Adsorptive Removal of Two Basic Dyes (Methylene Blue and Malachite Green) from Binary System using Low Cost Adsorbents

A thesis submitted by

Soumitra Banerjee

(Index No.: 179/15/E dated 11-12-2015)

Doctor of Philosophy (Engineering)

Department of Chemical Engineering
Faculty Council of Engineering & Technology
Jadavpur University
Kolkata, India

2021

Dedication

To
My Family
and Friends

Adsorptive Removal of Two Basic Dyes (Methylene Blue and Malachite Green) from Binary System using Low Cost Adsorbents

A thesis submitted by

Soumitra Banerjee

(Index No: 179/15/E dated 11-12-2015)

For the Award of

Doctor of Philosophy (Engineering)

Department of Chemical Engineering
Faculty Council of Engineering & Technology
Jadavpur University
Kolkata, India

2021

PROFORMA – 1

"Statement of Originality"

I Soumitra Banerjee registered on 11/12/2015 do hereby declare that this thesis entitled "***Adsorptive Removal of Two Basic Dyes (Methylene Blue and Malachite Green) from Binary System using Low Cost Adsorbents***" contains literature survey and original research work done by the undersigned candidate as part of Doctoral studies.

All information in this thesis have been obtained and presented in accordance with existing academic rules and ethical conduct. I declare that, as required by these rules and conduct, I have fully cited and referred all materials and results that are not original to this work.

I also declare that I have checked this thesis as per the "Policy on Anti Plagiarism, Jadavpur University, 2019", and the level of similarity as checked by Turnitin software is 8%.

____

Signature of Candidate:

Date: 17/05/2022

1. Prof. Siddhartha Datta

2. Prof. Anupam Debsarkar

CERTIFICATE FROM SUPERVISORS

This is to certify that, the thesis entitled ***"Adsorptive Removal of Two Basic Dyes (Methylene Blue and Malachite Green) from Binary System using Low Cost Adsorbents"*** *submitted by* ***Mr. Soumitra Banerjee****, who got his name registered on dated 15.12.2015, index no. 179/15/E , for the award of Ph.D. (Engineering) degree of Jadavpur University under Faculty of Engineering & Technology is absolutely based upon his own work conducted under the supervision of the* ***Prof. Siddhartha Datta*** *and* ***Prof. Anupam Debsarkar*** *and that to neither the thesis nor any part of it academic award anywhere before.*

(Prof. Siddhartha Datta) **(Prof. Anupam Debsarkar)**

Date: 17.05.2022 **Date: 17.05.2022**

Seal **Seal**

LIST OF PUBLICATIONS

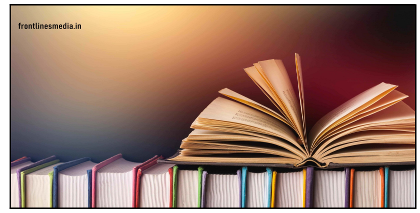

Journal Publications

1. **Soumitra Banerjee**, Dr. Anupam Debsarkar and Dr. Siddhartha Datta, *"Removal of basic dyes from aqueous solution by adsorption using rice husk ash-a fixed bed column study,"* **International Journal of Advanced Engineering, Management and Science**, March 2017, Volume 3 Issue-3,pp-325-330. ISSN 2454-1311. DOI: 10.24001/ijaems.3.4.7.

2. **Soumitra Banerjee**, Dr. Anupam Debsarkar and Dr. Siddhartha Datta, *"Adsorption of Methylene blue and Malachite Green in Aqueous Solution using Jack Fruit Leaf Ash as Low Cost Adsorbent,"* **International Journal of Environment, Agriculture and Biotechnology (IJEAB)**, May-Jun- 2017, Volume 2 Issue-3,pp 1369-1374. ISSN 2456-1878. http://dx.doi.org/10.22161/ijeab/2.3.45.

3. **Soumitra Banerjee**, Dr. Anupam Debsarkar and Dr. Siddhartha Datta, *"Adsorption of Methylene blue and Malachite Green onto Low Cost Adsorbent Rice Husk Ash: A Batch Study",* **International Journal of Agriculture, Environment, and Biotechnology**, June- 2018, Volume 11 Issue-3, pp 421-426, ISSN 0974-1712.DOI: 10.30954/0974-1712.06.2018.1

4. **Banerjee**, **Soumitra,** Datta Siddhartha and Debsarkar Anupam**,** *"Artificial neural network modeling for decolorization of textile dye mixture using low cost adsorbent",* **Research Journal of Chemistry and Environment**, May- 2020, Volume 24 Issue-5, pp 57-60, ISSN 0974-1712.DOI: 10.30954/0974-1712.06.2018.1

List of Conference Presentations

1. **Oral** Presentation on ***"Adsorption Potential of Selected Low Cost Adsorbents for Removal of Two Basic Dyes (Methylene Blue and Malachite Green) from Binary System: A Comparative Study"***, WEBINAR organized by R&D Committee, TEQIP-III, Jadavpur University during February 26-27, 2021.

ACKNOWLEDGEMENT

It is indeed my greatest pleasure to acknowledge my heartfelt gratitude to all my mentors, peers and well-wishers who have directly and indirectly contributed towards the successful completion of my thesis. It may not be possible to thank each one of them individually but I shall try my best to do the same.

At the outset, I would like to express my sincerest thanks and gratitude to my supervisors ***Prof. Anupam Debsarkar, Professor, Environmental Engg Division, Civil Engineering Department*** *and* ***Prof. Siddhratha Datta Ex-Professor Department of Chemical Engineering, Jadavpur University*** *for their unwavering guidance and help, without whose consistent support this thesis would not have seen the light of the present day.*

Special thanks are due to all the ***Faculty Members*** *and* ***Staff Members*** *of* ***Jadavpur University, Environmental Engineering Division, Civil Engineering Department and Chemical Engineering Department*** *for supporting me during my Ph.D work at this esteemed Institution.*

I am also thankful to Anirban and Snehil. I am sincerely grateful to Paramita, Sudipta, Sanjib Kumar Maiti, my fellow researchers of Environmental Engg Division. I convey my special thanks to Abhishek, my fellow scholar for his support during the completion of my thesis.

I would like to thank my family for believing in me. I would like to thank my late parents for their encouragement to pursue my research work. Lastly, I express my heartfelt thanks to my wife, for encouraging me to chase my dreams and for her continuous help and support.

Finally, I would like to express my sincerest thanks to all my well-wishers who have helped me in various capacities during my journey so far.

……………………………………

Jadavpur University **(Soumitra Banerjee)**

Contents

List of Tables

List of Figures

List of Abbreviations	
Full Form	**Full Form**
Neem Leaf Ash	NLA
Jack Fruit Leaf Ash	JFLA
Bagasse Fly Ash	BFA
Rice Husk Ash	RHA
Methylene Blue Malachite Green	MB MG
Break Through Curve	BTC
SEM-EDX Scanning Electron Microscopy	SEM
Sum of the Squares of the Errors	SSE
Sum of the Absolute Errors	SAE
Average Relative Error	ARE
Hybrid Fractional Error Function	HYBRIDF
Marquardt's Percent Standard Deviation	MPSD
Bed Depth Service Time	BDST
Mass Transfer Zone	MTZ
Artificial Neural Network	ANN

Executive Summary

The effectiveness of the abundant four agricultural waste materials viz. neem leaf ash, jack fruit leaf ash, bagasse fly ash and rice husk ash used non-expensive adsorbents was explored for adsorptive removal of mixture of two dyes Malachite Green (generic name: Aniline Green as referred afterwards) and Methylene Blue (generic name: Methylthioninium Chloride). These two dyes are referred hereinafter also by their generic name. Initially, investigation of batch study was done for adsorption of two basic dyes into solution mixture and for measuring the influence of different process inputs like adsorbent dose, initial concentration, shaker speed, pH and contact time of the initial dye solution. Capability of removal for neem leaf ash in the adsorption study was obtained as 99.2%, which showed the efficacy for the adsorbent. The adsorbent dosage as optimum amount was obtained as 4 gm as there was no significant effect upon dye removal over that dose. The dosage at optimum level for jack fruit leaf was obtained as 5 gm. The greatest efficiency for removal was recorded as 92.57%, which is highly satisfactory. The optimum dose of bagasse fly ash was 2 gm at equilibrium. High adsorption proves the effectiveness of the adsorbent for dye removal. The optimum dose for RHA was 4 gm, with the maximum removal percentage of dyes being 92.20%.

The optimum contact time for neem leaf ash, jack fruit leaf ash, bagasse ash and rice husk ash was recorded as 135, 165, 135 and 190 min respectively. The average adsorptive removal decreased from 95% to 60% as the concentration increased to 150 mg/L from original concentration of 25 mg/L. Increasing in shaker speed from 30 to 130 rpm increased the adsorptive removal to more than 97% for the adsorbents. The adsorptive removal was directly dependent on pH of adsorbate solution.

Adsorption isotherms viz. Freundlich, Temkin and Langmuir, were studied in the present research. The Langmuir isotherm model fitted best for all four low cost adsorbents as obtained in the present investigation. The error analysis was conducted considering five error functions to make out the best isotherm model. The statistical deviations of three isotherm models implied that Langmuir

equation best followed the data from equilibrium study for all four adsorbents, which was also supported by the results obtained from chi-square test. The values for separation factor (R_L) for all four adsorbents were obtained less than unity, which indicated favourable adsorption involving four low cost adsorbents.

The kinetic study for dye adsorption is an essential requirement for selecting the best option in terms of the operating condition for the full scale batch experiment. Pseudo-first-order and pseudo-second-order kinetic model explored in current investigation. Second-order model was found in superior conformity with experimental result showing best fit in the adsorption experiment.

Adsorption capacity has improved with rise in temperature. Thermodynamic study was also conducted in the present investigation. The magnitude of change of enthalpy (ΔH) was recorded as 43.14, 37.56, 54.03 and 40.36 kJmol^{-1} for neem leaf ash, rice husk ash , jack fruit leaf ash, and bagasse fly ash respectively, indicating the prevalence of the chemisorptions process. The adsorption process was characterized by activation energy.

The study under column adsorption was conducted under different varying input parameters like as adsorbent height, initial concentration of dye, pH and rate of inflow of the adsorbate solution. Removal of dye mixture through adsorption improved for raising bed height and adsorbent pH. It was also increased with reduced initial concentration and inflow rate of adsorbate solution.

Time for breakthrough raised 15 to 45 minutes during bed depth increased from 4 to 8 cm. Breakthrough time reduced to 50% for an increment of adsorbate concentration up to 100 mg/L from 25 mg/L for all four adsorbents.

The exhaustion time at high flow rate for the rice husk ash and bagasse fly ash was less than 10 min. The exhaustion time for neem leaf ash dropped from 30 to 8 min as flow rate was dropped down to 5 ml/min from its initial value of 10 ml/min. The exhaustion time for jack fruit leaf ash got reduced from 35 to 16 min as inflow rate was dropped to 5 ml/min from its initial value of 10 ml/min. Bed saturation time improved from 20 to 100 min with increased pH as 4.1 to 9.2 for all the four adsorbents.

In the current study Thomas, Yoon-Nelson, Adams-Bohart and Bed Depth Service Time (BDST) models were deployed to predict the dynamic response of the bed during the column study. Thomas model was employed successfully in process of adsorption for all the four adsorbents. The dye uptake rate increase with the increase in bed depth was inconsistent at initial concentrations. Uptake reduced with increasing value of initial concentration. The higher coefficient of regression value (R^2) implied that the data from experimental outcomes fitted better with the model analysis. In the Yoon-Nelson model, decreased constant (K_{YN}) and increased 50 percent breakthrough time (Γ) for all the four adsorbents were very distinct and it indicated that this model described the experimental run quite well. The higher coefficient of regression value for neem leaf ash and jack fruit leaf ash indicated better performance of the model compared to other two adsorbents viz. ashes of rice husk and bagasse fly. Influence of adsorbate pH over the adsorption for mixed dye solution may be described well this model. Application of Adams-Bohart model using experimental data for the variation of bed depth and concentration matched well. The higher coefficient of regression value (R^2) referred the effectiveness of the model. BDST model described the adsorption satisfactorily for all four adsorbents, particularly for bagasse fly ash. The higher coefficient of regression value (R^2) for neem leaf ash and bagasse fly ash was recorded. BDST model was the best fitted model compared to other three models.

Artificial Neural Network (ANN) model was introduced using experimental outcomes in the present research. This network is comprises of three layer. Transfer function with back propagation nature having structure 4:10:1 for column mode and 5:10:1 for batch mode operation were taken in present study. In training component, transfer function algorithm such as 'poslin' for hidden layer and 'purelin' in output has been utilized for developing model. MATLAB-2009a version was used in the present study. The variable operating parameters are used as input variables. The output variable is the percentage removal of dye mixture. The selection of neuron numbers in different layers and optimization of subsequent training and testing can be achieved by iteration. The performance of the model depends on the appropriate number of neurons in different layers. Selection of satisfactory neurons in hidden layer was decided with trial process for better understanding and prediction at the exit response. The overall performance of the ANN model to describe the adsorption experiment was satisfactory for all the four adsorbents. It proved the effectiveness of the model so developed.

Statistical t-test, a type of inferential statistical tools was used to compare between two sets of data, which might be related in certain aspects. The similarity between the laboratory experiment and the ANN simulated value was tested using Stata-10 statistical software. In the t-test comparison was made between the experimental outcomes with predictions. ANN model so developed, described the adsorption process during both column and batch mode studies successfully.

Introduction

1

1.1 Synthetic Colour and its Environmental Consequences

Over the last few decades, environmentalists are showing growing concern about the potential adverse effects of intensification of chemical industries in global scale. The number of various dyes and pigments use for the different purposes in dye bearing industries are more than 3000. The textile industry one of the major component of this group produces 5000 million kilogram of cloth and related items annually all the world over. Huge volumes of water is used for the production purposes. In India, the overall production of dyes in the year 2019-2020 has been nearly 191,000 metric tons ***(Chemical and Petrochemicals Statistics, 2020)***. This massive water used in textile sector has a major responsibility of water poisoning. Water is used in textile and other related industries for washing of machinery, shop floor and mainly in the processing operation. ***(World's Worst Pollution Problems Report, 2015)***. The colour manufacturing industries represent a significant part of the overall chemical industries.

The traces of using dye in textile dyeing have been discovered even before Neolithic era. The use of tree barks, vegetables and rodents in China has been evidenced by the archeologists in 1400 C.E. ***(Joylakshmi et al. 2013, C. Wang et al. 2011)***. Since prehistoric times, human civilization used natural colours for painting their surroundings and dyeing skin and their cloths ***(J.D. Saikhom et al. 2013)***. It is reported that organic dyes were used for this purpose by the common people. The use of inorganic pigments like manganese oxide, soot, and hematite are all from natural origin. On the other hand, the uses of textile dyes in earlier times are aromatic in nature and originated from plants, insects and fungi ***(G. Nagendrappa, 2010)***. It is true that till the middle of 19^{th} century, the use of this colour was more or less restricted within natural origin. The emergence of synthetic dyes as a result of industrial revolution has certainly limited the use of dyes extracted from the natural origin ***(I. Holme, 2006).*** The mass production of synthetic dyes has naturally replaced the natural dyes for earning more profits by the industrialists. The application of natural dyes has restricted only among the Art and Craft sector for shading with pure color and soft artistic purposes. ***(M.M. souse et al. 2008)***. In recent time synthetic dyes are being used in Paper, Food and Leather industries for dyeing purposes.

The dye component can absorb or emit spectrum of light for a particular range between 400 to 700 nm. This absorption of light is primarily due to electronic transition between the different orbital within the absorbing molecules and the wavelengths absorbed are determined by the energy differences between the orbital ***(W.A. Allen, 1970)***. It is the reason behind its colorful appearance. When an object absorbs light of a particular wavelength, it reflects all other wavelengths and thereby appears to have a colour complimentary to the wavelength absorbed. As an example, when an object absorbs light having wavelength within the range of (400-430) nm (violet portion of the visible spectrum), it accurately appears yellow, since it is the colour complementary to violet in the visible spectrum ***(M. Baranska, 2013)***.

The colour is divided into two major groups viz. organic and inorganic, which are further divided into natural and synthetic compounds for each group ***(S. Heli, 2015)***. Colour is also divided into two broad categories dyes and pigments out of which dyes are mostly responsible for colouring water bodies even in small concentrations. Pigments are insoluble materials, attached with polymer used in paints ***(G. Ahmet et al. 2016)***. Dyes are explored to colour different substances like clothing materials, tannery product, paper etc. This colour is present in the form of dye molecules in the effluent stream in partly or completely insoluble from resulting in pollution ***(A. Ameen et al. 2016)***.

1.2 Dyes

Dyes are classified in several ways. These are primarily classified based on the commercial names and chemical nature. Dyes have also different classifications based on commercial aspect or nature. The unsaturated aroma in the chemical structure is an unique property of dye resulting solubility, replacibility characteristics ***(C.L. Suriga, 2014)***. The soluble coloring pigments of different characteristics agglomerated within the dye molecule responsible for coloring cloths and other related materials. It can also able to impart different shading over the fabric due to this property ***(D. Robati et al. 2016)***.

Dyes give colour to the materials by chemical reaction with the different ways. Dyes have different structures including aryl rings with decolourized electron system and thus classified into cationic, non-ionic and anionic dyes. These can be further classified as acid dyes having chelating sites or not, basic, disperse, azo sulphur, substantive and reactive dyes. In reality, all basic and some particular reactive dyes are mainly responsible for water pollution because of their strong chemical bonding and there by cannot be removed by conventional treatment process ***(A. Kathryn et al. 2016)***. Now a day, there are almost 1,00,000 commercially available dyes used in different chemical industries like textile, paper, printing and foodstuff. These toxic and hazardous synthetic dyes are of major concern for the environmentalists at this time ***(A. Mazhar et al. 2018)***. The use of synthetic dyes was started in the year 1856 by **W.H. Perkin**, a British chemist during preparation of quinine. In the era of rapid industrialization, use of dyestuff has been increased remarkably ***(R. Kant, 2012)***. The commercial application of azo dyes which are mostly synthetic in nature has been increased by this time also. The main source of dye pollution is dye-contaminated industrial wastewater. The effluent wastewater of dye using industries comprises huge volume of color and toxic substances, really alarming to the environmentalists. The textile effluent is a complex mixture of pollutants comprising wastes varying from organo-choloride based pesticide wastes to heavy metals mixed with dyes. Most of these dyes have complex chemical structure and strong electro-chemical bonding and are almost impossible to remove from the effluent by conventional treatment methodology ***(R.K. Vital et al., 2016)***. A recent study reveals that 12% of synthetic dyes used annually is lost during industrial operation and 20% of that amount is directly enters into the environment through the effluent ***(R. Kant, 2012)***. The continuous exposure of the worker in these industries may create higher carcinogenic risk ***(S. Ahmed et al., 2019)***. The different organic compounds of dye components have carcinogenic effect on human and aquatic animals. The mixing of sulphur dyes into the water body results in rapid depletion of dissolved oxygen, affecting the life of fish and other aquatic organisms. Most of the dyes and their degradation products are toxic, mutagenic in nature. Reductive biotransformation of the azo connection of the dyes is mainly responsible for its mutagenic character. They are intractable to biodegradation rendering toxic environment to aquatic organism and other living beings.

Recent study shows textile industries discharge nearly 5.6 million liters ***(S. Sandhya, 2020)*** of effluent containing different types of dyes every day. The abnormal discharge of untreated effluent creates various problems like-

- **i)** Aesthetic problem by colouring the water bodies,
- **ii)** Limiting the penetration of sunlight into the water bodies thereby hampering the photosynthetic activities,
- **iii)** Causing mutagenic and carcinogenic effect on human beings.

The dye containing wastewater considering its huge negative impact on environment have to be treated before final disposal into natural water body ***(L. Alcaraz et al., 2018)***.

1.2.1 Anionic or Acid dye

Acid dyes which are also termed as anionic dyes explored to color soft fabric in the acid solution. The chemistry behind this operation is basically ionization involved between the anionic dye and cationic fabric materials ***(R.M. Kamel et al., 2019)***. The compositions of acid dye are sodium salts of phenolic organic acids. Sometimes it may be composed of sulfonic or carboxyl group of sodium salts. It is used for dyeing polyamide fabrics, wool and silk in textile industries ***(T. wang et al., 2016)***. These are water soluble and reactive in nature. These dyes are popularly used for its bright appearance ***(H. Kartik et al., 2014, S.G. Muntean et al., 2014)***.

1.2.2 Cationic or Basic dye

Basic dyes are formed from the basic radical of the organic salts. The molecule of basic dyes ionizes and converts the coloured component into positively charged radicals also terms as cationic dyes. ***(M. Siddique et al., 2014)***. The water soluble, cationic dyes are of this type. It has its use in the manufacturing of acrylic fiber. Acetic acid is a common facilitator for dyeing with cationic dyes on the acrylonitrile polymer based fiber. The another important use of basic dyes in paper coloration. The dyes are commercially used in wide range for colouring purposes. Aniline Green and Methylthioninium Chloride are most common and widely used basic dyes ***(Y. Yao et al., 2010, D. Tiwari et al., 2014)***. These two dyes have hazardous effect on aquatic as well as in the food chain. Methylene blue is responsible for permanent damage to the human eyes on the other hand malachite green has carcinogenic effect on human body ***(N. Sharm et al., 2014).*** Both these dyes have adverse effects on human breathing and nervous system during inhalation process. As the use of basic dyes is wide and common practices of the chemical industries, it is very necessary to treat the cationic dyes like aniline green and methylthioninium chloride before discharging to open environment ***(Chi Kim Lim and Ta Wee Seow, 2016)***.

1.2.3 Reactive dye

The responsible portion within the molecular orbital for reactive dyes instantly with the fibers are very active. The use of reactive dyes for the domestic purposes is common. The reactive dyes are very much stable, most permanent and cannot be treated by conventional treatment methodology due to its strong nitrogen double bonds. (N==N azo bonds). It has strong nitrogen covalent bonds between carbon, nitrogen atoms with oxygen, and nitrogen or sulphur atom of hydroxyl group. It is extensively used for colouring fibers due to its low energy consumption ***(V.S. Munagapati et al., 2018)***.

1.2.4 Direct dye

Direct dyes are used in printing process as well as at the timing of finishing operation in the textile industries. They are also commonly used on cellulose based fibers. These dyes are mixed in alkaline or neutral environment. The brightening properties are less for such category of dye but at the same time first, uniform application over the cotton fibers can be achieved easily. The hazardous and carcinogenic effects of direct dyes restrict its use, now a day, in many industries ***(F. Wali, 2015)***.

Direct dyes can be classified into two broad categories depending upon its charges used in the textile and other related industries ***(B. Mohamed et al., 2020)***.

1. **Positively charged or Cationic Direct Dyes**
2. **Negatively charged or Anionic Direct Dyes**

1.2.5 Azo dye

The azo dyes are broadly classified into three parts based on aryl functional group in its structure. The mono-azo, di-azo and tri-azo are the example of such categorization ***(H. Saeedeh et al., 2013)***.. There are more than thousands of azo dyes in the market used in the textile, paper and leather industries. It has restricted in various countries due to its adverse effect on human reproductive system ***(R. Ryan et al., 2010)***.

1.3 Hazardous effects of dyes and necessity of its treatment

Dyes are visible pollutant. It may cause colouring effect in the effluent even after a minor release ***(M.A. Shrafi et al., 2017)***. Hence the dye pollution easily draws the attention of the common people and authorities or local bodies. The industry should be cautious to minimize the release of colour even in little amount as it creates visible nuisance for the environment. In the chemical industries, especially in textile industries, incomplete exhaustion of dyes onto textile fiber during dyeing process ***(A. Mohamed et al., 2017)***. The dye producing constituents are often toxic in nature, responsible for mutagenesis and detrimental for life. The azo dye comprises of anililine in its structure is mainly responsible for cancer during discharging toxic amines into the water body ***(C.P. Huang and C. Huang 1996)***.

The good quality of dye compromises of chemicals which are again detrimental to the man and environment. Due to stringent regulation in early 19^{th} century health security issue of worker and supporting staff members have been restored. Review groups of the Pollution Control Agencies of different states reported miserable situation of the worker as per as their health is concerned. Textile industries require huge amount of colored water into which white fabrics are dipped for coloring and subsequent operations. This colored effluent is discharged to the natural water body creating problems associated with health hazards ***(M.K. Indana et al. 2016)***. The people awareness helps to introduce new stringent legislation in respect of environmental protection. As a result of this treatment of dye bearing wastewater in different forms and techniques become very popular day by day which helps in sustainable development ***(A.E. Al Prol, 2019)***. It is evident that dyes in general are toxic and responsible for critical health hazard issue for the human society. It is also not acceptable for aquatic environment. The physical detection and proper analytic quantification is essential to get rid of this difficulties. Generally, there are two decolourisation methods: by destruction of colourant molecules and the other is by separation of colourants from water.

1.4 Conventional treatment for dye removal

There are several techniques which are explored to eliminate the dye molecules from dye bearing wastewater. These treatment processes are broadly classified as the followings:

i) Biological process ii) Physical process iii) Chemical process and

ii) Physico-chemical process

In absence of costly chemical treatment of wastewater coupled with the necessary recovery of important chemicals mixed with the effluent, chemical treatment is used very rare in practice. At the same time lower efficiency of biodegradation of some dyes, the biological process of treatment for the dye bearing effluent has very limited use. The process as described above have definite reliable techniques and in true sense they are very effective methods for a particular dye in specific wastewater ***(S. Sumathi, 2015)***. Biological treatment is effectual for removal of BOD and TOC from coloured effluent but its decolournization capacity is limited due to non-biodegradable nature of most commercial dyes. Chemical and physical treatment techniques are considered to be very effective. ***(R. Istratie et al., 2015)***. The different effective technologies applied for this purposes are adsorption, filtration, coagulation, dissolved air floatation, chemical oxidation, membrane filtration, electro chemical methods etc. The suitability of different methods for the specific range of dye removal is given in the following tabular form:

Table-1.1: Suitability of different methods for dye removal

Treatment methods	Anionic dyes	Substantive dyes	Synthetic dyes	Cationic dyes
Adsorption	✓	✓	✓	✓
Coagulation	✓	✓	✓	✓
Chemical oxidation	×	✓	✓	✓
Membrane filtration	✓	✓	✓	✓
Electro chemical methods	✓	×	✓	×

✓ Suitable × Not suitable

The treatment of effluent containing dyes have been worked out for last few decades. Some of the important and potential technique are described below:

1.4.1 Physical methods

So far, the most popular treatment method for the dye removal from the wastewater using physical methods is membrane filtration technique. This includes nanofiltration, reverse osmosis, electro-dialysis etc. ***(Z. Yong et al., 2017)***. These are used very effectively in many textile and other dye related industries. Membrane filtration technique can clarify, concentrate and separate the dye molecules from the colour bearing wastewater. This method can even be operated at high temperature under huge microbial concentrations. But it has a problem regarding handling the residual dye molecules separated from the wastewater after membrane filtration. There is a possibility of clogging and replacement of membrane at a certain interval, resulting high capital cost of the operation. The method is suitable at lower concentrations of dye molecules in wastewater and recycling purposes in the interim operation in textile industries ***(M. Kharub et al., 2012)***.

1.4.2 Chemical methods

i) Coagulation and Flocculation

The treatment of coloured wastewater by coagulation- flocculation followed by filtration is very common and is widely used in dye industries. This method is cost-effective as well as promising for both the soluble and insoluble dyes ***(A. Naimabadi et al., 2009)***. The problem of employing this technique for the stated purpose is handling of sludge generated by the process. In case of cationic dyes, adoption of this method is quite difficult because of huge floc formation.

ii) Oxidation by hydrogen per-oxide

Chemical oxidation using hydrogen peroxide and ultra violet (UV) ray for exclusion of dye from the textile effluent is a promising and important method in present day industries. The dissociation of H_2O_2 molecules into two hydroxyl radicals, i.e. strong oxidants can take place by using UV ray. H_2O_2 itself produces hydroxyl radical when it comes in contact with wastewater. The hydroxyl radicals of strong oxidation property break organic compounds by extricating protons to yield organic compounds for the subsequent removal. This method has a limitation for its use because of its very slow removal rate of dye molecules ***(S. Thakur and M.S. Chauhan, 2016)***.

iii) Oxidation by ozone

Ozone is a strong oxidant, used for the exclusion of colour from the effluent. It is reported by several researchers that ozone can be used for the removal of colour up to 88.6% and it can simultaneously decrease the DOC concentration. Due to its strong oxidizing capacity, it can easily degrade chloride, coals, insecticides and unsaturated hydrocarbons ***(S. Venkatesh et al., 2017)***. The formation of residual colour in the form of sludge is less in this method but still the method is not acceptable widely due to the high cost of ozone.

iv) Oxidation by chlorine

The removal of colour from the wastewater by using chlorine is still not considered to be effective as this process releases aromatic amines, which causes cancer and produces other hazardous effects to the environment (***C. L. Suriga et al., 2011, A.K.M. Abdul Quader, 2010)***.

v) Photochemical degradation

Photo catalytic detoxification is an alternative approach for dye extraction from the industrial effluent. This method is capable by mineralizing toxic dye present in the wastewater with sunlight by combining the heterogeneous catalysis ***(H.T. Dang***

and P.T. Mai, 2017). Both batch and column mode operation can be employed in this technique, due to its zero sludge formation characteristics. The treatment methodology is suitable for mixed industrial wastewater.

1.4.3 Biological method

This method includes aerobic and anaerobic digestion, activated sludge and biosorption, microbial degradation. Some of the methods are comparatively much effective than physical and chemical process for decolourization ***(M kharub et al., 2012)***. But in the biological method of treatment for decolourization huge land area and sufficient sun light is required for the entire duration, which is impractical throughout the year in many occasions. On the other hand, this method of treatment is less effective for the removal of azo dyes. Some of the important biological methods are:

i) Aerobic digestion

The growth of naturally occurring aerobic micro-organisms helps in aerobic digestion of coloured wastewater. The principle of aerobic digestion is to change the energy level of organic compound from high to low value. In the aerobic digestion, the bacteria, present in the activated sludge, absorb heavy metals and dye molecules through its cell wall, made up with lipid, amino acids and other cellular compounds ***(A. Albihm, 2009)***. The major drawback of this process is continuous change in quantity and emission of odorous gases during storage.

ii) Anaerobic digestion

In anaerobic digestion treatment of the wastewater bearing colour molecules, methane, carbon dioxide and water are produced, which require less energy and produce low quantity of sludge. In anaerobic digestion, reductive decolorization of azo dyes could be achieved easily ***(A.M. Mir, 2016)***.

iii) Microbial degradation

Microorganisms have long been used for decolorization and metabolization of azo dyes. The use of particularly different species of microorganisms for treating coloured wastewater is very common and widely used by the environmentalists for quite a long time. Microbial treatment in the form of growth of white rot edible mushroom for reducing toxicity of dye bearing wastewater is a well-accepted technique for this purpose. However, it has got some limitations, as the technique is very selective and not effective for complicated dyes.

iv) Biosorption

Adsorption in biomass is a treatment technique where a particular types of inactive, non-alive, sticky microbial biomass concentrate and bind up the heavy metals and dye molecules from the wastewater, and thereby reducing the toxicity and colour from the industrial effluent. It is becoming effective alternative method of dye removal to replace the conventional methods. The use of different microorganisms in the form of fungi, obtained from the industrial fermentation processes make the removal process cheaper and helps for sustainable development. The common types of these dye absorbing fungi are Aspergillus, Niger, Rhizopus and Rhizopus oryzaea ***(C.P. Huang and C. Huang, 1996)***.

1.5 Physico-Chemical Method - Adsorption

Adsorption is a treatment method which includes physical, chemical as well as biological process to reduce the dye molecules from the coloured wastewater to the desired level and also to reuse the wastewater for the industry ***(M. Dogan et al., 2009)***. The principle followed in this adsorption is that the solid surface (adsorbent), initially coming in contact with solution of dyes (adsorbate). Due to difference surface force, the pore of the adsorbent surface gets saturated by adsorbent accumulation . In this method, the adsorbent of any form solid, liquid or gas moves from one phase to another crossing some boundary. It is an established fact through intensive research that adsorption achieved within the pores, present on the solid surface due to physical attraction. The attraction evolves due to interaction at phase interface and accumulation of substances also takes place over the sorbent surface. The interface comprises of boundary layer of any two medium made up of solid, liquids or gases. The adsorption capacity depends on the surface transfer ability of adsorbate molecules from one phase to another, may be of same or different in nature. In case of dye removal problem, most of the dyes used in the food industries and those direct dyes for textile industry are hydrophobic in nature and can easily be eliminated by the adsorbent from the aqueous media. Oxidation, filtration or other conventional methods for dye removal process are cost expensive compare to adsorption. So adsorption is the most competent and cost-effective process over all other treatment methodologies available for decolourization also due to its simple operational mode, less or nil production of toxic sludge, recovery and recycling of the adsorbent. This has encouraged the researchers now a day for the development of adsorbents that are abundantly available and economically feasible ***(A. Mittal et al., 2009)***.

In current time attempt has been made in different researches to examine the effect of size and shape of surface pores of sorbents and its morphology in different types of activated carbon and to compare this information with sorption properties**.** The surface characteristics in terms of pores structure of the adsorbent delivers a significant role in the process of adsorption. It may be classified into three components ***(C. L. Mangun et al., 1998)***.

1. The pores having diameter less than 2 mm on the surface of the adsorbent is known as micro-pores.
2. The pores and internal channels having diameter in between 2 to 50 mm is known as meso-pores.
3. The pores having diameter greater than 500 mm is known as macro-pores.

The process parameters influence they are of followings:

i) Physical properties i.e. particle size distribution and surface area.
ii) Chemical properties of adsorbent.
iii) The solution temperature and pH.
iv) The flow rate or contact time of the wastewater with adsorbent.

Factors influencing adsorption:-

i) Solubility factor for solute in the aqueous solution.
ii) Pore characteristics for the adsorbent
iii) Surface morphology of the adsorbent.
iv) pH and temperature of the solution.

Among a number of different techniques for elimination of dye pollutants from its aqueous medium described above it is reported that adsorption technique had been proved to be one of the best technologies and showed good results in the removal of different colours from the water system ***(H. Freundlich, 1906)***. Adsorption process has very simple operational technique due to its friendly design approach. It has a strong insensitivity towards toxic impurities in the effluent water ***(Langmuir, 1916)***. For the elimination of heavy metals, color and other impurities of organic nature adsorption proves its authority over other approaches of removal techniques ***(H.W. Vnder Marel, 1966)***.

1.5.1 Conventional adsorbents

Activated carbon, known as charcoal, has an wide use in the dye bearing industries for treating wastewater over thousands of year. The high percentage of carbon in the organic substances are used for the purpose of adsorption. Activated carbon may be used as conventional adsorbent as it contains less amount of volatile organic matter, long life and good stability in exchange reaction ***(A. Bhatnagar and A.K. Minocha, 2006).*** This may be prepared in two steps. Initially, carbonization of raw carbonaceous material is carried out in an inert environment followed by activation of resulting char (***C. Wang.* et al., 2011**). During carbonization process, the non-carbon portions are eliminated and residual carbon atoms group together to form amalgamated condensed aromatic ring. The pores of the char in this form cannot be accessible. Thus, further activation is necessary for enhancing the pore structure of the char. This activation may result in the formation of large internal area of carbon. This porosity of carbon can also be enhanced by chemical activation where chemical compounds like H_3PO_4. $ZnCl_2$ etc. are added to the stock prior to carbonization. These dehydrating agents influence the process of pyrolyic decomposition and inert formation of tar to increase porosity on the surface of carbon. The optimum temperature of this activation is nearly 555^0C.

The unique characteristics of activated carbon includes wide surface with effective pores along with the affinity towards molecules of solid in the adsorbate solution. The activated carbon is undoubtedly effective and most efficient adsorbent used in adsorption process for eliminating heavy metals and dyes from industrial effluent. The wide use of activated carbon has been started around 2000 B.C. In the year of 1789-90, ***Lowitz*** first used charcoal to remove bad taste and odors from the water ***(N.K. Mandal, 2014)***. Since early days so many researchers carried out exclusion of colour from the wastewater using activated carbon.

In spite of its high efficiency, at the same time activated carbon has high manufacturing cost. Similarly, polymers have proven to be efficient in dye adsorption due to their high regeneration capacity but less economical. In view of these, different locally available abundant materials have been tested as adsorbent during dye and heavy metals exclusion ***(F. Deniz and S.D. Saygideger, 2011)*** in recent time.

1.5.2 Non-conventional adsorbents

The effectiveness of conventional activated carbon over adsorption meant for removal of dyes in chemical, textile, leather industries is undoubtedly brilliant. But the commercially available carbon for this purpose is very costly and makes the entire process of adsorption expensive ***(C. Gregorio, 2015).*** In the developing countries, large scale application of costly activated carbon is restricted. The procurement as well as its cost force to search alternative low cost adsorbent by the scientists. The toxic, synthetic dyes are used in almost all the textile and similar other industries. The use of non-conventional, low cost, eco-friendly activated carbon as adsorbent is a challenging task of the environmentalists now a days ***(K. Abbas et al., 2018).***

The cost involvement by exploring commercially available activated carbon as adsorbent is become very high. The need for using abundant agricultural wastes of bio-origin as adsorbent is become very popular among the scientists at present time ***(Z.J. Song et al., 2017).***

The use of such non-conventional adsorbent may serve two ways. Firstly, the use of such waste materials reduce the cost of adsorption process for removal of dyes, secondly, it solves the problem of handling solid waste disposal in agricultural and industrial sectors, which in turn helps us for the sustainable development ***(X. Ma et al., 2016).***

Hence, adsorption has been focused for the removal of dyes to reduce adverse effects upon our environment. The cost-effective, non-conventional adsorbents generated from agricultural and industrial waste materials can be considered wisely by the environmentalists ***(M.R. Wual, 2019).*** The effluents of certain industries viz. fly ash, slag, slurry, mud are commonly used as low-cost adsorbents at present time. On the other hand, the waste produced from agricultural field such as neem leaf, bagasse, jack fruit leaf, rice husk, mango bark, cotton fiber are becoming very popular use as non-conventional adsorbents. The performances of such substances are tested and confirmed about their potential use in adsorption ***(M.K. Satpathy et al. 2015, Y. Dai, 2018).***

According to ***World Bank (2014),*** 20% of water pollution is caused by textile processing. The use of thousands of chemical s and allied compounds along with textile items coupled with dyeing operation in the industries are responsible for production of billions of dyestuff all over the world annually. Textile industries are the principal source of industrial pollution for any country like India. On the other hand, increased population and modernization of society gave rise to booming of textile sectors in India. Report states that textile generates 14% of total industrial production of the country and it earns 27% of foreign income annually. In the 2015-2016 financial year production of textiles was 1.34 million tons. As reported, water consumption and discharge of wastewater into the river by the Indian industries were 1123 MLD and 501 MLD respectively. In West Bengal it was 116 MLD and 87 MLD respectively, which is alarming. In the stretch of West Bengal the river Hooghly receives this amount of wastewater from more than twenty textile and allied industries. It is reported that those industries discharge more than seventy percent of total wastewater generated, followed by pulp and paper industries (20%) has a direct effect over man and environment ***(CPCB, 2013).*** Another important aspect of using low cost agricultural residue like neem leaf, jack fruit leaf, rice husk, bagasse etc. in form of ash (carbonization of the product) as adsorbent for adsorptive removal is that, resulting reuse for those abundant materials is also helpful for sustainable development. Thus, the treatment of dye bearing industrial wastewater using low cost agricultural wastes is becoming a challenging task ahead of the environmentalists and engineers at present day.

1.5.3 Removal of Mixed dye

The synthetic dyes are really a threat to the environment considering its chemical stability and resistant to exclusion from the wastewater using common removal approach. The annual use of such dyes all over the world is approximately 700 million tones. The component of pollution in the effluent coming out from the textile industries not only the toxic dye particles but also hazardous organics which jeopardize our ecological system ***(R. Jayalakshmi and J. Jeyanth 2015, J. Yu et al., 2020).*** There are more than 70% of used water and 40 % of dyes come out from the textile industries as effluent. The contamination of textile dyes creates unpleasant environment for aquatic life by disrupting photosynthesis, food chain and dissolved oxygen level of the water body. Textile effluents comprise different dyes ***(X. Li and Y. Li 2019)***. So exclusion of more than one dyes from the wastewater is essential to address real life problem. In this respect very few contributions are available ***(A. Dina and M. Scholz 2018)***.

The dye bearing industries contribute 11% to export earnings, 4% to GDP and they are responsible for providing direct employment of over 35 million people. On the other hand in Indian context, daily production of dyes is almost 64,000 tones out of which 11% is coming out with the effluent. It is most alarming that 9% of the effluent is directly discharged into the natural water body due to lack of proper treatment, which significantly reduce the aesthetic quality of the water body. It increases BOD, COD value of the water, inhibits photosynthesis, enter into the food chain, generates toxicity, mutagenocity and carcegenocity. So to safeguard our environment and as well as our economy, handling dye as pollutant is imperative ***(A. Alhujaily et al. 2020, V.K. Gupta et al. 2015)***.

The elimination of dyes in the industrial effluent has become a critical issue in the present society. Challenge is more formidable when more than one dye is to be removed from the effluent in a cost-effective manner ***(S. An et al. 2015)***. Removal of mixture of dye using inexpensive adsorbents is thus challenging task ahead before the researchers to solve a real life problem.

Literature Review 2

2.0 Literature review

2.1 Dye pollution

The various industries like textile, leather, plastic etc. use considerable amount of water for their operation particularly for dyeing purposes ***(Bruno et al. 2019).*** Contamination of color in the effluent solution can easily be detected in open eyes even it present a bit amount and not at all acceptable ***(Islam and Mostafa, 2019). Kavithayeni et al. (2019)*** reported that textile dye in wastewater is one of the most important sources of contamination. The concentrations of textile dyes in the natural stream of water at higher percentage restrict the re-oxygenation potentiality of the receiving water.

In the study of ***Noel and Rajan (2014)*** it was recorded that due to presence of plenty suspended solids, dyes and pigments long with COD and heavy metals such as Pb, Cu, Cd, Zn etc.

According to ***Charumati et al. (2011)*** the presence of colour in the natural stream evolved enormous hazards as per as aquatic life is concerned.
The dyes are important contributors to the pollution problem as it is estimated 50% of their amount is not fixed on fibers and go finally in wastewater ***(Kant, 2012).*** Contamination of dye is lower compare to other chemical pollution. But due to its visibility, the aesthetic characteristic is seriously affected at the time of disposal ***(Samchetshabam et al. 2016).***
Massoud et al. (2018) reported that organic dyes have mutagenic and carcinogenic effect on human beings and adsorption is one of the potential technique for their removal.

2.1.1 Dye categorization and formation

In spite of wide structural variety, the dyes are basically composed of chromospheres, responsible for imparting colour and auxo-chromes giving more sticking ability over the fabric surface ***(Malik 2004)***.

According to ***Banet et al. (2000),*** different types of dyes such as anionic, cationic, azo etc used in the textile industries.

In the paper ***Benkhaya et al. (2020)*** emphasized on the classification of dyes due to its numerous varieties and numbers. The different functional groups such as Anthraquinone, azo, phthalocyanine, sulfur, indigo, etc. have been considered in respect of chemical structure of dye classification ***(Kanna et al. 2016).*** In the present investigation, the dyes will be reviewed depending upon the three definite groups based on chemical structures. This is considered the color index numbers (CI) and the methods of application ***(Ahmet et al. 2016).***

Table 2.1: Some common classes of dyes and their uses

Type of dye	Properties	Applications	References
Acid	water soluble	nylon, wool, silk, acrylic printing, leather, ink-jet	***Naimabadi et al. (2009)*** ***David Noel and Rajan (2014)***
Cationic	water soluble	nylon, polyester, polythene	***Bhatti et al., (2017)*** ***Shahryari et al. (2010)***
Direct	water soluble affinity for cellulose	cotton, leather, rayon, nylon	**Guibal *et al.(1999)*** ***Gorzin et al. (2018)***
Reactive	chromophoric groups	cotton, wool, nylon, cellulose fibers	***Fkih et al. (2018)*** ***Saeedeh et al. (2013)***
Disperse, water soluble	non-ionic	polyester, nylon, acrylic, acetate	***Crini et al. (2008)*** ***(Kant 2012)***

2.2 Assessment of environmental impact and associated health risks of dyes

The Hazardous effect due to direct or secondary contamination in the effluent wastewater is a great concern and challenges before the environmentalists. The issue of direct or secondary pollution is being handled with equal care and seriousness ***(Baranska et al. 2013).***.

The contamination of dye with an little amount like 1 mg/L generates huge negative impact over the aesthetic nature of the water body and needs elimination using suitable approach ***(Dogan et al., 2009)***.

Many synthetic dyes for Textile industries are chemically stable and non-biodegradable in nature preventing sunlight entering into the water body and thereby disturbing photosynthetic activity ***(Sallash et al. 2011)***. This has harmful effect upon aquatic life. Dyes have different health hazard issue due to its toxic nature. The mutagenesis effect is also become growing concern to the scientists ***(Venkatesh 2017).***

Shahryari et al. (2010) reported the toxicity risks for cationic and diazo dyes (**Table 2.1**). Due to oral intake, chest congestion associated with irregular heart bits ***(Mahmoud et al. 2012)***, vomiting, weakness may occur ***(Nasuha et al. 2011).***

Mixing of synthetic dyes in natural water course obstruct sunlight entering into the water and affects photo synthesis ***(Nasuha et al., 2011, Crini and Badot et al. 2008).*** The hazardous Azo compounds are not acceptable due to its toxic properties ***(Sismanoglu et al. 2010).***

Reduction of dissolved oxygen level due to contamination of colour results insufficient growth of plants and animal ***(Staron, 2019).***

Brunolellis et al. (2019) reported that the textile industries and other dye bearing industries because of their anthropogenic activities, consume water and at the same time pollute water bodies. The dyes from the textile industries considerably negotiate with aesthetic quality of water bodies, increase biological and chemical oxygen demand (BOD and COD), weaken photosynthesis, reduce plant growth, destroy the food web, resulting bioaccumulation and encouraging toxicity, mutagenicity and associated risks **(*Nasuha et al., 2011).***

.

2.3 Dye removal methods

In the year ***2018, Katheresan et al.*** stated that the effluent from the dye bearing industries has serious harmful effect towards man and environment. The direct or even secondary contamination of dye molecules may leads to carcinogenic effect over civilians. In that paper the difficulties of selecting a particular method is pointed out for resolving contamination problem. Degradation of enzyme in polymer stabilization or accumulation of adsorbate over the surface and into the pores of the sorbent by attractive force are considered to be biological and physical processes of dye exclusion technique respectively. These processes are very useful methods of dye removal in recent time.

Ahmad et al. (2010) reported development of several novel techniques and methodologies for elimination of dyes from dye bearing solution. It is important that no single methodology likely to be recommended for treatment of all kinds of dye-bearing wastewater. The potentiality of the removal technique of dyes from the effluent water depends on the nature of dye to be treated and also the impurities there in and the wastewater characterization.

The categorization in respect of various chromophoric and auxochromic groups dyes are described as anionic, cationic and non-ionic dyes. It is difficult to remove anionic dyes by conventional techniques due to its high solubility in water The reactive and disperse dyes cannot be removed easily by the biological process. On the other hand, basic dyes like malachite green or methylene blue has a good response in adsorption or oxidation process ***(Isiuku 2018).***

Lcaraz et al. (2018) reported that there was no such universal method of remediating dye effluent. The best choice depends on the type of dyes to be removed, their composition and production flow into the wastewater. Different physical, chemical and biological methodologies are applicable for elimination of dyes from the effluent from quite a long time.

The effect of synthetic dyes and its impact has not been given proper attention a few decades ago ***(Gupta and Suhas 2009).*** But recently it is taken into account by introducing regulations and make it mandatory. Certain measures are taken by the Government agencies to safeguard our globe ***(Chinenye 2019).***

The treatment of dye bearing wastewater is not easy ***(Dogan et al. 2009)*** and inconsistent proportions of dye molecules in the effluent solution make the situation more complex ***(Crini, 2008).*** The biodegradability of synthetic dyes is poor due to its inherent structure ***(Mittal et al. 2014)*** and make it stable against temperature and sunlight ***(Mandal 2014).***

2.3.1 Biological treatment methods

Naimabadi et al. (2009) stated that the biological method explored in dye removal is often considered to be better approach in compare to physio-chemical process as per as cost and sludge formation is concerned. Decolorization of sulfur dye-containing wastewater using different bacterial strains are also reported in this paper.

According to ***Marisa Punzi et al. (2015),*** several biological treatment technique for exclusion of dye pollutants has been considered as effective approach. The usefulness of anaerobic method of dye stabilization in wastewater due to its low nutrient requirement has been reported.

Recepoglu et al. (2018) pointed out that in biological treatment involvement of microorganism for the treatment of dye pollutants are mostly acceptable and one of the promising approach in this aspect. At the same time according to ***Wang et al. 2016,*** the biological method has certain limitation in its use due to technical reason.

The use of fungus or microbes for stabilization of dye pollutants at early phase of treatment in biological method is very effective but at the same time process is slow due to slow metabolism rate of the microorganisms ***(Nguyen and Juang***

2013). The efficacy of a biological process depends on the pollutant load and nature of toxicity of the solution. This method exhibits better result in lower concentration of pollutant load ***(Patil, 2015).***

Batool et al. (2018) mentioned an interesting phenomenon regarding acceptability of biological treatment. It is reported that the toxicity level of generated sludge is more than the parent dye concentration.
Activated sludge and filter beds has been utilized in the biological treatment in the in the secondary stages ***(Gupta and Suhas, 2009).***

The presence of organic carbon as nutrients is essential in biological process **(*Crini, 2008*).** Due to absence of carbon in natural wastewater, this has to be added externally with constant supervision of pH level is another aspect of this method (***Chen et al., 2016***). The requirement of wide open land area with ample sunlight is another key requirement of this treatment technique ***(Siddique et al. 2014).*** So the removal of synthetic dyes in biological treatment is not so easy to handle and rejected accordingly **(*Bidi et al., 2019; Yu et al., 2020*).**
According to ***Wang et al. (2016),*** satisfactory results were generally obtained involving a biological treatment along with subsequent tertiary refinement of decolorization by adsorption using granulated activated carbon in a dynamic study.
Bhatia et al. (2017) reported that in India the textile sector contributes 14% of total industrial production and occupies nearly 4% of our GDP. Indian foreign exchange and employability of the common people is largely depends on this sector. This paper deals with the different treatment methods with their relative strength and shortcomings. It gives emphasis on biological method for its eco-friendly characteristics.

2.3.2 Chemical treatment methods

Kartik et al. (2014) used ferric oxide as adsorbents for the dye removal as an excellent example of chemical treatment. As per the observation, there are many techniques widely available for the removal of colour amongst and among them adsorption process is popular and effective. Many removal techniques have been applied. But, adsorption technique is cheaper and easily available to entrap the various pollutants from the industrial wastewater. The performance evaluation for the adsorption process primarily evaluated through batch rector due to its feasible and easy operation facilities associated with low cost involvement.

The chemical methods are generally referred as electro-chemical oxidation, advanced oxidation, or photo-catalysis. Highly competent oxidative catalysis and addition of oxidizing additives such as H_2O_2 are fundamental requirements of chemical methods ***(Kathryn et al. 2016).***

Another attempt of chemical treatment used by ***Pirkarami and Ebrahim (2017)*** for removal of Reactive Red 120 dye has been investigated. This paper also reported on the influence of process parameters such as electric loading and concentration of electrolyte solution. A constant monitoring over solution pH and regulating of temperature is another aspect of this study. This is an unique example of improved and economic dye removal process.

2.3.2.1 Coagulation and Precipitation

For the removal of sulfur and amino ketone dyes this technique is suitable ***(Rahdar et al. 2019).*** But at the same time not very effective for diazene groups and chrome dyes (as refereed in ***Table 2.1***) this is costly method and has limited use in practice ***(Crini, 2005).*** Disposal of large volume of sludge so generated in this process is another drawback as reported by ***Crini (2008)***.

2.3.2.2 Oxidation technique

This is another effective and important approach for lowering pollution load of the dye bearing industries ***(Gupta and Suhas 2009)***. Gaseous chlorine is used in this method with the associated risk for formation of toxic halogens. In some cases hydrogen peroxide is also explored for this purpose giving satisfactory result (***Table 2.1***), ***Sallesh et al.(2011)*** pointed out the problem in respect of generation of huge volume of sludge by this method.

Haber-Weiss reaction technique using Iron and Hydrogen peroxide is a recent development of this direction ***(Abdul Quader et al. 2010).***

Removing of manufactured dyes using oxidation approach is troublesome due to insensitive behavior of such dyes. The oxidizing agents are fail to give any impact over such dyes ***(An et al. 2015)***. Considering its wide range, single oxidizing agent often not enough for complete stabilization of effluent water.

Rahat and Umair (2019) mentioned using the metal catalyst other than Fenton origin, for dye elimination purpose in Advance Oxidation Process.

2.3.2.3 Advanced oxidation processes (AOPs)

Atalay and Ersoz (2015) explained the usefulness of advanced oxidation process (AOPs). In reality, one technique for complete stabilization of non-soluble dye is not at all possible as reported in this review. The most of the dyes used in modern days are of synthetic origin, have stable structure, difficult to remove from wastewater.

Al Prol (2019), was reported that advanced oxidation process has become an innovative approach by the researchers in recent times. This process produce highly sensitive genus to interact with organic dye pollutants as well as on pathogens present in wastewater for its complete stabilization.

Advance oxidation process is a powerful tool for decolourization as it uses more than one oxidizing agents simultaneously with different proportions. The use of chlorine along with UV ray has given better performance as reported by ***Rosales et al. (2012).*** Removal of organic dyes using AOPs is noted **(*Saeedeh et al. , 2013).***

The advantages of AOPs in the process of elimination of stable organic dyes over other conventional technique is due to use of combined oxidizing agents simultaneously act in a single process **(*Suriga et al. 2014).***

Oxidation process has still limited use due to high cost and rejected by the industries **(*Sarala et al. 2017).*** The accumulation of toxic sludge is another drawback of this treatment methodology ***(Sarala et al. 2017).***

2.3.3 Physico-chemical treatment

Adsorption is one of the popular approach in Physico-chemical technique other than membrane filtration ***(Kathryn et al. 2016, Yao et al. 2010).***

2.3.3.1 Membrane filtration

The filtration technique used for the reduction of dye loading from the effluent has achieved moderate success. Micro or nano level filtration has better performance over macro-level filtration due to small pores of the media ***(Gupta and Suhas 2009).***

The clogging of filtering media has certainly lowered the efficiency of ultra or nano level filtration needs monitoring and cleaning at regular interval. It has limited use for this hazard ***(Yawei et al. 2017).***

Tiwari et al. (2014) pointed out that when the effluent wastewater having high volume of dyes and at the same time sludge load is minimum the membrane separation technique such as nano-filtration and reverse osmosis technique is a suitable attractive method for the elimination of dyes from effluent. Here major disadvantage is that low water permeability and high energy cost.

Shah et al. (2015) noted that the organic dyes into negatively charged solution can be eliminated with the help of porous ceramic membrane. This type of sorbent is available with wide pH range and advantageous due to its surface charge characteristics (zeta potential).

Reverse osmosis is applicable in comparatively pure water or where the pollutant loading is less ***(Das et al. 2020).*** This method is still not become popular due to costly membrane and mechanical arrangements ***(Fkih et al. 2020).***

2.3.3.2 Adsorption

High solubility, structural complexity coupled with synthetic origin makes the diazine dye groups very difficult for exclusion from the textile effluent ***(David Noel et al. 2014).*** Use of physical and other conventional methods cannot be stabilized the dye loading completely. Comparatively adsorption is a better choice for adopting in dye bearing wastewater, considering its low cost and simple operational approach.

Adsorption is simple and cheaper alternative to treat the dye bearing wastewater. Wide ranges with variable capacity of the adsorbents make it popular among the scientists ***(Sharmeen Afroze et al. 2015).***

Extraction of solid pollutants from the liquid phase makes the adsorption technique more attractive before the industry ***(Venkatesh S. et al. 2017).***

The passive uptake of pollutants on the surface of the inert solid by the solid-liquid interaction either batch reactor or dynamic mode operation takes place in adsorption ***(Thakur and Chauhan, 2016; Wang et al. 2016).***

Adsorption method is low time consuming and simple cheaper approach in compare to available conventional methods adopted for dye exclusion purposes ***(Rafatullah et al. 2010).***

The inert adsorbents used in adsorption technique has low risk of sensitivity towards toxic pollutant, which is very important aspect specially in dye removal ***(Uddin et al. 2009; Sumathi, 2015).***

The problem associated with the generation of sludge is almost nil in adsorption followed by easy operational approach and simple design consideration ***(Diniz et al. 2008, Nguyen and Juang, 2013 Khoshnamvand et al. 2017).***

The generation of sludge needs pre-treatment before throwing to the natural water body increase the overall cost of the operation. Due to this, sometimes, it may become less attractive for the industry house ***(Kok et al. 2016).***

Adsorption technique shows better performance for removing certain heavy metals and dyes ***(Liang G. et al. 2019).***

Despite of many weakness, adsorption technique proves its effectiveness in large scale industrial operation ***(Islam, et al. 2019).*** The use of low cost agricultural waste and other biomass makes the process attractive as per as cost is concerned ***(Kharub and Rajor, 2012 and Joylakshmi and Jekendra, 2013, Kayode and Olugbenga 2015).***

Globally, the entire approach has shifted for searching alternative adsorbent such as rice husk, jack fruit leaf which are available locally with ample quantities and certainly having good carbonation properties ***(Heli et al. 2015).***

2.4 Adsorbent materials

The granulated carbon has high carbonation property which enhance the efficiency of the process. Due to its surface morphology adsorption of dyes or other heavy metals with wide variety can be achieved in effective manner ***(Bhatnagar and Minocha 2006, Alcaraz et al. 2018).***

The presence of small to large pores over the surface of the activated carbon depending upon the degree of carbonation is the key factor for describing the efficient operation of the process ***(Kamel et al. 2019, and Hasfalina et al. 2015).*** The charcoal readily available in the market possesses high cost and due to this reason it has limited use by the industrial house ***(Li et al. 2019; Mittal et al. 2009).*** The disposal problem specially in case of removal heavy metals is another serious issue to be considered ***(Mahmoodi et al. 2016). Senthil Kumar (2015)*** investigated into the adsorption of Pb by using treated cashew nut shell. It showed that Pseudo-second-order model followed the experiment well.

2.4.1 Low cost adsorbent materials

Adsorption is stated as one of the most widely accepted methods, particularly when low cost abundant materials are used as adsorbent ***(Indra et al. 2006, Deniz et al. 2013, Suresh 2016, Song et al. 2017). Manoj and Chaitali (2019)*** studied the effect of different parameters viz. dye concentration, adsorbent dose, contact time and pH of the solution on the adsorption of malachite green (MG) by using jack fruit leaf. The maximum dye concentration studied for adsorption experiments was found to be 100 mg/l.

Using of low cost abandon material such as neem leaf, bagasse, as sorbent in adsorption study becomes very popular ***(Sarvanen et al. 2018).*** Different papers in this respect have studied. One of the important paper for removing cationic dye

(MB) from the solution by ***Uddin et al. (2017)*** where they explored adsorbent as neem leaf. Langmuir isotherm model described the experimental outcome satisfactorily. Maximum adsorption was recorded as 156 mg/g.

Utilizing jack fruit leaf, bagasse mango leaf as low cost adsorbents for dye removal is another important findings as reported by ***Chen et al. (2016).***

According to ***Gupta (2015)***, agricultural products from renewable source which are less expensive, biodegradable and environmentally friendly ***(Gupta and Majumder, 2017)*** have been studied for dye removal ***(Heli and Juhani, 2015).***

Bagher and Niyaz (2012) explored the surface modification of activated carbon by chemical treatment with NaOH for Acid Red removal. From the paper it has been proved that adsorptive facility of the treated activated carbon increased from 2.5 to 11.77 mg/g. Surface modified activated carbon has proved its enhanced capacity for adsorption of NO_x and SO_2 gases from the renewable sources ***(Abdul Rasheed et al. 2018).***

Abundant agricultural wastes are potential inexpensive adsorbent ***(Mall et al., 2005; H. Patel, 2010, Mandal, 2014).*** Use of marine algae for Lead removal ***(Betiku et al., 2015),*** exploring wheat straw for removal of basic dyes ***(Mahmoodi 2011, Chowdhury et al. 2009).*** Pomegranate peel for exclusion basic dyes ***(Alhujaily, 2020, Yawei et al. 2017),*** are some of the important findings in this respect in Literature review section. Cell of the living and non-living microbes have been explored in different field of study efficiently ***(Abbas K et al., 2018).***

Hubbe et al. (2011) reported comparatively better performance of dead cell over live cell for exclusion of dyes from the effluent.

Another advantage for using dead cell in the process of adsorption is that there is no requirement of supplying nutrients and subsequent monitoring ***(Lan et al. 2014). Kathryn et al. (2016), Manoj (2012) and Liu (2012)*** highlighted the use of different agricultural waste materials for the adsorption method and compare the performances between treated and non-treated adsorbents.

Crini (2006) stated that the dye elimination technique using adsorption is effective specially using alternative abundant waste materials. In the paper of

Bhattacharya and Sharma (2005), it was reported that Neem in dust form found to be very effective in removing the dye, Brilliant Green, from aqueous solution. , The suitability of the adsorbent was tested by fitting the adsorption data with Langmuir and Freundlich isotherms.

2.4.1.1 Dye Removal in Single and Binary System

Adsorption of cationic dyes **viz.** methylene blue and malachite green in binary system has been achieved by using Thiourea-Modified polymer (acrylonitrite –co-acrylic acid) ***(Adeyi et al. 2015).*** Langmuir and extended Langmuir model described data well. The experimental data were better represented by Pseudo-second-order model.

Lin (2015), in his study on dye removal using cellulose based bio-adsorbent, concluded that adsorbent behaviors were dominated by the electrostatic interactions between the bio-adsorbent and the dye molecules in binary system. It is also reported that the bio-adsorbent could be reused for at least three cycles.

Removal of two dyes viz. Congo Red and Malachite Green in binary system has been achieved by using bentonite as adsorbent (***Abdil and Serkan 2009***). Optimum pH was recorded as 8.2 for maximum adsorptive removal of dye mixture. Langmuir, Freundlich, Redlich-Peterson and Temkin equations were used and Temkin isotherm described the experimental data well.

Sathy et al. (2006) utilized rice husk ash of two different origins to remove methylene blue. Highest removal capacity was recorded as 690 mg/L.

The removal of malachite green by using activated neem leaf was investigated by ***Kassa (2014).*** It was reported that the adsorption of dye was found to increase with the increase in the adsorbent dosage, but decreased with the increase in the initial concentration of the adsorbate due to presence of active site of the adsorbent at the initial stage of adsorption.

2.4.2 Water hyacinth

The use water hyacinth as alternative inexpensive adsorbent material for sorption for pollutant dye is another scope of study for the environmentalists ***(Mahamadi 2011, Mall et al. 2005).***

The economic value of water hyacinth is low. On the other hand it creats several hazards for aquatic life. Moreover, the accumulation of water hyacinth in the water body obstruct the hydra power generation and water intake project ***(Mamdouh, 2010 and Sanmuga et al. 2014).***

The availability of water hyacinth and its subsequent processing is easy and can be used directly for the adsorption purposes ***(Muntean et al. 2014).*** Metal adsorption by using dried roots of water hyacinth has conducted effectively as reported by ***Shrmeen Afroze (2015).Suresh and Tygi (2016)*** has emphasized upon pre-treatment of water hyacinth biomass prior to use as adsorbent. The efficiency of adsorption using water hyacinth is low as reported by ***Song et al. (2017).***

2.5 Biomass Immobilization

Over the decade, researchers have explored biomass in powdered form ***(Gupta et al. 2015).*** The notion behind this selection was availability of more surface area during adsorption process ***(Fayazi etal. 2015, Ghosh et al. 2015 , Indana et al. 2016).*** But using the powdered form biomass also has some disadvantages specially the chance of mixing of biomass powder with the effluent solution ***(Marisa Punzi et al. 2015).***

It is reported that powder form of biomass also reduce the rate of adsorption and the entire process gets slower ***(Mazhar et al. 2018).***

The different immobilization approach has been explored to produce granular biomass from its powder form for achieving better performance ***(Dogan et al., 2009; Charumathi and Das, 2012).*** Similar observation has also been reported by ***Ozdemir and Baysal (2004)*** during removal of Reactive Red dye.

The granulated biomass prevents chemical degradation by increasing mechanical properties of the adsorbents ***(Wang et al. 2011; Agarry et al. 2012).***
Immobilization technique is helpful for reuse of biomass and make the entire process cost effective ***(Abkenar et al. 2016; Li X. 2019).***

2.5.1 Immobilization Method

The method of capsulation or trapping physically the unrefined biomass is very popular approach in immobilization ***(Patil and Shrivastava 2015; Saeedeh et al. 2013; Rao and Kashifuddin 2016).*** The silica is very common and widely used immobilization agent that used in the industry ***(Saikhom et al. 2013, Sumathi 2015).***
The use of synthetic agent for the process of immobilization has limited use due to their sensitivity towards enzyme cell ***(Ajenifuja et al., 2017, Bidi et al, 2019).*** The use of alginate, a typical polymer, as immobilization agent has become popular day by day due to its diffusion capabilities ***(Betiku et al. 2015, Albihm, 2009).*** Another approach in recent past has explored by mixing biomass with alginate to achieve better result ***(An et al. 2015, Abbas et al. 2018; Awual et al. 2019).***
Immobilization process sometimes blocks the pore spaces and the affects the capacity of the adsorbent ***(Ahmet et al. 2015).*** Moreover, it reduces the kinetic rates of adsorption ***(Naja and Volesky, 2011; Oguz, 2005; Romero-Gonzalez et al., 2005).***
Immobilization of low cost abundant waste material explore for dye adsorption is very cost effective approach as discussed ***(Mall et al. 2005 ; Lan et al. 2014).***

2.6 Mode of operation: Static and Dynamic biosorption

The adsorption operation is conducted by two distinct mode-

1. Static or batch adsorption
2. Dynamic or column adsorption

In batch process the adsorbent –adsorbate are being kept in closed loop while in column adsorption the adsorbate solution passes over the adsorbent in open channel ***(Wang et al. 2018).***

2.6.1 Static or Batch operation

According to ***Tiwari and Singh (2014),*** batch equilibrium adsorption study, a requirement for design of adsorption column was conducted with set of Erlenmeyer flask containing dye solution at different concentrations.

Sharmeen et al. (2016) reported that batch study gives useful information in respect of adsorption phenomenon but this outcome cannot be utilized in column mode due to some limitation for contact time. ***Diwevdi et al. (2008) and Khoshnamvand et al. (2017)*** have narrated ***t***he requirement of dynamic study of adsorption for industrial use based on batch experiment. The study of different isotherm model coupled with kinetic equations have been explored.

In the paper of ***Dubey and Gopal (2007),*** the carbonation of groundnut has been done for exploring as cost effective sorbent for the exclusion of chromium. The removal of metal was recorded as 96.5% at pH 3.0.

In arsenic adsorption using cheaper laterite has been investigated in batch mode ***(Maji et al. 2008).*** The extraction of metal was recorded as more than 98%.

Removal of another heavy metal, Lead was investigated by taking Tamarind seed as low cost adsorbent. The effect of temperature over adsorption has been investigated along with isotherm models ***(Acharya et al. 2009).***

In the paper of ***Batzias (2007), Cazetta Vargas (2008) and Demirbas (2011)*** the usefulness of isotherm studies in adsorption has been narrated.

2.6.2 Thermodynamic Study

Exploration of thermodynamic investigation and determination of its parameters has been observed for adsorption of acetic acid. The activation energy and sticking probability have been investigated. It is reported that process is endothermic **(*Das et al. 2020*).**

The kinetic parameters coupled with thermodynamic tools for adsorption has been explored by ***Ebrahim et al. (2017).***

Ajenifuja (2017) conducted a study to examine the sorption ability of treated and non-treated saw dust onto chrysoidine. Thermodynamic parameters were determined. The influence of other process inputs was also investigated.
Teak leaf as potential sorbent has been explored for the exclusion of Congo red. The thermodynamic parameters have revealed that the process is spontaneous and endothermic ***(Batool et al. 2018).***

2.7 Mode of operation: Column study

Adsorption experiments by and large have conducted in batch mode. This practice is considered as a first phase operation for gathering information for adsorbent efficiency and the solid-liquid interface behavior ***(Ashrafi et al. 2017, Vinodhini and Das 2010).***
Experimental outcomes of batch experiment cannot be shared as first hand information in dynamic mode operation ***(Mallik, 2004).***
The approach of column study for industrial application has been discussed by ***Bidi (2019).*** In column operation the adsorbent solution is passed over the packed adsorbent bed kept in the column generally in downward direction ***(Uddin et al. 2009).***
The simple operational technique associated with time effective approach has proved the superiority of column sorption process ***(Ahemed et al. 2016 and Betiku, 2015).***
The dynamic operation is a better approach in respect of large scale operation due to quick achievement of breakthrough time ***(Rahdar et al. 2019; Patel, 2019).***

2.7.1 Breakthrough Study

The graphical representation of effluent to initial adsorbate concentration with feeding time of adsorbate over adsorbent is noted as breakthrough curve. The important process parameters and uptake value obtained from slope and intercept of s-shaped breakthrough curve ***(Kumar and Bandyopadhyay, 2006; Fkih et al. 2019).***

The study of break through curve for the adsorption process can be obtained either from laboratory observations or from mathematical derivation using conventional dynamic models. These of standard model for determining breakthrough curve is attractive due to its simple application ***(Chen D et al. 2016, Chinenye et al. 2019).*** The exhaustion time indicates the effectiveness of the adsorbent of process ***(Gupta, 2015).***

2.7.2 Column analysis

The determination of column performance is an essential tool in dynamic study. The effluent concentration coupled with initial percentage of adsorbate is a key parameter of this study. The time of exhaustion or saturation time should be considered for designing purpose ***(Volesky, 2011).***

The incorporation of experimental outcomes in the standard model equation as input is known as dynamic modeling. This is very attractive and popular practice for the scientists and environmentalists to study the performance of adsorption ***(Khataee et al. 2011; Kartick et al. 2014).***

The analysis of data from the dynamic study by using conventional models is complex one. The assistance of software in recent years makes the task easier ***(Kok et al. 2016, Okoniewska, 2021).***

The outstanding challenge of removing unsafe natural dyes from effluents has been investigated by ***He et al. (2018).*** In this investigation an exclusive discrete cationic structure was developed using mixed-ligand path way. The Zn metal was formed a metal organic combined structure having one dimensional pathway over gigantic molecular base. The external anionic molecules can effectively and smoothly adsorbed in the pathway. NH_4Cl and ethanol combination has accelerated the process noticeably.

Brion et al. (2018) has investigated Arsenic removal by anion exchange technique using chitosan adsorbent. Column study has been explored and maximum adsorption was recorded as 50 mg/g. Different conventional models for dynamic analysis of column performance has explored. Thomas model has a better agreement of the experiment result.

Adsorption in column operation is dependent on initial dye concentration and inflow rate of the adsorbate dye and also independent of other factors selected in the study. Revival of the exhausted bed can be achieved easily ***(Biswas and Mishra 2015, Canteli et al. 2014).*** Use of montmorillonite for removal of a cationic dye BY-2, the dynamic behavior has been investigated ***(Hassani et al. 2015).***

In the paper of ***Barquilha (2017),*** the biosorption of Nickel and copper has been investigated with free and immobilized biosorbents. It is noted that Calcium alginate matrix increased the maximum uptake of immobilized biosorbents. The column study result showed better performance for biosorption process.

Sharma et al. (2011) has conducted column experiment for exclusion of methylene blue with the help of rice husk as adsorbent. The influence of input variables of physical conditions evaluated and column analysis has been investigated.

2.8 Artificial Neural Networks (ANN) model

An alternative promising evaluation method was recommended in neural network mode for adsorbing methylene blue using Neptune grass as adsorbent material ***(Dang et al. 2017).***

Experiments were conducted by ***Saibaba et al. (2012)*** for judging adsorption efficiency of plant carbon. ANN study evaluated the efficiency of methylene blue exclusion from the experiment.

Sina and Raheleh (2017) has compared the performance between artificial neural networking and imperialist algorithm for UV-ray based stabilization of cationic dye. The correlation of experimental data with computation model suggested better performance of ANN model over imperialist algorithm.

Çoruh et al. (2014) has evaluated the performance of laboratory study by introducing ANN tool. The batch experiment for extracting malachite green using marbel dust as low cost waste has been used. The bias value along with the correct weights of the model operation was achieved by using different training algorithm in the ANN model so developed. The same observation also reported by ***Chinenye and Shahin (2019).***

Lekan (2019) has used ANN model for removing heavy metals by using agricultural waste. A 4-9-1 architecture of the model was developed for the purpose. The accuracy of the model has been proved. The development of 4-5-1 ANN model to compare the experimental performance. Sensitivity analysis has been conducted and influence of pH over the adsorption has been identified in the paper of ***Mohamed Gar Alalm and Mahmoud Nasrb (2018).***

2.8.1 Statistical t test

The adsorption of Zn metal using leaf dust has been investigated. The critical study for getting viability of the experiment has been performed with the statistical tools. The similarities between the experimental outcomes under different operating conditions has been explored. Statistical t-test based on null hypothesis has been noted ***(Kaushal and Singh, 2016).***

At lower pH of the of the adsorbate solution, the chromium adsorption has recorded maximum. The statistical hypothesis based on acceptance or rebuff of null hypothesis has been verified. ANOVA software has been used for the purpose ***(Sarvanen, 2018).***

In the paper of ***Dang and Mai (2017)*** the chi-square test along with t-test has been conducted. The tabular expression showed the good correlation between statistical and laboratory experiment.

Practically, effluent wastewater from the textile and other dye bearing industries has more than one dye. So the treatment of dye mixture by using low cost adsorbents is a challenging task for the environmentalists at present. The use of abundant agricultural waste materials as low cost adsorbents is another approach towards waste minimization. As per as present literature review we observe very *few contributions have so far been made*. Therefore, the adsorptive removal of dye mixture by using abundant agricultural wastes as low cost adsorbents is the principal focus for the present investigation.

Based on the available literatures on adsorptive removal of dye mixture using low cost adsorbents the following gaps are identified:

- In our real life, the wastewater coming out from the textile and other dye related industries contains more than one dye. The treatment of dye mixture is become a critical hazard for the scientists, and very few contributions has been made so far. Therefore, adsorptive removal of mixture of dyes from the effluent is a possible approach for achieving real life solution.
- Replacement of commercially available costly activated carbon by low cost abundant waste has become very popular since last few years which have been studied extensively in our literature review section. The reuse of abundant agricultural wastes as adsorbent would certainly reduce the solid waste loading. It is found that various agricultural waste materials viz. neem leaf, jack fruit leaf, rice husk straw etc. are some of the effective and probable adsorbents for the exclusion of basic dyes from binary culture.
- Use of such abundant agricultural waste materials for adsorptive removal of two common basic dye mixture, MG and MB, will simultaneously minimize the solid waste and dye loading from the environment.

Green Area, Objectives and Scopes of the Research 3

3.1 Green Area of the Research

Based on the available literatures on adsorptive removal of dye mixture using low cost adsorbents the following gaps are identified:

- In our real life, the wastewater coming out from the textile and other dye related industries contains more than one dye. The treatment of dye mixture is become a critical hazard for the scientists, and very few contributions has been made so far. Therefore, adsorptive removal of mixture of dyes from the effluent is a possible approach for achieving real life solution.
- To explore low cost abundant wastes in lieu of commercially available costly activated carbon has become very popular since last few years which have been studied extensively in our literature review section. The reuse of abundant agricultural wastes as adsorbent would certainly reduce the solid waste loading. It is found that various agricultural waste materials viz. neem leaf, jack fruit leaf ash, rice and raw sugarcane bark (bagasse) and rice husk are some of the effective and potential adsorbents to exclude mixture of two basic dyes Mg and MB.
- Use of such abundant agricultural waste materials for adsorptive removal of two widely explored Malachite Green and Methylene Blue in mixture will simultaneously minimize the solid waste and dye loading from the environment.

3.2 Objective

The present investigation has been carried out with the objective *to explore the possible use of the neem leaf ash (NLA), bagasse fly ash (BFA) , jack fruit leaf ash (JFLA), and rice husk ash (RHA) as alternative adsorbents for removal by exploring* *adsorption of two widely used cationic dyes Malachite Green (MG) and Methylene Blue (MB) from their aqueous solution i.e. simulated or synthetic wastewater in binary system.*

3.3 Scopes of the Study

The scopes of the present work considered for achieving the stated objective are given below:

- To conduct ***batch and fixed bed column study*** utilizing *neem leaf ash, jack fruit leaf ash, bagasse fly ash* and *rice husk ash* as alternative adsorbents to exclude MB and MG from mixed solution by adsorption technique.
- To explore into the effect of process factors like as ***sorbent dosages, initial concentrations of dye mixture, shaker speed, contact time*** and ***pH*** over adsorption process for the **batch study**.
- To investigate into the effect of process inputs i.e. the ***initial pH of the adsorbate solution, flow rate, influent concentration*** and ***adsorbent bed height*** for the column study.
- To undertake ***isotherm studies*** viz. ***Langmuir, Freundlich*** and ***Temkin models*** under batch mode operation for determining the **best fit isotherm model.**
- To conduct ***statistical analysis based on five different error functions due to error generation from linearization*** of non linear regression and also to detect the best fits model for the experimental data at equilibrium.
- To conduct ***chi-square (X^2) analysis*** for evaluating the accuracy of **isotherm model in adsorption study**.
- **Pseudo-first-order** and **pseudo-second-order equations to explore kinetic study. Determination of** solute uptake rate coupled with residence time also to be evaluated.
- To envisage the performance of the experiment and use the conventional dynamic model such as **Thomas model, Adams-Bohart model, BDST**

model and Yoon-Nelson model and **BDST model** for similar other study without conducting experimental run.

- To develop artificial neural network model to check the accuracy for the laboratory experiment and also to reduce the experimental run for making time and cost effective study.
- To perform statistical t-test to check the similarities between the two data sets artificial neural network (ANN) data and experimental outcomes.

Research Methodology

4

4.1 General

The study of adsorption isotherm coupled with kinetic model in dye removal problem of a multi-component systems has been explored in the present work using four different low-cost adsorbents in batch study and compare different kinetic models in dynamic mode (column study) taking same adsorbents.

4.2 Principle

Adsorption on most of the adsorbents including agricultural byproducts governs by the physical forces. Though there is some exception particularly for chemisorptions. Vander Waals force is one of the important force lies behind this group. Other than this force dipolar attraction and hydrogen bonding are also acting on this area ***(S.G. Mutean et al. 2009).*** The influence of such forces, particularly for the low cost , non-treated adsorbent substances are very important for the betterment of the performance of the process. The growing popularity of using inexpensive abundant wastes mainly depends upon this dipolar attraction. The interaction between adsorbent and adsorbate interface or the surface morphology of the adsorbent are important factors influencing the adsorption performance. The study of different influencing physical inputs are the subject of interest of any research related to this field.

4.3 Materials used for experiment

In the present work, the four low cost waste materials viz. neem leaf, jack fruit leaf, bagasse and rice husk were used for removing dye mixture under batch and column study in the laboratory.

4.3.1 Low cost adsorbents

- **Neem leaf ash (NLA) & Jack fruit leaf ash (JFLA)**

The raw leaves of neem and jack fruit procured from the Jadavpur University campus. The collected leaves were washed in the plain tap water and distilled water twice. After natural drying it has been dried in the woven around for 8 hours. Carbonation of the dried leaves have been achieved by placing it in muffle furnace at 600^0C for 1 hr. The produced ash, was sieved through 300 µm sieve and the portion retained was preserved for the experiment.

- **Bagasse fly ash**

Raw sugarcane stalks were procured from the area adjacent to Jadavpur University. The raw stalks were washed with the normal water in the laboratory, dried under sunlight, undersized and these pieces stalks then placed in furnace at 600^0C for a duration of 1 hr. for carbonation. Bagasse fly ash was sieving through 300 µm sieve and the portion retained was preserved for the experiment.

- **Rice Husk Ash (RHA)**

The adsorbent RHA was collected in the form of rice husk, a waste material from the local agricultural field near North 24 parganas, West Bengal. Rice Husk was taken into the muffle furnace at 480^0C for 1 hr. after conducting same operation like other three adsorbent materials.

The rice husk and all other materials, so selected for adsorption, were analyzed by SEM.

4.3.2 Adsorbate

In the present study the two basic dyes Methylthioninium Chloride (MB) and Aniline green (MG) were considered with the pH of the mixed dye solution varying in the range of (7.0 - 7.2).

Table- 4.1: Chemical formulae: MB and MG

Parameters	MB	MG
Colour Index Constitution Number	52015	42×10^3
Colour Index	Basic Blue- 9	Basic Green- 4
Molecular Formula	$C_{16}H_{18}N_3SCl$	$C_{22}H_{25}N_2Cl$
Molar mass	319.85	364.91
λ (nm)	664.1	617.3

4.3.3 Chemical used

- ✓ pH buffer
- ✓ nitric acid
- ✓ sulphuric acid
- ✓ acetone

4.3.4 Instruments for the experiment

The following equipments were utilized in present study:

- Electronic Balance
- Digital visible Spectrophotometer (Systronics Model 166)
- Digital pH meter (Electronic India Make, Model 101E)
- Hot air Oven
- Shaker Apparatus for Batch Study
- Column made up of acrylic (internal dia. 1.5 cm, height 50 cm)
- Peristaltic pump
- Centrifuge machine.

Other materials

- Borosil glassware-before commencement of experiment all glassware has been cleaned with nitric acid and distilled water
- 50 mL test tube
- Filter paper (Whatman-40, Ashless).

4.4 Experimental Method

Laboratory experiment was conducted at neutral pH (pH 7.0) i.e. the pH of the distilled water) unless otherwise mentioned. Distilled water was used for this purpose. Inflow rate was kept constant at 7.5mL/min except some special cases viz. during pH and inflow rate variation study.

4.4.1 Preparation of Stock Solution and Standard Curve

Stock solution of 100 mg/L is prepared for the two basic dyes Methylthioninium Chloride (MB) and aniline green (MG) taking in ratio 1:1 by weight (50 mg each) in 1000 mL distilled water followed by preparation of 10 mg/L of working solution. From this working solution 0, 4, 8, 12, 16 and 20 mg/L solution is prepared and the absorbance is measured at a wavelength 619.9 nm against blank distilled water. The best fit linear equation is obtained for the mixed dye solution as Y = 0.1014X, where Y = fractional absorbance and X = concentration (mg/L) with R^2=0.9978.

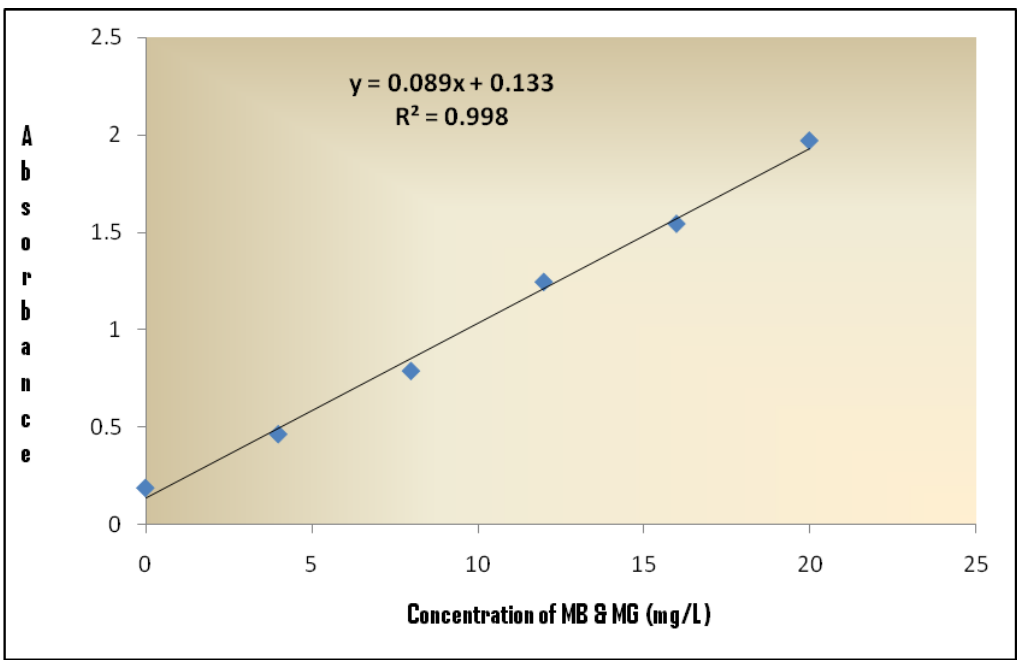

Fig. 4.1: Standard curve for dye mixture of MB and MG

Some of the photographs of experimental works are given below:

Fig.4.2: Muffle furnace for carbonization of adsorbents

Fig.4.3: Sieving of burnt adsorbent materials with 300 µm sieve

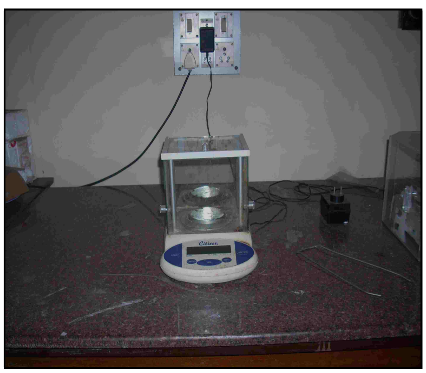

Fig. 4.4: Weighing Balance

Fig. 4.5: Spectrophotometer for measuring dye concentration

4.5 Experimental procedure

As per the objective of the study the experimental work is done separately in batch and column mode.

4.5.1 Batch Mode Operation

In batch study, series of 200mL of solution having known mixed dye concentration, pH and known adsorbent dosages were taken in a 250 mL stopped conical bottle. Speed of the shaker was 120 rpm unless otherwise mentioned. Different parameters like pH, shaker revolution, adsorbent dosage and shaking time (contact time) were varied as and when necessary to study the parametric effect over adsorption process. The fixed adsorbent dosages were maintained at 4.0, 2.0, 5.0 and 4.0 gm/L for the adsorbents NLA, JFLA, BFA and for RHA respectively. The sampling frequency was selected as 10 minutes. Sample dye concentration in effluent were measured from the supernatant in spectrophotometer after centrifuging at an rpm of 500. The removal of dyes and uptake q_e (mg/gm) can be worked out from the following relations:

$$\% \text{ removal} = 100 \times \frac{C_0 - C_e}{C_0}$$

$$Amountadsorbed q_e = (C_0 - C_e)V/w$$

where, C_0 = initial conc. for dyes in mg/L

C_e = equilibrium concentration in mg/L

V = adsorbate volume(L)

W = adsorbent weight (gm)

4.5.1.2 Effect of different process parameters

The influence of physical variables as input factors for batch adsorption like dose, concentration, pH, contact time and speed of the shaker has been investigated.

(a) Adsorbent dosages

200 mL dye mixture having concentration 25 mg/L at neutral pH was taken into 15 numbers of 250 mL plastic bottles. Different adsorbent dosages were varied from 0.1 to 12 gm/L and were poured into those bottles and reinstalled in the shaker for shaking at a constant speed and time duration for the respective adsorbents as discussed in the 'Results and Discussion' chapter. The samples were

taken out, centrifuged and concentrations were measured in the spectrophotometer.

(b) Initial concentrations

Dye mixtures each having 200 mL volume with varied early concentration of 25, 50, 75 and 100 mg/L were taken with fixed adsorbent dosages and neutral pH into the shaker. The shaker speed and shaking time were kept fixed for the respective four low cost adsorbents as discussed in the 'Results and Discussion' chapter. The samples were taken out after fixed shaking time and analyzed at spectrophotometer.

(c) Contact time

200 mL dye mixture having concentration of 25 mg/L has been poured in 250 mL plastic bottle along with respective optimum dosages as discussed in the 'Results and Discussion' chapter and was kept inside the shaker for shaking at an optimum speed for 3 hrs. Sampling frequency was fixed as 10 minutes. The samples centrifuged, and analyzed in the spectrophotometer to measure the dye concentration.

(d) **Shaker speed**

200 mL dye mixture having concentration of 25 mg/L has taken with fixed adsorbent dosages and neutral pH into the shaker as discussed in the 'Result and Discussion' chapter. The shaker speed was varied from 30 to 130 rpm. The samples centrifuged, and analyzed in the spectrophotometer to measure the dye concentration.

(e) pH of the initial dye solution

200 mL dye mixture having concentration of 25 mg/L has been poured in 250 mL plastic bottles with four different adsorbents at their respective optimum dosages as discussed in 'Results and Discussion' chapter and was kept inside the shaker for shaking at an optimum speed and time. The pH of mixed dye solution was varied

4.1 to 9.2 using pH capsules. Centrifuging samples and subsequent analysis in the spectrophotometer, measuring the effluent dye concentration, has been performed.

4.5.2. Column Study

Continuous flow adsorption experiment was carried out in column made of acrylic, having1.5 cm and 50 cm, internal diameter and tall respectively. The dye mixture was send downward direction into the column. Peristaltic pump was explored to control rate of flow. Adsorbent was packed into the column and was supported by glass wool, bids from top and bottom. Samples of dye solution were collected from the column exit. Sampling time was 10 minutes. Analysis in spectrophotometer keeping absorbance wavelength at maximum of619.9nm. Operation of the Column was closed at C_t/C_0 exceeding 99.5%.

The experimental methods adopted for the column study collected from the various literatures are given below.

Table 4.2: Experimental methods adopted for column study

Effect of system	**Initial conc.** (milligram/Liter)	**Adsorbent Height (centimeter)**	**Inflow rate** (milliliter/minute)	**pH**
Effect of initial conc.	25, 50, 75, 100	4,6,8	7.5	7
Effect of bed height	25, 50, 75, 100	4,6,8	7.5	7
Effect of flow rate	100	8	5, 7.5, 10	7
Effect of pH	100	8	7.5	4.1, 7, 9.2

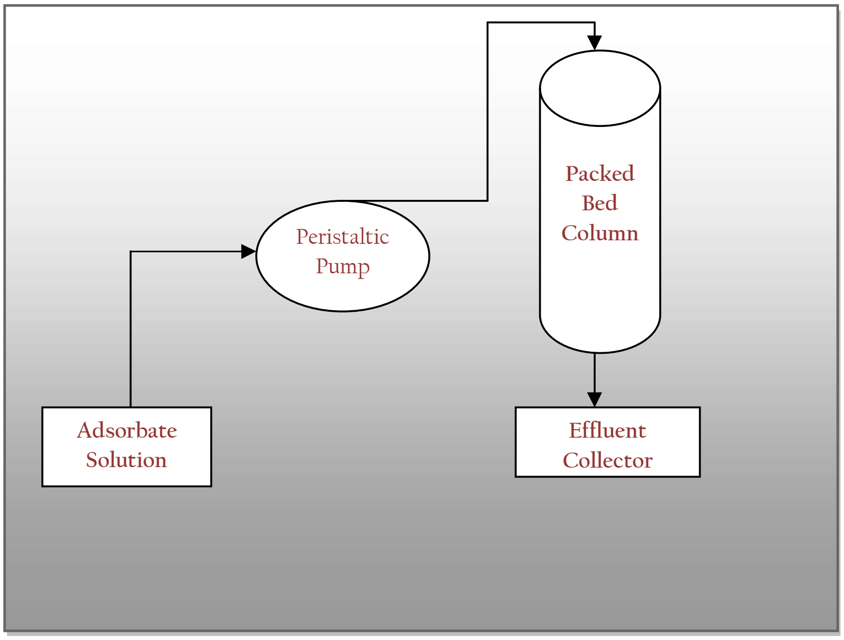

Fig.-4.6: Schematic diagram of column mode operation

Fig. 4.7: Batch reactor conducting batch study

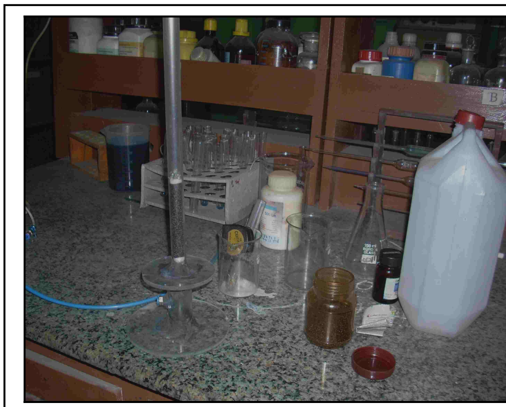

Fig. 4.8: Performing column study using peristaltic pump and column

4.5.2.1 Effect of different process parameters

Adsorbent height, concentrations of dye mixture, inflow rate and pH of the mixed dye solution have been considered as input parameters for the present investigation. The influence of the input factors has been evaluated from the time versus percentage dye removal graph as discussed in the 'Results and Discussion' chapter.

(a) Adsorbent height

The influence of sorbent height over sorption under column mode operation was investigated under fixed bed height and flow rate. It was kept as 4cm and 7.5 mL/min respectively at neutral pH. Initial concentration of mixed dye was taken from 25 to 100 mg/L as depicted in Table-4.1. The effluent concentration of dye mixture was analyzed in the spectrophotometer. Similar studies were undertaken for other adsorbent bed heights of 6 and 8 cm.

(b) Concentration of dye solution

In column mode operation, concentration effect was investigated under fixed mixed-dye concentration and flow rate. It was kept as 25 mg/L, and 7.5 mL/min respectively at neutral pH. The mixed dye solution was poured at fixed flow rate of 7mL/min in the downward direction. Sampling time was 10 minutes and samples were analyzed in the spectrophotometer to measure the concentration of the effluent solution. Similar studies were conducted with 50, 75 and 100 mg/L dye concentrations of in the similar fashion.

(c) Inflow rate of adsorbate

Effect of inflow rate over adsorption under column mode operation was investigated under fixed bed depth and initial concentration. Depth of adsorbent and concentration were taken as 4 cm and 100 mg/L respectively at neutral pH. The inflow rate was varied from 5.0 to 10 mL/min, illustrated in the Table-4.1. The effluent mixture concentration was analyzed in the spectrophotometer.

(d) pH of dye mixture

Effect of adsorbate pH has been reviewed under fixed bed height of 4 cm and concentration 100 mg/L. Initial pH of the adsorbate varied from 4.1 to 9.2 by using pH buffer. Inflow rate from 5 to 10 mL/min has been selected. Effluent concentration of dye mixture was analyzed in the spectrophotometer

4.6 Thermodynamic Study

Thermodynamic study is the measure of temperature effect upon adsorption. The equilibrium adsorption of dyes using non-expensive four wastes as adsorbent was conducted. The adsorption data at equilibrium has been utilized to determine dye uptake using Langmuir, Freundlich and Temkin isotherm model. Kinetic constants and feasibility studies were synthesized with facilitating of pseudo-first-order and pseudo-second-order model.

50 ml volume of mixture of two basic dyes MB and MG (equal proportion by weight) with concentrations varying from 25 to 150 mg/L was poured into 150 mL flasks. The optimum dosages of adsorbent as discussed in the 'Results and Discussion' chapter for the respective adsorbent were taken. The adsorbate solution were shaken at respective optimum speed and time in the water bath 290, 295, 300, 305 and 310 K temperature respectively. After shaking, the mixture of two dyes was analyzed by centrifugation supernatant solution in the spectrophotometer in the laboratory at a wavelength $\lambda = 619.9$ nm.
The different thermodynamic inputs such as Gibb's free energy (ΔG^0), enthalpy change (ΔH^0), entropy change (ΔS^0) have been obtained from this study. Sticking probability (S^*) and activation energy (E_a) can also be calculated. All these thermodynamic parameters help us understand the adsorption mechanism and adsorption study as a whole taking cost effective adsorbents.

4.7 Scanning Electron Microscope (SEM) Analysis

SEM study was conducted (Model: Nova Nano SEM 450 Make: FET Ltd) to understand the surface morphology and characterization of the four low cost adsorbents before and after adsorption of the dye mixture. Photographs of surface morphology in scanning machine at desired magnification has been taken in the laboratory. Acceleration voltage in the range of 5-20 KV at different magnification using image detector was performed ***(Das et al. 2020).*** This part of the study was performed in Bose Institute (Rajabazar) and Indian Institute of Cultivation of Science Jadavpur.

4.8 ANN Software

ANN study by using Mat lab (version 2009a) software has been explored in the present investigation. The training, testing and subsequent processing to validate the input was done.

The present ANN model can be classified into three components. Each such part is termed as layers. They are input, hidden and output layers. The variation of physical factors such as contact time, adsorbent dosage, pH, concentration etc. have been utilized as input data for the input layer. The outcome or objective of the study was determine or predicting removal percentage of adsorbate and accordingly the only one output data has been obtained from the output layer.

The training algorithm was adopted as Levenberg-Marquardt for the present wok. The weighted value in the training process within neurons have been applied to subside the differences between actual and predicted value. The objective of the training is to minimized the error between these two and subsequently after completion of the training process another set of data has been utilized for testing purposes. After successful execution of testing, the model can be used for predicting the output value.

The neurons in hidden coupled with other layers has been evaluated by setting learning rate within the domain of specific training goal.

In the present study the development of ANN model has been executed by testing data set by several iteration techniques with alteration of network weights.

4.9 Statistical t-test

Statistical t-test has been employed for comparing the means of two sets of data. A comparative study was conducted between the ANN simulated outcomes and the experimental results. As for both the datasets considered for the present research population is same, a paired t test was conducted. The statistical software named Stata-10 was used for this purpose. The determination of level of confidence or significance of the ANN modeling with reference to the experiment work is very important for this present study. The software output gives important information about the standard deviation(s), standard error(s), p value and t score under 95% confidence level and under certain degrees of freedom. The variations of different process parameters under batch and column study of all four low cost adsorbents were considered.

Theoretical Consideration 5

5.1 General

The utilization of synthetic dyes over other groups, in the textile and other dye bearing industries increases day by day due to its availability and cost aspect. Textile industry consumes considerable volume of water and also uses different types of synthetic dyes to colour their products. These pollutants are tricky to remove due to their composite aromatic structure and synthetic base ***(Ahmet et al. 2016).*** The uses of dyes are likely more than 100,000 over the world annually. Most of them are identified to be toxic and carcinogenic ***(Crini and Badot, 2008).***
Treatment of dye bearing wastewater is becoming a mandatory protocol of the industry house due to recent introduction of stringent regulations ***(Kant, 2012).*** In this aspect cost effective and eco-friendly approach towards dye emission has become the bird's eye of the researchers ***(Muntean et al. 2014).*** The different methods of dye removal are being explored by the scientists over the years. It is established fact that dye removal is dependent upon its type. Some of the popular approaches are adsorption, coagulation, ozonization etc. In spite of ample varieties of removal techniques, adsorption has proved its superiority over others. One of the basic reason behind this is its simple design approach nd operational technique. ***(Mittal et al. 2009).***

Granulated activated carbon, available in the market is considered to be most potential adsorbent. But at the same time it is very costly. Therefore to make the adsorption cost effective, replacement by inexpensive abundant wastes is become very popular in recent time. The adsorption process for single component system has practised widely in recent time. However, the investigation on adsorption of mixed dyes is uncommon ***(Ponda et al. 2017).*** Present investigation was explored to address the feasibility of adsorption of multiple dyes using four different low-cost adsorbents viz. neem leaf, jack fruit leaf, bagasse and rice husk in ash form in batch mode and compare different kinetic models in dynamic mode (column study).

5.2 Adsorption

The building up of solids over the surface or inner pores of another solid in two phase system under certain forces of attraction is generally refers to adsorption. The physical or chemical forces of attraction is responsible for this phenomenon.

Depending upon the character of force, the adsorption mechanism is divided in to the followings:

i) Physical process for adsorption

ii) Chemical process for adsorption

In the event of physical adsorption involvement of Van der Walls force, bonding strength of molecular hydrogen together with dipolar forces are very important. On the other side, chemical adsorption process is basically developed by molecular or ionic strength in between the solid interface ***(Saeedeh et al. 2013).***

The surface morphology or the characteristics of porous nature of the adsorbent associated with physical factors like temperature, concentration, pH of the two phase system influences the efficiency of the whole adsorption process ***(Gupta and Majumder, 2017).***

5.2.1 pH and adsorption

The adsorption is pH reliant. pH of adsorbate solution renders favourable adsorption environment depending upon the surface property of the adsorbent. The adsorbate solution pH is influenced by the cationic or anionic dye present within the system **(*Naimabadi et al. 2009*).**

An important factor 'zero charge' of the adsorbent influences the adsorption rate. This is obvious for agricultural wastes when used as adsorbent in adsorption study. It is reported that favourable adsorption is achieved in basic dyes if given pH is more than that pH at zero charge and for the acid dyes it is just opposite.

5.2.2 Initial concentration and adsorption

The adsorption is concentration dependent. Initial concentration is an indirect measure of the presence of active sites of the adsorbent exposed towards adsorbate ***(Dina and Scholz, 2018).***

The concentration of adsorbate at early stage, generates huge mass transfer resulting capacity development of the adsorbent favouarable for adsorption and simultaneously percentage exclusion of dye decreases.

5.2.3 Temperature and adsorption

Temperature can influence the adsorption capacity. Adsorption of dye from the adsorbate solution is directly proportional to rise in temperature of the system ***(Alhujaily et al. 2012).*** Endothermic process is a good example of temperature dependency of the adsorption. The increased energy is directly augment the potential sites of the adsorbent because of temperature increment. That is why, adsorption is temperature reliant.

5.2.4 Adsorbent optimum dosage and adsorption

Selection of proper dosage for the adsorbent is definitely is an important factor as per efficiency of the system is concerned. Dosages of adsorbent gives a primary information in respect of minimum amount of dye adsorption. It influence the capacity of adsorption by accumulation of porous area of the adsorbents. The increased dose of the adsorbent refers to accessibility of more porous sites for adsorption ***(Kok et al. 2020).*** Solution of mixed dyes (100 ml) and 12 mg of each adsorbent were thoroughly mixed in 250 ml Erlenmeyer flasks prior to storage for 24 h. The solutions were shaken for 3 h at 135 rpm in an orbital rotary shaker followed by filtering with Whatman no. 1 membrane filter (retention 11 µm) prior to measurement in the spectro photometer. The percentage removal of MB from aqueous solution was calculated. The most effective adsorbent or optimum dose was selected based on the removal efficiency of dyes in binary system.

5.3 Equilibrium study

Adsorption isotherm are significant issue for the study of adsorption mechanism. It can measure the interaction between adsorbent adsorbate at their interface ***(Batool et al. 2018).*** The theoretical study for the empirical formula to predict the adsorption behavior is important. Equilibrium study helps to determine the dye uptake at equilibrium based on certain assumption in respect of adsorbent, adsorbate nature ***(Stephen, 2018).***

5.3.1 Langmuir isotherm

This model speaks about single layer adsorption for the solute, present over the surface of adsorbent, under specific boundary condition, of the entire system. The static nature of adsorbate molecules and unaltered system temperature are the other important issues of this study ***(Langmuir, 1916).***

Expression of this model in single system is :

$$q_e = \frac{q_m k_L C_e}{1 + K_L C_e} ------(5.1)$$

The form of this equation for binary system can be expressed as:

$$q_i = \frac{q_{maxi} b_i C_{ei}}{1 + \sum_{i=1}^{n} b_i C_{ei}} ---------(5.2)$$

q_m = model constant expressing max adsorption capacity

K_L = model constant, represents energy distribution

These constants K_L and q_m derive from slope and intercept from equation (5.2)

5.3.2 Freundlich isotherm

Freundlich equation deals with the inconsistent enthalpy distribution over the uniform surface of the adsorbent ***(Yang et al., 2011).*** The empirical relation between the excluded solid from the adsorbate with the adsorbent holds good by this isotherm equation. The heterogeneous nature of active site is important submission of this model. The dye uptake can be mathematically expressed by this equation ***(Freundlich, 1906).***

Mathematically, it is expressed as

$$q_e = K_f C_e^{1/n} \text{------------------------------ (5.3)}$$

Taking log in the both sides,

$$\log q_e = \log K_f + \frac{1}{n} \log C_e \text{ --------- (5.4)}$$

K_f = equation constant refers to capacity of adsorption

1/n = another equation constant refers to concentration effect indicator

The correlation coefficient of the model can be obtained from the plot which can be drawn from the equation under reference (5.4).

This model rejects the single layer adsorption phenomenon.

5.3.3 Temkin isotherm

The consideration of phase interaction between adsorbate and adsorbent is the principal focus of this isotherm equation. The heat evolves in the process of adsorption reduces directly in connection with coverage. It deals with the single layer adsorption of adsorbate molecules onto the adsorbent ***(Temkin and Pyzhev, 1940).*** Under the equilibrium situation, concentration (C_e) and adsorbed quantity(q_e) the linear form of binding energy is the basic consideration for formulation of interaction formula of this isotherm models.

Mathematical expression for this model is given by,

$$q_e = \left[\frac{RT}{b_1} \log(K_T C_e)\right] \text{ ----------- (5.5)}$$

Linearization of the equation (5.5) is given by,

$$q_e = \frac{RT}{b_1} \log K_T + \frac{RT}{b_1} \log C_e \text{ -------- (5.6)}$$

where, R = universal gas constant (8.314 J/mol/K)

and T = absolute temperature (in K).

Isotherm constants (b_1 and K_T) value can be find out using equation (5.6).

5.4 Statistical Analysis

The linearization of the isotherm equation generates approximation error ***(Batool et al. 2018).*** The innate biasness towards this approximation can be determined by using five different functions deal with error analysis. Moreover, the relative accuracy of the isotherm model, describing the experimental study, by this process of approximate analysis can be determined with this tool.

Another important hypothetical tool for determining the best accurate model in respect of laboratory experiment is chi-square (X^2) test. Evaluation of noteworthy effects on process parameters upon dye elimination from the aqueous solution, chi-square test plays an important role.

5.4.1 Error Analysis

5.4.1.1 Summation of squares error (SSE)

This is commonly used error equation. Accuracy of the equation is maintained well at a upper end of the phase attention. The amount of error is directly proportional to adsorbate concentration.

$$\sum_{i=1}^{n}(q_{e\ cal}-q_{e\ meas})_i^2 \text{---------}(5.7)$$

5.4.1.2 Summation of absolute errors (SAE)

This approximation analysis by this equation yields better result as it has a better correlation of data at higher concentration.

$$\sum_{i=1}^{n}\left|\frac{(q_{e\ meas}-q_{e\ cal})}{q_{e\ meas}}\right|_i \text{--------}(5.8)$$

5.4.1.3 Average relative error (ARE)

This error equation covers the entire range of adsorbate concentration.

$$\frac{100}{n}\sum_{i=1}^{n}\left|\frac{(q_{e\ meas}-q_{e\ cal})}{q_{e\ meas}}\right|_i ------ (5.9)$$

5.4.1.4 Hybridization fraction error function (HYBRID)

This is the complementary error equation of SSE at lower concentration. The introduction of this equation due to the existing limitation at lower concentration of SSE can be achieved by dividing the difference by its measured value.

$$\frac{100}{n-p}\sum_{i=1}^{n}\left[\frac{(q_{e\ meas}-q_{e\ cal})}{q_{e\ meas}}\right]_i ------(5.10)$$

5.4.1.5 Marquardt's percent standard deviation (MPSD)

This error equation derives geometric mean error by considering degrees of freedom of the system of equations.

$$100\sqrt{\frac{1}{n-p}\sum_{i=1}^{n}\left\{\frac{(q_{e\ meas}-q_{e\ cal})}{q_{e\ meas}}\right\}_i^2} ------(5.11)$$

5.5 Selection of best isotherm model

Isotherm parameters are derived from each error function. So the correlation between a particular parameter over the different error analysis is quite difficult ***(K. Chowdhury et al. 2009).*** The normalization of approximation value can have a solution of this problem. Normalization is done by reducing the error value by the number of observations. By this process, the optimization of an isotherm model in consideration of describing experimental run can be achieved.

5.6 Kinetic Study

The study of reaction kinetics in the process of adsorption in an important tool to determine the operating condition of batch experiment. Kinetic study is developed on the concept of diffusion control. The solute uptake rate depends on the mass transfer within system and that can be achieved by solute residence over the surface of the adsorbents ***(Fkih et al. 2020).*** For designing the adsorption system, this rate is most important and can be evaluated from the kinetic study. Thus, by using different kinetic models the kinetics of anionic and cationic dyes onto various adsorbents can be analyzed very effectively.

5.6.1 Lagergren pseudo-first-order model

Pseudo-first-order equation describes reaction kinetics of any adsorption process ***(Oguz, 2005).***

The differential form of kinetics equation is given as:

$$\frac{\partial q_t}{\partial t} = K_1(q_e - q_t) ---------- (5.12)$$

where, q_e and q_t (in mg.g $^{-1}$) are amounts of dye molecules of two basic dyes adsorbed at equilibrium condition for any arbitrary time t, and K_1 is rate constant (min^{-1}).

Integrating considering initial condition q_y and t as zero, it generates

$$\log\left[\frac{q_e}{q_e - q_t}\right] = \frac{K_1}{2.303}t ---------- (5.13)$$

This can be written as :

$$\log(q_e - q_t) = \log q_e - \frac{K_1}{2.303}t ---- (5.14)$$

The slopes and intercepts of plots of log (q_e-q_t) versus t gives the unknown parameters K_1 and q_e of the equation kinetic which can be compared with the experimental outcomes.

5.6.2 Lagergren pseudo-second-order model

Pseudo-second-order equation describes reaction kinetics of any adsorption process ***(Batool et al. 2018).***

The differential equation is generally known and described as:

$$\frac{dq}{dt} = k_2(q_e - q_t)^2 \text{ ----------------------- } (5.15)$$

Here, k_2 is rate constant obtained from second order reaction kinetics of adsorption. Unit is min^{-1}.

Integration of the equation 5.15, we have

$$\frac{t}{q_t} = \frac{1}{k_2 q_e^2} + \frac{1}{q_e} t \text{ ---------------------------- } (5.16)$$

The rate constant can be evaluated using following equation 5.17 as

$$h = k_2 q_e^2 \text{ -------------------------- ----- } (5.17)$$

Plot t/q_t versus t evaluates reaction constant and dye uptake value from the slope and intercept respectively.

The intercept and slope of the plot of t/q_t versus t according to the equation (5.16) is referred accordingly.

5.7 Thermodynamic study

The communication between organic solute and porous solid in the form of adsorbent can be understood through the process of adsorption under present study. For better perceptive, various information regarding mechanism of the process is necessary. This can be resulting from the thermodynamic study for the adsorption process. This study is very much supportive to predict the adsorbent properties and also to know the heat requirements for the adsorbent process ***(Stephen, 2018).***

Thermodynamic study provides a practical tool to estimate the states of the adsorbent and solution. Thermodynamic inputs such as entropy, enthalpy , free energy etc. are to be calculated for describing the adsorption study ***(Wang et al. 2018).***

Thermodynamic parameters pertinent for the adsorption process viz. Gibb's free energy (ΔG^0), change in enthalpy (ΔH^0) and change in entropy (ΔS^0) are calculated using following equations:

$$\Delta G^0 = -RT \ln K_L \quad \text{---------------------------------} \quad (5.18)$$

$$\Delta G^0 = \Delta H^0 - T\Delta S^0 \quad \text{---------------------------------} \quad (5.19)$$

Where, R = universal gas constant (8.314 $Jmol^{-1}K^{-1}$)

T = absolute temperature (K).

Gibb's free energy (ΔG^0) can be determined from the Langmuir isotherm constant K_L .A plot of Gibb's free energy (ΔG^0) versus temperature T generates the enthalpy change (ΔH^0) and the entropy change (ΔS^0) as the intercept and slope respectively of the equation (19).

The activation energy (E_a) and sticking probability (S^*) can be derived from the experimental data using Arrehenius equation. Surface coverage (θ) is important factor in this aspect ***(Kok et al. 2016).***

$$\theta = \left[1 - \frac{C_e}{C_0}\right]$$

where, C_e and C_0 are the concentrations at equilibrium and initial stage of the experiment.

The theoretical relation between activation energy and sticking probability can be established by,

$$\ln(1-\theta) = \ln S^* + {E_a}/{RT} \quad \text{------------------} \quad (5.20).$$

The value of E_a and S^* was find out from the slope and intercept of the plot ln(1-θ) versus reciprocal of absolute temperature (1/T) respectively as given in the equation (5.20).

Some important inference can be drawn from the thermodynamic parameters derived by using above equations and plot. The negative value for Gibb's free energy refers the feasibility and spontaneity adsorption process. This is characterized by high activation energy. This coupled with the magnitude of the enthalpy change indicates whether the adsorption process is physi-sorption or chemisorption. The lesser value for the sticking probability refers a feasible adsorption process ***(Ebrahim et al. 2017).***

5.8 Breakthrough curve (BTC) and mass transfer zone (MTZ)

The breakthrough curve, its shape and break point is noteworthy for designing dynamic study. This curve is S- shaped, the time-resolved effluent concentration of the adsorptive under investigation. The feasibility for a practical use, study of BTC is very important consideration. The plot between exit to initial concentration versus lapse time throughout for a given column bed height is known as breakthrough curve (BTC) ***(Sarvanen et al. 2018).*** The performance of dynamic study is BTC dependent. The exhaustion time in the BTC is influenced by the concentration, flow, pH and several other factors like adsorbent height, shape of the column etc. Hence, the time-concentration outlining from the BTC is very important mapping for successful application of dynamic column ***(Kartick et al. 2014).***

BTC is usually depicted by plotting $C_{effluent}(C_t)$ /$C_{influent}(C_0)$ versus service time (t) for a fixed height of adsorbent. The area above the BTC (Fig.5.1) is proportional to the amount of sorbent adsorbed in the column where as the area below the curve is proportional the amount of sorbent goes out of the column. So the column capacity means the area above the BTC as depicted in the fig. below.

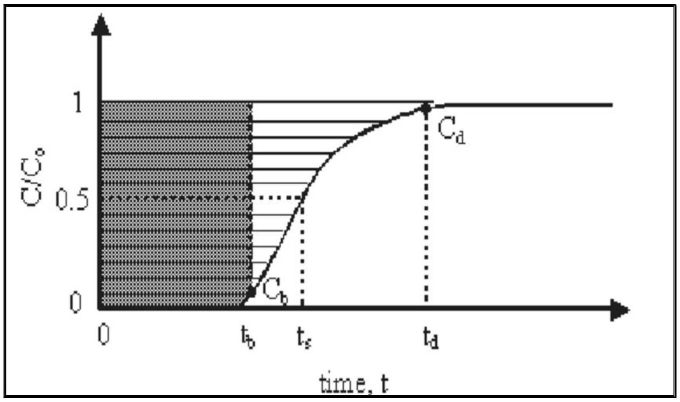

Fig. 5.1: Breakthrough Curve

A capacity of adsorption up to its full strength has been depicted above in the Fig. 5.1. Lower Concentration value at breakthrough has marked as C_b in the figure above. The concentration at any point of time C_t has reached almost 100% of its initial value (C_0) refers to full exhaustion of adsorbent bed. The area represented in the curve the adsorbed quantity of solutes under dynamic approach.

The derivation of column parameters are the function of time-concentration outline (***Indana et al. 2016***).

The mathematical submission for the performance study is given as

$$t_t = \int_{t=0}^{t=\infty} \left(1 - \frac{C_t}{C_0}\right) dt = A_1 + A_2 ------- (5.21)$$

Time equivalent to usable capacity is

$$t_u = \int_{t=0}^{t_b} \left(1 - \frac{C_t}{C_0}\right) dt = A_1 ----------- (5.22)$$

Actually, t_b represents the break through time corresponding to practical utilization of adsorbent which is nearly equal to usable time and given as

$$t_u = t_b$$

Mass transfer zone (MTZ) starts from the point of occurrence of adsorption in the column. It is influenced by the several characteristics of adsorbent and adsorbate solution. The porous nature of adsorbent along with character of solute in the solution under acidic or basic environment are some of the key features which influence the mass transfer phenomenon ***(Mahmoodi and Soltani-Gordefaramarzi, 2016).***

The relation between mass transfer zone with the idle bed for adsorbent can be given as ***(Shah et al. 2015):***

$$H_{UNB} = (1 - t_u/t_t)H_T = (1 - t_b/t_t)H_T \text{ ------------------------ (5.23)}$$

Where H_T is total bed height (cm),

H_{UNB} = Mass Transfer Zone --- (5.24)

The effective bed height H_B can be calculated as:

$$H_B = \left({t_b}/{t_t}\right) H_T$$

The gross volume of effluent collected at the end of study is important for BTC ***(Vital 2016).***

Mathematically, $V_{eff} = Q.\ t_{total}$ -------------------------------------- (5.25)

Here, Q = the volumetric rate (mL/min)

and t_{total} = total time for adsorbate flow (min).

Adsorbed dye (Q_{total}) during the process can be balanced with concentration of adsorbed dye with the flow rate within the boundary as explained in the Fig. 5.1 ***(Istratie et al. 2015).***

The total removal (%) of two mixed dyes can be calculated from the following equation

$$\% \text{ Removal} = (q_{total}/m_{total}) \text{ x100. ----------------- (5.26)}$$

5.9 Model study

The performance and application feasibility study of a column depends upon its perfect design ***(Heli et al. 2015).*** Conventional mathematical expression to envisage the dynamic performance of column bed has been developed and explored by the researchers ***(Thakur and Chauhan, 2016).*** In most occasions, kinetic study for column adsorption performances have been tested. Thomas, Adams-Bohart, Yoon-Nelson, and Bed Depth Service Time (BDST) models have provided a better description for the study. By finding out of kinetic parameters for setting out the efficiency of the dynamic study is an fundamental approach of using such dynamic models. The bed capacity is influenced by the different factors can be evaluated by this study.

5.9.1 Analysis of dynamic operation in column mode

The removal of solute by the column operation has been expressed by the influent and effluent ration (C_t/C_0) as a function of effluent volume ***(Munagapati et al. 2018).*** Area under the plot between adsorbate-adsorbent concentration (C_{ad}) represents the adsorption capacity q_{total} (mg). It can be expressed mathematically as :

$$q_{total} = \int_{v-0}^{V=V_{total}} C_{ad} dV \quad \text{--------------------- (5.27)}$$

The equilibrium uptake ($q_{eq(exp)}$) is expressed as

$$q_{eq}(exp) = \frac{q_{total}}{X} \quad \text{-------------------------- (5.28)}$$

where, X = adsorbent weight in the column (g).

Passing of adsorbate over adsorbent bed (W_{total}) can be find out from equation (29)

$$W_{total} - C_0 V_{total} - - - - - - - - - (5.29)$$

Percentage removal in terms of total adsorbate (W_{Total}) is represented as

$$Y = \frac{q_{total}}{W_{total}} \times 100 - - - - - - - - (5.30)$$

The aforesaid derivation can help a successful design of a column based on maximum adsorption capacity ***(Li and Li, 2019).***

5.9.2 Application of Thomas Model

Thomas model envisage exchanging of ion of hetorogenity in a flowing object **(*Thomas, 1944*).** The plug flowing following Langmuir isotherm consideration is the basis of this model ***(Futiam et al. 2011).*** It rejects the dispersion of axial flow observing reversible kinetics having degree of second order ***(Hassan et al. 2010)***.

Mathematical expression for Thomas equation as follows:

$$\frac{C_t}{C_0} = \frac{1}{1 + \exp\left[\frac{K_{Th}}{Q(q_0 X - C_0 V_{eff})}\right]} ------ (5.31)$$

where K_{Th} is the Thomas rate constant (mL/min.mg); q_0 is the maximum concentration of solute (mg/g). X is the amount of adsorbent (g); V_{eff} is the volume of effluent(L); q is the flow rate (mL/min).
After rearranging, the model can be expressed as follows:

$$\ln\left(\frac{C_0}{C_t} - 1\right) = \frac{K_{Th} q_0 X}{Q} - \frac{K_{Th} C_0}{Q} V_{eff} ------- (5.32)$$

Model equation has been used the experimental outcomes to study the adsorption performance for the dye MB and MG on the adsorbents. The ration of inflow and effluent concentration has been considered ranging from 0.0001 to 0.99 under different varying inputs, to find out the model constant K_{Th} and dye uptake q_0 from the equation 5.32.

5.9.3 Application of Yoon-Nelson model

Yoon-Nelson model ***(Yoon and Nelson, 1984)*** is considered as the most simplest model in dynamic adsorption study. There is no consideration is made regarding the character of adsorbate solution or the adsorbent in use. This model also cannot consider even the surface morphology of the adsorbent ***(Yao et al. 2010).*** This model is only consider that probability of decreasing solute adsorption upon sorbent molecules is proportional to its breakthrough probability.

Expression of Yoon-Nelson model is :

$$\ln\left(\frac{C_t}{C_0 - C_t}\right) - K_{YN} - K_{YN}T \text{ -------- } (5.33)$$

where, K_{YN} = the Yoon-Nelson rate constant (min^{-1}),

C_0 = the inlet concentrations of dye mixture (mgL^{-1}),

C_t = the effluent concentrations (mgL^{-1}),

t = the breakthrough time (min),

and T = the time required for 50% adsorbate breakthrough (min).

Rate constant K_{YN} and 50% breakthrough time T can be find out from eqn. (5.33).

5.9.4 Application of Adams-Bohart model

Bohart and Adams has established an equation between time (t) and influent-effluent ratio (C_t/C_0) during studying of chlorine adsorption onto activated carbon. From the early stage to later part of the experiment the adsorbent hs been changed from gaseous to liquid phase. In this context they changed the concept of pressure for gaseous state into concentration for liquid phase of the adsorbate.

Certain assumptions were put forth to analyze the model equations ***Sarala (2017)***:

1. The concentrations are weak.
2. When $t \rightarrow \infty$; $q \rightarrow N_0$ where N_0 represents the maximum adsorption capacity.
3. Mass transfer is slower down the rate of adsorption.

The model has been proposed during adsorption using granulated activated carbon as:

$$\frac{C_0}{C_t} = \frac{1}{1 + e^{a-bt}} \text{ ------------ } (5.34)$$

The linear equation of Adams-Bohart model is given by:

$$\ln\left(\frac{C_0}{C_t} - 1\right) = \frac{KN_0x}{u} - KC_0t \text{ ------------- } (5.35)$$

where C_0 = influent concentration (mg/L);

C_t = effluent concentration (mg/L);

K_{AB} = adsorption rate coefficient (L/mg.min);

N_o = adsorption capacity coefficient (mg/L);

x = bed depth (cm);

u = linear velocity (cm/min)

and t = time in minute.

The values of model parameters K_{AB} and N_0 can be determined from the equation (5.35).

5.9.5 Application of Bed Depth Service Time (BDST) model

The column adsorption is better alternative over batch adsorption due to some obvious reason. The uneven flow pattern with lesser dispersion in the column couples with non-exhaustion of packed bed before regeneration has some certain advantages for using in the industries ***(Venkatesh et al. 2017, Gupta et al. 2015).***

5.9.5.1 Objective of the model

From the traditional concept of determining breakthrough curve for designing column adsorption, Bed Depth Service Time (BDST) has ushered a new concept in line with irreversible isotherm model and introduced by ***Bohart and Adams (1920).*** The relation between the bed depth with time for breakthrough has been proposed in this model ***(Wang et al. 2016, Song, 2017).***

5.9.5.2 Assumptions of the model

The rejection of interaction between solids at the interface and idea of direct surface adsorption has been proposed by ***Hutchins (1973).***

5.9.5.3 Mathematical Formulation of the model

The correlation between the solid phase loading and time has been successfully utilized by this model ***(Agarry and Owabor, 2012).***

The representation of bed depth (Z) and service time (t) is as follows:

$$t = \frac{N_0 Z}{C_0 v} - \left({}^{1}/_{K_{ad} C_0}\right) \ln\left(\frac{C_0}{C_t} - 1\right) - - - - - - - - - (5.36)$$

The slope of the plot equal to N_0/C_0v

Bed capacity change against service time the necessary change of the equation (5.36) has been incorporated as follows:

$$t = N_0\left[1 - e^{-at1/2}\right] - - - - - - - - - - - (5.37)$$

Here root time dependence for mass transfer has been considered ***(Baranska et al. 2013).***

At higher flow rate introduces larger error in BDST analysis. As per ***Bohart and Adams (1920)*** this can be considered and the equation is introduced as follows:

$$\ln\left({}^{C_0}/_{C_t} - 1\right) = \ln(e^{K_{ad} N_0 Z} - 1) K_{ad} C_0 t - - - - - - - (5.38)$$

The modeling equation based on the laid down assumption is given as:

$$t - (N_0/C_0 F)Z - {}^{1}/_{K_2 C_0} \ln\left(\frac{C_0}{C_t}\right) - - - - - - - - - - - (5.39)$$

where ,

C_t = solute concentration in effluent (mg/L),

C_o = initial solute concentration (mg/L),

F = linear velocity for adsorbate (cm/min),

N_o = sorption capacity (mg/gm),

K_2 = rate constant of BDST model (in L/mg/min),

t = service time (min)

and Z = adsorbent depth (cm).

Later, Hutchins during phenol adsorption problem introduced ***(Mahmoodi, 2016)*** a simplified form of the BDST model as:

$$t = aZ - b \quad - - - - - - - - - - - - - - - - (5.40)$$

where, $a = \frac{N_0}{C_0 F}$ and $b = (1/K_2 C_0)\ln\left(\frac{C_0}{C_t} - 1\right)$ -------------------- (5.41)

5.10 Artificial Neural Network (ANN)

5.10.1 Layers of ANN

Artificial Neural Network (ANN) is basically effective and faster computing software functioning with the similar working principle of biological neural network of human brain. The main focal issue of using ANN in different engineering problems is to make the computation faster than practice. ANN is termed as artificial neural network, which processes data base for higher prediction based on certain inputs of known values.

The structural of artificial neural network indicates how the neural nodes/neurons are placed relative to each other. Interactions of neurons acts based on their weights. In general the artificial neural network consists of three layers as described below:

i) Input layer

This layer accepts information of experimental values from the certain known sources. These inputs are normalized within the specific limits (0.2 to 0.8 in our work) based on activation function.

ii) Hidden or intermediate or invisible layer

This layer composed of neurons and processes input data to give the final result as output .

iii) Output layer

The output layer also consists of neurons and liable to produce or represent the output of the entire network system, which comes out as a result of processing data from the input layer by the neurons of the preceding hidden layer.

The general structure of ANN is given below where we can find that each neuron is inter connected over the entire layers. The inputs are feeded and carried over the subsequent layer through neurons and multiplied by the weights for optimization error. Signals from other neurons can be either excitatory (positive) or inhibitory (negative), as shown in the Fig. 5.2 and Fig.5.3 below.

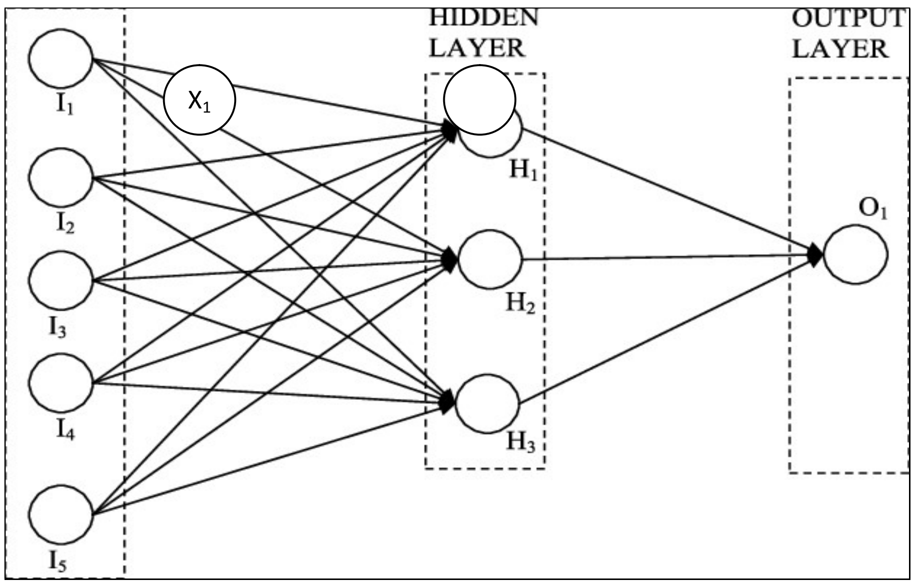

Fig. 5.2: Architecture of ANN Model

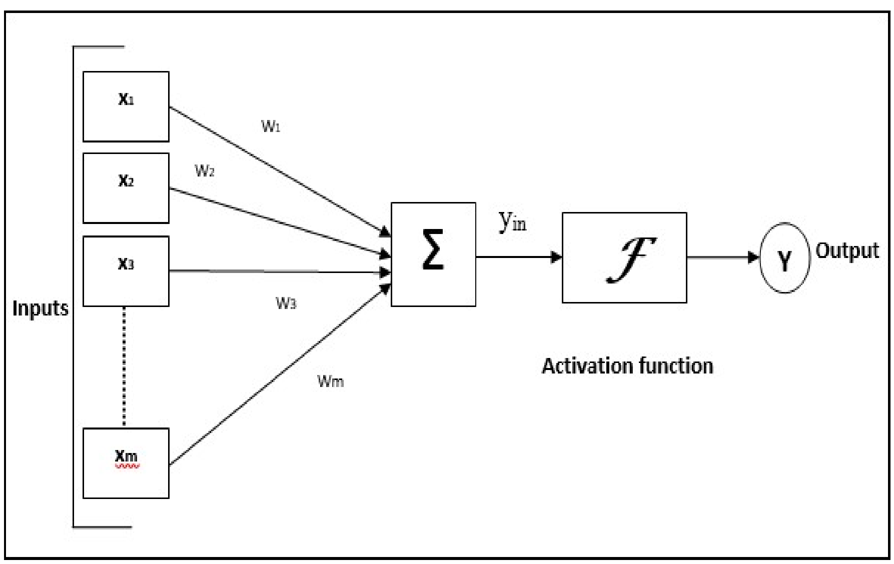

Fig. 5.3: Conversion of input signal to input feeding data to ANN

5.10.2 ANN Architecture

Architecture of ANN can be classified on the basis of orientation of neurons as well as their inter connectivity as follows:

- **i.** single layer feed-forward network
- **ii.** multiple-layer feed-forward network
- **iii.** recurrent network
- **iv.** mesh network

i) Single-layer feed-forward network

The single layer network having one input layer and output layer of single neuron. The processing instruction is unidirectional and flows from input to output direction. It is shown in the Fig. 5.4. This ANN is used in pattern classification and linear filtering problems. The perception is one of the most important types of feed-forward model. The main type of such ANN model belongs to Perception and the ADALINE.

The output O is defined by:

$$O = f(net) = f(\overline{w}\overline{x}) = f\left(\sum_{j=1}^{n+1} w_j x_j\right) = f\left(\sum_{j=1}^{n} w_j x_j - \Theta\right)$$

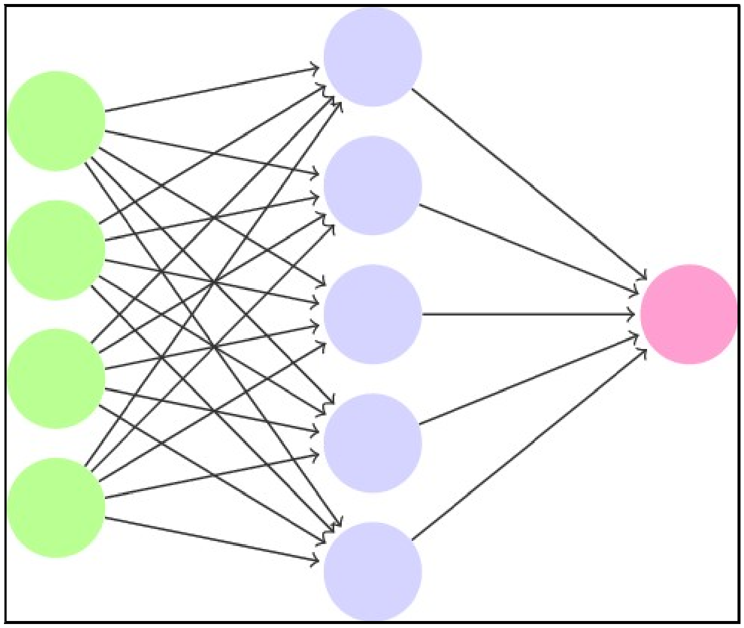

Fig. 5.4: Single-layer free-forward ANN

ii) Multiple-layer feed-forward architecture

The number of hidden layer for Multiple-layer feed-forward architecture is more than one to process more diverse problem. Generally functional approximation problem can be solved by this model. In the Fig.5.5, the architecture of a free forward network with multiple layers is shown. The number of hidden layer from the figure is two.

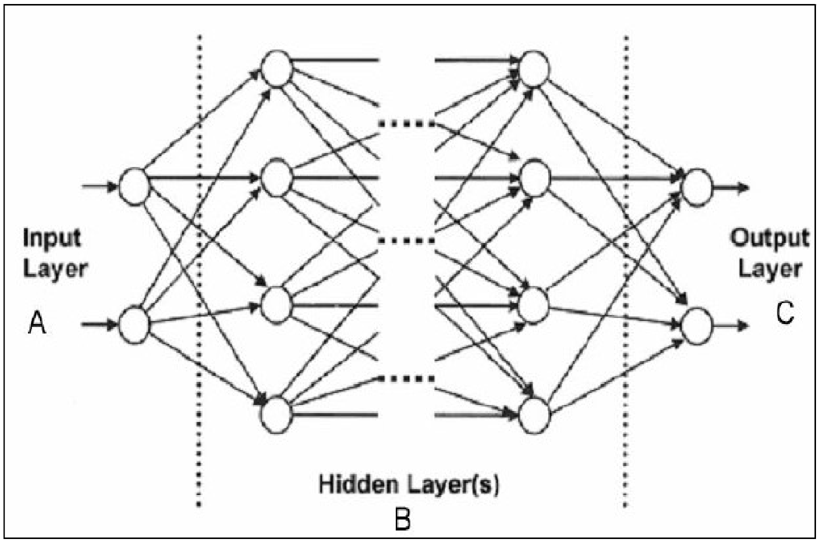

Fig. 5.5: Multiple-layer free-forward ANN

The number of neurons in different layer for this architecture is different. The number of neurons in the different layers of hidden layer may be same or different depending upon the problem. This is accuracy depending i.e. how far the degree of accuracy is required for processing data.

iii) Feedback Architecture

The output neurons can be utilized for giving feed back to its preceding layer as function of dynamic processing. The output processes the data again on the basis of given feed back in earlier occasion.

iv) Mesh Architecture

The main feature of network of such type is the two or more dimensional arrangement of neurons. Mesh structure has a wide use in the solving of data clustering problem. Moreover, optimization of graphical or spatial pattern recognition can be solved using accurate weight within particular thresholds. One of the well known structure of this category is Kohonen network where two dimensional neuron arrangement is noted as in the Fig. 5.6 below.

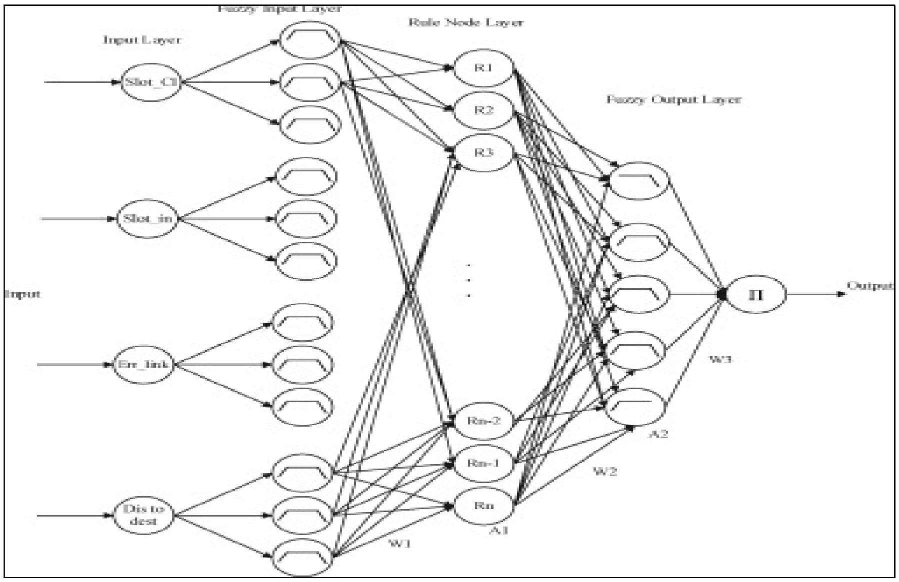

Fig. 5.6: Structure of the mesh network

5.10.3 Training and Learning in ANN

The ANN model accepts the data from a system of data set accordingly recognize the relation between system input with the output by successive iteration using appropriate weights etc. The understanding of input data for establishing the proper relation with the output is known as learning. The process by which a set of system data is converted from input to output level by applying appropriate weights under threshold by way of adjusting training epoch, is known as training.

In general, from the complete data set 60 to 90% of data are used for training purpose and rest 10 to 40% data are used for testing or validation of the model.

i) Supervised Learning

This learning process was invented by Donald Hebb in the year 1949. In this learning approach , input signal by way of using attribute generates output results for the predicted value. The construction of hypothesis for data prediction can be made accordingly under the supervision of this value table.
The repetitive adjustment of weights and threshold to minimize the gap between actual and desired level of output is maintained by this supervised learning.

ii) Un-supervised Learning

The interaction between input signal with desired level of output is not necessary for unsupervised learning. The adjustment of weights and threshold is necessary to coordinate the sub set data within the same layer specific data system.

iii) Reinforcement Learning

This learning process is an improved version of supervised learning. The continuous adjustment of weights and threshold over neurons for optimization output data up to desired level is the general fetures of any learning mechanism. Here additionally some satisfactory weights generating by the process of learning is added to improve the entire level of learning. This is sometimes termed as stochastic method.

5.10.4 Preprocessing and scaling of data

The discriminate response in the model analysis for the learning process is due to varying nature of data system and their different level of importance. The appropriate measure in the learning process by suitably adjusting the weights and network threshold can minimize the level of discrepancy.
The processing of data system for each layer is very important issue in this respect.

Generally as per as Metlab software is concerned, the range of data set scale in the input and output layer lies between 0.2 to 0.8.

The preprocessing is performed by using the following relation as below as shown in the equation 5.43.

$$X_i(\text{net}) = 0.2 + 0.6\,\frac{(X_{in} - \min(X_i))}{\max(X_i) - \min(X_i)} ------(5.43)$$

where,

X_i (net) = Value Normalization for any variable(i_{th}),

X_{in} = Observed value of i_{th} variable in data range,

min (X_i) = Minimum value of i_{th} observed variable during training ,

max (X_i) = Maximum value of i_{th} observed variable during training,

The new system of data set as evolved by this pre-possessing activity is used in training purpose with precision. The predicted output value so generated by the learning and processing is again rescaled to its original form. This form of data set of output is compared with the target value.

The rescaling operation is done with the help of the following equation as shown below:

$$Y_{i(p)} = \text{MinY}_i + \frac{(\text{MaxY}_i - \text{MinY}_i)}{0.6} \times (x_i(\text{net}) - 0.2)) ---------- (5.44)$$

where,

$Y_{i(p)}$ = Predicted value of i_{th} output variable;

X_i (net) = Normalized value of i_{th} output variable;

MinY_i = Minimum value of i_{th} observed variable for training data-set;

MaxY_i = Maximum value of i_{th} observed variable for training data-set.

The multi-layer perception (MLP) technique used in the present work was developed in METLAB 2017a with five input neurons for batch study and four input neurons for column study, single hidden layer having 10 neurons and one output layer (percentage elimination of dyes). It was analyzed and simulated by the ANN software. The input variables and the distribution of training and testing data are given in the Table 6.43, 6.44, 6.45 and 6.46 in the Results and Discussion chapter.

5.10.5 Optimization by ANN

The optimization of the gap between the output value from actual to desired level is very important ***(Ekici and Aksoy, 2009).*** This optimization process reduces the MSE of the model. The optimization of MSE is being achieved by increasing the number of neurons in the hidden layer(s).

MSE with the number of neurons in the hidden layer can be related as :

$$MSE = \frac{1}{N}\sum_{i=1}^{N}(T_i - A_i) \quad \text{..} \quad (5.45)$$

N = Number of observations

A_i = Experimental value at the i^{th} data.

T_i = Network predicted value at the i^{th} data.

i = range index of data.

ANN so developed in the present study has three layers. 60 to 85% of data from the system set is used for training and rests are used for testing or validation. The number of neurons in hidden layer is set as 10 while the input variables are set as per the experimental run. It is depicted that ANN as a powerful modeling tool, can predict the effluent concentrations of dye mixture for different operating conditions. High values for the regression coefficients prove the accuracy of the model.

5.11 Statistical t-test

Statistical t-test a type of inferential statistical tools was used to compare between two sets of data, which might be in related in certain aspect. It is stat hypothesis testing test. The three key parameters such as variance, t-score and p-value can be evaluated to judge the null hypothesis ***(Goulden, 1956).***

The t-test may be categorized into three types

1. Independent samples t-test
2. Paired t- test
3. One sample t-test

During processing of similarities between outcomes of two procedures, one should know the character of three data set, whether paired or independent ***(Fkih et al. 2020).***

So the mathematical approach of t-test by taking sample from each of two data sets and draw comparison on the basis of null hypothesis ***(Liang et al. 2019).***

The t-score of the hypothesis is the measure of similarities or dissimilarities between the two groups or within the same groups. Lower value indicates closeness of two sets of data.

Another important parameter is 'p' value in t-test. It indicates probability and varies from 0 to 100%. The value is expressed in decimal place. It is the measure of statistical significance. So to determine the level of significance of two sets, p-value is considered. If it is greater than 0.05 (i.e. 5% level), indicates a good agreement between two set of observations.

In the present study the statistical t-test has been employed to compare the ANN simulated outcome with the experimental results.

Results and Discussion

6

6.1 Effect of Different Operating Parameters on Adsorption

Batch adsorption was performed for examining the influence of diverse operating parameters viz. adsorbent dosage, initial concentration of dye mixture comprising of methylene blue (MB) and malachite green (MG), shaker speed, pH of the mixed dye solution and contact time. The curves obtained for the variation of operating conditions reveal the effect of the parameters over the adsorption process.

6.1.1 Influence of Adsorbent Dosage

The influence of adsorbent dose as input parameter for the adsorptive removal of mixture of two dyes viz. methylene blue (MB) and malachite green (MG) from the solution by using four low cost adsorbents was investigated. The results have been shown in the Annexure (Table-3, 7, 11 and 15). The amount of dosages for four low cost adsorbents viz. neem leaf ash (NLA), bagasse fly ash (BFA), jack fruit leaf ash (JFLA), and rice husk ash (RHA) ranged from (0.1 – 12) gm/L in 15 numbers of plastic bottles with fixed concentrations of dyes at 25 mg/L. The other operating parameters viz. shaker speed and pH of the adsorbate solution were maintained at 120 rpm and 7.0 respectively. The removal percentage of dye mixture in different adsorbent dosages was recorded after elapsing 3.0 hrs of shaking followed by successive centrifuging and analyzing the effluent concentrations in a spectrophotometer as given in the Fig. 6.1 to Fig. 6.4.

The results shows that when the neem leaf ash dosage was increased from 0.1 to 5 gm the dye exclusion augmented from 53.25% to 97.8% and then attained a stability. The removal efficiency for neem leaf ash in the process of adsorption was recorded as 99.2% which shows the degree of effectiveness of the adsorbent. Thus, the optimum dose of the adsorbent was obtained as 4.0 gm as there is no significant effect upon dye removal above that dose. In case of jack fruit leaf ash as adsorbent as the dosage was varied from 0.1 gm. to 6.0 gm the elimination of the dye mixture increased from 15.83% to 91.23% and then got at the saturation. The optimum dose for jack fruit leaf was obtained as 5.0 gm. The maximum removal efficiency was noted as 92.57% giving satisfactory result. For bagasse fly ash as adsorbent, as the amount of adsorbent dosages increased from 0.1 to 2.4 gm the percentage exclusion of the dyes increased from 91.37 to 98.12 and thereafter no significant effect was noticed. In the present study the dosage for bagasse fly ash was measured as 2.0 gm for equilibrium dosage. The removal efficiency of 98.57% establishes the potentiality of the adsorbent for dye elimination. By increasing the dosage of rice husk ash as adsorbent from (0.1 – 6.0) gm the percentage of dye removal was increased from 15.83% to 90.49% and thereafter no noticeable change was recorded. The optimum dose was determined as 4.0 gm for RHA. In the case of RHA, the maximum removal percentage was recorded as 92.20%.

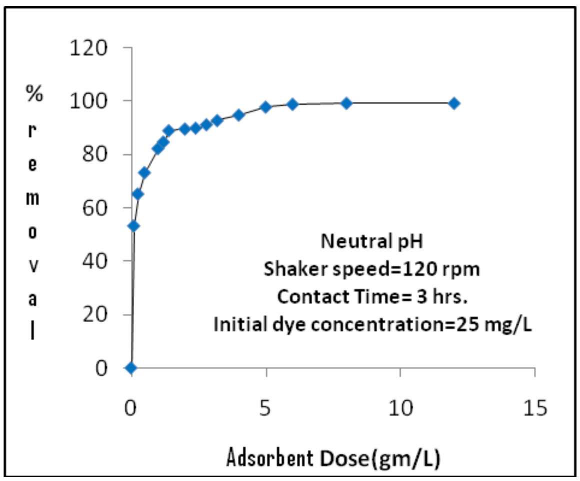

Fig.6.1: BTC under varying adsorbent dose using NLA

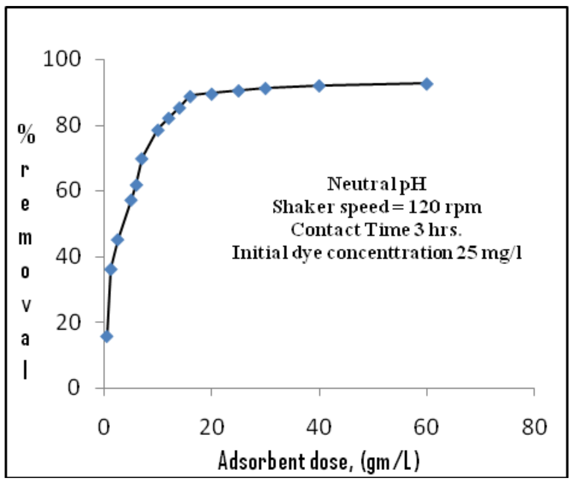

Fig.6.2: BTC under varying adsorbent dose using JFLA

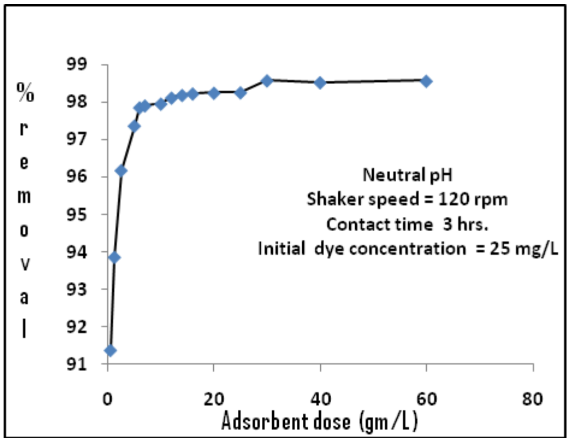

Fig.6.3: BTC under varying adsorbent dose using BFA

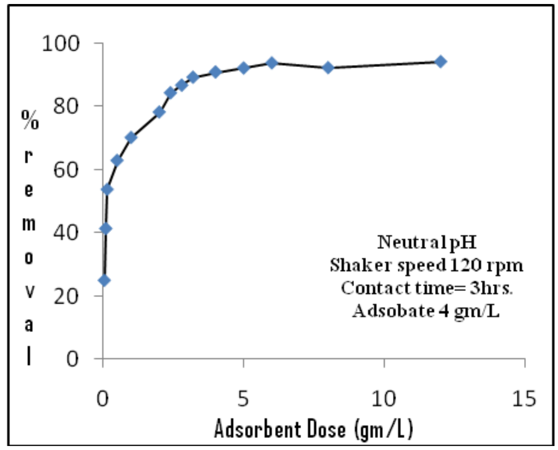

Fig.6.4: BTC under varying adsorbent dose using RHA

The Fig.6.1 to Fig.6.4, the removal percentage of mixed dyes using four low cost adsorbents is elaborated graphically. The elimination rate of dye molecules at initial stage was faster as adsorbent dose increased due to presence of more adsorption sites. Thereafter exhaustion of adsorption sites caused insignificant removal of dyes in spite of increasing adsorbent dosage.

6.1.2. Influence of Contact Time

Influence of another important input variable, contact time, for adsorptive removal of two basic dyes viz. methylene blue (MB) and malachite green (MG) by means of four inexpensive adsorbents was investigated in the current study. Removal of dye mixture data in percentage are furnished in the Annexure of the thesis (Table 4, 8, 12, and 16). The amount of adsorbent taken for the four low cost adsorbents viz. neem leaf ash, bagasse fly ash, jack fruit leaf ash, and rice husk ash at their optimum value was 4, 2, 5, and 4 gm respectively. The plastic bottles for shaking purposes was taken in 15 numbers at fixed concentrations of dye mixture of 25mg/L. The other variable parameters such as shaker speed and pH of the adsorbate solution was kept constant as 120 rpm and 7.0 respectively. The percentage removal of dyes with different adsorbent dosages was observed at regular interval of time of shaking and effluent samples were taken out, centrifuged and analyzed in a spectrophotometer to determine the concentrations of dyes in the solution as shown in the Fig.-6.5 to Fig.-6.8. The experiment was done for a period of 5.0 hrs.

The spectrophotometer analysis of effluent concentration for the percentage removal of dye mixture at different time interval was recorded. The percentage removal increased over the time varying from 10 to 135 min in case of neem leaf ash while it was recorded as 165 min, 135 min and 190 min for jack fruit leaf ash, bagasse fly ash and rice husk ash respectively. After that no significant removal was achieved in spite of the exposure of adsorbents to the dye molecules. Accordingly the time for equilibrium was recorded all the four adsorbents viz. neem leaf ash, jack fruit leaf ash, bagasse fly ash and rice husk ash as 135 min, 165 min, 135 min and 190 min respectively.

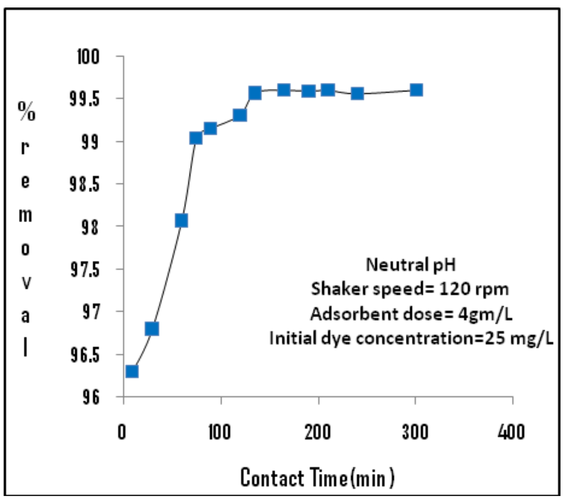

Fig. 6.5: BTC under varying contact time using NLA

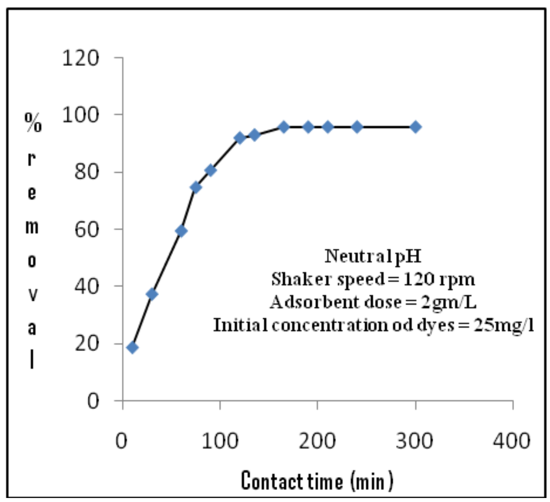

Fig. 6.6: BTC under varying contact time using JFLA

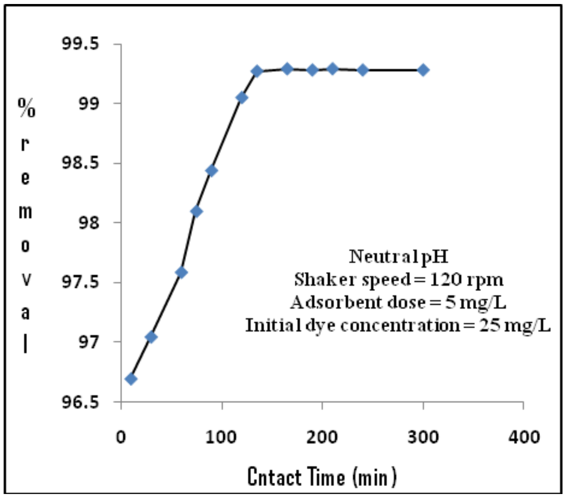

Fig. 6.7: BTC under varying contact time using using BFA

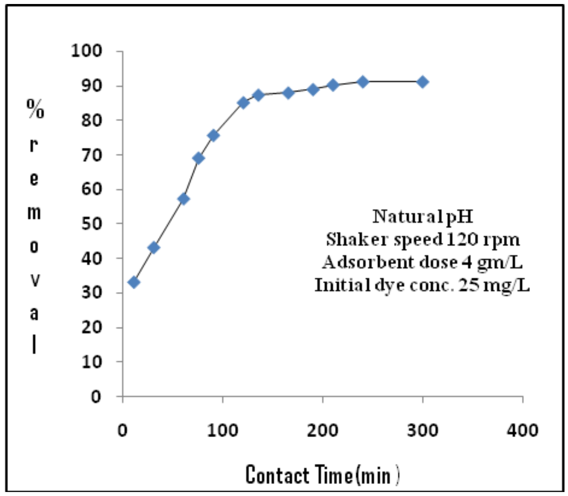

Fig.6.8: BTC under varying contact time using RHA

It is observed that initially, the adsorption rate under several other fixed operating conditions jumped rapidly and thereafter beyond a certain time interval no considerable alteration in the percentage removal was observed. This was because of the presence of strong cohesive forces between the molecules of two dyes and the adsorbents at early stage of adsorption process and thereafter pore saturation of the adsorbent surfaces certainly reduced the capacity of adsorption.

6.1.3. Influence of Initial Adsorbate Concentration

The early concentration effect of mixture of two basic dyes with equal proportion by weight was investigated using four low cost adsorbents. The amount of adsorbent dosages was kept fixed at their individual optimum dosage for all the four adsorbents. The varying amount of initial concentration of two dyes in mixture was taken as 25, 40, 50, 75, 100 and 150 mg/L. Other operating variables such as shaker speed, pH and contact time for mixed dye solution were kept fixed at 120 rpm, 3.0 hrs and 7.0 respectively during course of experiment. The percentage removal with respect to varying initial concentration of mixed dye solution is depicted in Fig.-6.9 to Fig.-6.12. The experiment outcomes are given in the Table-1, 5, 9 and 13 in the Annexure.

The percentage removal of dye mixture from its aqueous solution decreased at the initial phase but there was no significant effect at higher initial concentration. Percentage removal of dye mixture lowered from 98.78% to 67.74% for increased initial concentration as 25 mg/L to 150 mg/L for neem leaf ash. The removal percentage for jack fruit leaf ash decreased from 88.53% to 58.25% for was noted. The removal percentage for the bagasse fly ash decreased from 98.54% to 86.49%, while for the rice husk ash removal percentage decreased from 88.53% to 58.25% during raising of initial or primary concentrations from 25 mg/L to 150 mg/L.

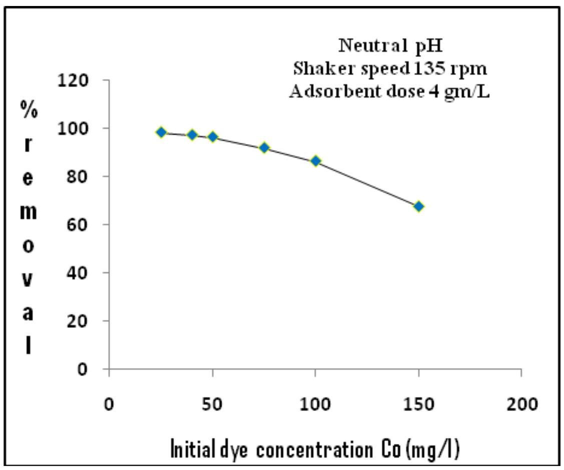

Fig. 6.9: BTC under varying concentration using NLA

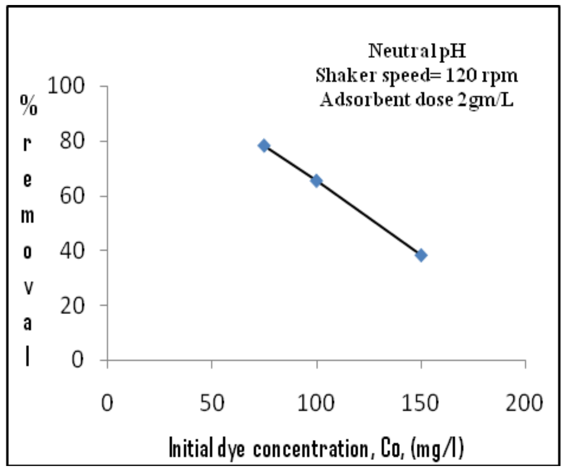

Fig. 6.10: BTC under varying concentration using JFLA

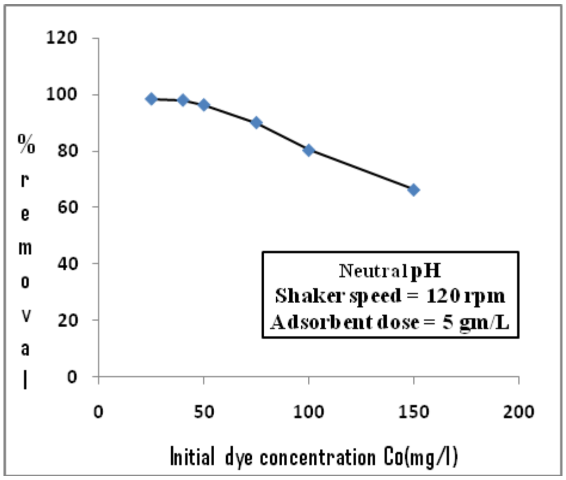

Fig. 6.11: BTC under varying concentration using BFA

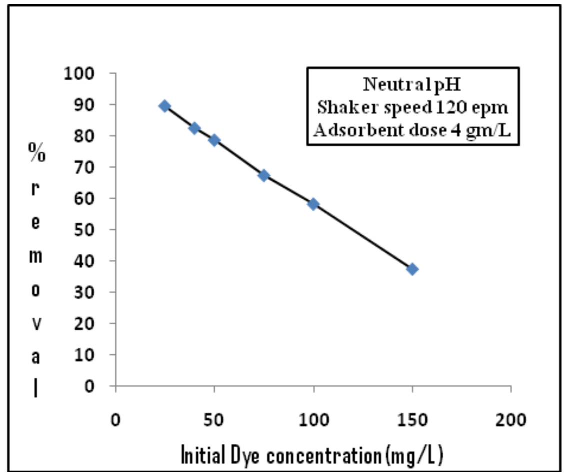

Fig. 6.12: BTC under varying concentration using RHA

The increased concentration of dyes directly reduced the adsorption capacity as the pores of the adsorbent got saturated. As a result, the surface of the adsorbent molecules could not adsorb extra dye molecules from the queous solution at a fixed amount of contact time. The percentage removal decreases at the initial stge and after that at the further state of time it becomes insignificant.

6.1.4. Effect of Shaking

The revolution of shaker is another important factor influencing the removal of dye mixture. The effect of the shaker speed in several other fixed operating conditions was studied for the adsorptive exclusion of dye mixture using all four inexpensive adsorbents as shown in the Fig. 6.13 to 6.16. The initial dye concentration of 25 mg/L along with their respective optimum adsorbent dosages under normal pH was considered at varying shaker speed ranging from (30 –130) rpm. The time for contact was fixed at 3 hrs for the experiment. The experimental results are furnished in the Annexure (Table-2, 6, 10 and 14).

It is observed from the experiment data that adsorptive removal increased from 93.13% to 98.52% with the increase in shaker speed from 30 rpm to 130 rpm for the neem leaf ash. The percentage removal increased 96.28% to 98.43% for the jack fruit leaf ash, 95.54% to 98.24% for the bagasse fly ash and 66.48% to 90.95% for the rice husk ash as recorded for the increased shaker speed from 30 rpm to 130 rpm.

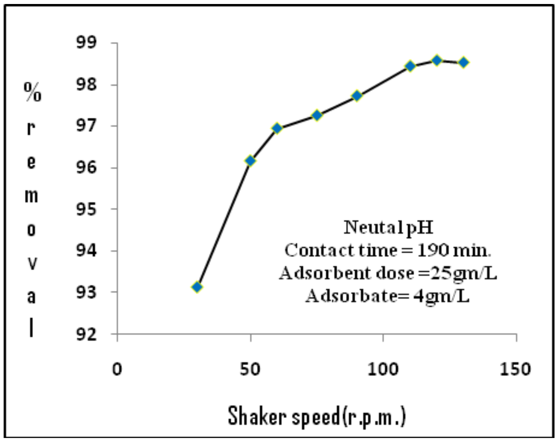

Fig. 6.13: BTC under varying shaking rpm using NLA

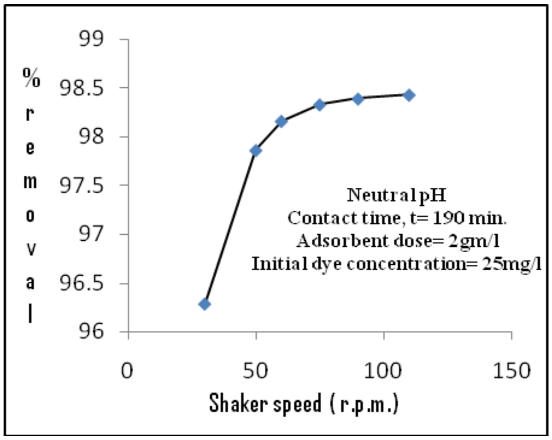

Fig. 6.14: BTC under varying shaking rpm using JFLA

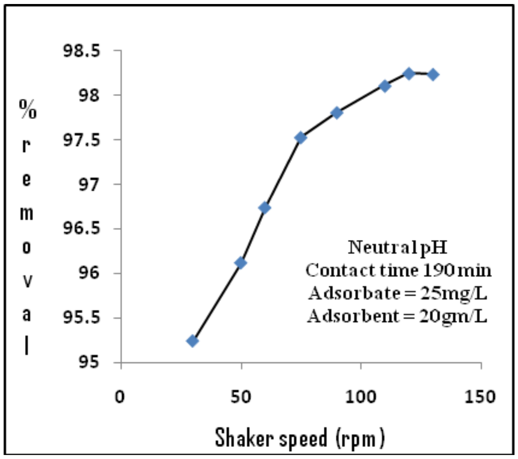

Fig. 6.15: BTC under varying shaking rpm using BFA

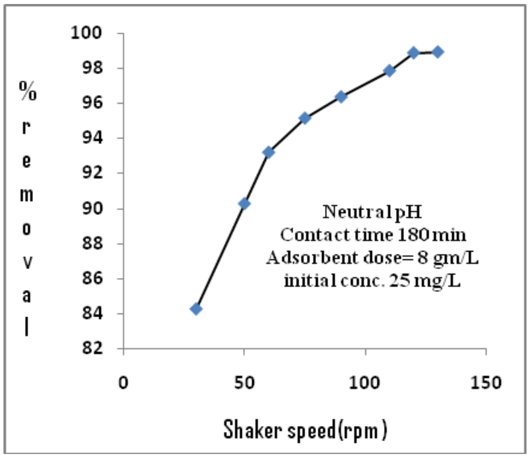

Fig. 6.16: BTC under varying shaking rpm using RHA

As the shaker speed increased, the chances of larger number of adsorbate molecules to come in contact with the adsorbent surface were also increased, resulting in greater adsorptive removal of dyes. In case of all the four adsorbents the removal of dyes at the early stage of the experiment increased rapidly and after certain time period percentage rate of elimination decreased due to exhaustion of sorbent surfaces. The higher removal percentage of the neem leaf ash and jack fruit leaf ash proved their effectiveness as good quality adsorbent.

6.1.5 Influence of Adsorbate pH

Effect of adsorbent pH onto the adsorptive removal by using low cost adsorbents was also under purview of the present research. Adsorbate pH varied from 3.0 to 9.1. in the present work under fixed values of shaker speed (120 rpm), initial dye concentration (25 mg/L), time of contact (optimum time) and adsorbent dose (respective optimum dosage) as shown in the Fig. 6.17 to 6.20. The experimental results for the four adsorbents are given in the Table-17 to 20 in the Annexure.

The adsorptive removal of dye molecules from adsorbate solution, increased as the pH of the solution increase, over a range from 4.1 to 9.2, was considered for the study. It can be concluded from the experiment data that adsorptive removal increased from 93.76% to 99.16% with the increase pH from 3.0 to 9.1 for the neem leaf ash. The percentage removal increased 94.87% to 99.18% for the jack fruit leaf ash, 95.72% to 99.08% for the bagasse fly ash and 65.44% to 98.73% for the rice husk with the increased pH from 3 to 9.1 of the mixed dye solution.

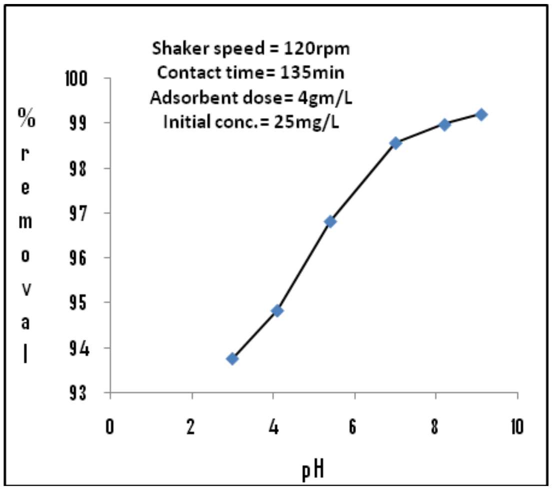

Fig. 6.17: BTC under varying adsorbate pH using NLA

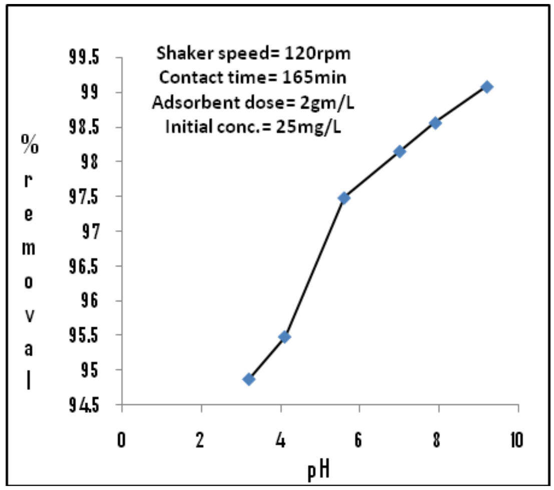

Fig. 6.18: BTC under varying adsorbate pH using JFLA

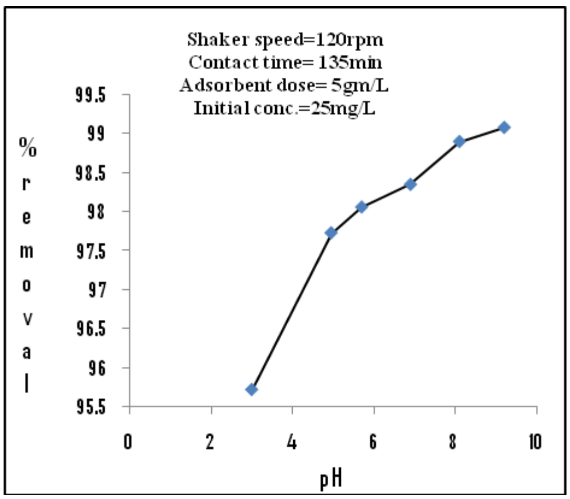

Fig 6.19: BTC under varying adsorbate pH using BFA

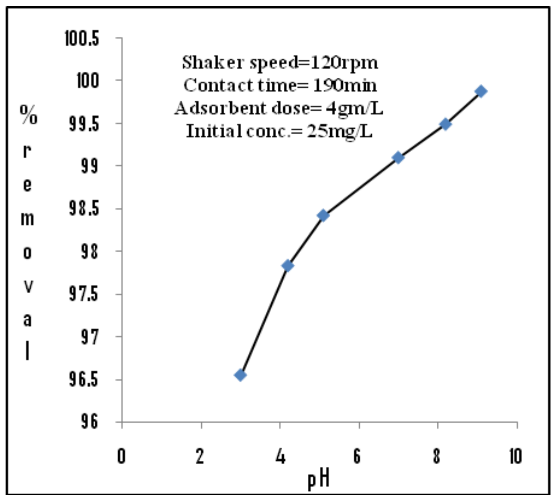

Fig 6.20: BTC under varying adsorbate pH using RHA

Effect of pH upon removal of dye molecules in binary system onto the four adsorbents is shown in the Fig. 6.17 to Fig. 6.20. The adsorptive removal directly depends on the solution pH. Surface characteristics of adsorbent and solution pH of the adsorbate are interactive factor which influences the adsorption process.

Surface acidity and basicity influences the present adsorption study. It can be explained below:

Adsorbent (OH^-) + Adsorbate (OH^-) $\rightarrow$ $O^- + H^+$ --------(A)

Adsorbent (H^+) + Adsorbent (H^+) $\rightarrow$ OH_2^+ ---------(B)

Equation (A) and (B) surface basicity for higher pH and surface acidity for lower pH is shown.

Thus, MB and MG being two cationic dyes adsorbed onto all four adsorbents spontaneously at high pH values as shown above. Therefore, adsorption of Methylthioninium Chloride or MB and Aniline Green or MG in binary system achieved better removal at increased solution pH while it showed reverse effect at lower pH.

6.2. Equilibrium study

Mechanism of adsorption can b explained from isotherm study. It is an important tool for understanding of solid phase interaction as well as fixing of optimum dosing ***(Rahdar et al. 2019).*** Adsorption result depends on correlation of equilibrium outcomes. Homogeneous or heterogeneous nature of surface of adsorbent, phase interaction and coverage are some of the important consideration before studying sorption isotherm ***(Das et al. 2020).*** The dye uptake at equilibrium concentration (C_e) may be evaluated using few conventional models as discussed followings.

6.2.1 Langmuir isotherm model

Langmuir model states the maximum occurrence of adsorption on the surface of sorbent during the presence of a saturated monolayer of solute molecules. It also considers steady adsorption energy and the transportation of adsorbate molecules over surface plane is not possible ***(Langmuir, 1916).***

This Langmuir isotherm model is

$$q_e = \frac{q_m k_L C_e}{1 + K_L C_e} - - - - - - -(6.1)$$

This can be represented as,

$$\frac{1}{q_e} = \frac{1}{q_m} + \frac{1}{q_m K_L}\frac{1}{C_e} - - - -(6.2)$$

Equations parameters and determination methodology are explained in section 5.3 in Chapter 5.

Batch adsorption experiment was carried out using all the four low cost adsorbents viz. neem leaf ash, jack fruit leaf ash, bagasse fly ash and rice husk ash.

From the Fig. 6.21 to Fig.-6.24, isotherm derivatives fitted well (R^2>0.923) for this model. Isotherm model value, K_L and q_m evaluated from slope and intercept of the line. The isotherm constants (K_L) for neem leaf ash, jack fruit leaf ash, bagasse fly ash and rice husk ash was obtained as 13.9, 14.0, 8.46 and 18.5 L/mg respectively. The values of dye uptake (q_m) for the adsorbents were recorded as 40.0, 20.41, 52.63 and 29.41 mg/g respectively. The experimental results for all four adsorbents are shown in the Table-21 to Table-24 in the Annexure.

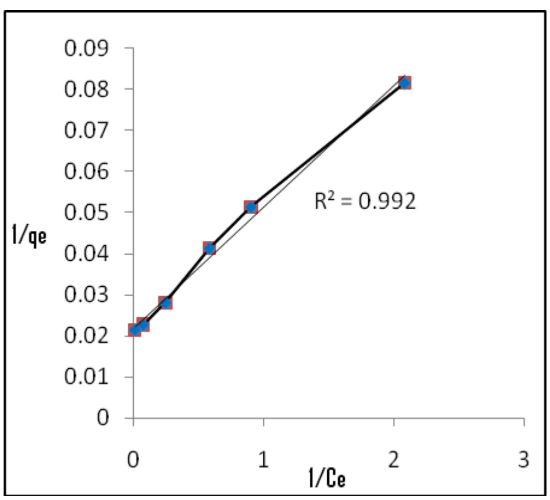

Fig.-6.21: Langmuir model using NLA

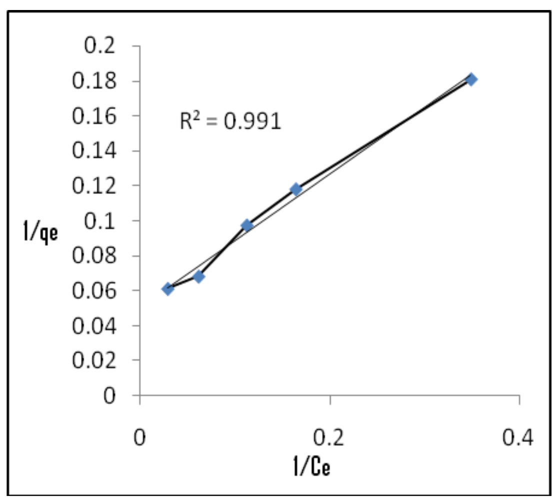

Fig.-6.22: Langmuir model using JFLA

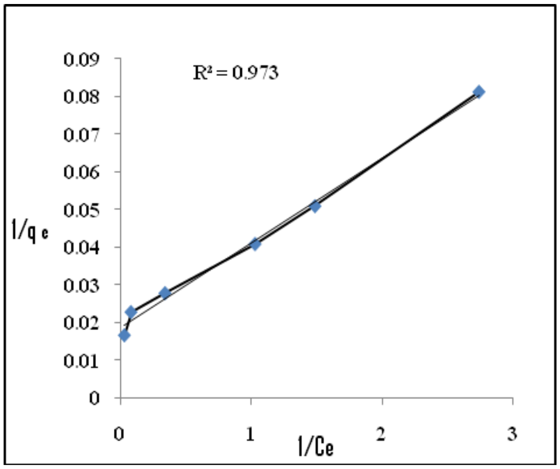

Fig.-6.23: Langmuir model using BFA

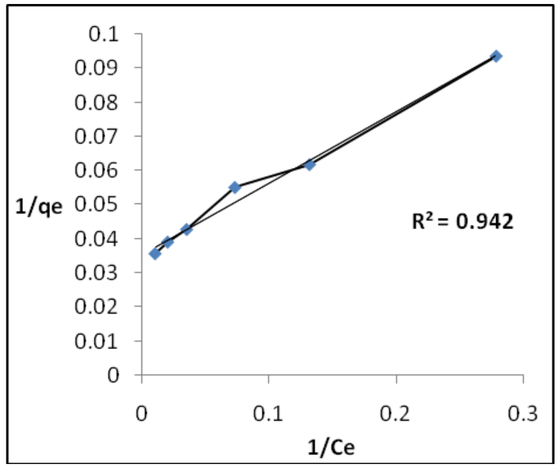

Fig.-6.24: Langmuir model using RHA

6.2.2 Freundlich isotherm model

This isotherm describes about surface homogeneity with non-even distribution of adsorption enthalpy ***(Freundlich, 1906).*** This model is given an empirical relationship for interaction between the solutes from a liquid and the solid surface. It refers the involvement of active sites with variable adsorption energies. Here in present investigation, Freundlich adsorption draws relation between the adsorbed amount of two dyes in mixture for unit mass of adsorbent (q_e) with equilibrium concentration of dyes (C_e) .

Mathematical expression for this isotherm is given by

$$q_e = K_f C_e^{1/n} \text{-------------------------------------} \quad (6.3)$$

Taking log in the both sides, the equation becomes,

$$\log q_e = \log K_f + \frac{1}{n} \log C_e \text{ ---------}(6.4)$$

Equation parameters are given in section 5.3.1 in chapter 5.

The parameter 1/n and constant (K_f) evaluated from the intercept and slope of the equation (6.4). This isotherm has wide application with the limitation over mono-layer adsorption detailing contrary to Langmuir model ***(Panda et al. 2017).***

Plotting log C_e versus log q_e was developed for all four adsorbents to get K_f and 1/n from intercepting and gradient value. Isotherm constants K_f and 1/n for Freundlich isotherm model were calculated for all the four low cost adsorbents (Fig. 6.25 to Fig. 6.28). The K_f values for the neem leaf ash, jack fruit leaf ash, bagasse ash and the carbonized rice husk were calculated as 19.77 ,3.639, 20.56 and 6.47 mg/g respectively. The adsorption intensity (1/n) was noted for all the four adsorbents as 0.197, 0.291, 0.342 and 0.417 respectively. This indicates easy separation of dye molecules from its aqueous solution. Freundlich model is fitted well with high correlation coefficient value (R^2 >0.924). The experimental results are given in Table-25-28 in the Annexure.

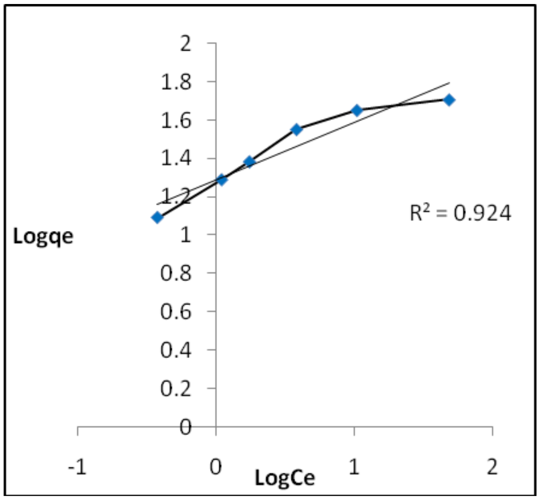

Fig. 6.25: Freundlich isotherm model using NLA adsorbent

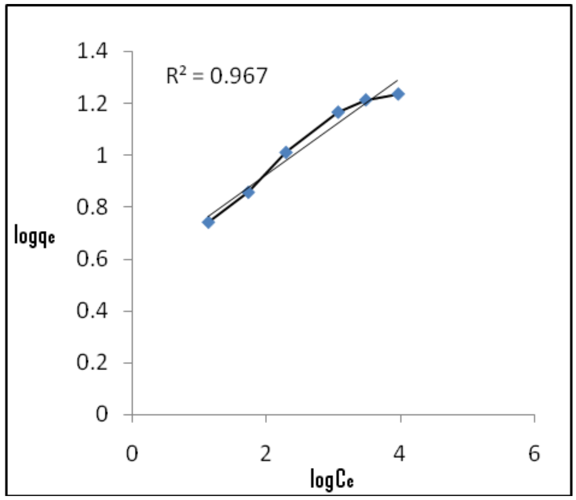

Fig.6.26: Freundlich isotherm model using JFLA adsorbent

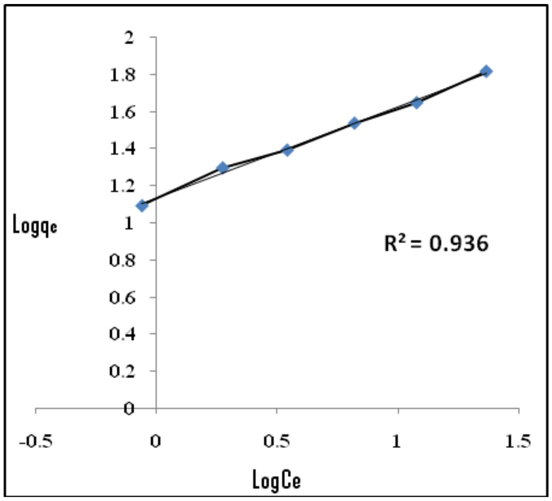

Fig. 6.27: Freundlich isotherm model using BFA adsorbent

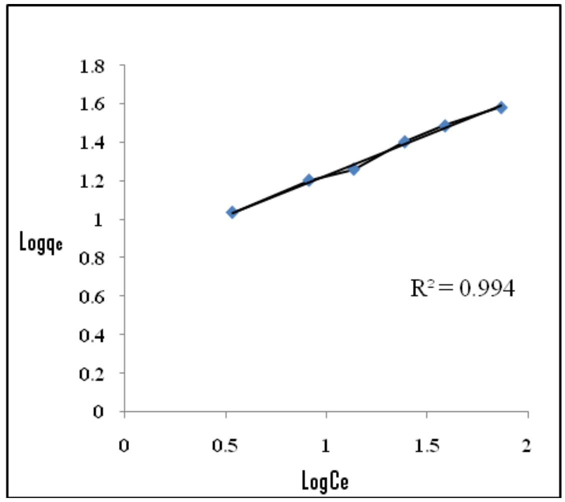

Fig.6.28: Freundlich isotherm model using RHA adsorbent

6.2.3 Temkin isotherm model

Temkin and Pyzhev (1940) during derivation of isotherm deduced the interaction between the adsorbate and adsorbent. They concluded that the heat generated during adsorption of the entire molecular layers decreased proportionately with coverage.

This isotherm consider specific interaction of sorbent-adsorbate. The transportation of uniform binding energy is the focl point of this model consideration. The adsorbed quantity (q_e) and equilibrium concentration (C_e) can be related.

Mathematical expression of the isotherm is given by

$$q_e = \left[\frac{RT}{b_1}\log(K_T C_e)\right] - - - - - - - - - - - (6.5)$$

The linearized form of the equation (5) is given by,

$$q_e = \frac{RT}{b_1}\log K_T + \frac{RT}{b_1}\log C_e \ - - - - - - - - (6.6)$$

The sorption outcomes can be deduced from equation (6.6).

Therefore, plot q_e versus C_e enables one to determine the constant K_T and b_1.

The linear plot (q_e) versus log(C_e) has been plotted for all the four adsorbents for adsorptive removal of dye mixture as shown in the Fig. 6.29 to Fig. 6.32. The results are depicted in the Table-29 to Table-32 in the Annexure.

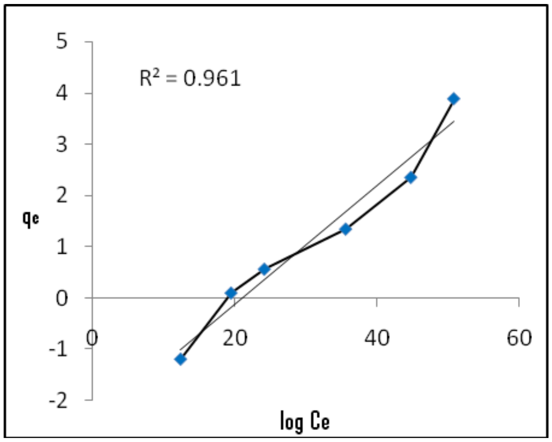

Fig. 6.29: Temkin isotherm plot for NLA

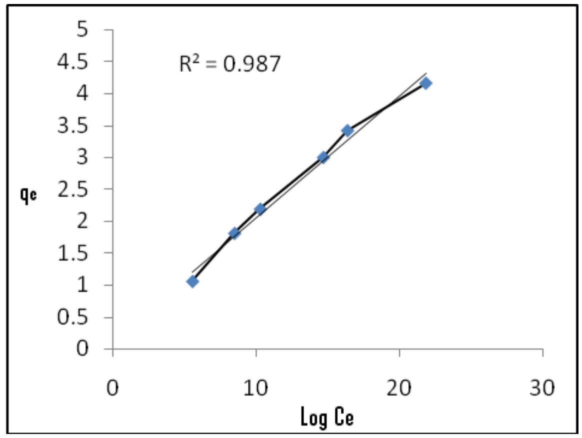

Fig.6.30: Temkin isotherm plot for JFLA

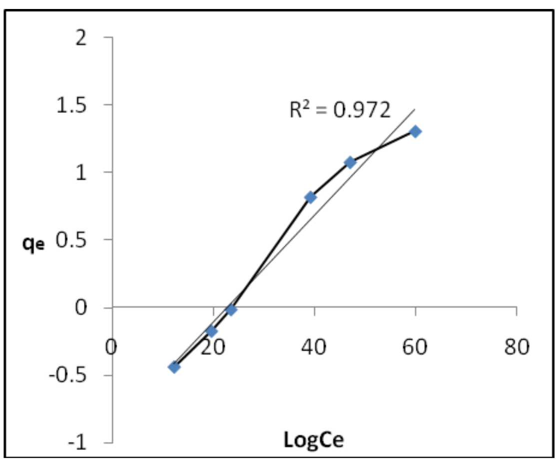

Fig.6.31:Temkin isotherm plot for BFA

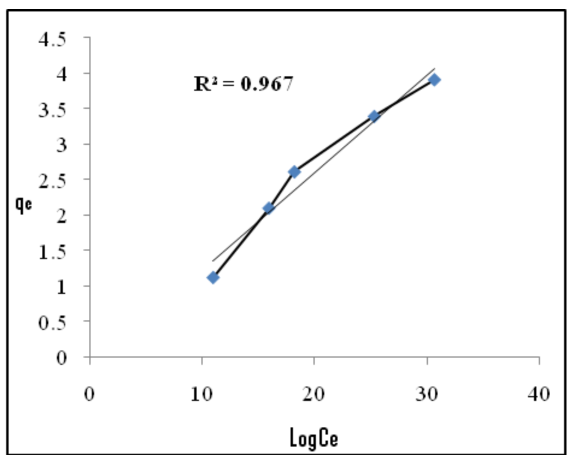

Fig.6.32: Temkin isotherm plot for RHA

The high bivariate correlation (R^2> 0.96) for neem leaf ash and jack fruit leaf ash implies excellent conformity with Temkin isotherm model (Fig. 6.29 to Fig. 6.32). The comparatively lower correlation coefficient value for bagasse fly ash and rice husk ash (R^2>0.865) indicates that these two adsorbents did not follow Temkin isotherm well. The isotherm constant K_T and b_1 were worked out from slope and intercept of the equation for the neem leaf ash, jack fruit leaf ash, carbonized bagasse and rice husk. The K_T value for the four adsorbents are found to be 1.118, 1.050. 1.056 and 6.182 L/mg while b_1 values are obtained as 21.78, 11.95, 30.71 and 17.39 for the neem leaf ash, jack fruit leaf ash, bagasse fly ash and rice husk ash respectively (Table 6.1).

Table 6.1: Parametric values of different adsorbents using different isotherm models

Adsorbent	Langmuir Isotherm			Freundlich Isotherm			Temkin Isotherm		
	q_m (mg/g)	K_L (L/mg)	R^2	K_F (L/mg)	1/n	R^2	K_T (L/mg)	b_1	R^2
Neem leaf ash	40.0	13.9	0.992	19.77	0.291	0.924	1.118	21.78	0.961
Jack fruit leaf ash	20.41	14.0	0.991	3.636	0.197	0.967	1.050	11.95	0.987
Bagasse fly ash	52.63	8.46	0.973	20.56	0.342	0.936	1.056	30.71	0.972
Rice husk ash	29.41	18.5	0.942	6.47	0.417	0.994	6.182	17.39	0.967

6.3 Statistical Analysis

This was used in the present work due to acquired error as result of linearization of isotherm equation ***(Kaushal, 2016).*** The selection of best fitted model with experimental data has been explored. Accordingly, five error functions as discussed in the Chapter 5 were considered. For getting more specific correlation another hypothetical test, Chi-square test has been considered.

6.3.1 Error analysis

The isotherm parameters are evaluated by each error function. So the correlation between a particular parameter over the different error analysis is quite difficult. The normalization of approximation value can have a solution of this problem. Normalization is done by reducing the error value by the number of observations. By this process, the optimization of an isotherm model in consideration of describing experimental run can be achieved.

The normalization of error is an important steps towards finalizing the best model through error analysis. The normalized errors for each parameter set are presented in the Table-6.2.

Table 6.2: Error analysis data using five error functions for four inexpensive adsorbents

Error Equation	Neem Leaf Ash			Jack Fruit Leaf Ash		
	Langmuir	Freundlich	Temkin	Langmuir	Freundlich	Temkin
Sum of the squares of the error	**7.623**	**37.321**	**222.135**	**0.312**	**5.658**	**23.726**
Sum of the absolute errors	**5.291**	**13.431**	**34.254**	**0.432**	**5.044**	**12.145**
Average relative error function	**0.756**	**46.125**	**90.258**	**0.213**	**234.257**	**95.853**
Hybrid fractional error function	**0.327**	**54.252**	**135.247**	**0.509**	**18.0124**	**214.146**
Marquardt's percent standard deviation	**18.215**	**75.412**	**270.187**	**12.056**	**76.126**	**378.224**

Table 6.2: Error analysis data using five error functions for four inexpensive adsorbents (contd.)

Error Equation	Bagasse Ash			Rice Husk Ash		
	Langmuir	Freundlich	Temkin	Langmuir	Freundlich	Temkin
Sum of the squares of the error	**0.442**	**71.727**	**130.812**	**3.741**	**99.612**	**140.524**
Sum of the absolute errors	**1.227**	**14.125**	**24.105**	**3.451**	**34.742**	**24.315**
Average relative error function	**0.233**	**44.321**	**90.526**	**0.441**	**69.278**	**73.312**
Hybrid fractional error function	**5.571**	**10.521**	**135.743**	**2.052**	**16.452**	**109.824**
Marquardt's percent standard deviation	**16.721**	**64.813**	**270.523**	**12.512**	**60.121**	**219.154**

The normalized error value as shown in the Table 6.2 proves that Langmuir equation 'best follows' the equilibrium data for selected low cost sorbents. The similar conclusion is obtained from regression analysis of the isotherm model.

6.3.2 Chi-square values for various isotherm models

The normalization of error value by statistical hypothesis is more accurately performed by chi-square test. The dependency of this test regarding selection of optimized model is more than other error analysis data.

The result obtained from chi-square test, for all four adsorbents for isotherm models are depicted in the Table-6.3. It is observed that the sorption result follows Langmuir isotherm very well (minimum values ranging from 0.0001 to 1.054). The adsorption in case of jack fruit leaf ash shows the best result among the other three adsorbents. It can be also seen that Freundlich and Temkin isotherms also fit well for jack fruit leaf adsorbent (X^2 values are 1.73 and - 9.27 for Freundlich and Temkin isotherm respectively). For RHA adsorbent the Freundlich isotherm also fit moderately well with the minimum X^2 value of 11.2.

Table-6.3: Chi-square values

Adsorbate	Langmuir Isotherm	Freundlich Isotherm	Temkin Isotherm
Neem leaf ash	**1.054**	**21.452**	**165.524**
Jack fruit leaf ash	**0.004**	**6.542**	**8.115**
Bagasse fly ash	**0.412**	**265.214**	**254.221**
Rice husk ash	**0.107**	**11.242**	**661.147**

6.3.3 Separation Factor

Separation factor (R_L), is a dimensionless constant and is a good indicator of adsorption characteristics. R_L, can be expressed in the following equation:

$$R_L = \frac{1}{1+K_L C_0} \quad \text{-------------------------} \ (6.7)$$

where,

C_0 (milligram /Liter) = concentrations of the adsorbate (as the mixture of two dyes methylthioninium chloride blue and aniline green) and K_L (Liter/milligram) = Isotherm constant derived from Langmuir.

The R_L indicates sorption parameters. If R_L is in fraction (i.e. in between 0 and 1) the adsorption is considered favourable otherwise it will be unfavourable for R_L greater than unity. The zero value for R_L indicates irreversible process **(*Ajenifuja et al. 2017*).**

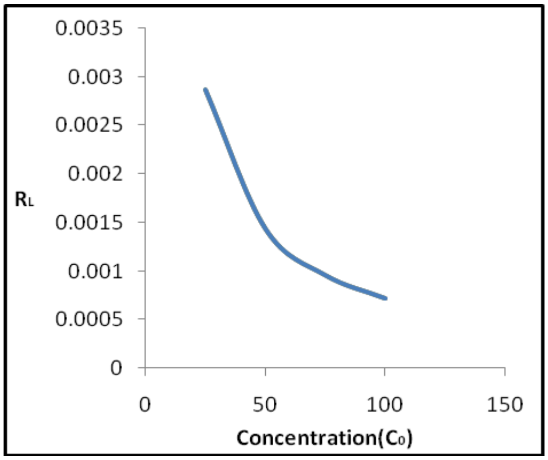

Fig. 6.33: Plot of separation factor at different concentration of dye mixtures at 27⁰ temperature for NLA

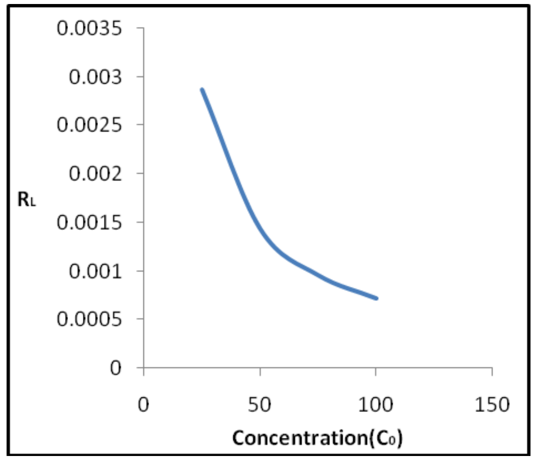

Fig. 6.34: Plot of separation factor at different concentration of dye mixture at 27⁰ temperature for JFLA

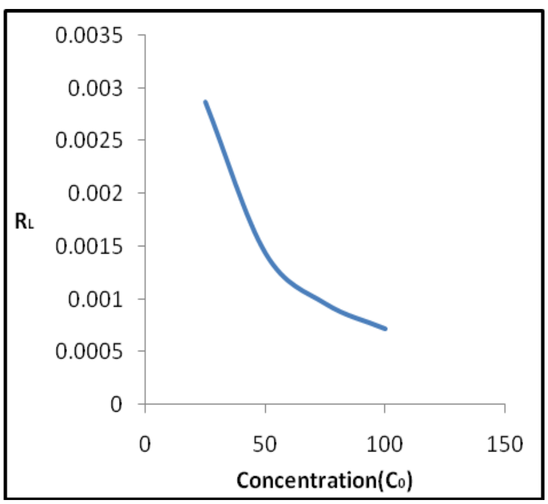

Fig. 6.35: Plot of separation factor at different concentration of dye mixture at 27⁰ temperature for BFA

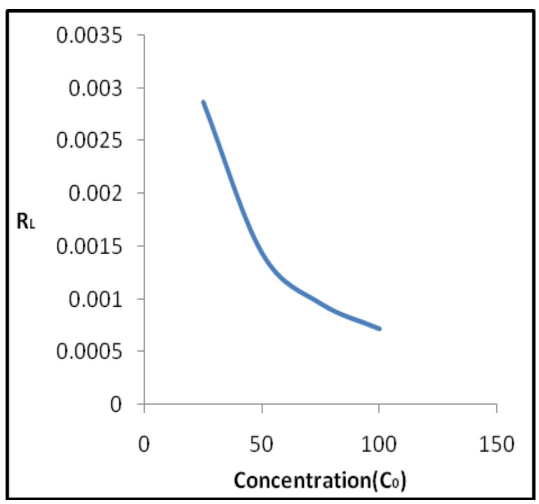

Fig. 6.36: Plot of separation factor at different concentration of dye mixture at 27⁰ temperature for RHA

The various plots of R_L versus concentration of dye mixture (C_0) at 27°C are shown in the Fig. 6.33 to Fig. 6.36. Separation factor (R_L) lies in the range 0.0005 to 0.003 for the neem leaf ash, 0.0007 to 0.003 for jack fruit leaf ash, 0.0008 to 0.0027 for bagasse fly ash and 0.0007 to 0.0028 for the rice husk ash which are less than unity, indicating that the sorption of selected two dyes on four low cost adsorbents are favorable process, and the data fits Langmuir isotherm model quite well.

6.4 Kinetic study

The study of reaction kinetics in the process of adsorption in an important tool to determine the operating condition of batch experiment **(*Fayazi et al. 2015*).** Kinetic study is developed on the concept of diffusion control. The solute uptake rate depends on the mass transfer within system and that can be described by solute residing time over the surface of the adsorbents **(*Fkih et al. 2020*).**
Thus two kinetic models pseudo first-order and second order equations have been analyzed very effectively for mixture of two cationic dyes onto four low cost sorbents **(*Oguz et al. 2005*).** The rate constants and deviation (Δ) of the laboratory result from the calculated ones are given in tabular form for all the four adsorbents.

6.4.1 Adsorbent: Neem leaf ash

Table 6.4: Reaction kinetics and deviation of NLA by pseudo-first-order

C_0 (mg/L)	Linear equation	R^2	q_e (mg/gm)		K_1 (min^{-1})	Δ (%)
			Expt.	Cal.		
25	Y=-0.004x+0.366	0.205	1.44	23.43	0.0092	87.41
50	Y=-0.008x+0.308	0.668	1.36	46.27	0.018	90.12
100	Y=-0.006x+0.494	0.675	1.63	90.58	0.014	94.05
150	Y=-0.008x+0.864	0.660	2.37	144.86	0.018	94.70

Table 6.5: Reaction kinetics and deviation of NLA by pseudo-second-order

C_0 (mg/L)	Linear equation	R^2	q_e (mg/gm)		K_2 (min^{-1})	Δ (%)
			Expt.	Cal.		
25	Y=0.042x+0.026	>0.999	23.8	23.43	$1.3x10^{-3}$	0.017
50	Y=0.021x+0.016	>0.999	47.60	46.27	$2.8x10^{-3}$	0.028
100	Y=0.011x+0.009	>0.998	90.92	90.58	$6.8x10^{-3}$	0.011
150	Y=0.006x+0.008	>0.999	166.67	144.86	$8.5x10^{-3}$	0.006

6.4.2 Adsorbent: Jack fruit leaf ash

Table 6.6 : Reaction kinetics and deviations of JFLA by pseudo-first-order

C_0 (mg/L)	Linear equation	R^2	q_e (mg/gm)		K_1 (min^{-1})	Δ (%)
			Expt.	Cal.		
25	Y=- .003x+0.672	0.477	2.95	23.43	0.023	87.41
50	Y=-.005x+1.074	0.715	4.57	46.27	0.023	90.12
100	Y=-.009x+1.647	0.878	5.39	90.58	0.018	94.05
150	Y=-.010x+2.295	0.891	7.67	144.86	0.021	94.70

Table 6.7: Reaction kinetics and deviation of JFLA by pseudo-second-order

C_0 (mg/L)	Linear equation	R^2	q_e (mg/gm)		K_2 (min^{-1})	Δ (%)
			Expt.	Cal.		
25	Y=0.039x+0.60	0.998	23.8	23.43	$2.98x10^{-3}$	-1.70
50	Y=0.020x+0.29	0.998	45.50	46.27	$1.36x10^{-3}$	1.67
100	Y=0.010x+0.18	0.997	90.90	90.58	$5.46x10^{-4}$	-0.35
150	Y=0.006x+0.21	0.990	156.25	144.86	$1.99x10^{-4}$	-7.86

6.4.3 Adsorbent: Bagasse fly ash

Table 6.8: Reaction kinetics and deviations of BFA by pseudo-first-order

C_0 (mg/L)	Linear equation	R^2	q_e (mg/gm)		K_1 (min^{-1})	Δ (%)
			Expt.	Cal.		
25	Y=-0.008x+0.060	0.421	1.06	23.43	0.018	95.47
50	Y=-0.005x+0.283	0.267	1.32	46.27	0.012	97.14
100	Y=-0.007x+0.496	0.675	1.64	90.58	0.016	98.19
150	Y=-0.010x+1.030	0.664	1.03	144.86	0.023	99.29

Table 6.9: Reaction kinetics and deviation of BFA by pseudo-second-order

C_0 (mg/L)	Linear equation	R^2	q_e (mg/gm)		K_2 (min^{-1})	Δ (%)
			Expt.	Cal.		
25	Y=0.041x+0.038	>0.999	24.39	23.43	$1.7x10^{-3}$	4.09
50	Y=0.022x+0.014	>0.999	45.45	46.27	$3.5x10^{-3}$	-1.77
100	Y=0.011x+0.0.007	>0.998	90.90	90.58	$4.4x10^{-3}$	0.35
150	Y=0.0062x+0.007	>0.999	161.30	144.86	$5.5x10^{-4}$	11.34

6.4.4 Adsorbent: Rice husk ash

Table 6.10: Reaction kinetics and deviations of RHA by pseudo-first-order

C_0 (mg/L)	Linear equation	R^2	q_e (mg/gm)		K_1 (min^{-1})	Δ (%)
			Expt.	Cal.		
25	Y=-0.022x+1.389	0.217	4.01	23.43	0.05	82.90
50	Y=-0.011x+1.744	0.851	5.72	46.27	0.03	87.60
100	Y=-0.013x+2.285	0.810	9.83	90.58	0.03	89.15
150	Y=-0.010x+2.191	0.711	8.94	144.86	0.02	93.82

Table 6.11: Reaction kinetics and deviation of RHA by pseudo-second-order

C_0 (mg/L)	Linear equation	R^2	q_e (mg/gm)		K_2 (min^{-1})	Δ (%)
			Expt.	Cal.		
25	Y=0.041x+0.038	0.999	23.80	23.43	$3.71x10^{-3}$	1.58
50	Y=0.022x+0.014	0.994	47.61	46.27	$9.12x10^{-4}$	2.90
100	Y=0.011x+0.0.007	0.986	90.90	90.58	$3.43x10^{-4}$	0.35
150	Y=0.0062x+0.007	0.970	142.85	144.86	$1.53x10^{-4}$	1.38

The adsorbed dye quantity may be evaluated by using pseudo reaction model of first and second order kinetic ***(Patil et al. 2015).*** This can be achieved for different concentrations as shown in the Table 6.4 to 6.11 above. The kinetic study results were compared with the experiment outcomes. The regression analysis has conducted from the equation 5.14 and 5.16 as discussed in Theoretical Discussion in chapter 5.

To determine different parameters using **pseudo-first-order model**, log(q_e-q_t) versus time(t) graph was drawn. This enables to calculate the kinetic constant (k_1) from slope and adsorbed density $(q_e)_{exp}$ from intercept respectively. The plot for the pseudo-first-order model, for four inexpensive sorbents explored in current study are shown in the Fig.6.37 to Fig.6.40**.** The theoretical q_e values, calculated by using best fit equation as shown in the graph, do not have reasonable matching as depicted in the Table 6.4, 6.6, 6.8 and 6.10. This reveals that the present study of adsorption not followed pseudo-first-order reaction.

The reaction kinetics is a function of initial sorption rate (h) as represented follows:

$$h = K_2 q_e^2 \text{ -------------------- } (6.8)$$

The important kinetic inputs like kinetics(h), model constant (K_2) and dye uptake (q_e) can be evaluated from this current study. The graphical representation between t/q_t and t are depicted in the Fig. 6.41 to 6.44. The deviation between experiment and calculated value for this kinetic is minimum for all four adsorbents. It indicates a better description of experimental result by second-order kinetic model as shown in the Table 6.5, 6.7, 6.9 and 6.11.

The increment in K_2 value resulting from increased solute concentrations as in the case of neem leaf ash and bagasse fly ash have also supported by few literature review (***Suresh, 2016***). At the same time most of the survey also suggested that decrease k_2 value for increasing adsorbate concentration which is experienced for jack fruit leaf and rice husk adsorbent in the present study.

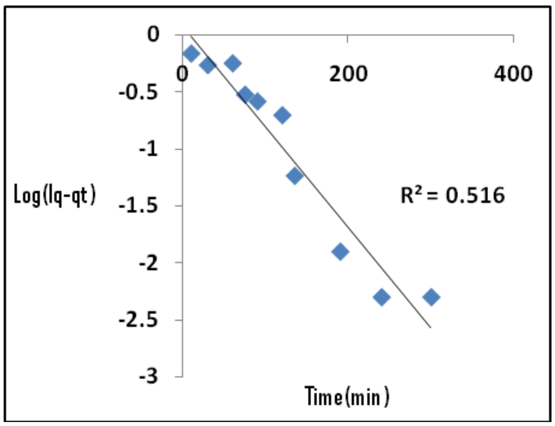

Fig. 6.37: Plot of pseudo-first-order model for NLA

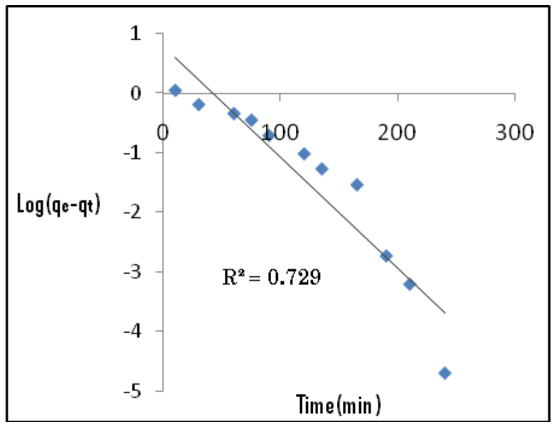

Fig. 6.38: Plot of pseudo-first-order model for JFLA

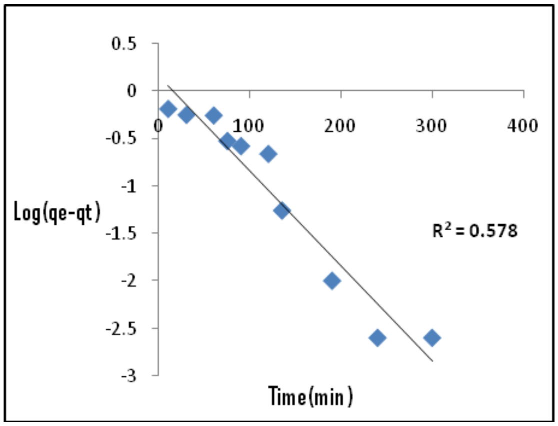

Fig. 6.39: Plot of pseudo-first-order model for BFA

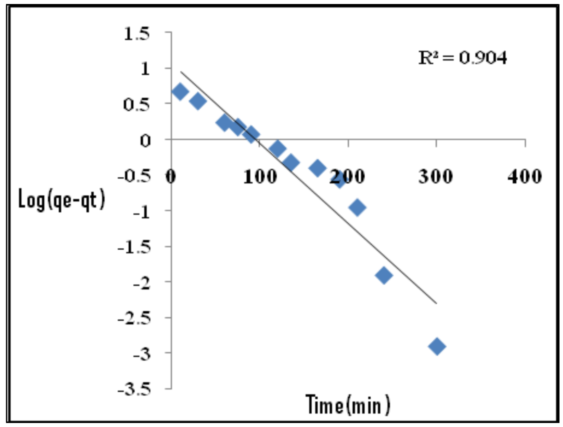

Fig. 6.40: Plot of pseudo-first-order model for RHA

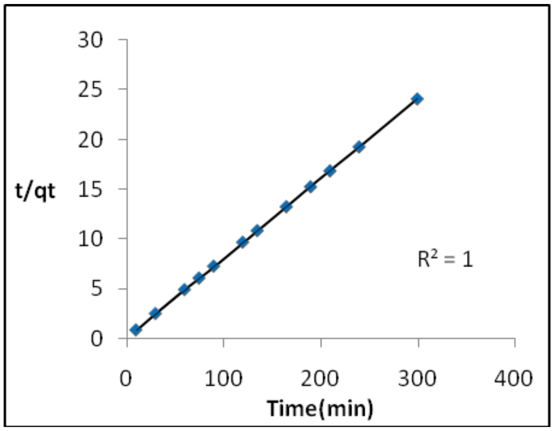

Fig. 6.41: Plot of pseudo-second-order model for NLA

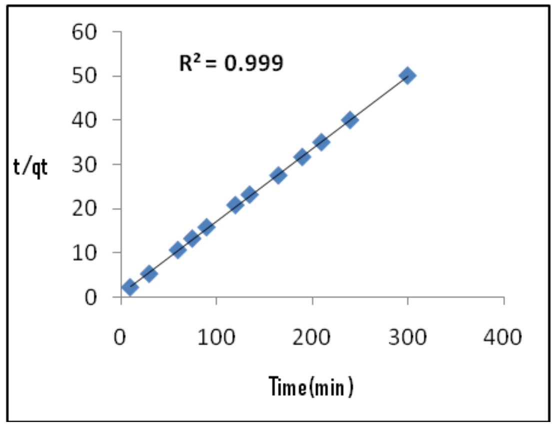

Fig. 6.42: Plot of pseudo-second-order model for JFLA

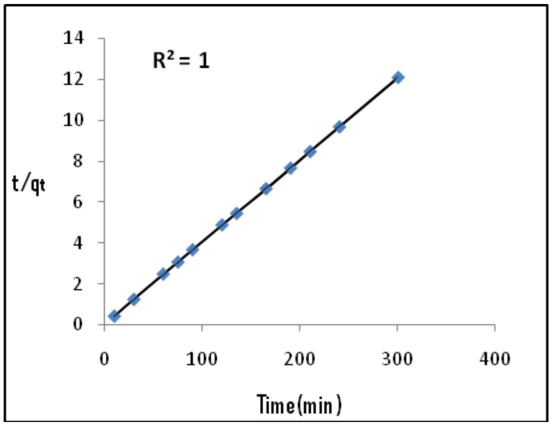

Fig. 6.43: Plot of pseudo-second-order model for BFA

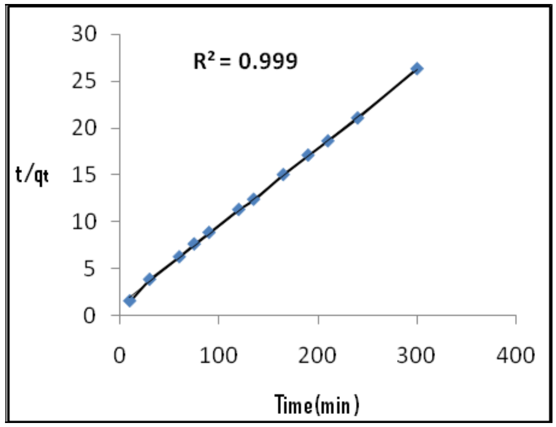

Fig. 6.44: Plot of pseudo-second-order model for RHA

The small bivariate correlation (R^2) from first-order model are depicted in the Fig 6.37 to Fig.6.40. On the other hand, the correlation coefficient (R^2) is >0.996 for all the cases, studied in this second-order model as shown in Fig.6.41 to Fig.6.44. The experimental results are given in the Table-33-40 in the Annexure. This ensures that second order kinetics fitted satisfactorily for the present adsorption study.

6.5 Thermodynamic Study on Adsorption of Cationic Dyes (MB and MG in Mixed Solution)

Mechanism of cationic dye adsorption adopted in the current research onto low cost adsorbent was also investigated using thermodynamic approach ***(Romero-Gonzalez et al. 2005).*** The four agricultural waste materials viz. Neem leaf ash, jack fruit leaf ash, bagasse fly ash and rice husk ash was selected as low cost adsorbents for this purpose. Thermodynamic study for an adsorption experiment helps to draw a conclusion regarding reaction spontaneity. The 'negative' Gibb's free energy value refers the spontaneous ,feasible process ***(Mangun et al. 1998)***. The change of enthalpy (ΔH^0) and change of entropy (ΔS^0) refers the randomness and nature of adsorption.

The innate energy change associated with the adsorption process can be expressed by the thermodynamic parameters in a better manner. The thermodynamic parameters are therefore, important tools for an entire approach of defining the adsorption chemistry.

The thermodynamic parameters such as **Gibb's free energy change (ΔG^0), enthalpy change (ΔH^0) and entropy change (ΔS^0)** are determined from the following equations:

$$\Delta G^0 = -RT\ln K_L \text{ -------------------------------- } (6.9)$$

$$\Delta G^0 = \Delta H^0 - T\Delta S^0 \text{ -------------------------------- } (6.10)$$

where,

R = the universal gas constant (8.314 $Jmol^{-1}$),

T = the absolute temperature in K,

and K_L = Langmuir isotherm constant

The Gibb's free energy (ΔG^0) versus temperature (T) generates a linear equation. The enthalpy (ΔH^0) and entropy (ΔS^0) change for thermodynamic study can be determined from the equation (6.10).

Modified Arrhenius equation considering the adsorbent surface coverage may the essential tool to find out the activation energy (E_a) and sticking probability (S^*) for thermodynamic study for adsorption.

$$\Theta = \left[1 - \frac{C_e}{C_i}\right] \text{-------------------------------- } (6.11)$$

where, C_e is the equilibrium concentration, C_i is the initial concentration of mixture of two dyes (adsorbates) and θ is the surface coverage **(*Batool et al. 2018*).**

The sticking probability represents the system of adsorption under investigation. The expression for activation energy and the sticking probability is given as:

$$\ln(1-\theta) = \ln S^* + \frac{1}{T}\left(\frac{E_a}{R}\right)$$ ---------------- (6.12)

E_a and S^* can be calculated as discussed in section 5.7 in the chapter 5 earlier and also depicted in (6.12) above.

6.5.1 Experimental Method

A fixed concentration of 25 mg/L for mixed dye solution was taken into a 250 ml bottle. The four adsorbents with their respective optimum dosages measured earlier were poured into the solution dyes. The bottles were shaken at a constant speed of 120 rpm at varying temperature of 290, 295, 300, 305 and 310 K respectively for 3 hours in water bath. After completion of the shaking, the bottles were taken out and the solution was filtered, centrifuged to get the clear supernatant. Effluent concentration has been find out by using spectrophotometer.

6.6 Determination of Thermodynamic Parameters

The calculation for thermodynamic parameters for different low cost adsorbents are depicted below:

6.6.1 Adsorbent: Neem Leaf Ash (NLA)

Outcomes from Langmuir Isotherm Study

Table 6.12: Determination of Gibb's free energy from Langmuir constant using NLA

T (K)	290	295	300	305	310
q_m (mgg^{-1})	37.8	39.6	40.0	41.2	42.6
K_L (Lmg^{-1})	11.3	12.7	13.9	14.8	15.6
ΔG^0 (KJmol^{-1}) *	-19.98	-20.96	-22.45	-23.37	-24.22
R^2	0.951	0.965	0.923	0.912	0.925

* $\Delta G^0 = -RT\ln(K_L)$

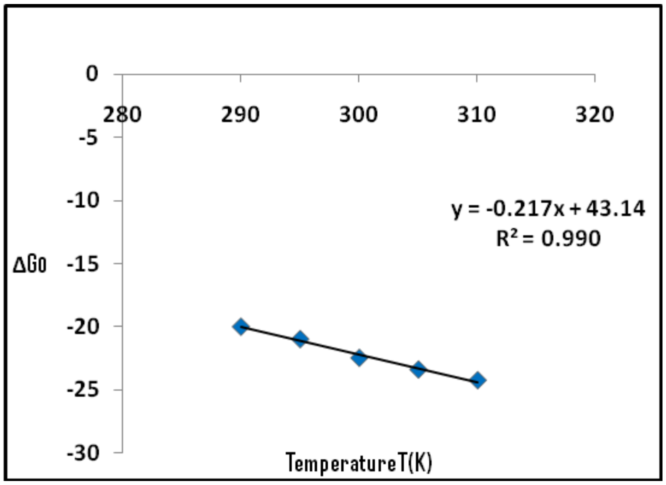

Fig. 6.45: Graphical representation between Free Energy and Temperature for NLA

The plot of ΔG^0 versus T generates the equation of the line Y = -0.217X + 43.14, which is compared with the standard equation $\Delta G^0 = -T\Delta S^0 + \Delta H^0$.

we have obtained,

Entropy Change = ΔS^0 = 0.217 $KJmol^{-1} K^{-1}$ and

Enthalpy Change = ΔH^0 = 43.14 $KJmol^{-1}$

6.6.2 Adsorbent: Jack Fruit Leaf Ash (JFLA)

Outcomes from Langmuir Isotherm Study

Table 6.13: Determination of Gibb's free energy from Langmuir constant using JFLA

T (K)	290	295	300	305	310
q_m (mgg^{-1})	18.43	19.78	20.41	22.50	23.17
K_L (Lmg^{-1})	12.6	13.2	14.0	15.6	16.7
ΔG^0 ($KJmol^{-1}$) *	-20.89	-21.64	-22.51	-23.83	-24.82
R^2	0.921	0.925	0.919	0.915	0.926

* $\Delta G^0 = -RTln(K_L)$

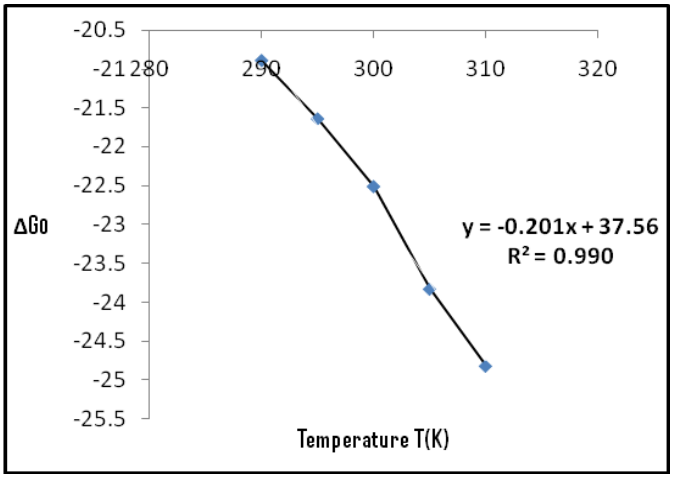

Fig.6.46: Graphical representation between Free Energy and Temperature for JFLA

The plot of ΔG^0 versus T generates the equation of the line Y= - 0.2017X + 37.56, which is compared with the standard equation $\Delta G^0 = -T\Delta S^0 + \Delta H^0$

From the slope and the intercept , we have

Entropy Change= ΔS^0 = 0.201 $KJmol^{-1} K^{-1}$ and

Enthalpy Change= ΔH^0 = 37.56 $KJmol^{-1}$

6.6.3. Adsorbent: Bagasse Fly Ash (BFA)

Outcomes from Langmuir Isotherm Study

Table 6.14: Determination of Gibb's free energy from Langmuir constant using BFA

T (K)	290	295	300	305	310
q_m (mgg^{-1})	49.20	50.83	52.63	54.16	55.92
K_L (Lmg^{-1})	6.87	7.52	8.46	9.24	10.51
ΔG^0 ($KJmol^{-1}$) *	-15.89	-16.92	-18.21	-19.28	-20.73
R^2	0.957	0.952	0.973	0.926	0.951

** $\Delta G^0 = -RT\ln(K_L)$*

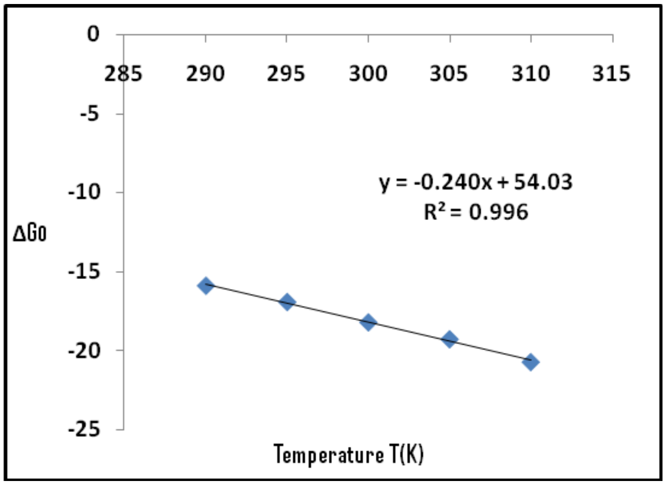

Fig.6.47: Graphical representation between Free Energy and Temperature for BFA

The plot of ΔG^0 versus T generates the equation of the line Y= - 0.2407X + 54.03, which is compared with the equation $\Delta G^0 = -T\Delta S^0 + \Delta H^0$.

As discussed earlier, we have

Entropy Change = ΔS^0 = 0.240 $KJmol^{-1}$ K^{-1} and

Enthalpy Change = ΔH^0 = 54.03 $KJmol^{-1}$

6.6.4 Adsorbent: Rice Husk Ash (RHA)

Outcomes from Langmuir Isotherm Study

Table 6.15: Determination of Gibb's free energy from Langmuir constant using RHA

T (K)	290	295	300	305	310
q_m (mgg^{-1})	37.8	39.6	40.0	41.2	42.6
K_L (Lmg^{-1})	11.3	12.7	13.9	14.8	15.6
ΔG^0 ($KJmol^{-1}$) *	-19.98	-20.96	-22.45	-23.37	-24.22
R^2	0.951	0.965	0.923	0.912	0.925

*$\Delta G^0 = -RTln(K_L)$

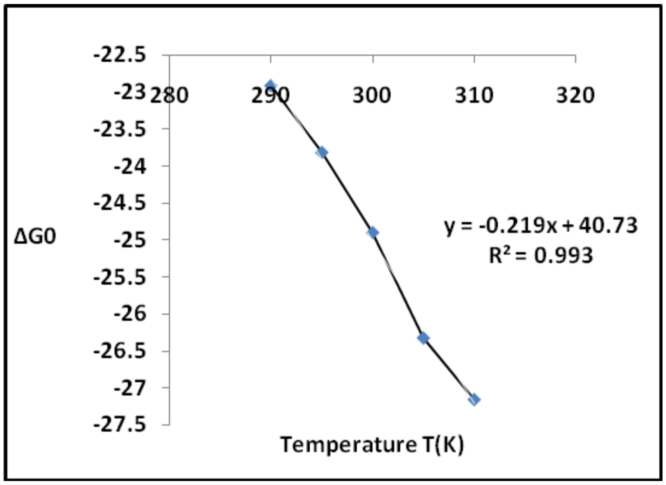

Fig. 6.48: Graphical representation between Free Energy and Temperature for RHA

Now the plot of ΔG^0 versus T generates the equation of the line Y = - 0.2407X + 54.03 which is compared with the equation $\Delta G^0 = -T\Delta S^0 + \Delta H^0$. From the slope and the intercept as discussed earlier we get

ΔS^0 = 0.218 KJmol^{-1} K^{-1} and

ΔH^0 = 40.36 KJmol^{-1}

The free energy (ΔG^0) is negative at all temperatures and it becomes progressively more negative with increasing temperature **in case of all four adsorbents**, implying amount of adsorbed dyes at equilibrium increased with temperature. Here, negative sign directs the process feasibility and spontaneity. It also indicates that strengthening of adsorbate-adsorbent interaction at higher temperature. The equilibrium constant is temperature dependent and the amount by which its value changes, is related to the standard change in enthalpy of the system.

The value of change of entropy (ΔS^0) is 0.217, 0.201, 0.240 and 0.218 KJmol^{-1}K^{-1}, for neem leaf ash, jack fruit leaf ash, bagasse fly ash and rice husk ash respectively. The positive and high entropy value suggests the growing disorder and randomness in solid-liquid boundary of dyes and that too for all the four adsorbents.

The magnitude of change in enthalpy (ΔH^0) for all the four adsorbents viz. neem leaf ash, jack fruit leaf ash, bagasse fly ash and rice husk ash are 43.14, 37.56, 54.03 and 40.36 $KJmol^{-1}$ respectively, which is clearly indicative of the chemisorptions process as we know that the physical adsorption is characterized by enthalpy value in the range of 5 to 20 $KJmol^{-1}$.

6.7 Determination of Activation Energy and Sticking Probability

6.7.1 Adsorbent: Neem Leaf Ash (NLA)

As $\theta = \left[1 - \frac{C_e}{C_i}\right]$, the θ values are calculated against different values of T as given in Table 6.16.

Table 6.16: Values of θ at different concentrations and temperature for NLA

C_0 (mgL^{-1})	290	295	300	305	310
25	0.9615	0.9712	0.9878	0.9895	0.9917
40	0.9602	0.9645	0.9724	0.9789	0.9824
50	0.9510	0.9578	0.9649	0.9680	0.9715
75	0.9382	0.9405	0.9489	0.9524	0.9610
100	0.8801	0.8872	0.8953	0.8994	0.9105

On plotting $\ln(1-\theta)$ versus 1/T for the different concentrations of dye mixture we get the five straight lines for the respective five dye concentrations as shown in the Fig. 6.49. The different equations generated for different concentrations are given below Table-6.17 below.

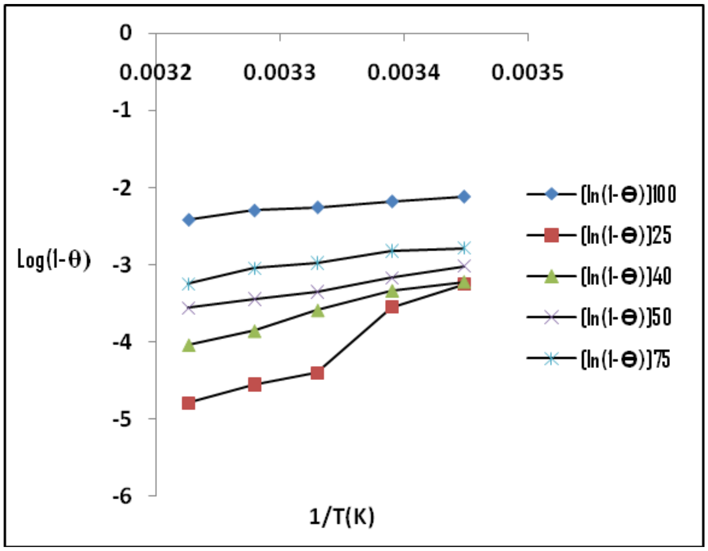

Fig. 6.49: Graphical representation of θ versus 1/T for NLA

Table 6.17: Equations for different concentrations of dyes for NLA

C_0	Equation	R^2
25	Y=4396X-18.77	0.939
40	Y= 3876X-16.50	0.981
50	Y=3458X-11.50	0.992
75	Y=2452X-9.818	0.945
100	Y=2356X-6,445	0.972

Comparing with the standard equation $\ln(1-\theta) = \ln S^* + \frac{1}{T}\left(\frac{E_a}{R}\right)$, activation energy and sticking probability for neem leaf ash are calculated as given in the Table-6.18.

Table 6.18: Activation Energy and Sticking Probability at different concentrations of Dyes for NLA

C_0	$E_a(KJmol^{-1})$	S*
25	36.55	$7.1x10^{-9}$
40	32.33	$6.8x10^{-7}$
50	28.44	$1.01x10^{-7}$
75	27.11	$5.4x10^{-5}$
100	22.44	$1.5x10^{-3}$

6.7.2 Adsorbent: Jack Fruit Leaf Ash (JFLA)

As $\theta = \left[1 - \frac{C_e}{C_i}\right]$, the θ values are calculated against different values of T as given in Table 6.19.

Table 6.19: Values of θ at different concentrations and temperature for JFLA

C_0 (mgL^{-1})	290	295	300	305	310
25	0.8774	0.8801	0.8853	0.8910	0.8987
40	0.7901	0.7992	0.8476	0.8916	0.9018
50	0.7814	0.7901	0.8220	0.8715	0.8914
75	0.7692	0.7714	0.7829	0.7992	0.8142
100	0.6015	0.6421	0.6546	0.6598	0.7214

On plotting $\ln(1-\theta)$ versus 1/T for the different concentrations of dye mixture we get the five straight lines for the respective five dye concentrations as shown in the Fig.6.50. The different equations generated for different concentrations are given Table-6.20 below.

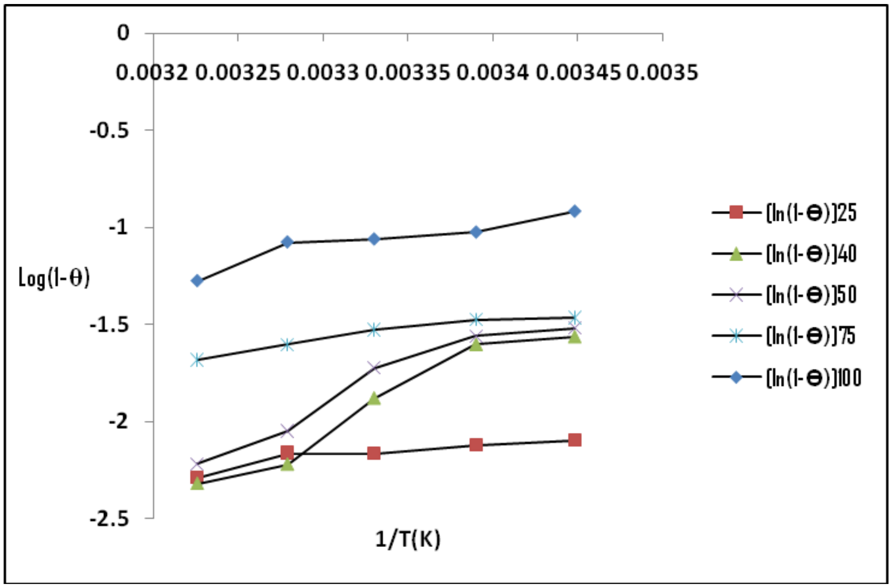

Fig. 6.50: Graphical representation of θ versus 1/T for JFLA

Table 6.20: Equations for different concentrations of dyes of JFLA

C_0	Equation	R^2
25	Y=2759.4X-4.70	0.815
40	Y= 3819X-14.65	0.914
50	Y=3382X-13.09	0.928
75	Y=3006X-4.909	0.924
100	Y=3374X-5.665	0.862

Comparing with the standard equation $\ln(1-\theta) = \ln S^* + \frac{1}{T}\left(\frac{E_a}{R}\right)$ activation energy and sticking probability for neem leaf ash are calculated as given in the Table-6.21 below.

Table 6.21: Activation Energy and Sticking Probability at different concentrations of dyes (JFLA)

C_0	$E_a(KJmol^{-1})$	S^*
25	24.62	$4.3x10^{-7}$
40	31.75	$4.1x10^{-6}$
50	28.12	$2.1x10^{-5}$
75	27.16	$1.82x10^{-5}$
100	30.42	$6.3x10^{-5}$

6.7.3 Adsorbent: Bagasse Fly Ash (BFA)

As $\theta = \left[1 - \frac{C_e}{C_i}\right]$, the θ values are calculated against different values of T as given in Table-6.22.

Table-6.22: Values of θ at different concentrations and temperature for BFA

C_0 (mgL^{-1})	290	295	300	305	310
25	0.9798	0.981	0.9854	0.9892	0.9902
40	0.9762	0.9801	0.9832	0.9871	0.9894
50	0.971	0.9782	0.9806	0.9856	0.9829
75	0.9001	0.9054	0.912	0.9157	0.9216
100	0.8705	0.8715	0.8804	0.8915	0.8995

On plotting $\ln(1-\theta)$ versus 1/T for the different concentrations of dye mixture we get the five straight lines for the respective five dye concentrations as shown in the Fig. 6.51. The different equations generated for different concentrations are given Table-6.23 below.

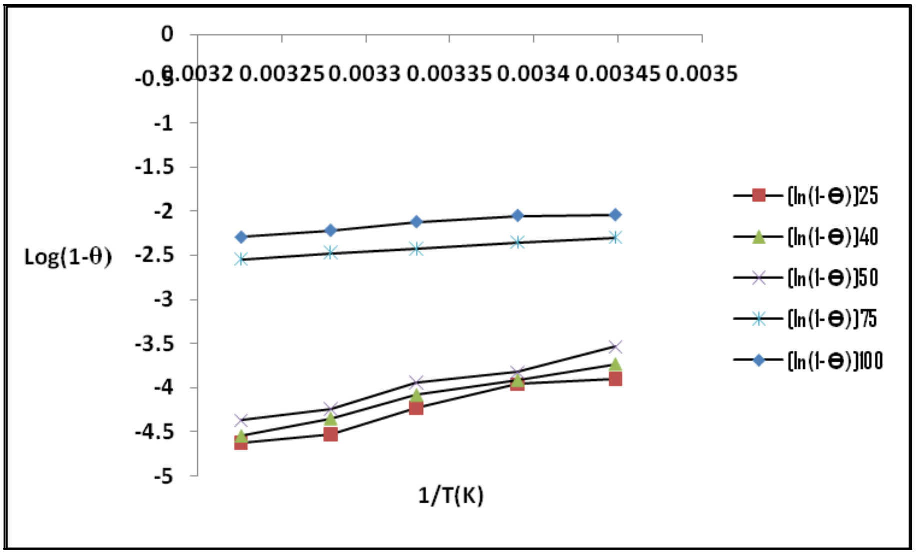

Fig. 6.51: Graphical representation of θ versus 1/T for BFA

Table 6.23: Equations for different concentrations of dyes (BFA)

C_0	Equation	R^2
25	Y=3614X-16.30	0.951
40	Y=3683X-16.41	0.988
50	Y=3670X-12.83	0.790
75	Y=3081X-6.027	0.995
100	Y=3209X-6,182	0.933

Comparing with the standard equation $\ln(1-\Theta) = \ln S^* + \frac{1}{T}\left(\frac{E_a}{R}\right)$ activation energy and sticking probability for bagasse fly ash are calculated as given in the Table-6.24 below.

Table 6.24: Activation Energy and Sticking Probability at different concentrations of dyes (BFA)

C_0	E_a ($KJmol^{-1}$)	S*
25	30.05	8.3×10^{-8}
40	30.62	7.5×10^{-8}
50	22.19	2.6×10^{-6}
75	28.98	2.4×10^{-3}
100	27.44	2.1×10^{-3}

6.7.4 Adsorbent: Rice Husk Ash (RHA)

As $\theta = \left[1 - \frac{C_e}{C_i}\right]$, the θ values are calculated against different values of T as given in Table-6.25.

Table 6.25: Values of θ at different concentrations and temperature for RHA

C_0 (mgL^{-1})	290	295	300	305	310
25	0.8756	0.8816	0.8853	0.8874	0.8992
40	0.7392	0.8412	0.8476	0.8712	0.8814
50	0.8104	0.8175	0.822	0.8293	0.8316
75	0.7723	0.7792	0.7829	0.7874	0.7892
100	0.6416	0.6472	0.6546	0.6592	0.6615

On plotting $\ln(1-\theta)$ versus 1/T for the different concentrations of dye mixture we obtain the five straight lines for the respective five dye concentrations as shown in the Fig.6.52. The different equations generated for different concentrations are given in the Table-6.26 below.

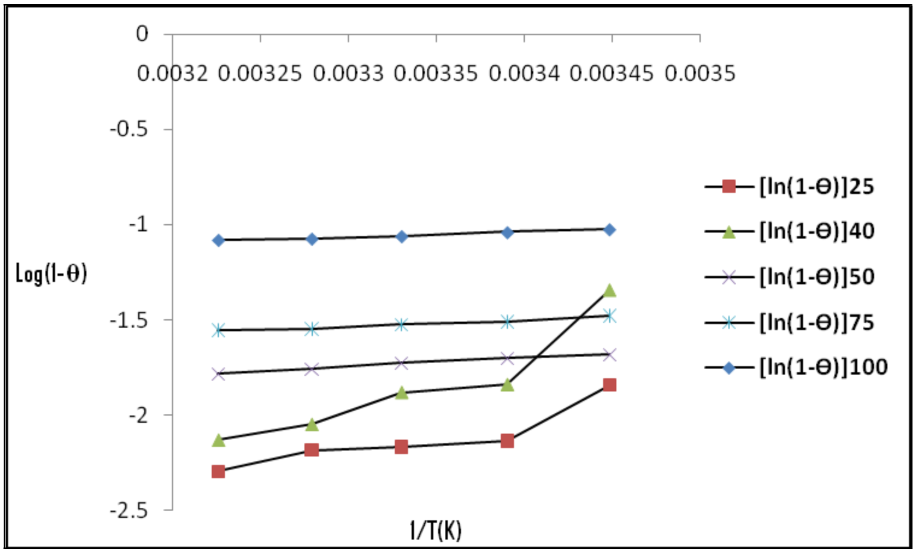

Fig.6.52: Graphical representation of θ versus 1/T for RHA

Table 6.26: Equations for different concentrations of dyes for RHA

C_0	Equation	R^2
25	Y=3744X-4.986	0.90
40	Y=3236X-12.64	0.857
50	Y=3547.8X-3.554	0.982
75	Y=3417.2X-2.682	0.971
100	Y=3619.2X-1.955	0.979

Comparing with the standard equation $\ln(1-\theta) = \ln S^* + \frac{1}{T}\left(\frac{E_a}{R}\right)$ activation energy and sticking probability for neem leaf ash are calculated as given in the Table-6.27.

Table 6.27: Activation Energy and Sticking Probability at different concentrations of dyes (RHA)

C_0	E_a ($KJmol^{-1}$)	S^*
25	27.02	$6.8x10^{-3}$
40	26.904	$3.3x10^{-6}$
50	24.55	$2.8x10^{-5}$
75	32.89	$6.8x10^{-5}$
100	34.24	$3.6x10^{-4}$

The values for activation energy ranging from 34.24 to 22.19 $KJmol^{-1}$ confirms the chemisorptions process as observed in the earlier findings in the case of change in enthalpy (ΔH^0). High activation energy is the important characteristics of chemisorptions as the heat is evolved in the adsorption.
The sticking probability (S^*) values are very much less than unity indicates the probability of attachment of the dye molecules over surface of the adsorbent is very high. The S^* value ranging from $7.1x10^{-9}$ to $2.1x10^{-3}$ indicates preferable process which depends on the system temperature.

The adsorption of two basic dyes in adsorbate, using four low cost adsorbents viz. neem leaf ash, jack fruit leaf ash, bagasse fly ash and rice husk ash is influenced by the temperature. The adsorption capacity was directly proportional to temperature. By using the Langmuir constant obtained from respective isotherm, thermodynamic parameter (ΔG^0) is evaluated. The parameter value for ΔH^0 and ΔS^0 are obtained exploring the relation between ΔG^0 and absolute temperature as shown earlier. The negative ΔG^0 and positive ΔH^0 value supports the spontaneity and type of adsorption onto low cost adsorbents. The adsorption reaction is endothermic ***(Stephen, 2018).*** The positive value of ΔS^0 indicates growing randomness at phase differential during the adsorption of dyes onto the adsorbents. The adsorption process is possessed high activation energy. This coupled with the magnitude of the enthalpy of adsorption is clearly established that the adsorption process can be characterized as chemisorptions ***(Gorzin et al. 2018).***

6.8 Column adsorption of dye mixture using low cost adsorbents

Fixed bed columns study have wide industrial application. In practice the columns are used for the adsorption of pollutants from wastewaters. Batch study has certain limitations in respect of describing the process and disseminating important information.

Therefore, it is very important to conduct down-flow tests using columns before obtaining design models ***(Isiuku et al. 2018).*** The design models target the time prediction of column operation before replacement or regeneration becomes necessary. The influence of different process inputs such as adsorbents bed height, inlet concentrations, influent flow rate and pH of the dye mixture have been explored. The experimental outcomes have been used in the different well known and widely used models viz. Thomas, Yoon-Nelson, Adams-Bohart and Bed Depth Service Time (BDST) for checking accuracy of the study ***(Chen et al. 2016).***

6.8.1 Effect of different operating parameters

6.8.1.1 Influence of adsorbent bed height

The influence of adsorbent height for all four low cost adsorbents onto breakthrough curve was investigated in the present study. The height 4, 6 and 8 cm was selected. The adsorbate flow rate and concentration was kept fixed during the experiment respectively as 25 mg/L and 7.5 mL/min. The similar effects for other concentrations of 50, 75 and 100 mg/L were also studied for all four adsorbents. As the bed height increases, breakthrough time also increased and decreased in breakthrough slope of the curve is noted. The movement of mass transfer zone is from entrance to exist end within the column. As the bed height increases for unaltered adsorbate concentration, the zone of mass transfer also increased. So the time of travel by the adsorbate solute gets more time before exhaustion of the bed. Naturally breakthrough time is lengthened. For higher bed depth, the increased adsorbent mass would provide more active binding sites leading to an effective sorption. The experimental breakthrough curve obtained in the present study followed an ideal adsorption process with perfect 'S' shaped curve profile.

The percentage removal increased from 80 to 90% when bed depth increased from 4 to 8 cm at 25 mg/l for the neem leaf ash as shown in the Fig. 6.53(a). The percentage removal for the varying bed depth for other fixed concentrations such as 50, 75 and 100 mg/l also shows the same trend as given from Fig. 6.53(b) to 6.53(d). The experimental results for effect of bed height for NLA are given in the Table- 41-44 in the Annexure.

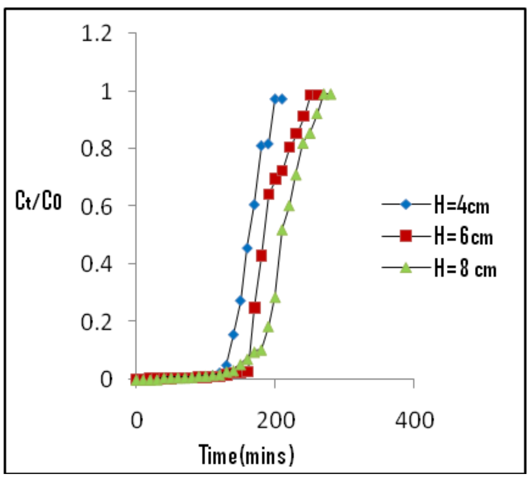

Fig. 6.53(a): Influence of bed depth at C_0 = 25 milligram/Lit and q= 7.5 milliliter/min

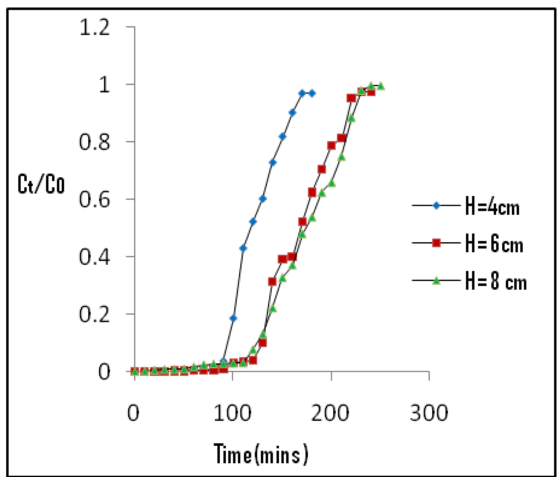

Fig. 6.53(b): Influence of bed depth at C_0 = 50 milligram/Lit and q= 7.5 milliliter/min

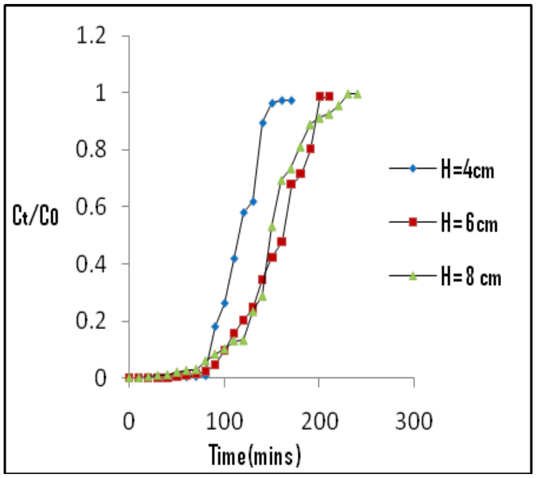

Fig. 6.53(c): Influence of bed depth at C_0 = 75 milligram/Lit and q= 7.5 milliliter/min

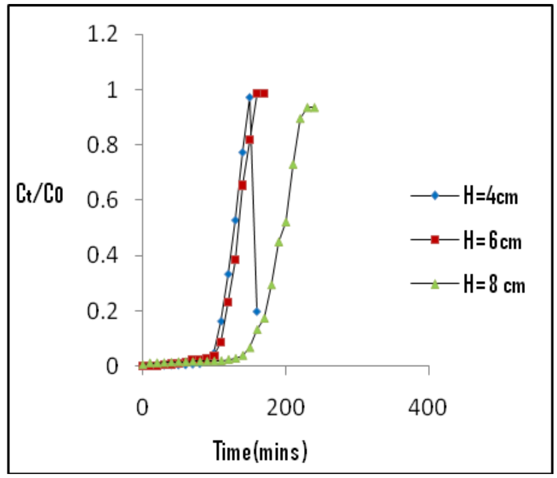

Fig. 6.53(d): Influence of bed depth at C_0= 100 milligram/Lit and q= 7.5 milliliter/min

For the jack fruit leaf ash as shown in the Fig.6.54 (a) to 6.55 (d), the adsorption system shows 'S' shaped profile properly. For sorbent depth increased from 4 to 8 cm, percentage elimination increased 75 to 95%. The laboratory results pertaining to the study on the effect of adsorbent for JLFA are given in the Table-47-50 in the Annexure.

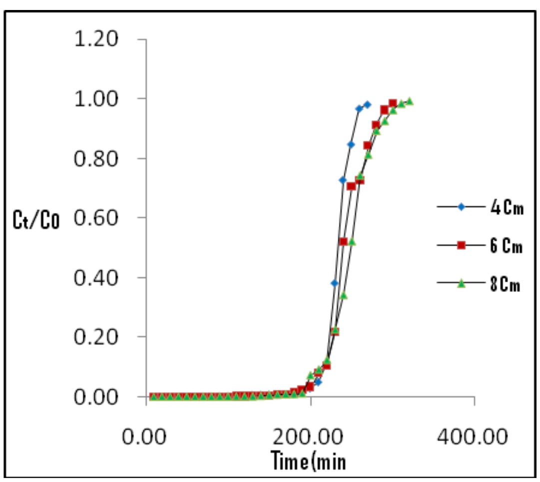

Fig.6.54(a): Influence of bed depth at C_0 = 25 milligram/Lit and q= 7.5 milliliter/min

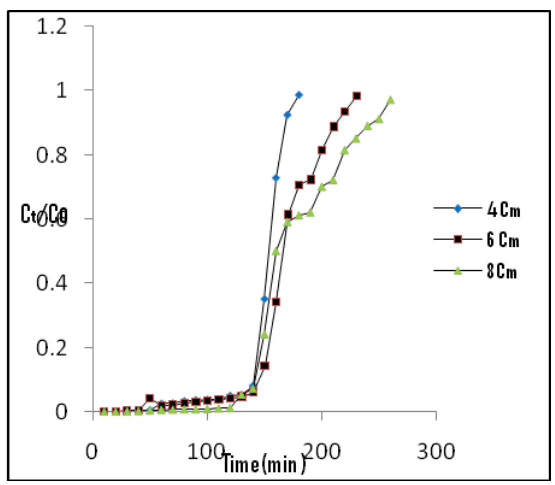

Fig.6.54(b): Influence of bed depth at C_0 = 50 milligram/Lit and q = 7.5 milliliter/min

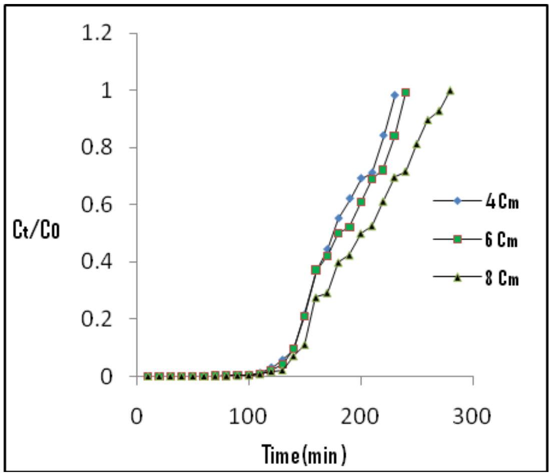

Fig.6.54(c): Influence of bed depth at C_0 = 75 milligram/Lit and q= 7.5 milliliter/min

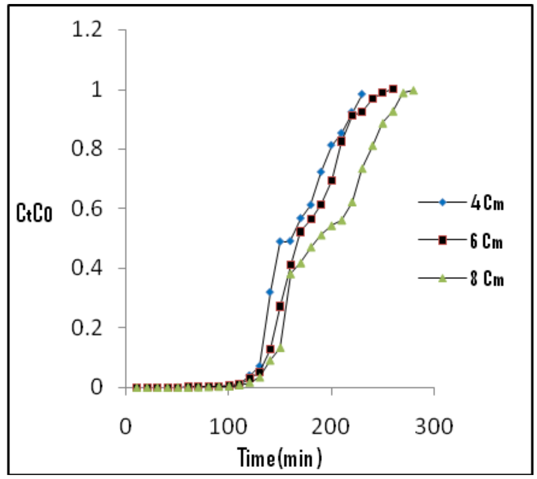

Fig.6.54 (d): Influence of bed depth at C_0 = 100 milligram/Lit and q = 7.5 milliliter/min

For bagasse fly ash as shown in the Fig. 6.55(a) to Fig. 6.55(d), increment of percentage elimination of MB and MG was recorded as 55 to 70 % for same increment of bed height. Overall removal percentage of dye mixture at all four concentrations varied within 60 to 70%, which reveals the limitations regarding the effectiveness of the adsorbent. The experimental results are given in the Table 53-56 in the Annexure.

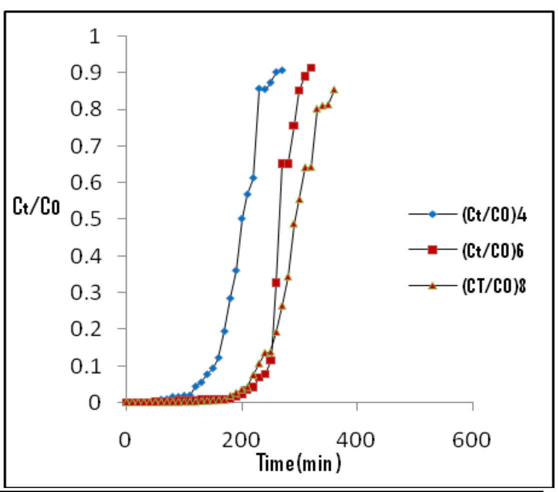

Fig. 6.55(a): Influence of bed depth at C_0 = 25 milligram/Lit and q= 7.5 milliliter/min

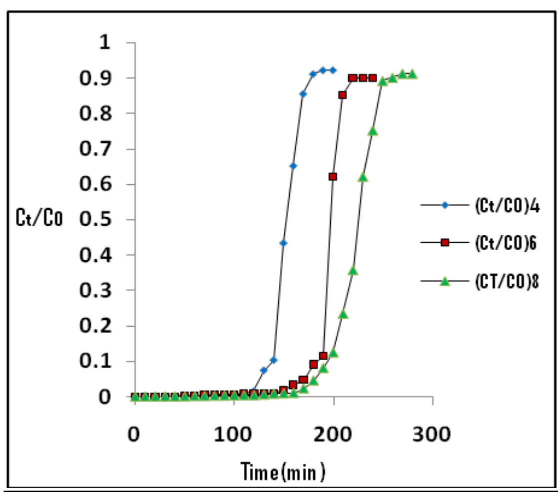

Fig. 6.55(b): Influence of bed depth at C_0 = 50 milligram/Lit and q = 7.5 milliliter/min

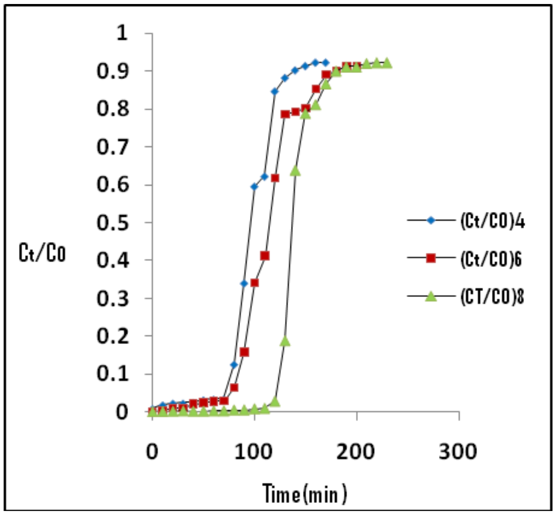

Fig. 6.55(c): Influence of bed depth at C_0 = 75 milligram/Lit and q = 7.5 milliliter/min

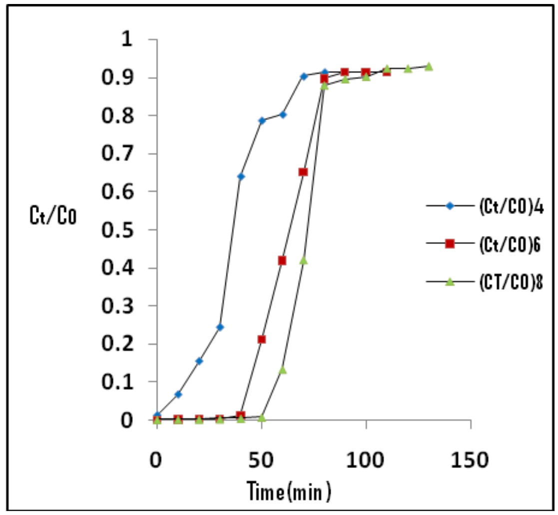

Fig. 6.55(d): Influence of bed depth at C_0 = 100 milligram/Lit and q = 7.5 milliliter/min

In the Fig. 6.56(a) to Fig. 6.56(d), with **rice husk ash** the percent removal for dye mixture increased from 55 to 75% when adsorbent bed height increased from 4 to 8 cm. Breakthrough profile for all the concentrations follows smooth 'S' curve. The experimental outcomes are given in the Table-59-62 in the Annexure.

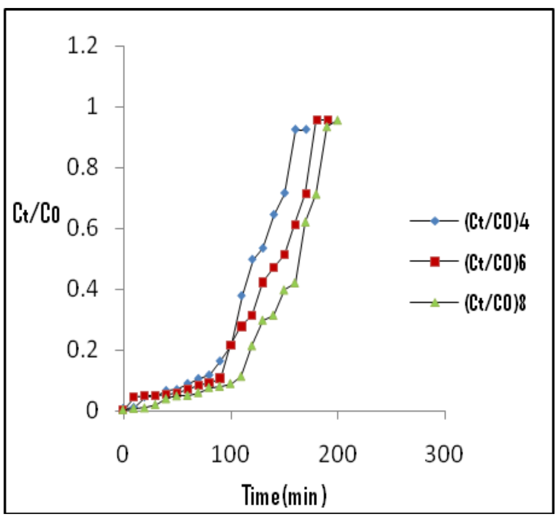

Fig. 6.56(a): Influence of bed depth at C_0 = 25 milligram/Lit and q = 7.5 milliliter/min

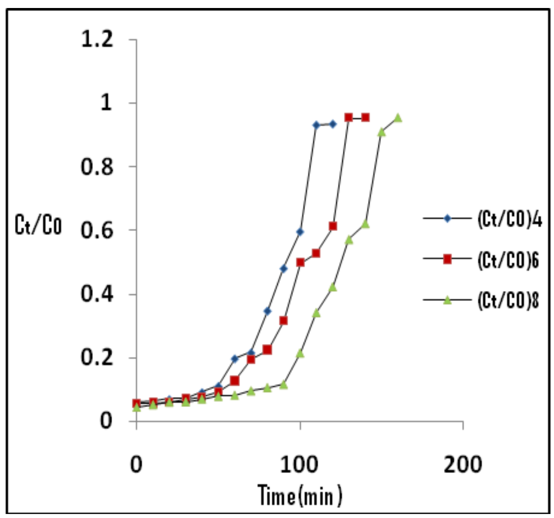

Fig.6.56(b): Influence of bed depth at C_0 = 50 milligram/Lit and q = 7.5 milliliter/min

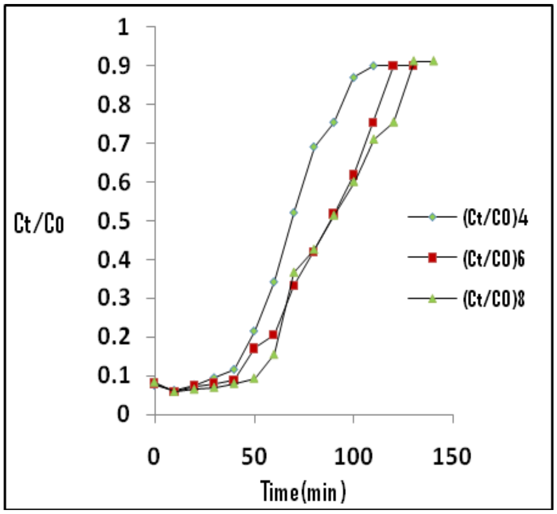

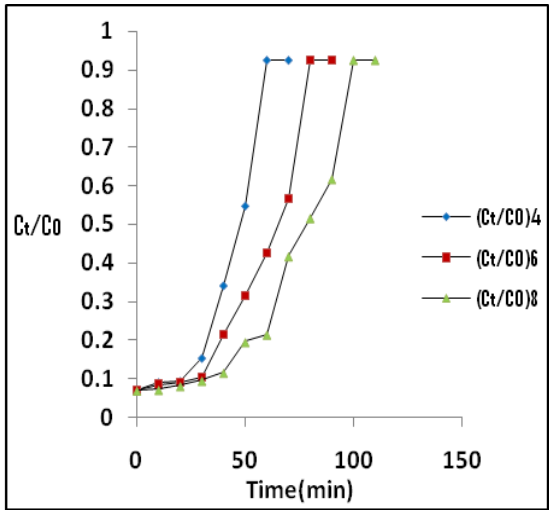

Fig. 6.56(c): Influence of bed depth at C_0 = 75 milligram/Lit and q = 7.5 milliliter/min

Fig. 6.56(d): Influence of bed depth at C_0 = 100 milligram/Lit and q = 7.5 milliliter/min

6.8.1.2 Effect of initial feed concentration

The adsorbate solution has been taken in four different concentration as 25, 50, 75 and 100 mg/L for this study. The adsorbent height, pH and rate of flow have been kept fixed as 4cm, 7 and 7.5 mL/min respectively during performing the experiment. At lesser concentration, the driving force within mass transfer zone was smaller and as a result breakthrough time has lengthened. So the exclusion of dye molecule was less at higher adsorbate concentration. The variation of inlet concentration under other fixed bed depths of 6 and 8 cm was also investigated separately for the present study for all the four adsorbents. The plots for effect of initial concentration at 4 cm bed depth were only shown for all four adsorbents.

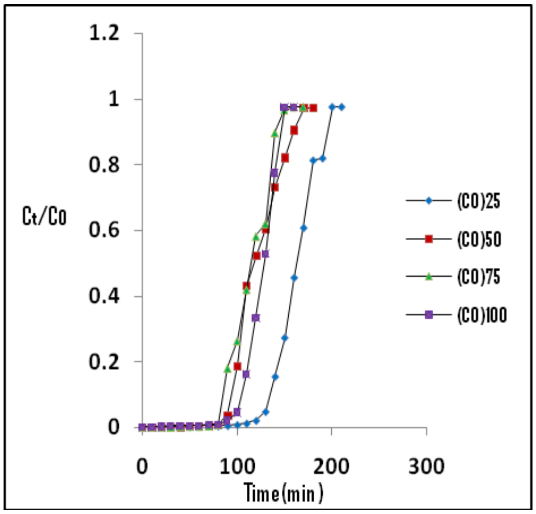

Fig.6.57(a): Influence of initial concentration for NLA at H = 4 cm, q = 7.5 milliliter/min

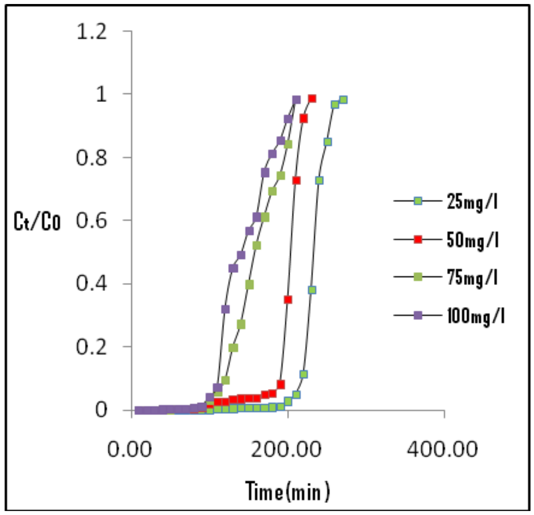

Fig.6.57(b): Influence of initial concentration for JFLA at H = 4 cm, q = 7.5 milliliter/min .

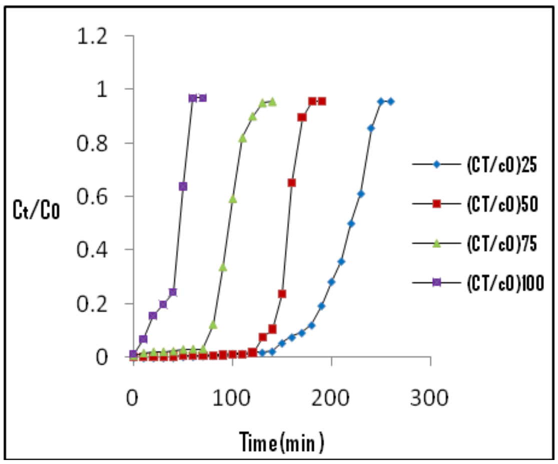

Fig.6.57(c): Influence of initial concentration for BFA at H = 4 cm, q = 7.5 milliliter/min

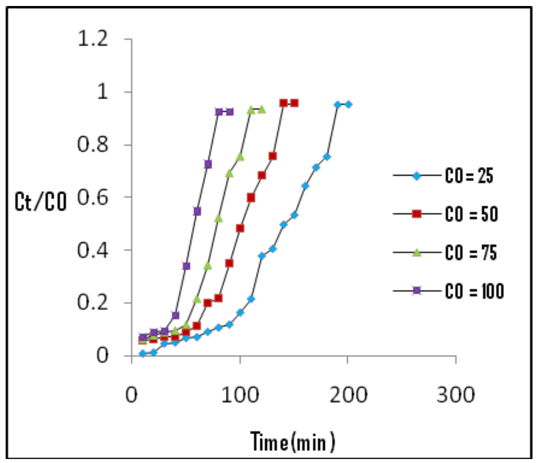

Fig.6.57(d): Influence of initial concentration for RHA at H = 4 cm, q = 7.5 milliliter/min

The effect of initial feed concentration on breakthrough time for all four adsorbents are shown in the Fig-6.57(a) to (d). The experimental results are given in the Table 53 to 56 in the Annexure. The variation of initial feed concentration was 25 to 100 mg/L for entire study. The noticeable decreased from 210 to 170 minutes for NLA and JFLA was recorded. The decrease in breakthrough time from

180 to 50 minutes was observed for RHA under same situation. BFLA was also exhibited same trend as shown above.

6.8.1.3 Influence of inlet flow

Adsorbate solution inflow rate has been taken in three different values as 5, 7.5 and 10 mL/min for this study. The pH, column depth and feed concentration have been fixed as 7, 4cm and 100 mg/L during performing laboratory experiment. Graphical representations of experimental results are furnished in the fig. 6.58(a) to 6.58(d). The breakthrough took place faster at higher flow rate. Mass transfer is flow rate dependent. So the adsorbent exhaustion time is decreased by the increasing flow rate. The laboratory outcomes for studying the effect of inflow rate onto adsorption are given in the Table 45, 51, 57 and 63 in the Annexure.

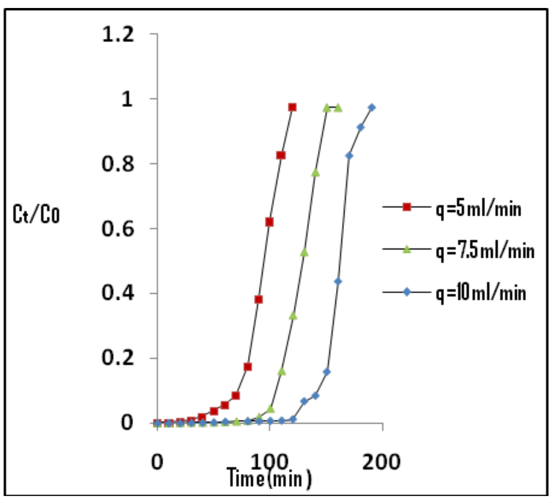

Fig. 6.58 (a): Influence of flow rate onto neem leaf ash at H = 4 cm, C_0 = 100 milligram/L

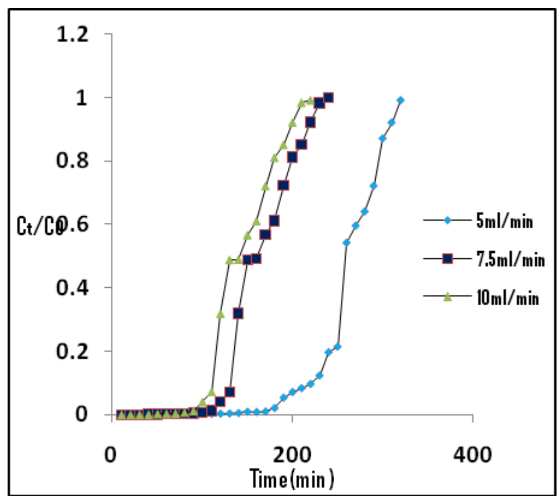

Fig.6.58(b): Influence of flow rate onto jack fruit leaf ash at H = 4 cm, C_0 = 100 milligram/L

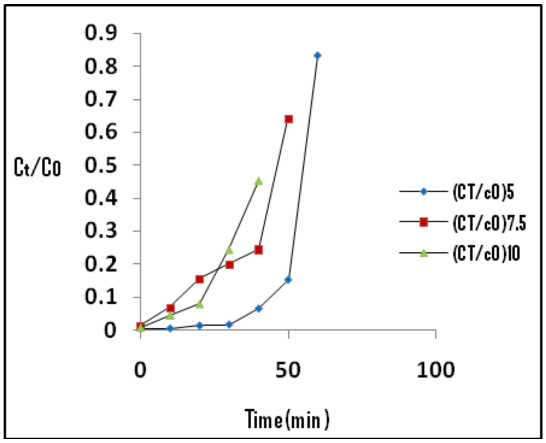

Fig.6.58(c): Influence of flow rate onto bagasse fly ash at H = 4 cm, C_0 = 100 milligram/L

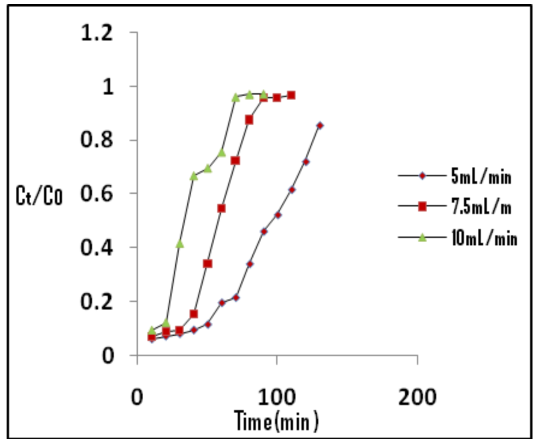

Fig.6.58(d): Influence of flow rate onto rice husk ash at H = 4 cm, C_0= 100 milligram/L

The exhaustion time at high flow rate for the BFA and the RHA was found less than 50 minutes. The exhaustion time by using neem leaf ash reduced from 180 minutes to 70 minutes for reduction in flow rate from 10 to 5 mL/min. The saturation time of jack fruit leaf ash was reduced from 200 min to 70 min during reduction of flow rate from 10 to 5 mL/min. As flow rate increased, time for breakthrough was reduced sharply. At low flow rate of dye mixture, the adsorbent had greater contact time (residence time) with the dye molecules, resulting higher removal efficiency. The adsorbed capacity and breakthrough slope has been governed by mass transfer concept. The experimental breakthrough curve obtained in this study followed ideal 'S' shaped profile as shown in the Fig. 6.58(a) to 6.58 (d).

6.8.1.4 Influence of pH on adsorption

Adsorbate pH has significant effect on biosorption. This is n important factor to be considered in current research. The influence of pH on dye removal problem onto all four low cost adsorbents is shown in the Fig. 6.59(a) to 6.59 (d) below. The percentage removal increased with adsorbate pH as recorded. Surface phenomenon is responsible for this as discussed in the section 5.2.1 in chapter 5.

This can be explained by the following equations also as below:

$$Adsorbent - OH \quad Adsorbent -= O^- + H^+ \quad \text{-------------------------(6.13)}$$

$$Adsorbent - OH + H^+ \quad Adsorbent - - -\xrightarrow{yields} OH_2^+ \quad \text{------------(6.14)}$$

The basic nature at higher pH and acidic nature in lower pH exposure is depicted in the above equation 6.13 and 6.14 respectively. Thus better adsorption of basic dyes MB and MG at high pH was achieved as also recorded in the investigation. The pH of dye mixture was controlled as 4.1 and 9.2 by adding buffer casuals.

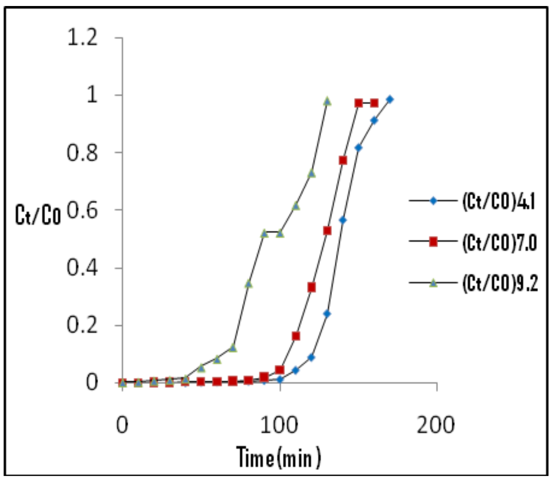

Fig.6.59(a): Influence of pH of the adsorbate at H= 4m, C_0= 100 milligram/Lit, and q = 7.5 milliliter/min for NLA

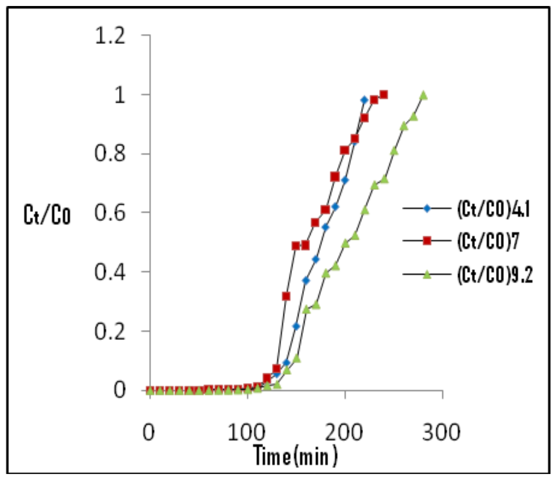

Fig. 6.59(b): Influence of pH of the adsorbate at H = 4m, C_0 = 100 milligram/Lit, and q = 7.5 milliliter/min for JFLA

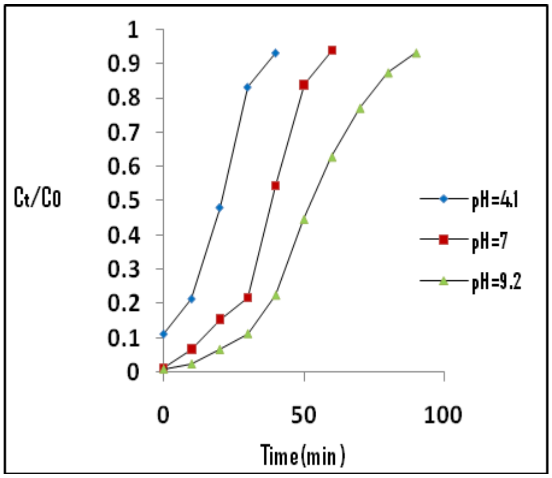

Fig. 6.59(c): Influence of pH of the adsorbate at H = 4m C_0 = 100 milligram/Lit and q = 7.5 mL/min for BFA

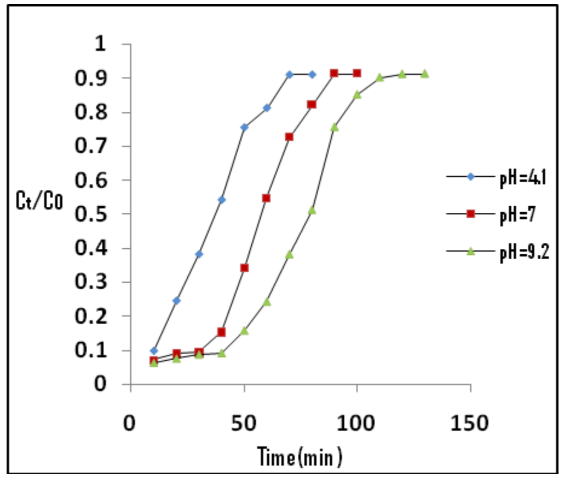

Fig. 6.59(d): Influence of pH of the adsorbate at H= 4m, C_0 = 100 milligram/Lit and q = 7.5 mL/min for RHA

The effect of pH onto adsorption is given in the Fig. 6.59(a) to 6.59(d) for all the four adsorbents. The breakthrough time increased from 30 to 100 minutes for neem leaf ash for an increase in pH from 4.1 to 9.2. The breakthrough time in case of bagasse fly ash increased greatly from 20 to 100 minutes for an increase in pH from 4.1 to 9.2. The same trend was also observed for the other two adsorbents jack fruit leaf and rice husk ash. The experimental results are given in the Table 46, 52,58 and 64 in the Annexure.

6.9 Model Study under Dynamic Column

Column study has better performance for describing the adsorption process compared to batch study. Due to this superiority of column study, it has wide industrial application. The liner flow of adsorbent with little dispersion in the column information appropriately.

The performance of column can be validated by the conventional mathematical models. This dynamic analysis has been conducted by using Thomas, Yoon-Nelson, Adams-Bohart and Bed Depth Service Time model. Present study deals with finding the most appropriate model, describing the experiment in better manner and also find the maximum dye uptake for the present investigation. Thus the model study for dynamic column mode operation judge the accuracy of the laboratory scale performance and determine the sorption capacity from the different kinetic parameters so evaluated ***(Adebowale et al. 2014).***

Analysis of dynamic operation in column mode

The loading pattern of dye molecules (adsorbate) that to be removed from the aqueous solution of mixture of two widely used basic dyes in dynamic column s function of influent-effluent ratio. The percentage removal of dye depends on the time for bed exhaustion ***(Guibalet al. 1995).***

Maximum capacity for adsorption q_{total} (in mg per gm of adsorbent) under fixed initial concentration and flow rate can be evaluated from area of the curve generated from adsorbate concentration versus volume of the effluent(V) and is evaluated from equation below:

$$q_{total} = \int_{v=0}^{V=V_{total}} C_{ad}\, dV \text{ ------}(6.15)$$

The equilibrium uptake ($q_{eq(exp)}$) is calculated in terms of total adsorbent present in column as :

$$q_{eq}(exp) = \frac{q_{total}}{X} \text{ -------- } (6.16)$$

where X = total mass of the adsorbent in column (gm).

Adsorbate amount passing to the column (W_{total}) is calculated from equation (6.16) as

$$W_{total} = C_0 V_{total} \text{ --------}(6.17)$$

Removal percentage (Y) of adsorbate is the ratio of maximum column capacity (q_{total}) to total adsorbate passed to the column (W_{total}) during experiment.

It can be given as:

$$Y = \frac{q_{total}}{W_{total}} \times 100 \text{ ------}(6.18)$$

The appropriateness of column design needs accurate outlining of breakthrough curve. The maximum dye uptake is the key factor for model description ***(L. Yang et al. 2014).***

In order to ascertain the most befitting model, standard error should be determined ***(Hasfalina etal. 2015).***

The expression for Standard deviation (SS) is as follows :

$$SS = \frac{\sum[(C_t/C_0)_c - (C_t/C_0)_e]^2}{N} \text{---------------------------} (6.19)$$

where, $(Ct/C_0)c$ = calculated effluent to influent ratio of dynamic models and $(Ct/C_0)e$ = calculated effluent to influent ratio from experiment N = the number of the observations

6.9.1 Application of Thomas Model

Thomas model envisage exchanging of ion of heterogeneity in a flowing object ***(Thomas, 1944).*** The plug flowing following Langmuir isotherm consideration is the basis of this model ***(Futiam et al. 2011).*** It rejects the dispersion of axial flow observing reversible kinetics having degree of second order ***(Hassan et al. 2010)***. Thomas model can be given as:

$$\frac{C_t}{C_0} = \frac{1}{1 + exp\left[\frac{K_{Th}}{Q(q_0X \quad C_0V_{eff})}\right]} ------(6.20)$$

The parameters are explained in the chapter 5.

Rewriting by using logarithm of equation 6.20, we get,

$$\ln\left(\frac{C_0}{C_t} - 1\right) = \frac{K_{Th}q_0X}{Q} - \frac{K_{Th}C_0}{Q}V_{eff} --------(6.21)$$

The experimental outcomes are feeded into the Thomas model equation . The C_t/C_0 ratio varies from 0.0001 to 0.99 as discussed in the Theoretical Discussion chapter earlier and respective Tables are given in the Annexure also. The model constant and dye uptake can be determined from the equation ***(Thomas, 1944).***

In the present investigation, Thomas model has been utilized taking laboratory outcomes as inputs under all varying parameters of four adsorbents considered.

The regression coefficient value (R^2) was obtained using nonlinear regression analysis, recorded as more than 0.95.

6.9.1.1 Adsorbent: Neem leaf ash

In the case of neem leaf ash (NLA) as adsorbent, during augmentation of concentration 25 to 100 mg/L, q_e increased from 12.36 to 50.58 mg/g and K_{Th} decreased from 1.0 to 0.30 mL/mg.min as shown in the Table 6.28. Similar trend has also recorded for higher bed depth of 6 and 8 cm. This is because of more driving force of higher concentration of dye mixture resulted in better uptake of dye molecules.

During increment of flow rate (from 5 to 10 mL/min) q_e decreased from 39.51 to 34.35 mg/g but K_{Th} increased from 0.57 to 0.81 mL/mg.min.

For the increased bed height from 4 to 8 cm, q_e increased and K_{Th} decreased significantly.

For both the two case, the mass transfer zone plays a significant ole and availability of more active sites are responsible for increased dye uptake.

The higher feed concentration and bed height with lower adsorbate flow rate developed adsorption capacity.

The higher R^2 value and smaller SS value also supported the feasibility of the model. The experimental data described well by this model.

No significant effect was observed for pH variation over the model values during study. The values of respective parameters are shown in the Table 65(a) to 65(c). The model graphs are shown in the Fig.11 to 15 in the Annexure-II.

Table 6.28: Thomas model factors, bivariate correlation and standard deviation using neem leaf ash

C_0 (mg/L)	q (mL/min)	H (cm)	pH	q_e (mg /gm)	K_{Th} (mg /mL.min)	R^2	SS (10^{-3})
25	7.5	4	7.0	12.36	1.0	0.994	1.42
100	7.5	4	7.0	50.58	0.30	0.986	1.18
100	5.0	4	7.0	39.51	0.57	0.992	2.04
100	10.0	4	7.0	34.35	0.81	0.997	1.45
25	7.5	8	7.0	61.51	0.13	0.981	1.62
100	7.5	4	4.1	43.56	0.68	0.993	1.71
100	7.5	4	9.2	44.34	0.71	0.998	1.66

6.9.1.2 Adsorbent: Jack fruit leaf ash

In the case of jack fruit leaf ash as adsorbent, under increasing initial concentration the q_e value increased sharply from 14.09 to 37.12 mg/g and K_{Th} decreased from 1.56 to 0.57 mL/mg.min indicating better agreement with the column experiment as shown in the Table 6.29. But when the flow rate onto the adsorbent column was increased, q_e value decreased insignificantly and K_{Th} value increased inconsistently as shown in the Table 6.29. Thus, at lower flow rate the model described the process of adsorption not so well for JFLA. Furthermore, as the bed depth augmented from 4 to 8 cm at 25 mg/l, the q_e value augmented marginally from 12.20 to 12.72 mg/g, while K_{Th} decreased slightly from 1.72 to 1.64 mL/mg.min. The coefficient of regression (R^2) and SS value ranged from 0.84 to 0.98 and $1.12x10^{-3}$ to $1.52x10^{-3}$, as depicted in the Table 6.29. During the variation of pH, the solid phase concentration increased from 16.65 to 40.80 mg/g and rate constant reduced from 0.25 to 0.16 mL/mg.min. Higher coefficient of regression value suggested good agreement of experimental data. The experimental results are depicted in the Table-68(a)-68(c) in Annexure-I. The graphical representations are given in the Fig.-16 to Fig.-21 in the Annexure-II.

Table 6.29: Thomas model factors, bivariate correlation and standard deviation using jack fruit leaf ash

C_0 (mg/L)	q (mL/min)	H (cm)	pH	q_e (mg /gm)	K_{Th} (mg /mL.min)	R^2	SS (10^{-3})
25	7.5	4	7.0	14.09	1.56	0.989	1.12
100	7.5	4	7.0	37.12	0.57	0.991	1.23
100	5.0	4	7.0	4.60	1.66	0.998	1.14
100	10.0	4	7.0	3.73	2.55	0.988	1.24
25	7.5	8	7.0	12.72	1.64	0.982	1.23
100	7.5	4	4.1	16.65	0.25	0.997	1.52
100	7.5	4	9.2	40.89	0.16	0.967	1.23

6.9.1.3 Adsorbent: Bagasse fly ash

In the case of BFA as adsorbent, the increase in initial concentration from 25 to 75 mg/L, q_e increased sharply from 9.56 to 21.53 mg/g while the K_{Th} value decreased from 1.36 to 0.59 mL/mg.min. Thereafter no significant increase or decrease was noticed for those two parameters at higher value of 100 mg/L. Thus, model described the experiment well up to a value of 75 mg/L. Flow rate augmentation from 5 to 10 mL/min, the q_e value reduced from 13.65 to 11.78 mg/g, whereas K_{Th} increased insignificantly from 0.82 to 1.86 mg/mL.min, indicating marginal agreement with the experimental data.

As bed height increased from 4 to 8 cm, q_e raised from 9.56 to 13.78 mg/g and K_{Th} decreased from 1.36 to 0.84 mL/mg.min. Thus, at higher concentration (upto 75 mg/L) and bed depth and at lesser flow rate the adsorption capacity increased consistently as observed also from the laboratory experimental results shown in the Table 6.30. For increase in pH, the uptake of dye mixture also increased significantly indicating good agreement of the model. The coefficient of regression value (R^2) lies between 0.929 to 0.998, indicating better conformity with the experimental data [Table 71(a)-71(c) in the Annexure-I]. The graphical representations are given in the Fig.-22 to Fig.-28 in the Annexure-II.

Table 6.30: Thomas model factors, bivariate correlation and standard deviation using bagasse fly ash

C_0 (mg/L)	q (mL/min)	H (cm)	pH	q_e (mg /gm)	K_{Th} (mg /mL.min)	R^2	SS (10^{-3})
25	7.5	4	7.0	9.56	1.36	0.989	1.12
100	7.5	4	7.0	21.53	0.59	0.987	2.14
75	7.5	4	7.0	22.38	0.57	0.991	1.23
100	5.0	4	7.0	13.65	0.82	0.998	1.14
100	10.0	4	7.0	11.78	1.86	0.988	1.24
25	7.5	8	7.0	12.72	1.64	0.982	1.23
100	7.5	4	4.1	5.011	0.86	0.997	1.52
100	7.5	4	9.2	14.31	0.56	0.967	1.23

6.9.1.4 Adsorbent: Rice husk ash

In case of RHA, when the initial concentration raised from 25 to 100 mg/L, the equilibrium uptake q_e, increased significantly from 10.98 to 18.77 mg/g and K_{Th} decreased from 0.52 to 0.23. Raising of flow rate from 5 to 10 mL/min, q_e decreased from 27.79 to 6.04 mg/g and K_{Th} increased from 0.15 to 0.31 mL/mg.min quite significantly. For the increased bed depth up to 6 cm, the sharp change in model parameters was recorded. Thus at higher concentration and bed depth up to 6 cm with low flow rate the model described the experimental value very well. During incrementing adsorbate pH from 4.1 to 9.2, the solid phase concentration also increased from 7.18 to 12.32 mg/g and the K_{Th} value decreased from 0.34 to 0.26 indicating favourable adsorption of two basic dyes in aqueous mixture. The model data are depicted in the Table 6.31. The adsorption results are given in the Table

74(a) to 74(c) in the Annexure-I. The graphical representations are given in the Fig.-29 to Fig.-35 in the Annexure-II.

Table 6.31: Thomas model factors, bivariate correlation and standard deviation using rice husk ash

C_0 (mg/L)	q (mL/min)	H (cm)	pH	q_e (mg /gm)	K_{Th} (mg /mL.min)	R^2	SS (10^{-3})
25	7.5	4	7.0	10.98	0.52	0.974	1.52
100	7.5	4	7.0	18.77	0.23	0.932	2.74
100	5.0	4	7.0	27.79	0.15	0.978	0.14
100	10.0	4	7.0	6.04	0.31	0.998	1.14
25	7.5	8	7.0	18.77	0.23	0.980	1.30
100	7.5	4	4.1	7.18	0.34	0.992	1.02
100	7.5	4	9.2	12.32	0.26	0.967	2.13

6.9.2 Application of Yoon-Nelson Model

The Yoon-Nelson model ***(Yoon and Nelson, 1984)*** is considered to be the most simplest approach in dynamic adsorption study. There is no consideration is made regarding the character of adsorbate solution or the adsorbent in use. This model also cannot consider even the surface morphology of the adsorbent ***(Yao et al. 2010).*** This model is only consider that the reducing probability of solute adsorption directly relates to the probability of its breakthrough upon adsorbent molecules

The expression for Yoon-Nelson model is :

$ln(C_t / C_0 - C_t) = K_{YN} - K_{YN}T$ ------------------------(6.22)

The model parameters in the equation are discussed in section 5.9.3 of chapter 5.

The graphical representation of $\ln[C_t/(C_0 - C_t)]$ versus sampling time (t) as per equation (6.22) generates a straight line at different bed heights (4, 6, 8 cm), different concentrations (25, 50, 75, 100 mgL^{-1}), different flow rates (5.5, 7.5, 10.0 mLmin^{-1}) and different pH of the solution mixture (4.1, 7.0 9.2). This model was applied to investigate the column performance. Evaluation of rate constant (K_{YN}) and Γ, for 50% breakthrough time was done to predict the laboratory performance.

6.9.2.1 Adsorbent: Neem leaf ash

The concentration increased of adsorbate solution as laboratory study from 25 to 100 mg/L, model constant increased marginally but **Γ** value decreased significantly from 136.51 to 49.85 L/min as shown in the Table 6.32. This is due to the fact that increase in competition in between the solute in the adsorbate with that on the active sites results increased uptake rate. This trend was also observed for higher bed depth such as 6 and 8 cm.

During increment of bed depth (4 to 8 cm), K_{YN} value decreased marginally from 0.031 to 0.025 L/min where as **Γ** value sharply increased from 136.51 to 181.60 min. Increasing flow into the column bed from 5 to 10 mL/min, K_{YN} increased from 0.013 to 0.029 L/min and 50% breakthrough time decreased from to 237.30 to 88.31 min. This is because of the lesser contact between sorbent and solute within packed column during increased flow rate condition resulting in reduction of breakthrough time for adsorption.

As pH increased, rate constant raised from 0.032 to 0.040 L/min and breakthrough time reduced from 67.86 to 111.34 min indicating favourable adsorption of basic dyes. The model parameters are depicted in the Table 6.32. The experimental results are given in the Table 65(a) to 65(c) in the Annexure-I.

Table 6.32: Yoon-Nelson model factors, bivariate correlation and standard deviation using neem leaf ash

C_0 (mg/L)	q (mL/min)	H (cm)	pH	Γ (min)	K_{YN} (L/min)	R^2	SS (10^{-3})
25	7.5	4	7.0	136.51	0.031	0.984	3.52
100	7.5	4	7.0	49.85	0.061	0.952	2.12
100	5.0	4	7.0	237.30	0.013	0.928	1.26
100	10.0	4	7.0	88.31	0.039	0.956	1.17
25	7.5	8	7.0	181.60	0.025	0.992	1.14
100	7.5	4	4.1	67.86	0.032	0.996	1.48
100	7.5	4	9.2	111.34	0.040	0.997	1.21

6.9.2.2 Adsorbent: Jack fruit leaf ash

In the case of the adsorbent jack fruit leaf ash, a significant increase in the rate constant (K_{YN}) and decreased in 50% breakthrough time were observed during augmenting in concentration and flow rate. The model constant decreased but 50% breakthrough time for adsorption increased during raising of bed height from 4 to 8 cm. For increasing pH of the mixed dye solution, rate constant increased with the decreasing breakthrough time as given in the Table 6.33.

Table 6.33: Yoon-Nelson model factors, bivariate correlation and standard deviation using jack fruit leaf ash

C_0 (mg/L)	q (mL/min)	H (cm)	pH	Γ (min)	K_{YN} (L/min)	R^2	SS (10^{-3})
25	7.5	4	7.0	167.02	0.053	0.974	1.52
100	7.5	4	7.0	0.077	115.61	0.932	2.74
100	5.0	4	7.0	165.84	0.057	0.978	0.14
100	10.0	4	7.0	91.79	0.081	0.998	1.14
25	7.5	8	7.0	206.0	0.039	0.980	1.30
100	7.5	4	4.1	71.97	0.052	0.992	1.02
100	7.5	4	9.2	172.85	0.079	0.967	2.13

6.9.2.3 Adsorbent: Bagasse fly ash

In the case of Bagasse fly ash, the increment in rate constant was marginal whereas the breakthrough time for 50% adsorption was significant for the increased initial concentration and inflow rate in adsorption study. In case of increased bed depth the rate constant had significant value upto a depth of 6 cm. At high bed depth of 8 cm, the increment was insignificant as recorded in the Table 6.34. The breakthrough time for 50% adsorption with the increased bed depth was very significant. The adsorption capacity was increased for getting more active sites at higher adsorbent height. The effect on the model parameters for increased pH of the mixture solution had no significant effect, which indicates that the model could not describe the experiment well in case of pH variation (Table 72(a) to 72(c) in Annexure-I).

Table 6.34: Yoon-Nelson model factors, bivariate correlation and standard deviation using bagasse fly ash

C_0 (mg/L)	q (mL/min)	H (cm)	pH	Γ (min)	K_{YN} (L/min)	R^2	SS (10^{-3})
25	7.5	4	7.0	229.42	0.036	0.996	1.02
100	7.5	4	7.0	46.23	0.045	0.915	1.14
100	5.0	4	7.0	270.20	0.052	0.947	2.01
100	10.0	4	7.0	166.40	0.057	0.984	0.24
25	7.5	6	7.0	379	0.022	0.980	1.30
25	7.5	8	7.0	402	0.021	0.994	1.17
100	7.5	4	4.1	167.63	0.059	0.987	2.14
100	7.5	4	9.2	170.59	0.053	0.998	1.17

6.9.2.4 Adsorbent: Rice husk ash

Using RHA as adsorbent, the increment of rate constant and reduction of 50% breakthrough time was significant for the increased initial concentration and inflow rate in adsorption study. The model outputs are shown in the Table-6.35. The reason behind this observations are same as discussed for other adsorbents.

In case of increased bed depth and adsorbate pH, reduction in rate constant was insignificant though significant increment of 50% breakthrough time (136.51 to 181.60 min) was observed. This is because of the fact that increased bed provides more active sites and greater adsorbate pH creates favorable environment for basic dye adsorption. The experimental results are given in the Table 75(a) to 75(c) in the Annexure-I.

Table 6.35: Yoon-Nelson model factors, bivariate correlation and standard deviation using rice husk ash

C_0 (mg/L)	q (mL/min)	H (cm)	pH	Γ (min)	K_{YN} (L/min)	R^2	SS (10^{-3})
25	7.5	4	7.0	136.51	0.031	0.971	1.14
100	7.5	4	7.0	49.85	0.061	0.995	1.53
100	5.0	4	7.0	237.30	0.013	0.997	1.11
100	10.0	4	7.0	88.31	0.039	0.992	2.14
25	7.5	8	7.0	181.60	0.027	0.986	2.41
100	7.5	4	4.1	67.86	0.040	0.987	1.44
100	7.5	4	9.2	111.34	0.032	0.993	1.59

6.9.3 Application of Adams-Bohart Model

Bohart and Adams has established an equation between time (t) and influent-effluent ratio (C_t/C_0) during studying of chlorine adsorption onto activated carbon. From the early stage to later part of the experiment the adsorbent has been changed from gaseous to liquid phase. In this context they changed the concept of pressure for gaseous state into concentration for liquid phase of the adsorbate. ***Oulman*** suggested Bed Depth Service Time (BDST) model for simulating analysis during his experiment over granular activated carbon (GAC) beds.

Certain assumptions were put forth to analyze the model equations ***Sarala (2017)***:

1. The concentrations are weak.
2. When $t \rightarrow \infty$; $q \rightarrow N_0$ where N_0 represents the maximum adsorption capacity.
3. Mass transfer is slower down the rate of adsorption.

The model has been proposed during adsorption using granulated activated carbon as:

$C_0/C_t = 1/(1+e^{a-bt})$---------------------------(6.23)

The linear equation of Adams-Bohart model is given by:

$\ln(C_0/C_t-1) = (KN_0x/u)- KC_0\ t$ -----------------------------(6.24)

The model unknowns have been discussed in the section 5.9.4 of chapter 5.

The model parameters K_{AB} and N_0 was find out by equating from the intercept and slope using equation (6.24). They can be worked out under different feed concentrations (25, 50, 75 and 100 mg/L); different bed depths (4, 6 and 8 cm); different flow rates (5.0, 7.5 and 10 mL/min); and different pH of the dye solution (4.1, 7 and 9.2).

6.9.3.1 Adsorbent: Neem leaf ash

The Adams-Bohart model was explored to predict the experimental performance conducted through column mode operation. For the increase of initial feed concentration from 25 to 100 mg/L, the model constant raised from 0.53 to 1.6 L/mg.min and maximum adsorptive ability increased marginally from 0.0005 to 0.0015 mg/L for neem leaf ash. During increment of flow rate from 5 to 10 mL/min, model constant increased significantly from 0.46 to 0.61 L/mg.min, where as adsorption decreased marginally from 1.83 to 1.06 L/mg.min due to less residence time of the dye molecules. Raising bed depth from 4 to 8 cm, model constant decreased insignificantly from 1.6 to 1.12 L/mg.min, and adsorption capacity got developed from 0.0005 to 0.0009 mg/L, as more adsorption sites were available at higher bed depth . The parametric values of the model are given in the Table 6.36. The experimental results are given in the Table 67(a) to 67(c) in the Annexure.

Table 6.36: Adams-Bohart model factors, bivariate correlation and standard deviation using neem leaf ash

C_0 (mg/L)	q (mL/min)	H (cm)	pH	Γ (min)	K_{YN} (L/min)	R^2	SS (10^{-3})
25	7.5	4	7.0	0.0005	0.53	0.996	3.18
100	7.5	4	7.0	0.0015	1.6	0.990	2.83
100	5.0	4	7.0	1.83	0.46	0.989	2.13
100	10.0	4	7.0	1.06	0.61	0.995	3.14
25	7.5	8	7.0	0.0009	1.12	0.993	3.41
100	7.5	4	4.1	0.94	0.53	0.997	2.44
100	7.5	4	9.2	1.88	0.43	0.995	2.09

6.9.3.2 Adsorbent: Jack fruit leaf ash

In the case of jack fruit leaf ash as adsorbent, raising up of feed concentration K_{AB} value got augmented from 0.45 to 1.24 L/mg.min while N_0 value got decreased from 0.75 to 1.90 mg/L, which is very significant for better description of the experiment by the model. The K_{AB} increased from 1.33 to 1.87 L/mg.min and simultaneously N_0 decreased from 0.295 to 0.187 mg/L as flow rate was increased. The increasing pH from 4.1 to 9.2 have very marginal effect over the model parameters K_{AB} and N_0 as given in the Table 6.37. The experimental results are given in the Table 70(a) to 70(c) in the Annexure.

Table 6.37: Adams-Bohart model factors, bivariate correlation and standard deviation using jack fruit leaf ash

C_0 (mg/L)	q (mL/min)	H (cm)	pH	Γ (min)	K_{YN} (L/min)	R^2	SS (10^{-3})
25	7.5	4	7.0	0.75	0.45	0.993	2.14
100	7.5	4	7.0	1.90	1.24	0.987	1.23
100	5.0	4	7.0	0.295	1.33	0981	1.74
100	10.0	4	7.0	0.187	1.87	0.997	1.05
25	7.5	8	7.0	0.42	1.24	0.987	2.61
100	7.5	4	4.1	1.99	0.211	0.924	1.27
100	7.5	4	9.2	2.28	0.170	0.978	1.42

6.9.3.3 Adsorbent: Bagasse fly ash

When bagasse fly ash was used as adsorbent, K_{AB} value got raised from 0.29 to 0.52 L/mg.min while N_0 got decreased very inconsistently at the time of increasing feed concentration. The K_{AB} increased from 0.34 to 0.41 L/mg.min and simultaneously N_0 got decreased from 0.702 to 0.448 mg/L as flow rate was increased. The increasing pH from 4.1 to 9.2 had marginal effect over the model parameters as K_{AB} decreased from 0.25 to 0.19 L/mg.min and N_0 increased from 0.356 to 0.836 mg/L as given in the Table 6.38. The higher coefficient of regression and smaller SS value suggested good agreement of the model. The experimental results are given in the Table 73(a) to 73(c) in the Annexure.

Table 6.38: Adams-Bohart model factors, bivariate correlation and standard deviation using bagasse fly ash

C_0 (mg/L)	q (mL/min)	H (cm)	pH	Γ (min)	K_{YN} (L/min)	R^2	SS (10^{-3})
25	7.5	4	7.0	0.42	0.29	0.994	1.14
100	7.5	4	7.0	0.53	0.52	0.994	1.17
100	5.0	4	7.0	0.702	0.34	0.995	1.21
100	10.0	4	7.0	0.448	0.41	0.991	1.48
25	7.5	8	7.0	0.69	0.32	0.993	1.14
100	7.5	4	4.1	0.356	0.25	0.998	1.18
100	7.5	4	9.2	0.836	0.19	0.978	0.17

6.9.3.4 Adsorbent: Rice husk ash

The trend of increase or decrease in the values of model parameters during the variation in initial concentration , flow rate, , bed depth and pH of the mixed dye solution was recorded very significant like other three adsorbents for rice husk as, depicted in the Table 6.39. Moreover regression coefficient and SS value indicated that model parameters described the adsorption process well. The experimental results are given in the Table 76(a) to 76(c) in the Annexure.

Table 6.39: Adams-Bohart model factors, bivariate correlation and standard deviation using rice husk ash

C_0 (mg/L)	q (mL/min)	H (cm)	pH	Γ (min)	K_{YN} (L/min)	R^2	SS (10^{-3})
25	7.5	4	7.0	0.14	0.76	0.992	1.45
100	7.5	4	7.0	0.40	0.35	0.989	0.24
100	5.0	4	7.0	1.20	0.10	0.997	1.14
100	10.0	4	7.0	0.39	0.17	0.998	1.36
25	7.5	8	7.0	0.29	0.32	0.989	1.26
100	7.5	4	4.1	0.57	0.11	0.923	1.51
100	7.5	4	9.2	1.38	0.10	0.999	0.11

6.9.3.5 Comparative study for the models

The overall performance of the Thomas, Yoon-Nelson and Adams-Bohart model in present study for all four adsorbents are found satisfactory as indicated by higher coefficient of regression and SS values given in the Table 6.28 to 6.39 above. These three models have good conformity with the experimental values for variation of four input parameters viz. adsorbent height, initial concentration, rate of inflow and pH for all four low cost adsorbents as shown in the Fig.6.60 (a) to Fig.6.63 (b).

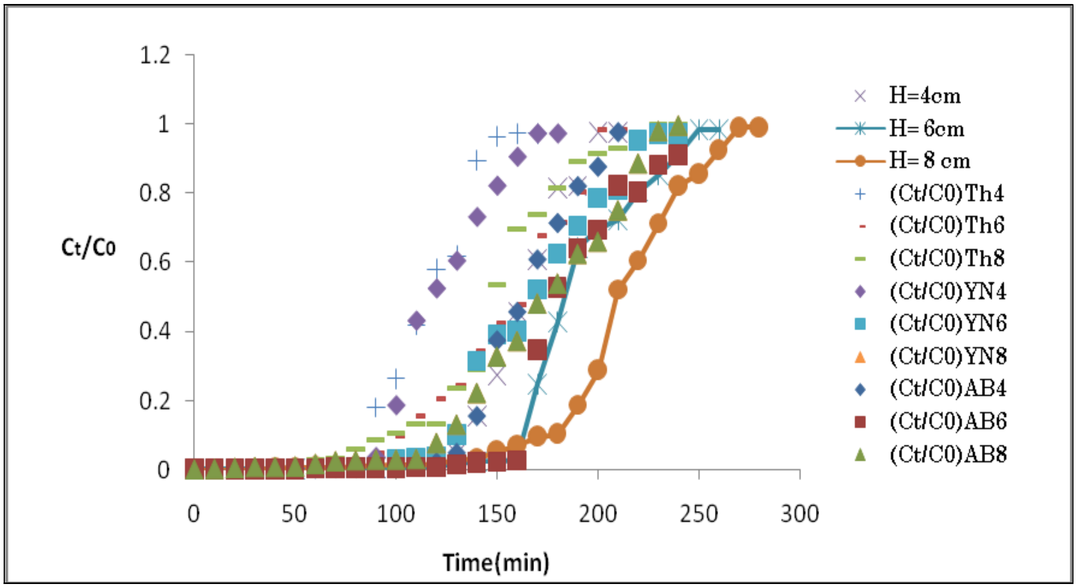

Fig. 6.60(a): BTC for NLA: the influence of adsorbent height on adsorption of dye mixture MB and MG (*C_0 = 75mgl^{-1}*, q = 7.5 ml min^{-1})

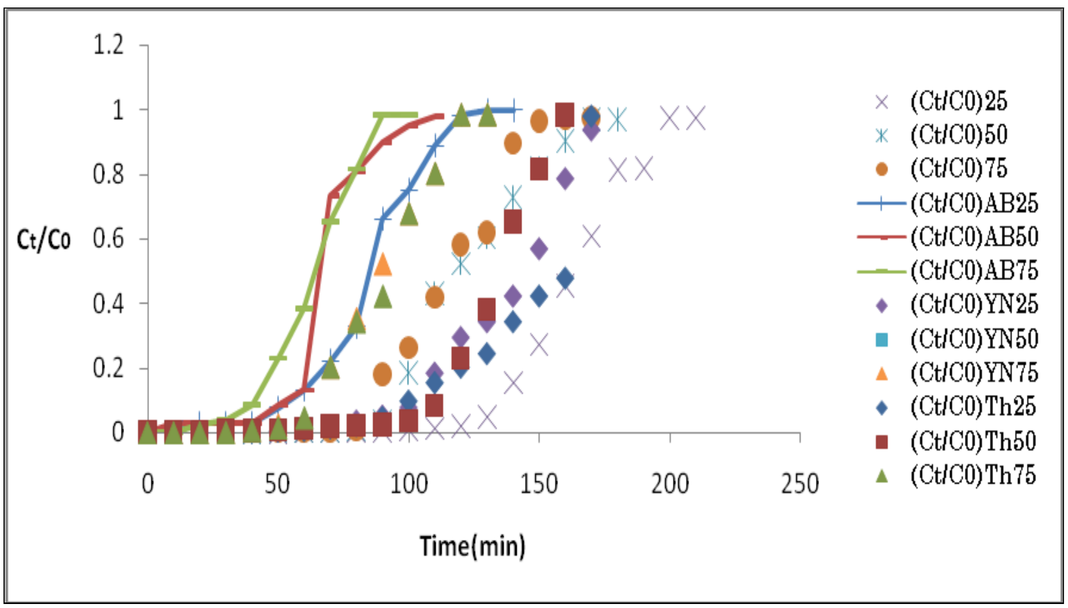

Fig. 6.60 (b): BTC for NLA: the influence of different initial concentrations on adsorption of dye mixture MB and MG (H = *4 cm*, q = 7.5 ml min^{-1})

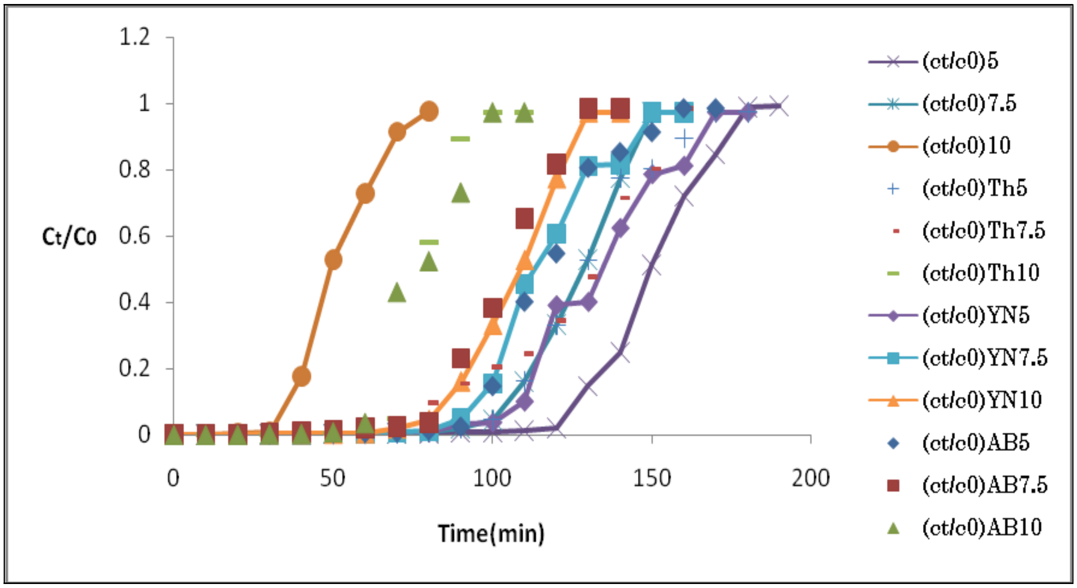

Fig. 6.60(c): BTC for NLA: the influence of different inflow rate on adsorption of dye mixture MB and MG (C_0 = *100 mgl⁻¹*, H = 4 cm, pH = 7.0)

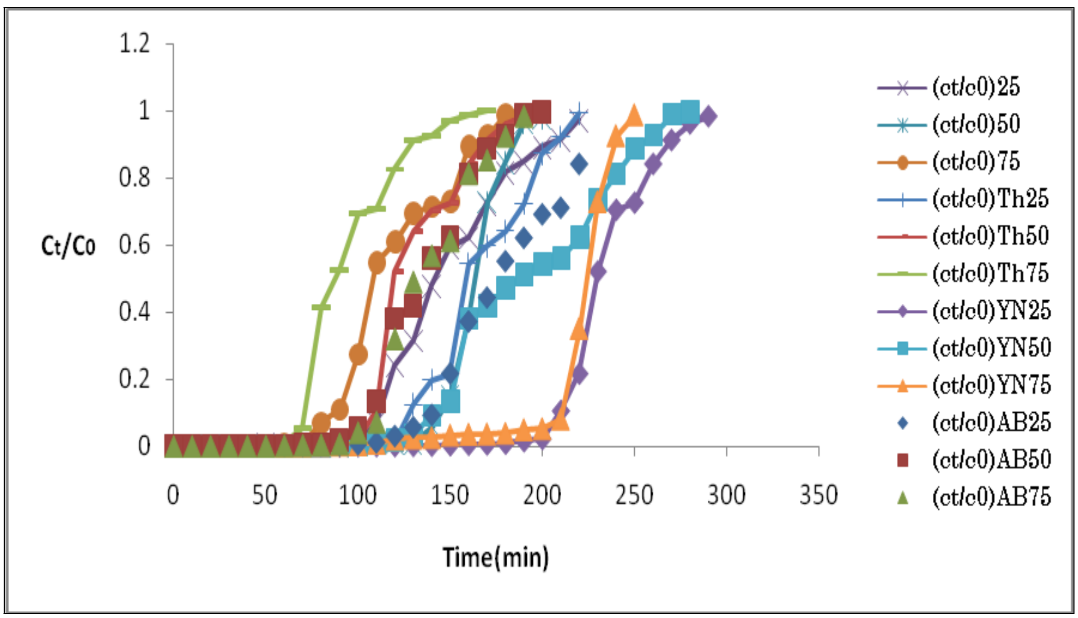

Fig. 6.61(a): BTC for JFLA: the influence of different initial conc. on adsorption of dye mixture MB and MG (H = *6 cm*, q = 7.5 ml min^{-1})

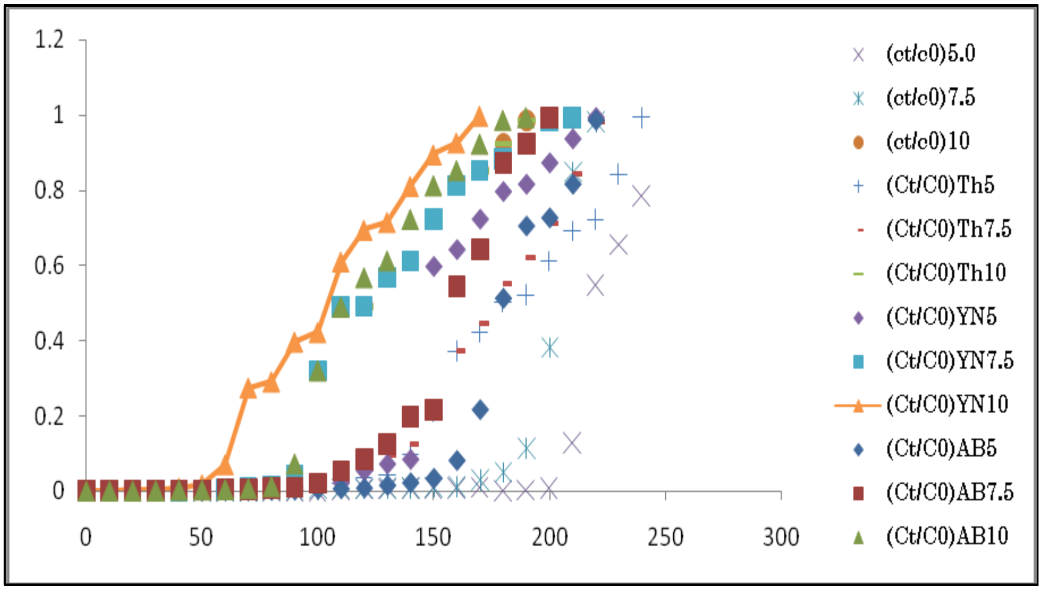

Fig.6.61(b): BTC for JFLA: the influence of different inflow rate on adsorption of dye mixture MB and MG (*C_0 = 100 mgl^{-1}*, H = 4 cm).

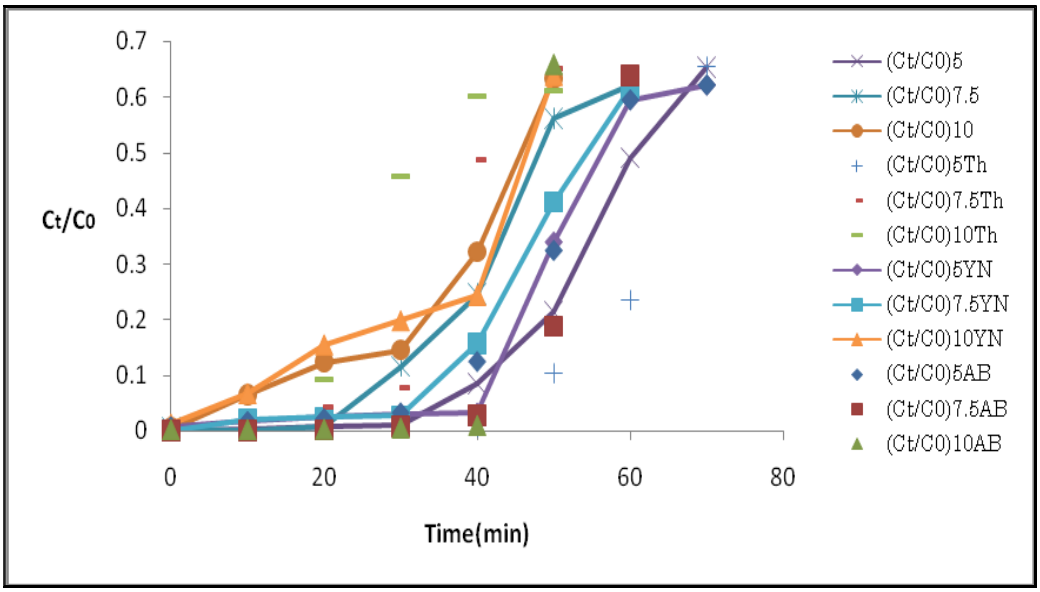

Fig. 6.62(a): BTC for BFA: the influence of different inflow rate on adsorption of dye mixture MB and MG (C_0 = 100 mgl^{-1}, H = 4 cm)

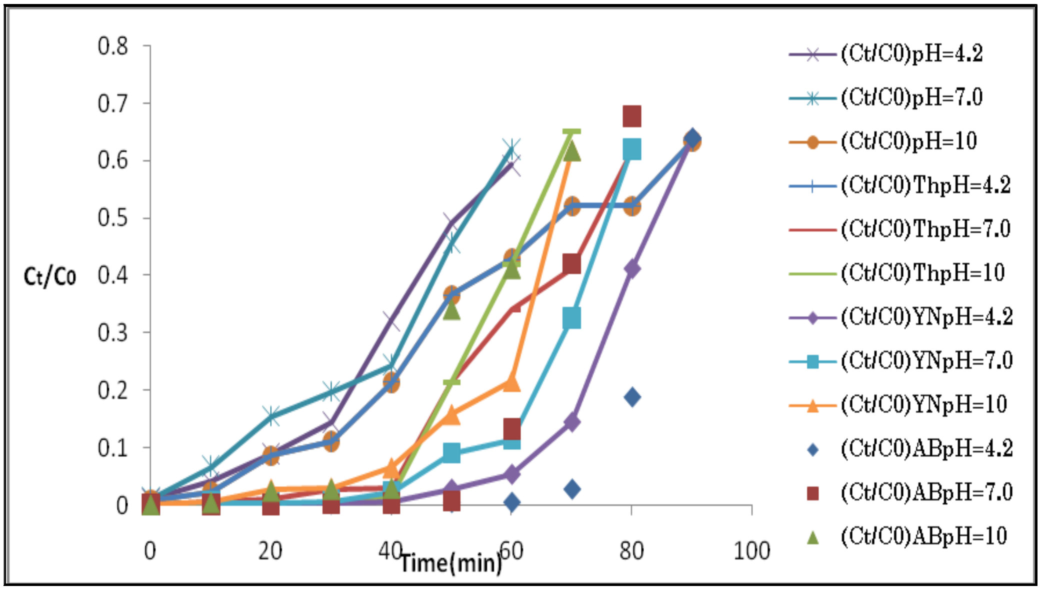

Fig. 6.62(b): BTC for BFA: the influence of different initial pH on adsorption of dye mixture MB and MG (*C_0 = 100 mgl^{-1}*, H = 4 cm)

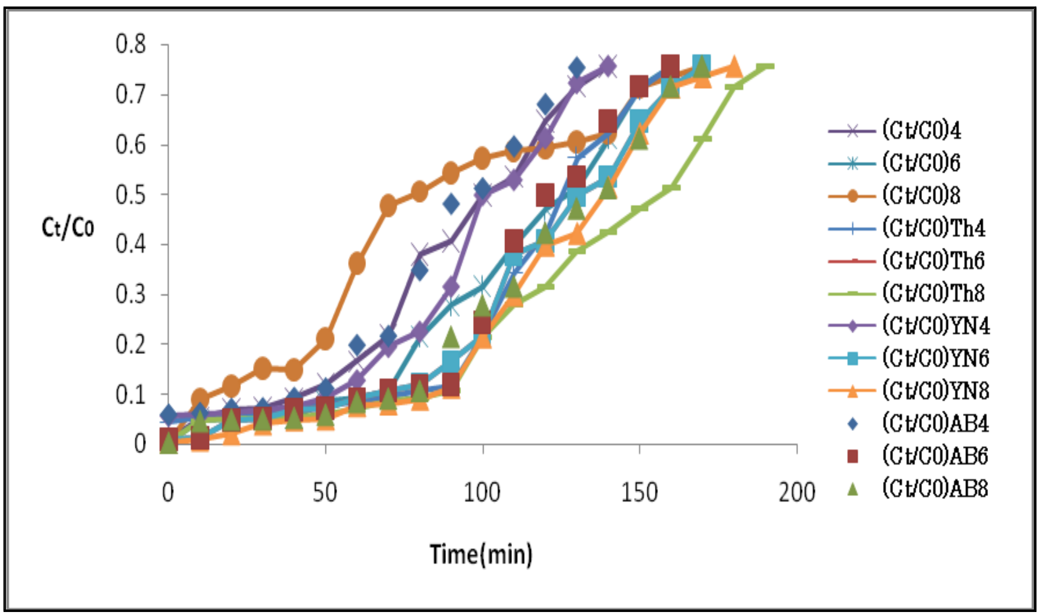

Fig. 6.63(a): BTC for RHA: the influence of different bed depths on adsorption of dye mixture MB and MG (*C_0 = 25 mgl^{-1}*, q = mL/min)

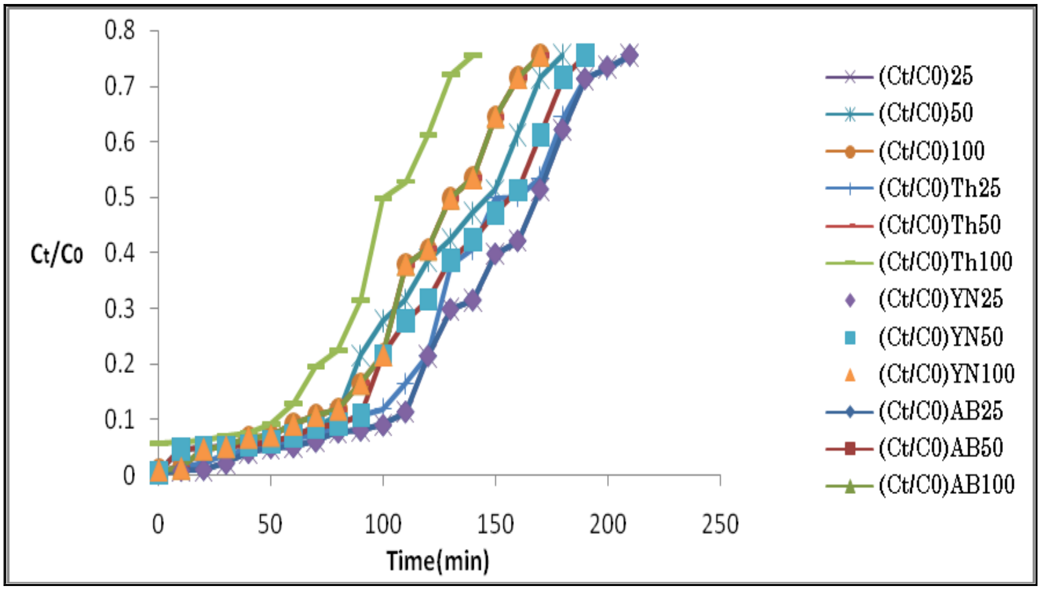

Fig. 6.63(b): BTC for RHA: the influence of different initial concentrations on adsorption of dye mixture MB and MG (*H* = *6 cm*, q = mL/min)

Here we plot few model values under selected operating conditions for thre different models namely Thomas, Yoon-Nelson and Adams-Bohart for comparison. Comparative investigation of the plots under these three models for different operating variables establishes the accuracy of all the models as they follow s-shaped curve. It may be concluded that there is a excellent conformity of model values and the outcomes from the experiments. It is also corroborated by the high regression coefficient values and smaller SS values as depicted in the Table 6.28 to 6.39.

6.9.4 Application of BDST Model

According to ***(Ayawei et al. 2017),*** BDST model is used to envisage the potentiality of adsorbent bed by using the different breakthrough values. The modified equation used in this study is given as:

$$t = \left(\frac{N_0}{C_0 F}\right) Z + \frac{1}{\ln\left[\frac{C_0}{C_t} - 1\right]} \quad \text{------------------------} \quad (6.25)$$

The equation unknowns are explained in section 5.9.5.3 of chapter 5.

$$t = aZ - b \quad \text{-------------------------------------} \quad (6.26)$$

The adsorption capacity (No) and rate constant (K_0) can be calculated from the BDST model. Generally, the related constants of BDST model are calculated from the slopes and intercepts of the t–Z curves at Ct/Co varying from 0.1 to 0.9. As the value of Ct/Co increased, the adsorption capacity of the bed per unit bed volume (N_o) was also increased. The values of R^2 establishes the validity of the BDST model for the present system.

6.9.4.1 Adsorbent: Neem leaf ash

The different service time for dye concentration in the effluent solution can be evaluated.

Table-6.39(a): C_t/C_o and t values at 0.1, 0.2 and 0.5 at bed depth 4, 6 and 8 cm for NLA as adsorbent

Z (cm)	t (min)	C_t/C_0	$t_{(Ct/C0)0.1}$ (min)	t (min)	C_t/C_0	$t_{(Ct/C0)0.2}$ (min)	t (min)	C_t/C_0	$t_{(Ct/C0)0.5}$ (min)
4	130	0.0483		140	0.1549		160	0.4556	
	140	0.1549	**134.84**	150	0.2730	**143.82**	170	0.6071	**162.93**
	160	0.0258		160	0.0258		180	0.4273	
6	170	0.2472	**163.35**	170	0.2472	**167.87**	190	0.6417	**183.40**
	170	0.0973		190	0.1862		200	0.2876	
8	180	0.1052	**173.42**	200	0.2876	**191.36**	210	0.5214	**209.08**

Interpolating C_t/C_0 for 0.1, 0.2, 0.5, corresponding t values were evaluated. The plotting of the equation (6.26) for t against Z. The values of different parameters were calculated by using equations 2, 3 and 5 and are shown in the Table - 6.39 (b).

Table-6.39 (b): Parameters under BDST model using NLA

C_t/C_0	Equation	a	b	N_0 (mg/gm)	K_0 (L/mg.min)	R^2
0.1	Y=23.07X+138.9	23.12	11.67	219.17	0.00036	0.995
0.2	Y=23.77X+120.1	23.77	14.87	225.82	0.0006	1.0
0.5	Y=19.29X+118.6	19.29	55.44	283.26	0.0005	0.929

Here capacity of adsorption in terms of bed volume (N_0) was evaluated under fixed operating conditions of concentration and liner flow (0.38 cm/min). The value can be determined by using slope of the equation derived above. Similarly, the rate constant was determined from the intercept of same equation under similar operational condition from the intercept. BDST model values so deduced can be effective information for extending similar study without conducting further experiment trial for its higher coefficient of regression values.

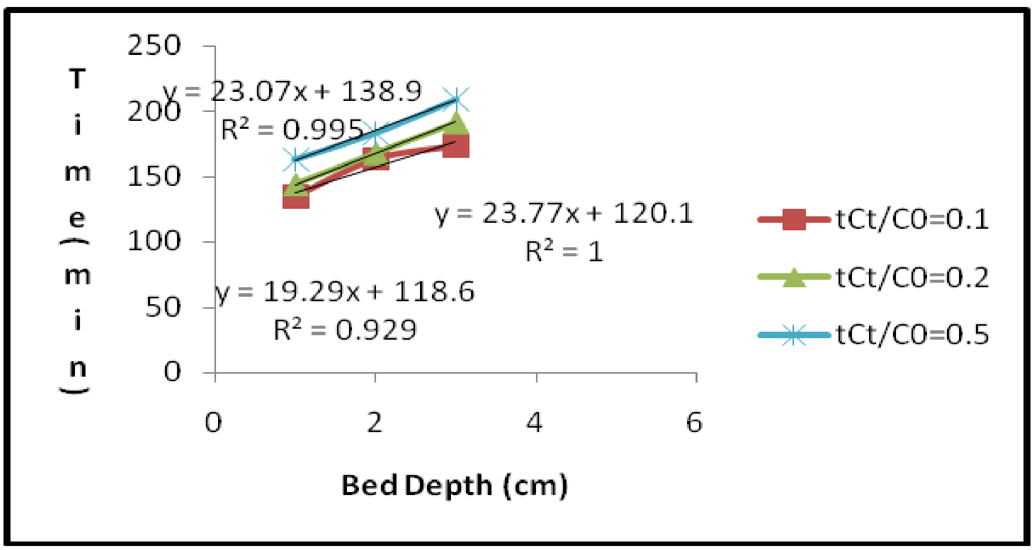

Fig. 6.64(a): BDST plot for neem leaf ash adsorbent at C_t/C_0= 0.1, 0.2 and 0.5 for a concentration of 25 mg/L

BDST analysis was also conducted for other concentrations viz. 50 and 75 mg/L. Plotting service time against Z for this study was presented in the Fig. 6.64 (b). The model parameters (N_0 and K_0) were worked out from this plotting, and depicted in the Table 6.39(b). During increment of C_t/C_0 value N_0 and K_0 values were also increased for all four concentrations we considered. Moreover, the regression coefficient value (R^2) indicated the effective use of this model for the present investigation.

Table 6.39(c): BDST constant for the column at different inlet concentrations and bed depths

C_0	C_t/C_0	R^2	K_0	N_0
50 mg/L	0.1	0.837	0.00003	142.96
	0.2	0.810	0.0006	171.52
	0.4	0.808	0.00016	256.70
75mg/L	0.1	0.968	0.000002	164.73
	0.2	0.897	0.00005	244.15
	0.4	0.90	0.0001	340.36

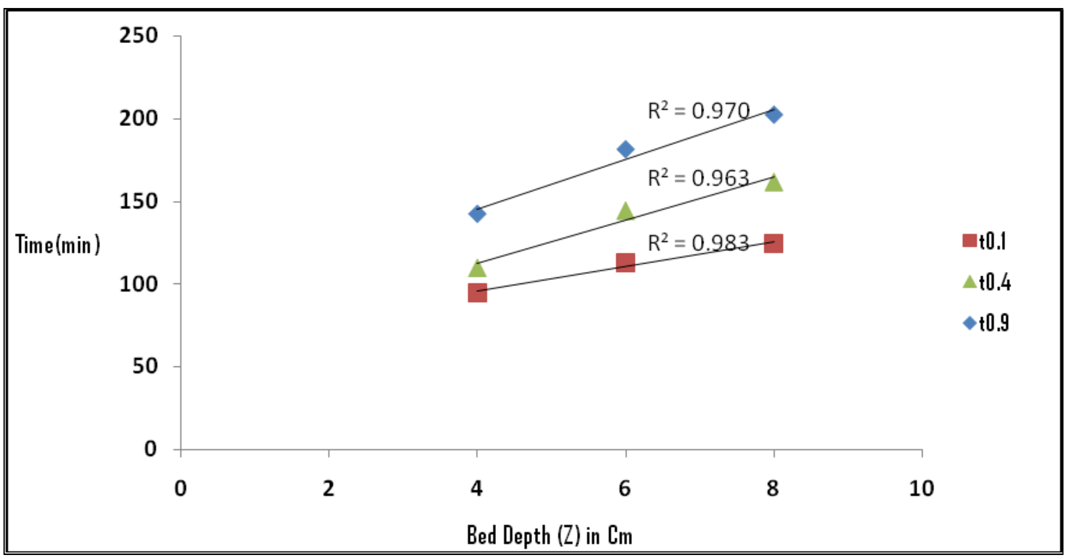

Fig. 6.64(b): BDST Model at constant inlet concentration C_0= 50 mg/L and q = 7.5 mL/min

6.9.4.2 Adsorbent: Jack fruit leaf ash

The C_t/C_0 values at 0.1, 0.2 and 0.5 and corresponding values of t at bed depth 4, 6 and 8 cm are taken for jack fruit leaf ash as:

Table - 6.40(a): C_t/C_0 and t values at 0.1, 0.2 and 0.5 at bed depth 4, 6 and 8 cm for JFLA as adsorbent

Z(cm)	t(min)	C_t/C_0	$t_{(Ct/C0)0.1}$ (min)	t(min)	C_t/C_0	$t_{(Ct/C0)0.2}$ (min)	t(min)	C_t/C_0	$t_{(Ct/C0)0.5}$ (min)
4	230	0.0497		240	0.1128		250	0.3817	
	240	0.1128	**237.97**	250	0.3817	**243.24**	260	0.7281	**253.41**
	240	0.0817		250	0.1058		260	0.2167	
6	250	0.1058	**247.60**	260	0.2167	**258.50**	270	0.5211	**269.30**
	260	0.0917		270	0.1241		290	0.3416	
8	270	0.1241	**262.56**	280	0.2253	**277.50**	300	0.5217	**298.79**

Interpolating the C_t/C_0 for 0.1, 0.2, 0.5, the values of t at were obtained. The values of different parameters are being calculated by using equations as shown in the Table-6.40(b).

Table-6.40(b): Parameters under BDST model using JFLA

C_t/C_0	Equation	a	b	N_0 (mg/gm)	K_2 (L/mg.min)	R^2
0.1	Y=12.29X+224.7	12.29	350	116.76	$1.21x10^{-4}$	0.984
0.2	Y=17.13X+225.4	17.13	225.2	162.74	$3.96x10^{-5}$	0.996
0.5	Y=22.69X+228.4	22.69	229.09	215.56	$1.21x10^{-5}$	0.970

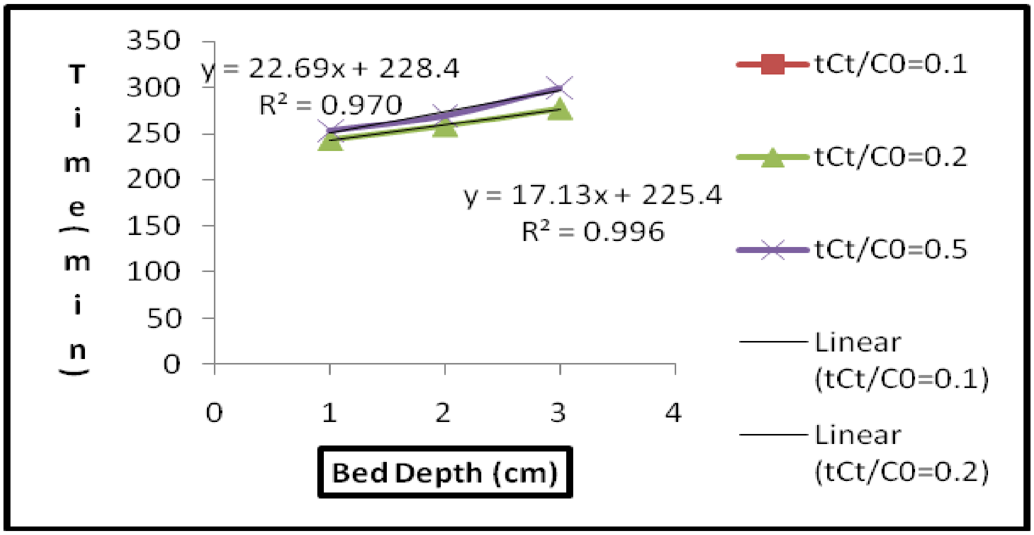

Fig. 6.65(a): BDST plot for jack fruit leaf ash adsorbent at C_t/C_0= 0.1, 0.2 and 0.5 for a concentration of 25 mg/L.

BDST analysis was done also for other concentrations such as 50 and 75 mg/L and the linear plot is given in the Fig. 6.65(a). From the plot, N_0 and K_0 were worked out and depicted in the Table 6.40(b). Due to increasing C_t/C_0 ratio, the N_0 and K_0 value also got increased for all four concentrations we considered. The R^2 value proved the potentiality of JFLA as adsorbent for present adsorption study.

Table 6.40(c): BDST constant for the column at 50 mg/L concentrations and bed depths 4 cm

C_0	C_t/C_0	R^2	K_0	N_0
50mg/L	0.3	0.837	$3.73x10^{9}$	84.08
	0.5	0.810	$6.79x10^{-9}$	104.57
	0.8	0.842	$4.21x10^{-9}$	117.54
75 mg/L	0.3	0.872	$3.86x10^{-9}$	
	0.5	0.824	$4.71x10^{-9}$	180.92
	0.8	0.812	$4.53x10^{-9}$	195.23

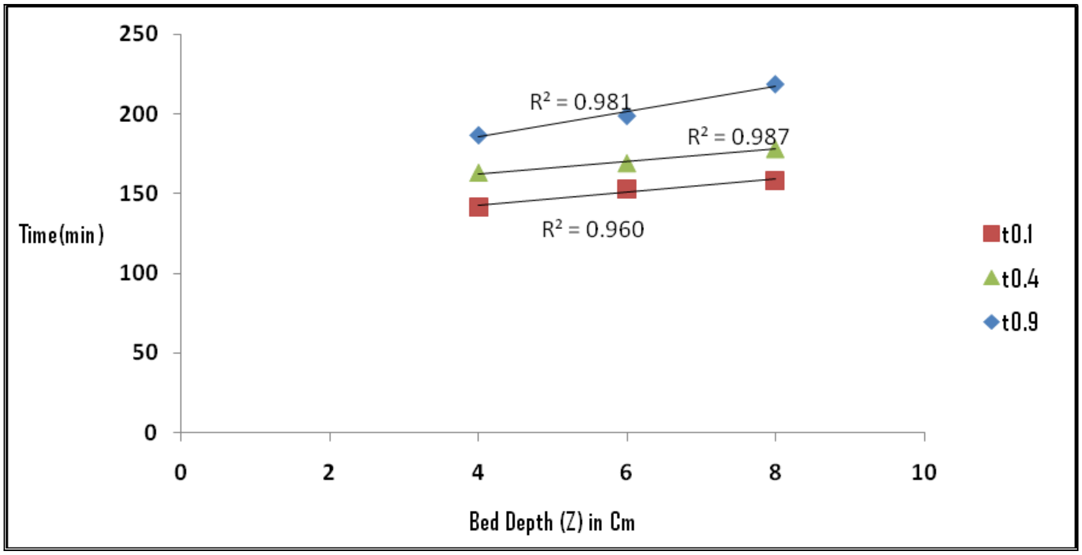

Fig. 6.65(b): BDST Model at constant inlet concentration C_0 = 75 mg/L at q = 7.0 mL/min

6.9.4.3 Adsorbent: Bagasse fly ash

The C_t/C_o values at 0.1, 0.2 and 0.5 and corresponding values of t at bed depth 4 cm, 6 cm, and 8 cm are taken for BFA as :

Table-6.41(a) : C_t/C_o and t values at 0.1, 0.2 and 0.5 at bed depth 4, 6 and 8 cm for BFA as adsorbent

Z (cm)	t (min)	C_t/C_o	$t_{(Ct/Co)0.1}$ (min)	t(min)	C_t/C_o	$t_{(Ct/Co)0.2}$ (min)	t(min)	C_t/C_o	$t_{(Ct/Co)0.5}$ (min)
4	170 180	0.0935 0.122	 **172.28**	190 200	0.1944 0.2841	**190.62**	210 220	0.3602 0.5014	**219.90**
6	280 290	0.0780 0.115	**281.61**	290 300	0.1150 0.326	**294.03**	310 320	0.487 0.651	**317.90**
8	280 290	0.0747 0.1063	**288.00**	320 330	0.1925 0.2642	**321.05**	350 360	0.4879 0.5542	**351.80**

Interpolating the C_t/C_o ratios, the corresponding values of t at C_t/C_o = 0.1, 0.2, 0.5 are calculated. The plot of t versus Z in the Fig. 6.66(a) gives the following equations. The values of different parameters were calculated by using equations 2, 3 and 5 are shown in the tabular form.

Table-6.41(b): Parameters under BDST model using BFA

C_t/C_o	Equation	a	b	N_o (mg/g)	K_0 (L/mg.min)	R^2
0.1	Y= 57.86x+131.5	57.86	250	549.67	1.68×10^{-4}	0.991
0.2	Y=65.21x+138.1	65.21	1382	619.50	6.45×10^{-5}	0.997
0.5	Y=65.95x+164.6	65.95	16500	626.53	1.68×10^{-5}	0.927

Here capacity of adsorption in terms of bed volume(N_0) was evaluated under fixed operating conditions of concentration and liner flow (0.38 cm/min). The value can be determined by using slope of the equation derived above. Similarly, the rate constant was determined from the intercept of same equation under similar operational condition from the intercept. BDST model unknowns so deduced would be important information for extending for other inflows without conducting further experimental trials for its higher coefficient of regression values. C_t/C_0 was directly proportional to N_0 but inversely related to its model constant K_2 as recorded.

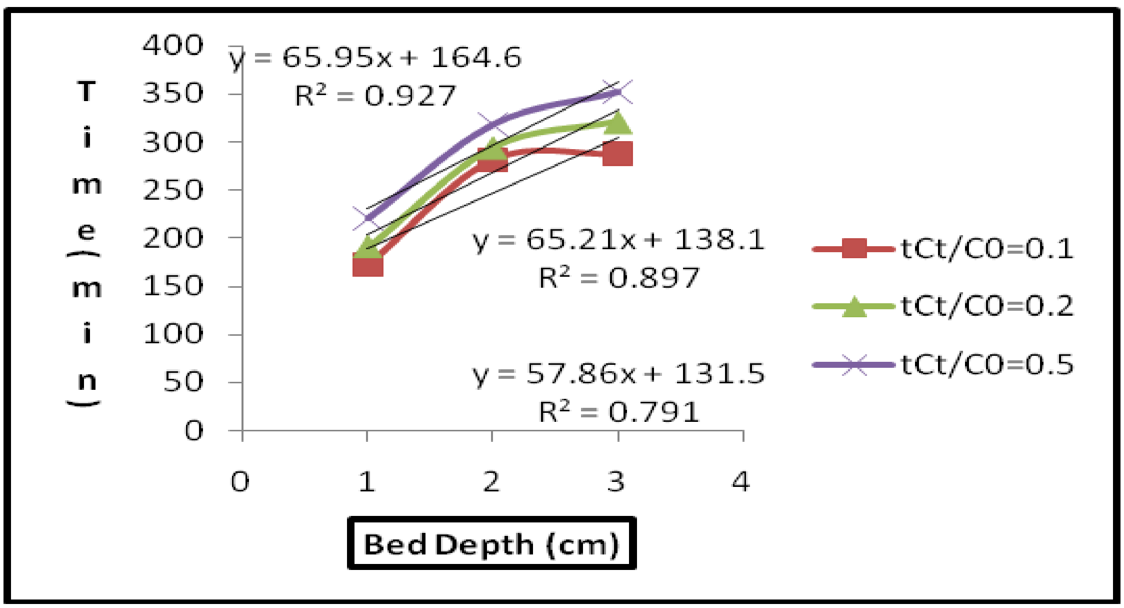

Fig.6.66(a): BDST plot for bagasse fly ash adsorbent at C_t/C_0 = 0.1, 0.2 and 0.5 for a concentration of 25 mg/L.

BDST analysis was done also for other concentrations such as 50, 75, 100 mg/L and the linear plot is given in the Fig. 6.66(a). From the plot, N_0 and K_0 were worked out and depicted in the Table 6.41(b). Due to increasing C_t/C_0 ratio, the N_0 and K_0 value also got increased for all four concentrations we considered. The R^2 value proved the potentiality of BFA as adsorbent for present adsorption study.

Table 6.41(c): BDST constant for the column at different inlet concentrations and bed depths

C_0	C_t/C_0	R^2	K_0	N_0
50 mg/L	0.1	0.886	0.000023	265.79
	0.2	0.925	0.000081	284.32
	0.3	0.966	0.000087	304.58
75 mg/L	0.1	0.853	0.000058	339.93
	0.2	0.906	0.0001	349.67
	0.3	0.945	0.0012	351.10
100 mg/L	0.1	0.996	0.0001	224.9
	0.2	0.994	0.0003	261.2
	0.3	0.998	0.000032	261.4

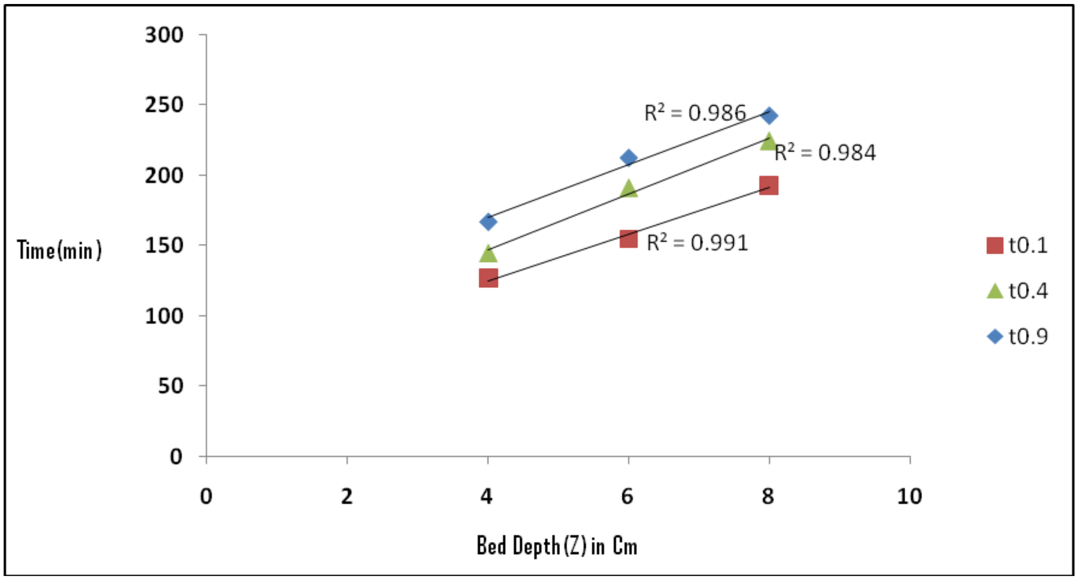

Fig. 6.66(b): BDST Model at constant inlet concentration C_0 = 50 mg/L and q = 7.5 mL/min

6.9.4.4 Adsorbent: Rice husk ash

The C_t/C_o values at 0.1, 0.2 and 0.5 and corresponding values of t at bed depth 4 cm, 6 cm, and 8 cm are taken for BFA as given in Table-6.42 (a). :

Table-6.42(a): C_t/C_o and t values at 0.1, 0.2 and 0.5 at bed depth 4, 6 and 8 cm for RHA as adsorbent

Z (cm)	t (min)	C_t/C_o	$t_{(Ct/Co)0.1}$ (min)	t(min)	C_t/C_o	$t_{(Ct/Co)0.2}$ (min)	t(min)	C_t/C_o	$t_{(Ct/Co)0.5}$ (min)
4	60 70	0.0915 0.1074	**65.35**	90 100	0.165 0.2164	**96.81**	130 140	0.4981 0.5346	**130.38**
6	80 90	0.0917 0.1072	**85.35**	90 100	0.1072 0.2151	**98.60**	150 160	0.4716 0.5127	**156.91**
8	100 110	0.0905 0.1142	**104.08**	110 120	0.1142 0.2147	**118.53**	160 170	0.4217 0.5141	**168.47**

Interpolating the C_t/C_o values the values of t are calculated at C_t/C_o = 0.1, 0.2 and 0.5. The values of different parameters are calculated by using equations 2, 3 and 5 are shown in the tabular form.

Table-6.42(b): Parameters under BDST model using RHA

C_t/C_o	Equation	a	b	N_o (mg/g)	K_0 (l/mg.min)	R^2
0.1	Y= 19.36X+46.19	19.36	35.29	183.92	$1.19x10^{-3}$	0.999
0.2	Y=10.91X+82.86	21.43	367.07	203.64	$2.43x10^{-4}$	0.911
0.5	Y=19.04X+113.8	25.88	2590	245.88	1.07x10-4	0.951

Here capacity of adsorption in terms of bed volume (N_0) was evaluated under fixed operating conditions of concentration and liner flow (0.38 cm/min). The value can be determined by using slope of the equation derived above. Similarly, the rate constant was determined from the intercept of same equation under similar operational condition from the intercept. BDST model parameters so deduced would be significant for extending for other flow rates without conducting further experimental trials for its higher coefficient of regression values. C_t/C_0 was directly proportional to N_0 but inversely related to its model constant K_2 as recorded.

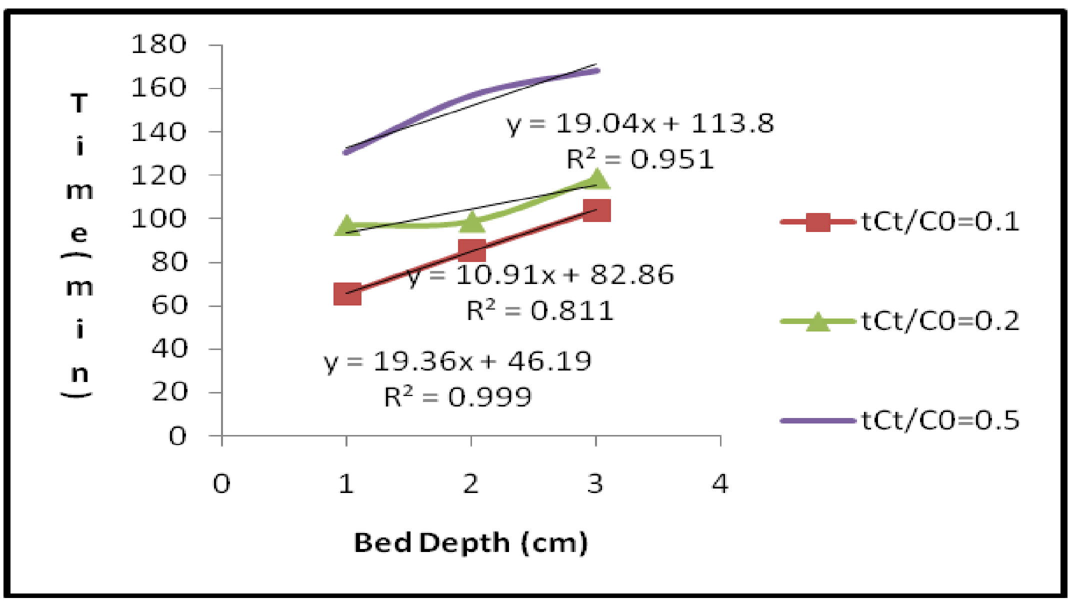

Fig. 6.67(a): BDST plot for rice husk ash adsorbent at C_t/C_0 = 0.1, 0.2 and 0.5 for a concentration of 25 mg/L

BDST analysis was done also for other concentrations such as 50 , 75, 100 mg/L and the linear plot is given in the Fig. 6.67(a). From the plot, N_0 and K_0 were worked out and depicted in the Table 6.42(b). Due to increasing C_t/C_0 ratio, the N_0 and K_0 value also got increased for all four concentrations we considered. The R^2 value proved the potentiality of RHA as adsorbent for present adsorption study.

Table 6.42(c): BDST constant for the column at different inlet concentrations and bed depths

C_0	C_t/C_0	R^2	K_0	N_0
50 mg/L	0.1	0.928	0.000175	143.82
	0.2	0.940	0.000209	147.73
	0.3	0.959	0.000210	158.91

Table 6.42(c): BDST constant for the column at different inlet concentrations and bed depths

C_0	C_t/C_0	R^2	K_0	N_0
75 mg/L	0.1	0.853	0.000050	84.29
	0.2	0.906	0.000054	83.95
	0.3	0.945	0.000112	87.44
100 mg/L	0.1	0.996	0.000107	107.72
	0.2	0.994	0.000198	191.07
	0.3	0.998	0.000300	251.05

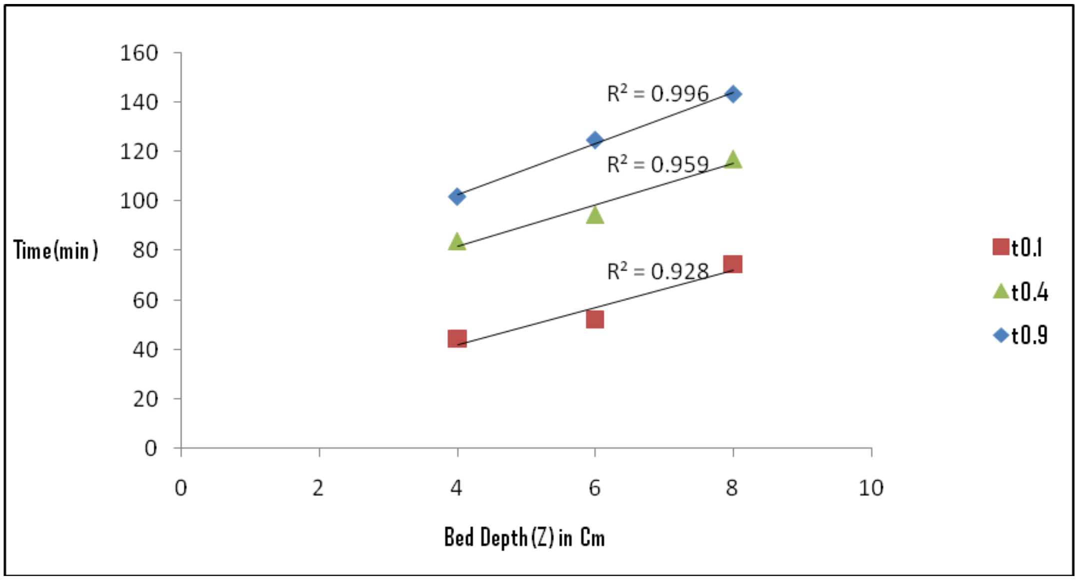

Fig. 6.67(b): BDST Model at constant inlet concentration C_0 =75 mg/L and q = 7.5 mL/min

BDST model described the adsorption system very satisfactorily for all the four adsorbents, specially for bagasse fly ash. The high values for adsorption capacity (N_0) indicate the unique features of this model i.e. the adsorbate molecules adsorbed directly onto the adsorbents. The higher value of coefficient of regression for neem leaf ash and bagasse fly ash was obtained. BDST model is the best approach over the other three models in the present study.

6.10 Evaluation of adsorption potential by using ANN tool

An artificial neural network (ANN) model is developed on the logic of deep learning. It is simple numerical algorithm operated through computer simulation. It is operated similar to biological neural network analysis ***(Ghosh et al. 2015).*** Three layer architecture having transfer function with linear propagation has been selected. In the present study, network neurons has been chosen 4:10:1 for column mode and 5:10:1 for batch mode operation.

The transfer function 'poslin' for hidden layer and 'purelin' for output was selected for training purposes. METLAB-2009a software was utilized to validate the experimental outcomes.

Variable operating parameters were used as input variables. The output variable was the percentage removal of dye mixture.

6.10.1 ANN model in Column Study

In the present study of adsorption the ranging of operating variables was selected as follows:

Table 6.43: Input data ranging in column study for ANN

Operating variables	Range
Adsorbent bed height	4 to 8 cm
Initial concentrations of mixed dyes solution	25 to 100 mg/L
Influent flow rate of dye solution	5 to 10 mL/min
pH of the dye solution	5.1 to 9.2

The multi-layer perception system explored in the present work was developed in METLAB 2009a with four input which are the independent variables (adsorbent bed height, initial concentrations of mixed dye solution, flow rate and pH of the dyes in solution mixture), one hidden layer of 10 neurons and one output layer of one neuron (percentage removal of dyes). It was analyzed and simulated by the ANN software ***(Betiku et al. 2015).***

The Neural Fitting APP (n f tool) was used for selecting data, subsequent learning and training. The performance was evaluated through mean square error (MSE) and R^2 value, inbuilt in the software. The training with Leven berg-Marquardt back propagation algorithm (trainlm) has been performed for the given network.

The training operation was stopped as optimization of mean square error has been achieved.

By successive trials, using weights to the neurons and giving appropriate threshold to the network optimization can be achieved. The number of neurons selected as 10 for the hidden layer for all the operating variables for all the four adsorbents ***(Gupta and Majumder, 2017).***

The percentage fraction of data used for training and testing purposes was given in the Table 6.44.

After selecting the appropriate number (10) of neurons in hidden layer by trial the network was simulated nearly 600 iterations produced regression coefficient quite satisfactory result for all the four adsorbents as shown in the Fig.6.68 to Fig.6.71.

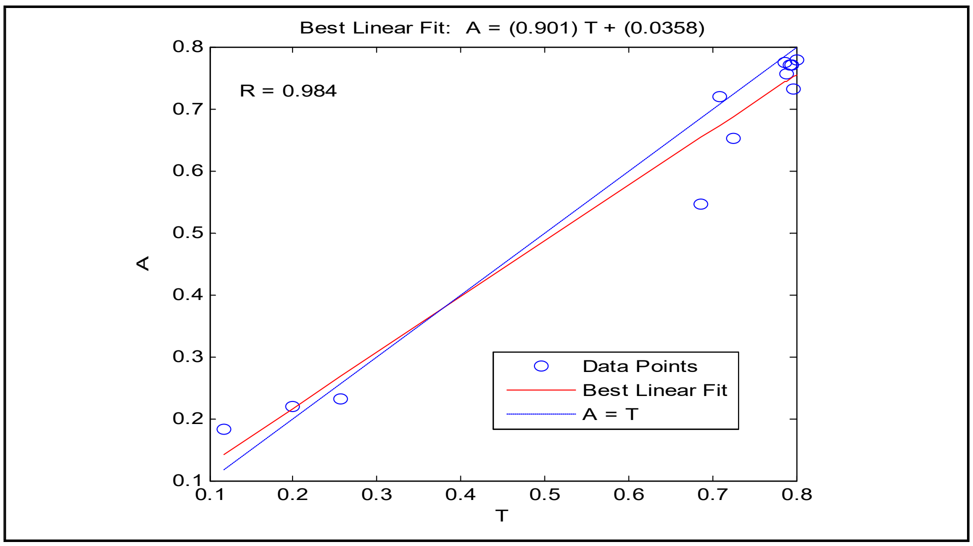

Fig. 6.68: MSE and regression coefficient value for neem leaf ash

Table 6.44: Data used for Training and Testing for all the four adsorbents at different process parameters under column study

Variable Parameters	Neem leaf ash			Jack fruit leaf ash			Bagasse fly ash			Rice husk ash		
	Total Data	Training Data	Testing Data	Total Data	Training Data	Testing Data	Total Data	Training Data	Testing Data	Total Data	Training Data	Testing Data
Bed Depth at C_0 = 25mg/l	75	56	19	102	78	24	92	73	19	83	65	18
at C_0 = 50mg/l	66	47	19	—	—	—	40	30	10	—	—	—
at C_0 = 100mg/l	56	42	14	81	57	24	23	14	9	24	14	10
Concentration at H = 4 cm	72	55	17	113	77	36	59	44	15	59	42	17
at H = 8 cm	101	78	23	130	103	27	75	55	20	80	62	18
Flow rate	48	33	15	81	62	19	19	13	6	27	17	10
pH	49	33	16	77	60	17	20	13	7	29	21	8

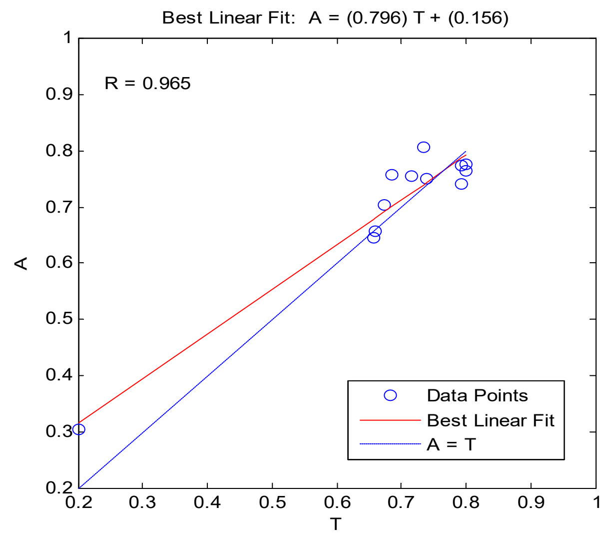

Fig.6.69: MSE and Regression coefficient value for jack fruit leaf ash

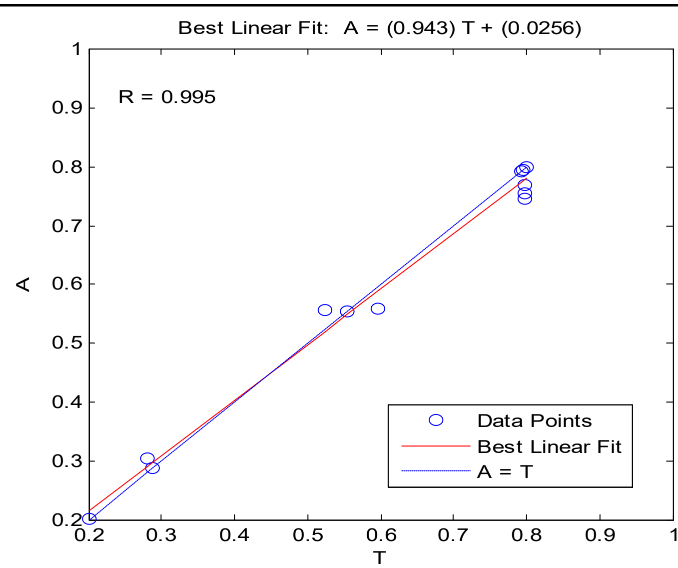

Fig.6.70: MSE and Regression coefficient value for Bagasse fly ash

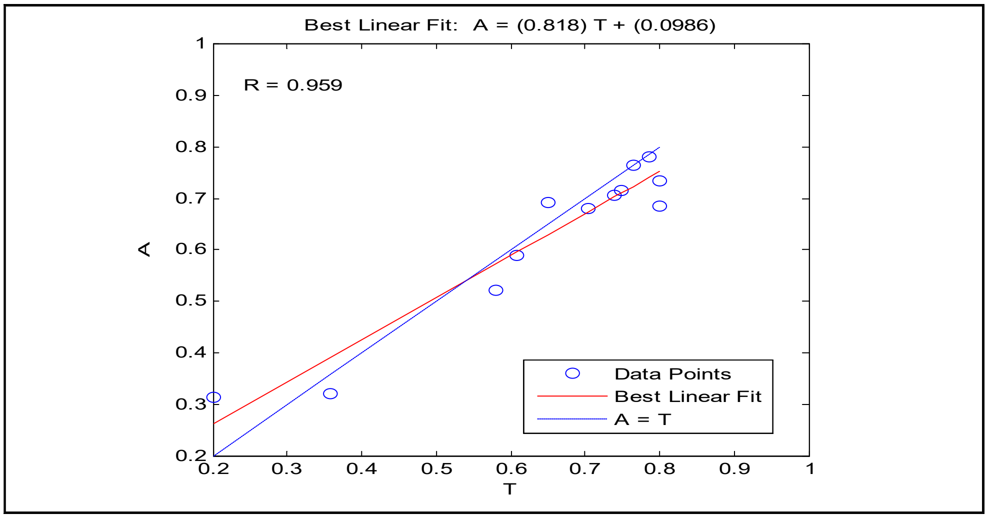

Fig. 6.71: MSE and Regression coefficient value for Rice husk ash

The linear fit model so obtained was used to predict the ANN model outcomes. Based on the test results showed that the percentage decolorization resulting from ANN is not much different from the experimental results. The comparison between the laboratory and ANN simulation under various operation conditions for all the four low cost adsorbents are represented graphically in the fig. 6.72(a) to Fig. 6.75(c) for all the four low cost adsorbents.

Adsorbent: Neem leaf ash (NLA)

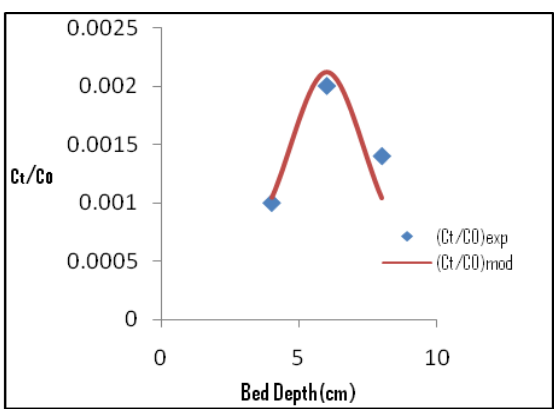

Fig.6.72(a): Laboratory study and ANN outcomes for NLA for different bed depth at C_0 = 25mg/l

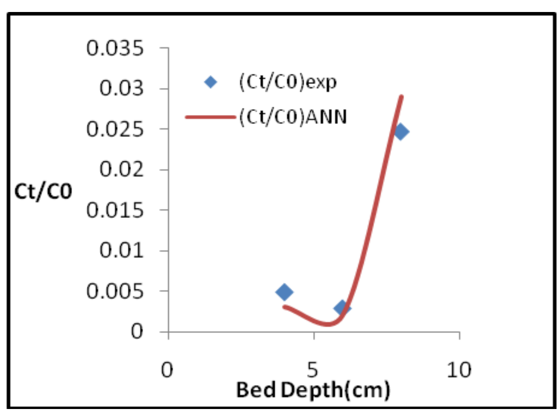

Fig.6.72(b): Laboratory study and ANNoutcomes for NLA for different bed depth at C_0 = 50mg/l

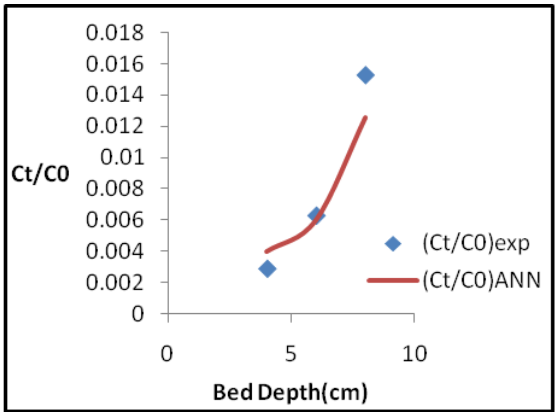

Fig.6.72(c): Laboratory study and ANN outcomes for NLA for different bed depth at C_0 =100 mg/l

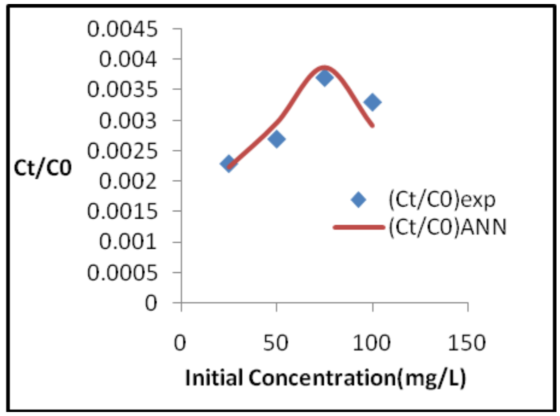

Fig.6.72(d): Laboratory study and ANN outcomes for NLA for different concentrations at H = 4 cm

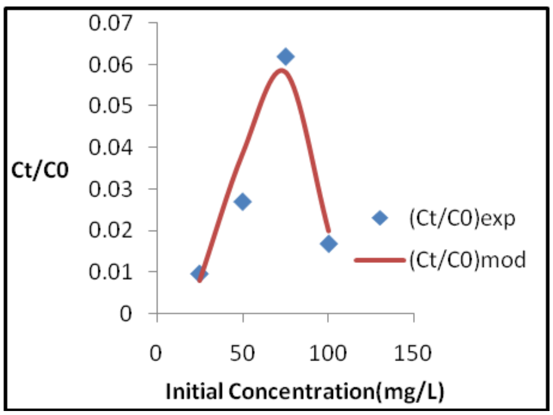

Fig.6.72(e): Laboratory study and ANN outcomes for NLA for different concentrations at H = 8 cm

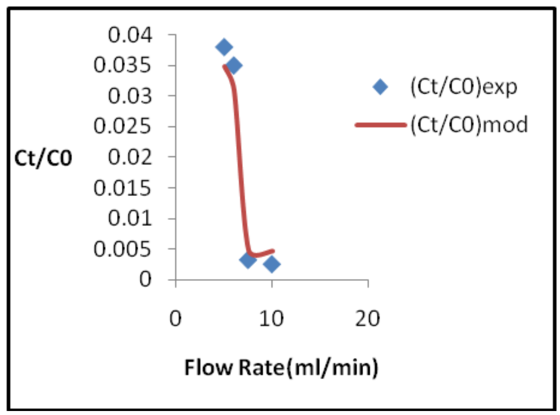

Fig.6.72(f): Laboratory study and ANN outcomes for NLA for different flow rate at H = 4 cm C_0 =100 mg/L

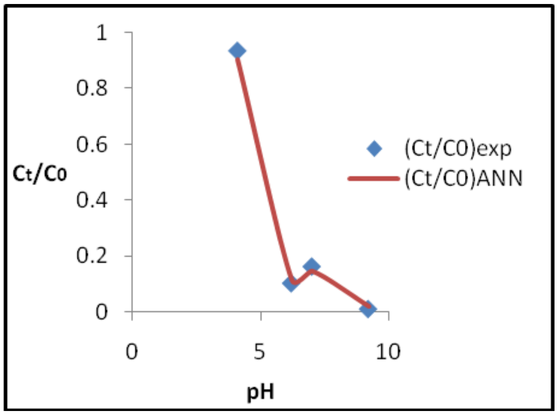

Fig.6.72(g): Laboratory study and ANN outcomes for NLA for different pH at H = 4 cm C_0 =100 mg/L

For the neem leaf ash as adsorbent, the deviation was noted during variation of bed depth at lower concentration as shown in the Fig.6.72(a). The deviation of experimental data from the ANN simulated outcome was recorded at higher bed depth of 8 cm as shown in the Fig. 6.72(e). The excellent matching between ANN and experimental result observed for neem leaf ash during variation of pH and inflow rate of the mixed dye solution as shown in the Fig. 6.72(f) and 6.72(g).

Adsorbent: Jack fruit leaf ash (JFLA)

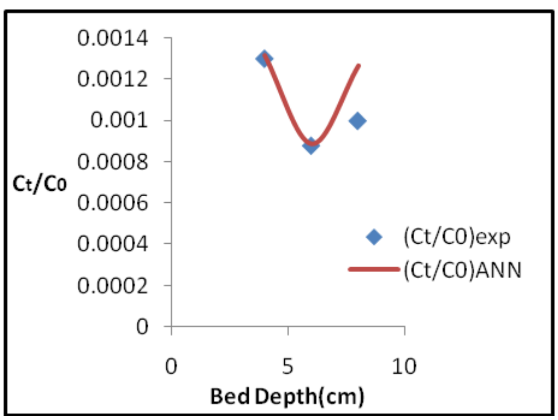

Fig.6.73(a): Laboratory study and ANN outcomes for JFLA for different bed depth at C_0 = 25 mg/l

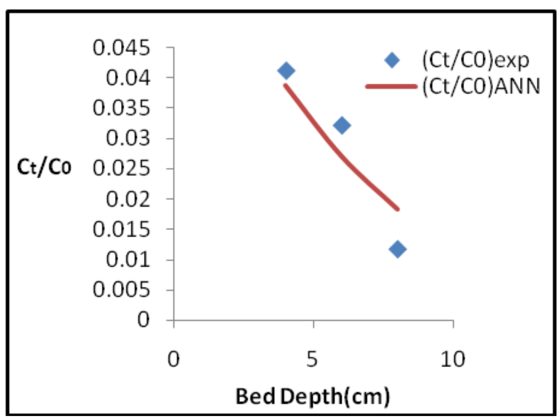

Fig.6.73(b): Laboratory study and ANN outcomes for JFLA for different bed depth at C_0 = 100 mg/l

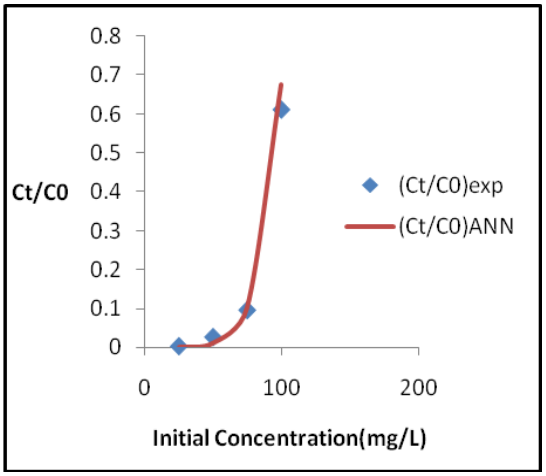

Fig.6.73(c): Laboratory study and ANN outcomes for JFLA for different concentrations at H = 6 cm

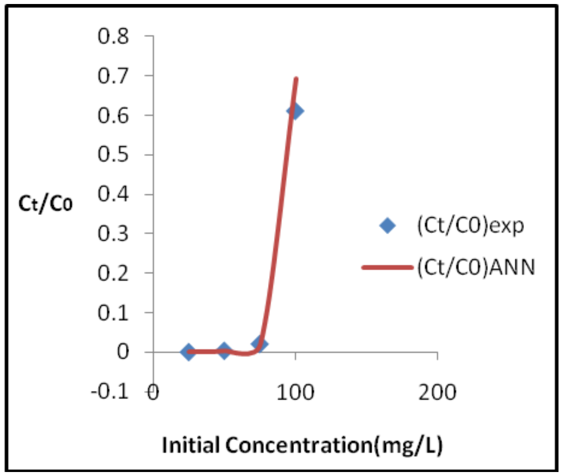

Fig.6.73(d): Laboratory study and ANN outcomes for JFLA for different concentrations at H = 8 cm

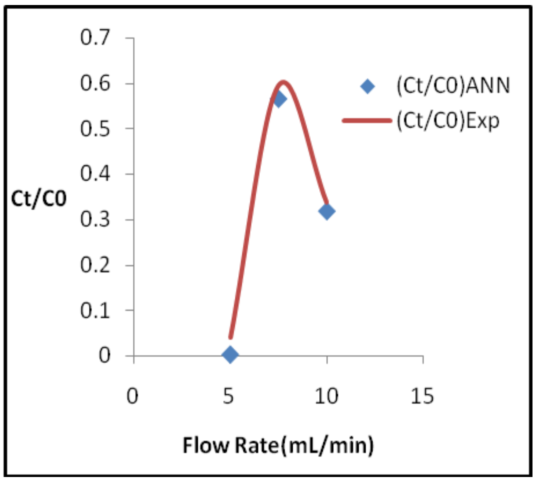

Fig.6.73(e): Laboratory study and ANN outcomes for JFLA for different flow rate at H = 4 cm C_0 = 100mg/L

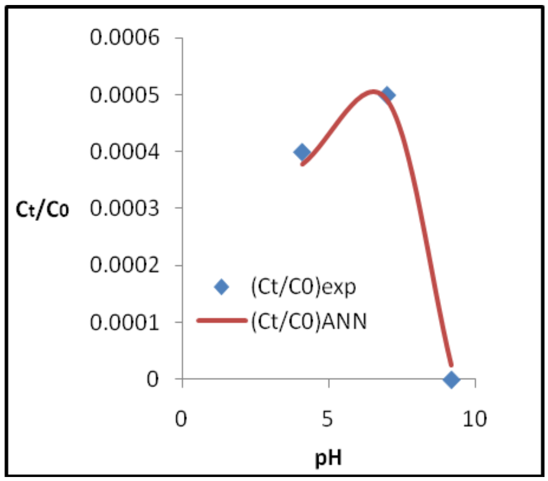

Fig.6.73(f): Laboratory study and ANN outcomes for JFLA for different pH at H = 4 cm C_0 = 100 mg/L

For the adsorption study using jack fruit leaf ash s adsorbent, considerable deviations have been observed during variation of bed depth at all ranges of concentration as shown in the Fig.6.73(a) and 6.73(b). The perfect matching between the experimental and ANN derived data for the variation of concentrations was recorded. ANN simulation correctly described the experimental data during variation of pH and inflow rate as depicted in the Fig. 6.73(e) and 6.73(f).

Adsorbent: Bagasse fly ash (BFA)

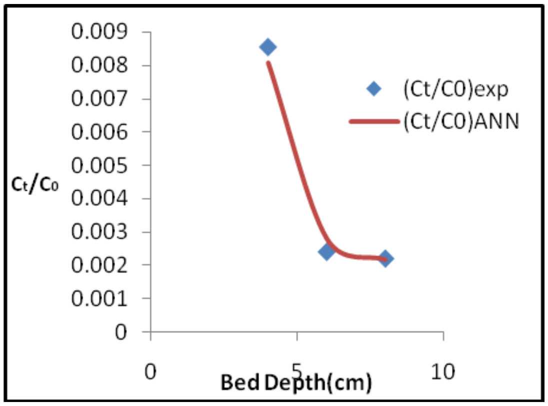

Fig.6.74(a): Laboratory study and ANN outcomes for BFA for different bed depth at C_0 = 25 mg/l

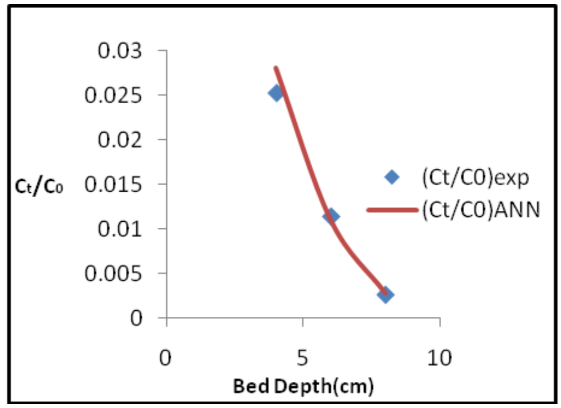

Fig.6.74(b): Laboratory study and ANN outcomes for BFA for different bed depth at C_0 = 75 mg/l

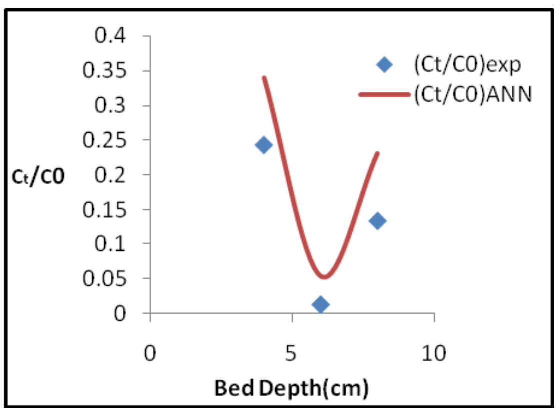

Fig.6.74(c): Laboratory study and ANN outcomes for BFA for different bed depth at C_0 = 100 mg/l

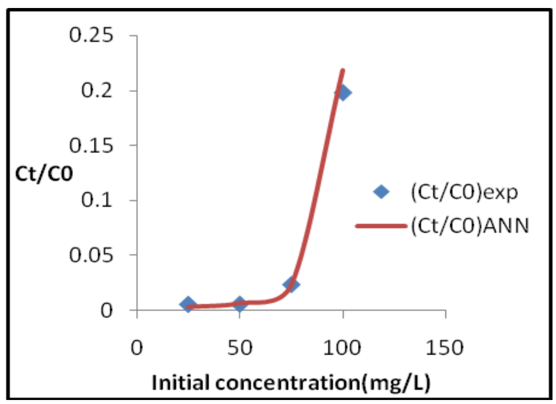

Fig.6.74(d): Laboratory study and ANN outcomes for BFA for different concentrations at H = 4cm

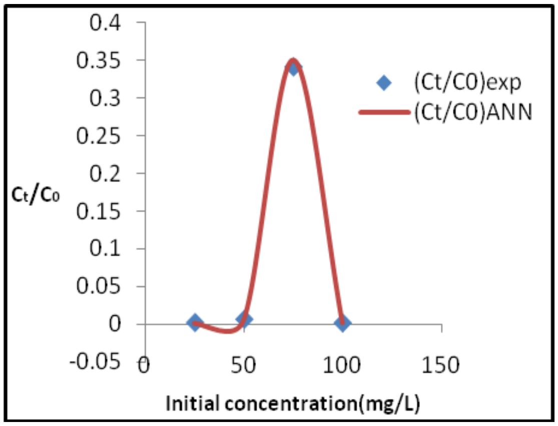

Fig. 6.74(e): Laboratory study and ANN outcomes for BFA for different concentrations at H = 6 cm

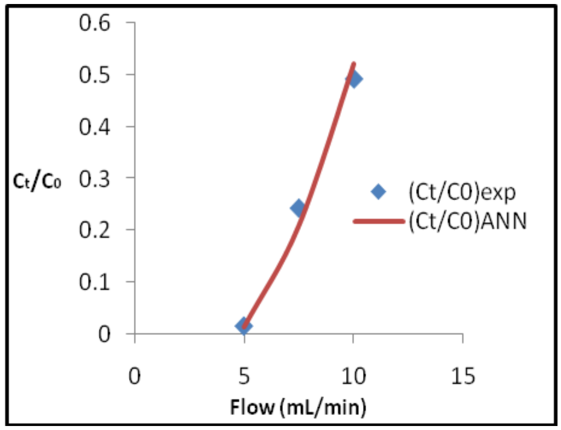

Fig. 6.74(f): Laboratory study and ANN outcomes for BFA for different flow rate at H = 4 cm C_0 =100 mg/L

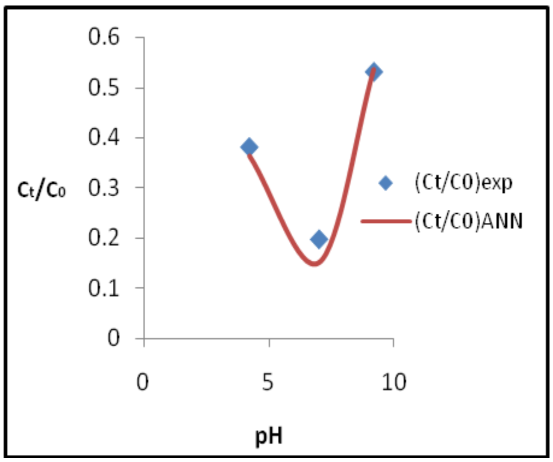

Fig.6.74(g): Laboratory study and ANN outcomes for BFA for different pH at H = 4 cm C_0 = 100 mg/L

At lower concentration 25 mg/L as shown in Fig. 6.74(a) for the bagasse fly ash, a notable deviation was observed between two data sets, whereas perfect matching was noted at higher concentration such as 75 and 100 mg/L shown in the Fig. 6.74(b) during the variation of adsorbent bed depth. The two sets of data correlated well during variation in initial concentration. The adsorption process during variation of initial pH of the dye mixture and also in the case of inflow rate was described satisfactorily by the ANN model so developed as depicted in the Fig. 6.74(d) to 6.74(g).

Adsorbent: Rice husk ash (RHA)

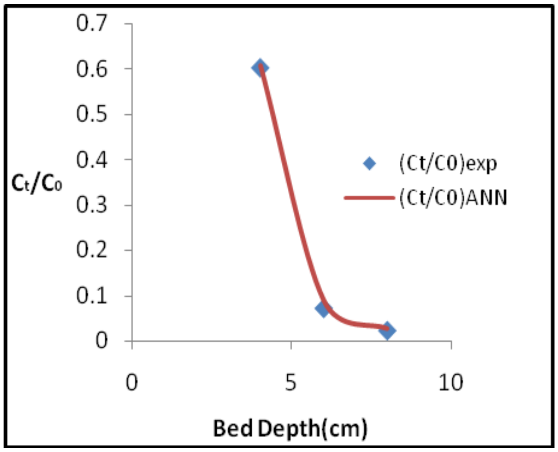

Fig.6.75(a): Laboratory study and ANN outcomes for RHA for different bed depth at C_0 = 25 mg/l

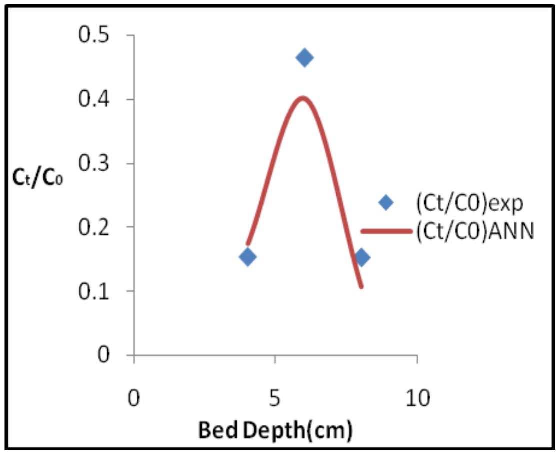

Fig.6.75(b): Laboratory study and ANN outcomes for RHA for different bed depth at C_0 = 100 mg/l

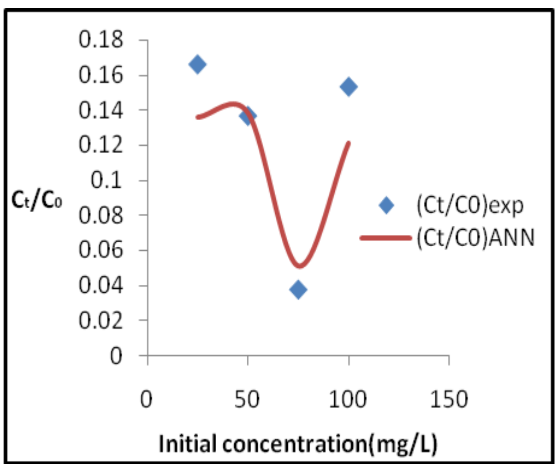

Fig.6.75(c): Laboratory study and ANN outcomes for RHA for different concentrations at H = 4 cm

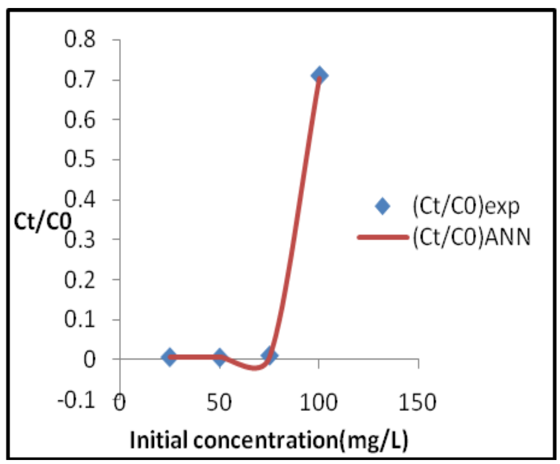

Fig.6..75(d): Laboratory study and ANN outcomes for RHA for different concentrations at H = 6 cm

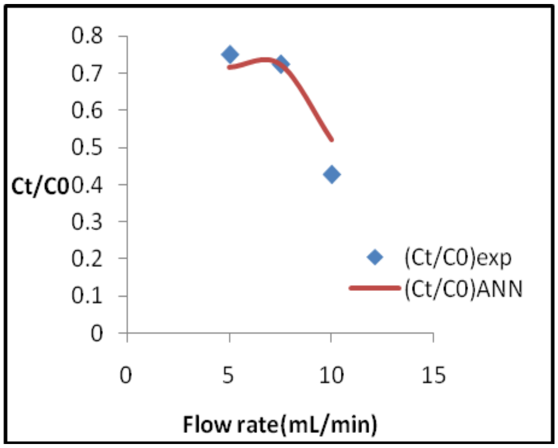

Fig.6.75(e): Laboratory study and ANN outcomes for RHA for different flowrate at H = 4 cm C_0 = 100 mg/L

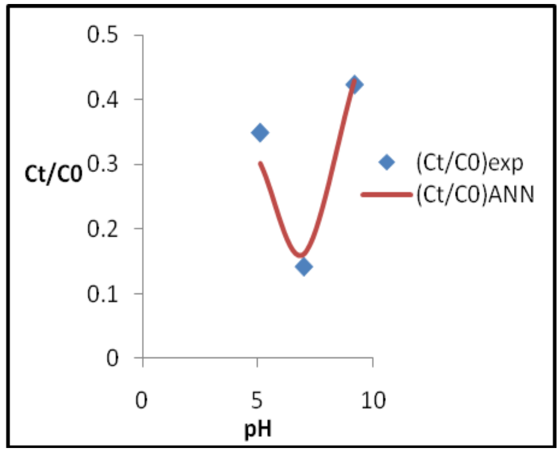

Fig.6.75(f): Laboratory study and ANN outcomes for RHA for different pH at H = 4 cm, C_0 = 100 mg/L

For the RHA adsorbent, the deviation of ANN simulated data from the experimental outcomes at higher concentration of 100mg/L was recorded as shown in the Fig. 6.75(b). This deviation was also recorded for lower bed depth of 4 cm during variation of concentrations from 25 to 100 mg/L. The deviation between two data sets at upper part of the experimental run during variation of inflow is shown in the Fig. 6.75(e). Mere deviation was also noted during the variation of pH as shown in the Fig. 6.75(f).

6.10.2 ANN Model for Batch Study

The ANN model so developed was also used for Batch study of the present investigation. The different operational variable parameters were taken as output as follows:

Table 6.45: Input data ranging in batch study

Operating variable	Range
Adsorbent dosage	0.1 to 5 gm
Contact Time	10 to 190 min
Initial Concentrations	25 to 150 mg/L
Shaker speed	30 to 165 r.p.m.
pH	4.1 to 9.2

The multi-layer perception (MLP) system explored in the present work was developed in METLAB 2009a with five input independent variables (adsorbent dosage, initial concentrations of mixed dye solution, contact time, shaker rpm and pH of adsorbate), one hidden layer and single output layer of one variable (percentage removal of dyes). It was analyzed and simulated by the ANN software.

The percentage fraction of data used for training and testing purposes is given in the Table 6.46.

The experimental data obtained under different variable physical paramenters for all the four adsorbents were used in the ANN model so developed. These data were used for trainging and target value derivation. The ANN simulated values for each of the operating parameters were compared with the experimental outcomes. The graphical representation is given below for all the four adsorbents separately for a comparative study between the performance of the ANN model so developed as well as the experimental performance study.

Table 6.46: Data used for Training and Testing for all the four adsorbents at different process parameters under batch study

Variable Parameters	Neem leaf ash			Jack fruit leaf ash			Bagasse fly ash			Rice husk ash		
	Total Data	Training Data	Testing Data	Total Data	Training Data	Testing Data	Total Data	Training Data	Testing Data	Total Data	Training Data	Testing Data
Adsorbent dosage	15	10	5	15	10	5	15	9	6	14	9	5
Contact time	12	6	6	12	7	5	12	6	6	12	8	4
Initial time	6	3	3	6	3	3	6	3	3	6	3	3
pH	6	3	3	6	3	3	6	3	3	6	3	3
Shaker speed	8	4	4	8	4	4	8	4	4	8	5	3

Adsorbent: Neem leaf ash (NLA)

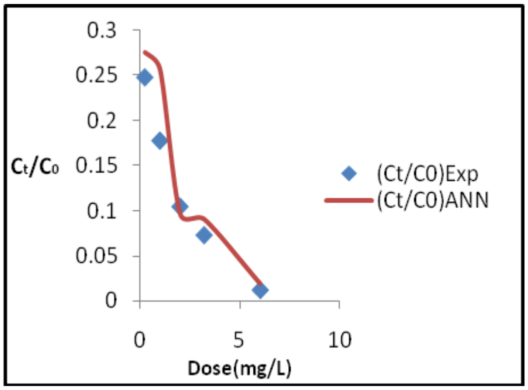

Fig. 6.76(a): Laboratory study and ANN outcomes of NLA for varying adsorbent dosage

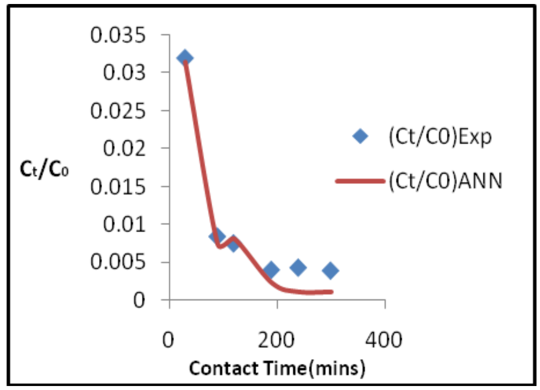

Fig. 6.76(b): Laboratory study and ANN outcomes of NLA for varying contact time

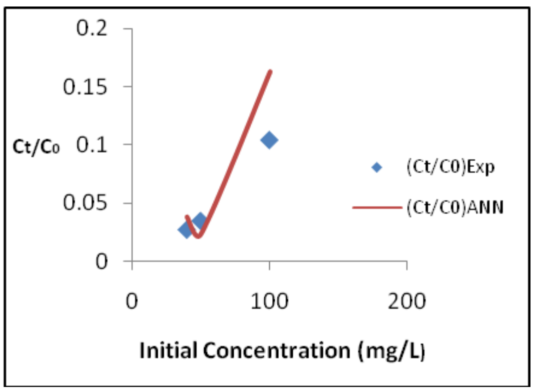

Fig. 6.76(c): Laboratory study and ANN outcomes of NLA for NLA for varying initial concentration

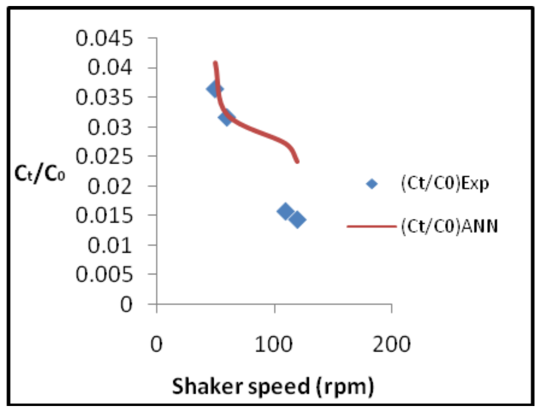

Fig. 6.76(d): Laboratory study and ANN outcomes of NLA for varying shaker speed

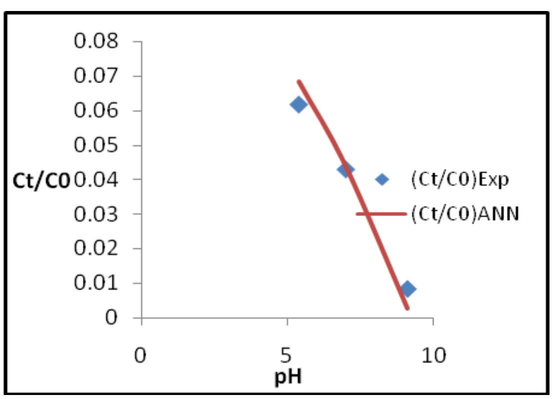

Fig. 6.76(e): Laboratory study and ANN outcomes of NLA for varying pH of the dye solution

Adsorbent: Jack fruit leaf ash (JFLA)

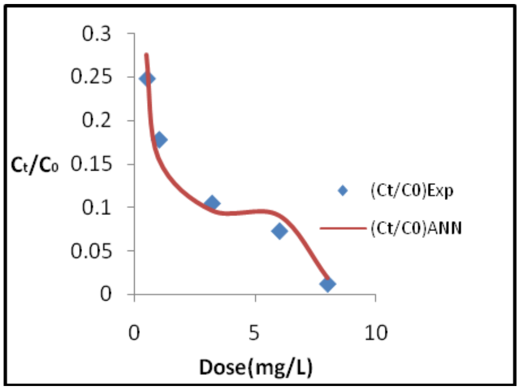

Fig. 6.77(a): Laboratory study and ANN outcomes of JFLA for varying adsorbent dosage

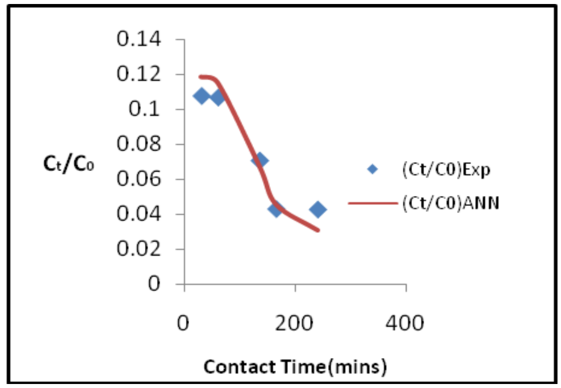

Fig. 6.77(b): Laboratory study and ANN outcomes of JFLA for varying contact time

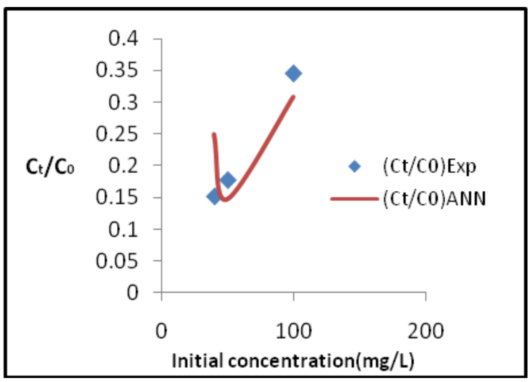

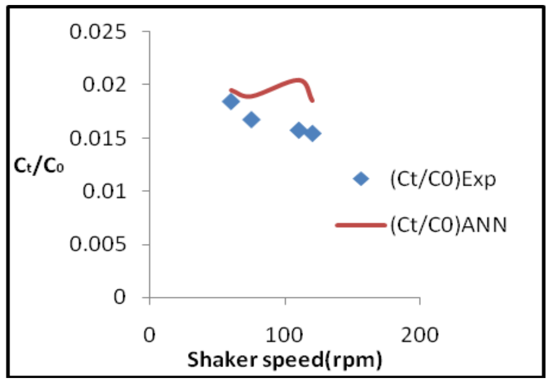

Fig. 6.77(c): Laboratory study and ANN outcomes of JFLA for varying initial concentration

Fig. 6.77(d): Laboratory study and ANN outcomes of JFLA for varying shaker speed

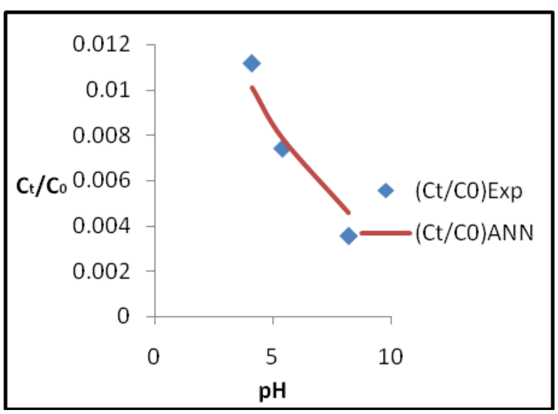

Fig. 6.77(e): Laboratory study and ANN outcomes of JFLA for varying pH of the dye solution

Adsorbent: Bagasse fly ash (BFA)

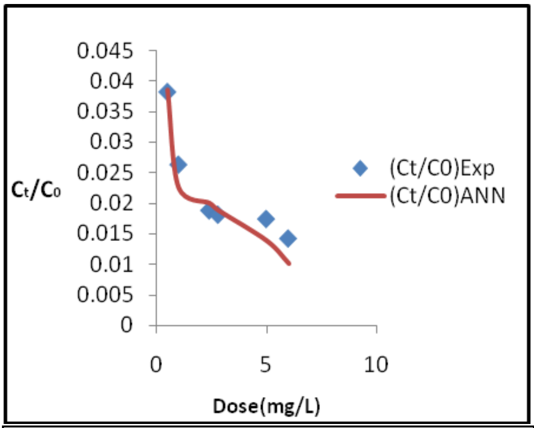

Fig. 6.78(a): Laboratory study and ANN outcomes of BFA for varying adsorbent dosage

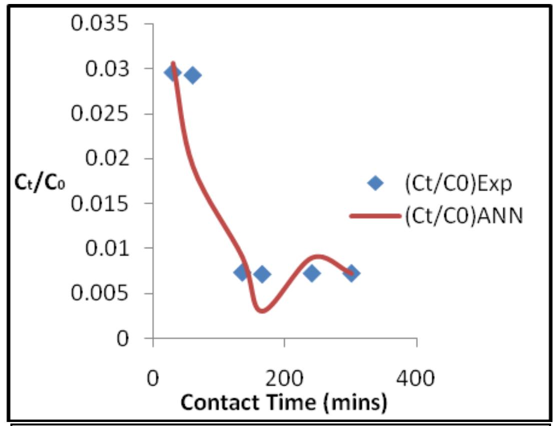

Fig. 6.78(b): Laboratory study and ANN outcomes of BFA for varying contact time

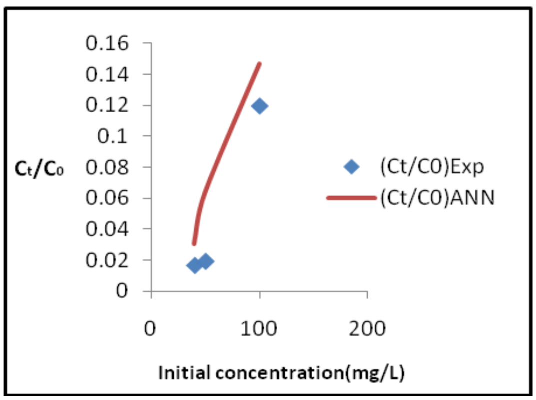

Fig. 6.78(c): Laboratory study and ANN outcomes of BFA for varying initial concentration

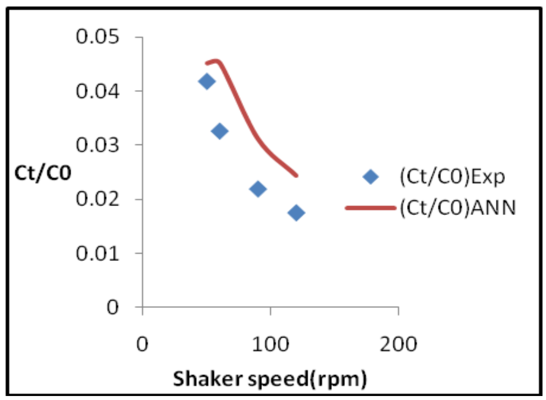

Fig. 6.78(d): Laboratory study and ANN outcomes of BFA for varying shaker speed

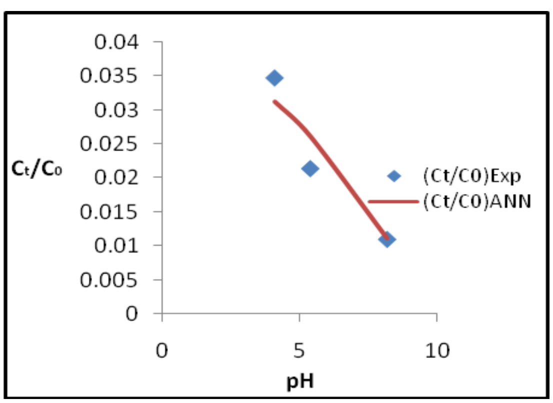

Fig. 6.78(e): Laboratory study and ANN outcomes of BFA for varying pH of the dye solution

Adsorbent: Rice husk ash (RHA)

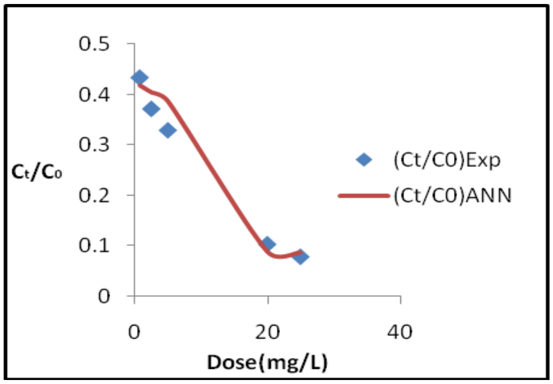

Fig. 6.79(a): Laboratory study and ANN outcomes of RHA for varying adsorbent dosage

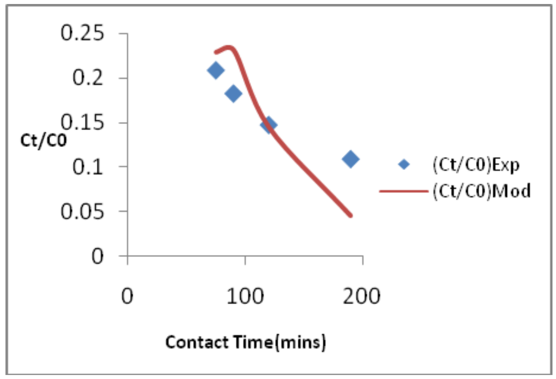

Fig. 6.79(b): Laboratory study and ANN outcomes of RHA for varying contact time

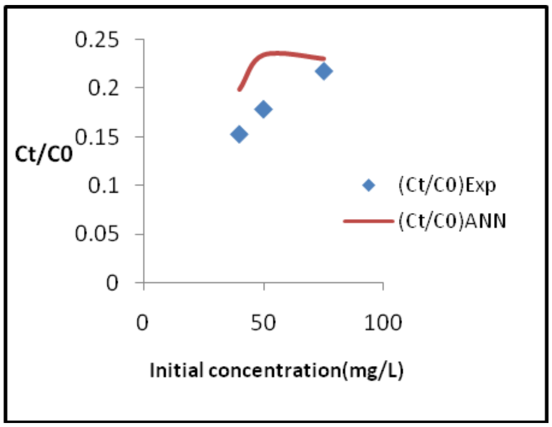

Fig. 6.79(c): Laboratory study and ANN outcomes of RHA for varying initial concentration

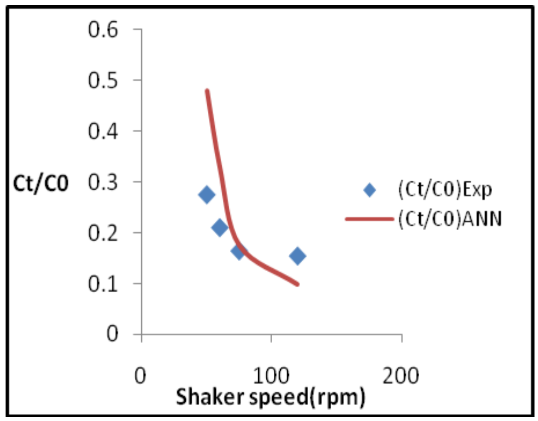

Fig. 6.79(d): Laboratory study and ANN outcomes of RHA for varying shaker speed

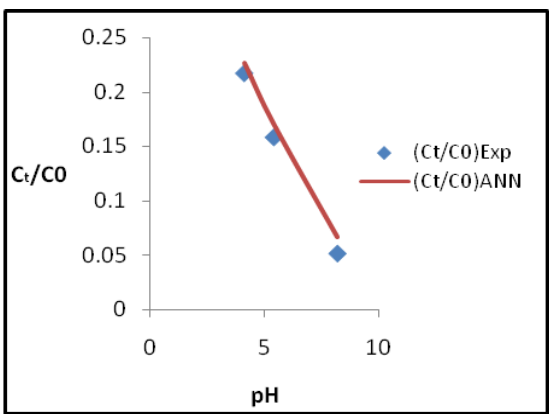

Fig.6.79(e): Laboratory study and ANN outcomes for varying pH of the dye solution

The deviation of experimental data from the ANN simulated outcome for the neem leaf ash in the adsorbent dosage and shaker speed is observed in the Fig.6.76(a) and 6.76 (d). A large deviation is also observed in case of pH variation data as shown in Fig. 6.76(e).

For jack fruit leaf ash adsorbent, slight deviation for the parameters in the case of adsorbent dosage and shaker speed is observed in the Fig. 6.77(a) and 6.77(d) respectively. The large deviation for the pH variation is observed in the Fig. 6.77(e). For the bagasse fly ash the experimental and ANN simulated data matches well except in the case of varying contact time as shown in the Fig. 6.78(b). A slight deviation is also noted for the contact time and initial convcentration for the rice husk ash as shown in the Fig. 6.79(b) and 6.79(c) respectively. The overall comparison between these two sets of data is satisfactory and proves the well performance of the ANN model so developed.

6.11: Statistical Significance Test (t-test) for evaluating performance of ANN model

Statistical t-test a type of inferential statistical tools was used to compare between two sets of data, which might be in related in certain aspect. It is stat hypothesis testing test. The three key parameters such as variance, t-score and p-value can be evaluated to judge the null hypothesis (**Kaushal and Singh 2017**).

The t-test may be categorized into three types

1. Independent samples t-test
2. Paired t- test
3. One sample t-test

During analyzing process similarities between outcomes of two procedures, one should know the character of three data set, whether paired or independent (**Adeniy et al. 2021).**

So the mathematical approach of t-test by tking sample from each of two data sets and draw comparison on the basis of null hypothesis (**Liang et al. 2019).**

The t-score of the hypothesis is the measure of similarities or dissimilarities between the two groups or within the same groups. Lower value indicates closeness of two sets of data.

Another important parameter is 'p' value in t-test. It indicates probability and varies from 0 to 100 %. The value is expressed in decimal place. It is the measure of statistical significance. So to determine the level of significance of two sets, p-value is considered. If it is greater than 0.05 (i.e. 5% level), indicates good agreement between two set of observations (***Fatima and Wihato et l. 2017***).

In the present study adsorptive removal of mixture of two dyes methylene blue and malachite green was investigated both in batch and column mode operation. In batch experiment the effect of different operating conditions viz. adsorbent dose, initial concentrations, shaker speed, contact time and pH of the dye solution were investigated. In column study, the operating variables viz. adsorbent bed height, initial dye concentrations, influent flow rate and pH of the solution were taken for consideration.

The experimental data and ANN simulated data were selected as two sets of variance for statistical t-test for each of this variable paraters for all the four adsorbents by using Stata 10 statistical software.

6.11.1: Statistical t-test between experimental and ANN simulated data : *Column study*

The experimental and ANN simulated data for adsorbent bed height, feed concentration, flow rate and pH of the dye solution were taken as two sets of variance for t-test analysis at 95% confidence level in Stata 10 statistical software ***(Kaushal et al. 2016 ; Kaushal and Singh, 2017).***

The outcomes of t-score, degree of freedom and standard deviations are given in tabular form in the Annexure for each of the operating parameters and for all the four adsorbents as follows under different operating conditions.

Here we illustrate statistical output for bed depth variation results for all four adsorbents in the Table below.

Table 6.47(a): Statistical test under column study for variable adsorbent height

	Parameters	NLA	JFLA	BFA	RHA
	Mean	-0.0005095	-0.0059446	0.0000934	0.0010075
	Standard Deviation	0.3260255	0.355709	0.1639928	0.1996772
	Standard Error	0.0683576	0.1037908	0.0539402	0.0675306
95% Confidence	Lower level	-0.1324933	-0.2148646	-0.1093024	-0.1382461
	Upper level	+1352949	+2029754	+0.1094892	+0.1362311
	t-value	-0.0075	-0.573	0.0017	-0.0149
	Degrees of freedom	90	46	36	34
	p-value	0.9941	0.9546	0.9986	0.9882

In this case we performed statistical t-test (paired t-test) considering two independent data sets one from the experimental outcomes as A and the other one from the ANN simulation as B. These two data sets as designated by A and B were entered in two columns in Stata 10 software one after another to check the null hypothesis. Different variable inputs like bed depth, initial concentration, inflow rate and pH variation were taken into consideration under column study.

Here, the null hypothesis might be;

H_o: There is no difference in between mean of the experimental and ANN simulated outcomes i.e.

$$\mu_1 - \mu_2 = 0.$$

And alternative hypothesis might be;

H_a: There is a difference in mean between the experimental and ANN simulated outcomes i.e.

$$\mu_1 - \mu_2 \neq 0$$

Output result refers the significant evocative decision about two groups A and B i.e. the experimental results and the ANN predicted values, that we compared in the present investigation. During this comparison, we took mean and standard deviation, as well as the outcomes from the independent t-test which contains the p-value and t-score. The t-test study data are represented as Stata 10 software output under different operating conditions for all four adsorbents. The output of the results have been depicted above.

In the output chart, H_o is the null hypothesis that is being tested.

Mean of two data sets var (1) and var (2) calculated by software and given as below:

$$diff. = \{mean(var\ 1) - mean(var\ 2)\} = 0$$

In our case **this is equal to zero as stated earlier** and is given in the Stata 10 output **as H_o : *diff* = 0** for all the four adsorbents under all operating conditions. So null hypothesis is correct and acceptable.

Degree of freedom of a t-test equals to sample size minus the number of parameters need to calculate during statistical analysis. In the preent study **two independent parameters were considered**. Thus the **degree of freedom** is determined by **subtracting 2 from the combined number of observations** for each cases as depicted above in the output chats for four low cost adsorbents.

The standard error of the mean for each level of the independent variable is shown in the Stata 10 output. It can be evaluated by dividing standard deviation with square root of sample sizes. The standard error varies from 0.01 to 0.13 for all column study results for all the four low cost adsorbents under various operating conditions. The small value for the standard error data indicates the **degree of precision with which the sample mean estimates the population means.**

The dependent variable under correlation with independent variable is standard deviation. Standard deviation is depicted in the output result for the present study. **In the output result we find that the deviation is nearly similar and also very small, indicating the similarities between the two data sets**.

p-value indicates significance of the null hypothesis considering the probability of observations. In the present investigation for both column and batch study the output results are given in the Stata 10 output format below considering four low cost adsorbents. It can be observed that the group means are considerably same as the p-value in the $\mathbf{P_r(|T| > |t|)}$ row under $\mathbf{(Ha: diff! = 0)}$ is high and greater than 0.97 in all the cases. In the **Mean** column we can observe that the percentage removal under different operating conditions under two data sets are almost similar. The two-tailed p-value for the **neem leaf ash** varied from 0.97 to 0.99 under different operating conditions. This value varied from 0.93 to 0.99 for jack fruit leaf ash, 0.95 to 0.99 for bagasse fly ash and 0.91 to 0.99 for rice husk ash respectively. The corresponding **two-tailed p-values were always greater than 0.05 under column study, which supported the null hypothesis** under 95% confidence level. The graphical representation of experimental data with ANN simulated outcomes also supported these similarities.

$\mathbf{P_r(T < t)}$ and $\mathbf{P_r(T > t)}$ are the one-tailed p-values evaluating the null against the alternatives i.e. mean difference < 0 and mean difference > 0 respectively. Like $\mathbf{P_r(|T| > |t|)}$, they are computed using t distribution. Here in the present study for all low cost adsorbents under different operating conditions, we observe that the value was greater than 0.05 (i.e. corresponding to 95% confidence level) from which we may conclude that mean is significantly equal to the null hypothesis i.e. difference between the two data sets are equal to zero.

't' is the ratio of difference between the sample mean and the mean of the given standard error. If t-value is equal to zero, it means the results exactly equal to the null hypothesis i.e. difference is zero. With the increased difference in between the sample data and null hypothesis, the absolute t-value also increases. In batch study two-tailed test was conducted for 95% confidence level. The critical region indicates how far the results are from the null hypothesis value. The result of t-test for bed depth variation in dynamic study for adsorbents is given in Table-6.47(a).

6.11.2 Statistical t-test between experimental and ANN simulated data : Batch study

The experimental and ANN simulated data for various inputs such as adsorbent dosage, initial concentrations off dye mixture solution, contact time, shaker speed and pH of the dye solution were taken as two sets of variance for t-test analysis at 95% confidence level in Stata 10 statistical software.

The outcomes of t-score, degree of freedom and standard deviations are given in Tabular form for each of the operating parameters for all the four adsorbents to evaluate the similarities of the two set of data in the Annexure.

Output data for batch study under different operating conditions provides important and useful descriptive statistical information for the two groups i.e. experimental result and ANN outcomes. It includes the mean(s) and standard deviation, coupled with outcomes of paired t-test.

Similar to column study, here we performed statistical t-test (paired t-test) considering two independent data sets; one from the experimental outcomes as A and the other one from the ANN simulation as B. These two data sets as designated by A and B were entered in two columns in Stata 10 software one after another to check the null hypothesis ***(Fatima and Wiharto, 2017).***

Here, the null hypo thesis might be;

H_o: There is no difference in between mean of the experimental and ANN simulated outcomes in batch mode i.e.

$$\mu_1 - \mu_2 = 0.$$

And alternative hypothesis might be;

H_a: There is a difference in mean between the experimental and ANN simulated outcomes i.e.

$$\mu_1 - \mu_2 \neq 0$$

In the output chart using Stata 10 software, Ho is the null hypothesis that was tested. In the present batch study **this is equal to zero, which supports the null hypothesis.**

The standard error of the mean for each level of the independent variable is shown in the column 3 of Stata 10 output. **From the output result we find that the deviation is nearly similar for all low cost adsorbents under all operating conditions.**

Here we represent an output data for variable adsorbent dosages in the Table below. *Rest of the computerized outputs are given in the Annexure as mentioned earlier.*

Table 6.47(b): Statistical test under batch study for variable adsorbent dosage

	Parameters	NLA	JFLA	BFA	RHA
	Mean	-0.0050295	-0.0011277	-0.0005041	-0.000673
	Standard Deviation	0.1173046	0.2357143	0.0203382	0.1607068
	Standard Error	-0.042149	0.0907885	0.0075573	0.0618984
95% Confidence	Lower level	-0.0911093	-0.187746	-0.0149764	-0.1278713
	Upper level	+0.0810502	+0.1854908	+0.0159845	+0.1265967
	t-value	-0.1193	-0.0124	0.0667	-0.0103
	Degrees of freedom	30	26	28	26
	p-value	0.9058	0.9902	0.9473	0.9919

Statistical significance is function of p-value. To determine level of significance of the model so developed, the p-value was considered. The p-value ranged from 0.92 to 0.99 for the batch study as recorded in the Stata 10 output. Thus, the p value was always greater than 0.05. The experimental values are not much differ from the predicted values as shown in the output.

The t-score, the ratio of difference between the sample mean and the mean of the said standard error for the present investigation varied from -0.0057 to 0.11, which also supports the similarities of two data sets.

From the statistical t-test performance, the developed ANN successfully describes the adsorption process both for column and batch mode study.

From the statistical t analysis it can be concluded that using paired t test, the ANN model prediction for the adsorption of dye mixture onto low cost adsorbent does not differ much from the experimental result.

The result of t-test for bed depth variation in batch study for adsorbents is given in Table-6.47(b). The entire software generated results for other inputs in batch study for four adsorbents are given in the Annexure.

6.11.3 Scanning Electron Microscope Study

The objective of carbonization is to enhance and reinforce the functional group potential and consequently to increase the number of active sites. Agricultural waste products containing cellulose in its structure have been extensively studied. The sorbents before adsorption, as shown in the Fig. 6.80(a), 6.81(a), 6.82(a) and 6.83(a) have a dirty and rough surface which can be attributed to presence of impurities of cellulose that spread over the surface pores. In the present study, the carbonization process was carried out to break down cellulose into carbon elements and remove non-carbon materials, which has ultimately enhanced the capacity of adsorption. This process has also removed water content helping adsorption of more dye molecules from the aqueous solution. This is shown in the Fig. 6.80(b), 6.81(b), 6.82(b) and 6.83(b).

Neem leaf ash

SEM study was conducted for neem leaf ash material for assessing morphology and surface characteristics as depicted in the Fig. 6.80(a) and 6.80(b) before and after adsorption. It composed of tiny particles having irregular, variable shapes and sizes. The highest size was recorded as 9 µm in diameter. The broken edge with uneven topography indicates effectiveness of such adsorbent.

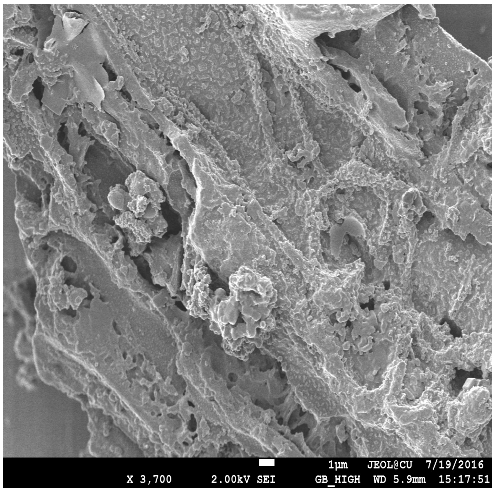

Fig. 6.80(a): SEM photograph for NLA before adsorption

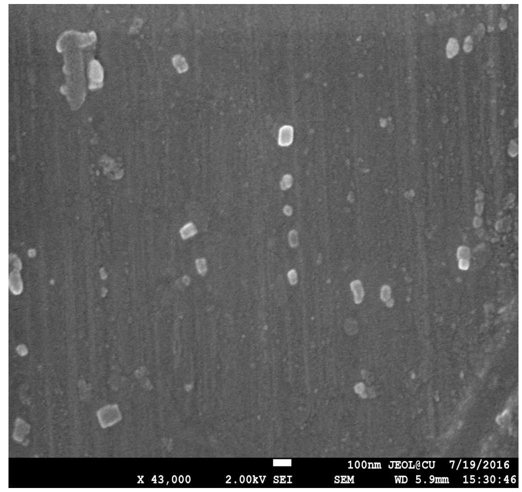

Fig. 6.80(b): SEM photograph for NLA after adsorption

Jack fruit leaf ash

SEM study was conducted for jack fruit leaf ash material for assessing morphology and surface characteristics as shown in the fig. 6.81(a) and 6.81(b). The particles are very small in size and stick like pores was observed which distributed non-uniformly on the surface. This indicates the heterogeneity of surface favourble for adsorption. After adsorption the surfaces adsorb dyes evenly and gives smooth exhausted surface visibility.

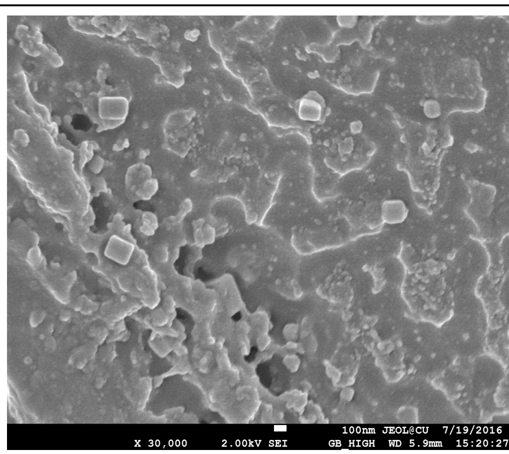

Fig. 6.81(a): SEM photograph for JFLA before adsorption

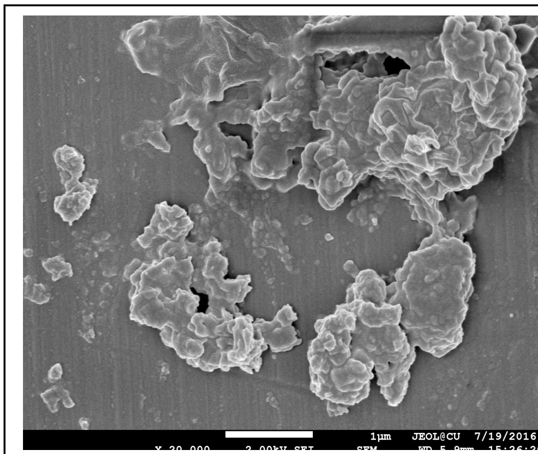

Fig. 6.81(b): SEM photograph for JFLA before adsorption

Bagasse fly ash

The SEM photograph for before and after adsorption is given in Fig. 6.82(a) and Fig. 6.82(b). It reveals that numerous pores of specific geometrical shape such as circular oval type are present on the surface. The cellulose sheet like pattern can be observed in Fig. 6.82(a). The after adsorption figure appeared as smooth texture as shown in the fig 6.82(b).

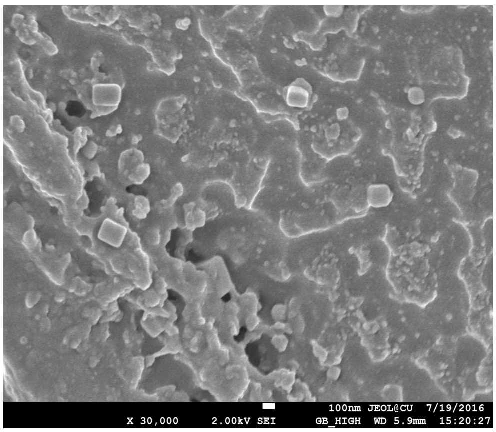

Fig. 6.82(a): SEM photograph for BFA before adsorption

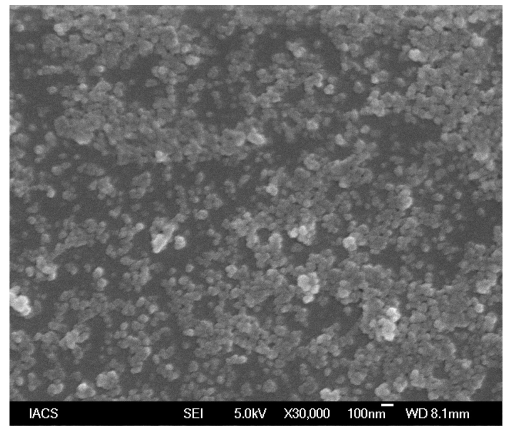

Fig. 6.82(b): SEM photograph for BFA after adsorption

Rice Husk Ash

SEM study was conducted for RHA in present investigation as shown in the fig. 6.83(a) and 6.83 (b). Small pores were distributed over the surface. The presence of silica on the surface is observed. SEM images of samples show the aggregates of clearly defined layers of loose flakes as shown in Fig. 6.83(a) and Fig. 6.83(b).

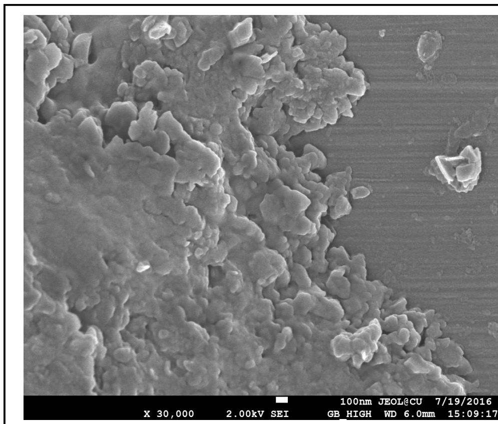

Fig. 6.83(a): SEM photograph for RHA before adsorption

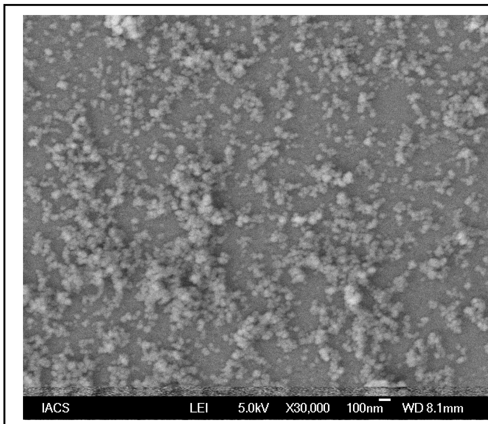

Fig. 6.83(b): SEM photograph for RHA after adsorption

Conclusions and Future Scopes of the Study

7

7.1 Conclusion based on experimental analysis

The present research investigation has been conducted with the objective of investigating into the feasibility of the adsorptive removal for mixture of two basic dyes viz. Methylene Blue and Malachite Green from the effluent by using four agricultural waste materials as low cost adsorbents.

The following inferences can draw on the basis of the outcomes of the experimental work and subsequent analysis of results.

- ***Effect of process parameters in the batch study***
  - ✓ The initial removal of dyes for all the four adsorbents increased from 53.25% to 97.8% with increasing in the adsorbent dosage from 0.1 to 10mg/L and thereafter removal rate decreases.
  - ✓ The removal percentage of dye increased for increase in contact time from 135 to 165 minutes for the four adsorbents.
  - ✓ The percentage removal of dye mixture decreased from 97% to 67 % with the increase in initial concentrations of dyes from 25 mg/L to 150 mg/L.
  - ✓ With the increase in shaker speed from 30 to 130 rpm, the dye removal percentage increased from 93% to 98% for all the four adsorbents.
  - ✓ Percentage exclusion of two basic dyes increased up to 99% as the solution pH increased from 4.1 to 9.2.

- ***Adsorption isotherm study***
  - ✓ Langmuir isotherm model described experimental data well as also revealed from high value of coefficient of regression value (R^2> 0.99).

- ✓ The isotherm constants (K_L) for neem leaf ash, jack fruit leaf ash, rice husk ash and bagasse fly ash were obtained as 13.9, 14.0, 8.46 and 18.5 respectively. The dye uptake values (q_m) for the adsorbents were found to be 40.0, 20.41, 52.63 and 29.41 respectively.
- ✓ In Freundlich isotherm study the adsorption intensity (1/n) for the four adsorbents was noted as 0.197, 0.291, 0.342 and 0.417 respectively, which indicates easy separation of dye molecules from the aqueous solution of two dyes.
- ✓ High correlation coefficient value (R^2> 0.96) for the neem leaf ash and jack fruit leaf ash indicates the adsorption data also fitted well in Temkin isotherm model. The comparatively lower correlation coefficient value for bagasse fly ash and rice husk ash (R^2>0.865) indicates that these two adsorbents did not follow the Temkin isotherm equally well.

➢ *Error analysis*

- ✓ Statistical analysis was employed with five individual error equations to select the optimum isotherm model. The normalized error value ranged from 7.623 to 18.215 for NLA, 0.312 to 12.056 for JLFA, 0.442 to 16.721 for BFA and 3.741 to 12.512. It indicates that Langmuir equation fitted best for the experimental data for all the four low cost adsorbents.

➢ *Kinetic study under batch mode*

- ✓ The coefficient of correlation (R^2) have obtained from pseudo-first-order and pseudo-second-order kinetic equation. It has been observed that pseudo-second-order model followed well (R^2>0.996) in compare to pseudo-first-order model R^2 varied from 0.2 to 0.89.

➢ *Thermodynamic study*

- ✓ The free energy (ΔG^0) was obtained negative at all temperatures and it became increasingly negative with an increase in temperature in case of all four adsorbents ranging from -15 to -24 $KJmol^{-1}$ which indicating feasibility and spontaneity of the process.
- ✓ Positive and high value for entropy (>0.2 $KJmol^{-1}K^{-1}$) suggests an increasing disorder and randomness at solid-liquid interface of dyes and that too for all the four adsorbents.
- ✓ The magnitude of change in enthalpy (ΔH^0) for all the four adsorbents viz. neem leaf ash, jack fruit leaf ash, bagasse fly ash and rice husk ash were obtained as 43.14, 37.56, 54.03 and 40.36 $KJmol^{-1}$ respectively, which is clearly indicative of the chemisorptions process.
- ✓ The negative ΔG^0 and the positive ΔH^0 value refers the spontaneous and endothermic character of adsorption respectively.
- ✓ The magnitude of activation energy ranging from 34.24 to 22.19 $KJmol^{-1}$ confirms the prevalence of chemisorption process.
- ✓ The sticking probability (S^{*}) ranged from $7.1x10^{-9}$ to $2.1x10^{-3}$, which indicates suitable process and temperature dependent.

➢ *Effect of process parameters in column study*

- ✓ The percentage removal of dye mixture increased for increasing bed height, influent rate of flow and adsorbate pH and decreased with increasing initial concentration of the dye mixture.

➢ *Dynamic model analysis under column study*

- ✓ In Thomas model the **higher coefficient of regression value (R^2)** means experimental outcomes fitted well with the existing model. Therefore, with higher initial concentration of mixture of two dyes, lesser flow rate and high adsorbent bed height certainly increase the adsorption of two cationic dyes from the aqueous solution mixture.

- ✓ Neem leaf ash as adsorbent described the model reasonably well.
- ✓ The dye uptake for all the bed depths decreased for increased initial concentration for the adsorbents, describing the consistency of adsorption process.
- ✓ Dynamics of the adsorption of dye mixture onto all four low cost adsorbents and pattern of breakthrough curves were best described by Adams-Bohart model. The balance of the process is not quick but is an averaged value of the entire process. The breakthrough curves were observed to be steeper as the initial concentrations of dye mixture increased.
- ✓ The BDST model is an effective tool to compare the performance of adsorbent bed functioning under different process variables. BDST model gave very rational approximation of the experimental model for understanding the effect of different process parameters over adsorption.
- ✓ The performance of BDST model as per as regression coefficient is concerned, for the present study reveals that it may be utilized to other similar investigation without adopting experiment further.

➢ *Evaluation of adsorption potential by ANN model*

- ✓ A slight departure from the experimental outcome was observed for the ANN simulated outcomes during the variation of concentration at higher adsorbent bed depth (8 cm) for the neem leaf ash.
- ✓ In the cases of jack fruit leaf ash and bagasse fly ash as adsorbent, the deviation during the variation of adsorbent bed depth at higher concentration (100 mg/L) was noted.
- ✓ During the variation of concentration at lower bed depth similar type of deviation was noted for the rice husk ash.

- ✓ The excellent matching between ANN and experimental data was observed during the variation of flow rate and pH of the adsorbate solution for all the four adsorbents.
- ✓ Deviation of experimental data from the ANN simulated outcome for the neem leaf ash in the adsorbent dosage and shaker speed was observed.
- ✓ For jack fruit leaf ash adsorbent, a slight deviation for adsorbent dosage and shaker speed was noted. Considerable pH variation was also observed.
- ✓ For the bagasse fly ash the experimental and ANN simulated data matched well.
- ✓ A slight deviation was noted for the contact time and initial concentration for the rice husk ash.
- ✓ The overall comparison between these two sets of data is satisfactory and it proves the good performance of the ANN model so developed.

7.2 Overall Conclusions

The overall conclusions which could be drawn from the above are as follows:

- ➢ The present study confirmed that the abundant agricultural wastes viz. neem leaf ash, jack fruit leaf ash, bagasse fly ash and carbonized rice husk can be used as substitute to commercially available activated carbon for exclusion of two basic dyes MB and MG.
- ➢ The ANN model predicts the experimental performance and decreases the number of experimental run. This phenomenon is certainly a cost and time effective approach necessary to judge the accuracy of the experiment. Moreover, it can be concluded that the ANN model so developed for the experiment using all four adsorbents agrees with the experimental outcomes well.

- The statistical t-test results in the form of small t-score and high p-value obtained for both batch and column mode operation for the adsorbents proves the accuracy and closeness between the experimental outcomes and ANN simulated data.
- It also provides idea for disposal of mixed dye solutions by using low cost adsorbents. The findings of the present laboratory-scale studies could be applicable in the process of industrial wastewaters adsorption.

7.3 Scopes for future study

The scope of the present study can be further expanded encompassing the following aspects:

- Dye removal using any raw low-cost adsorbent material yields poor results. However, carbonization of raw substances give noteworthy improvement in the capacity for adsorption. This ultimately enhances decolourization of dyes from the wastewater. Therefore, different reagents such as phosphoric acid, organic cation substitutions and mixture of reagents can be used to prepare activated carbon material, which could be improving its adsorption capacity.
- One of the popular approaches is to combine activated carbon with cationic polymers and organic cations which are able to decolorize the dye bearing wastewater. Activated carbon blends with cationic polymers and results in possible ionic interaction that tends to increase the adsorption efficiency of sorbent onto anionic dyes.
- Adsorbents used should be subjected to further studies i.e. for the removal of other classes of dyes, e.g. they can be used for the colour removal from the wastewater of paper and pulp industry.
- In the Indian context, agricultural waste materials such as rice straw, cluster seed shells, coconut coir are available in huge quantities. This can be

modified by suitable reagents and used in decolourization of dye bearing wastewater.

- Cost analysis of adsorption of dyes onto the inexpensive adsorbents used in the present study can be worked out and compared with the cost of commercially available activated carbon with these four adsorbents used in the study.
- The efficiency of the four low cost sorbents for the elimination of other pollutants such as phenols, heavy metals can be explored.
- The applicability of other adsorption isotherms such as Flurry Huggins and Redlich-Peterson can be explored during the batch study.
- The applicability of other kinetic models such as Clark, Wolborska and modified dose–response model can be explored for future work.
- Artificial intelligence (AI) is very useful technique for validating the process of adsorption of dyes. It can be classified into four different types. These are multivariable linear regression (MLR), artificial neural network (ANN), least square version of support vector machine (LS-SVM) and ensemble method of machine learning models. They have their specific application with certain strength and weakness. Out of these four models, ANN is practiced in the present study. Thus, beside ANN, other three models can be explored for the purpose.

Soumitra Banerjee

Date: 17.05.2022

1. **Prof. Siddhartha Datta** **(Examiner)**

2. **Prof. Anupam Debsarkar**

References

A

- *Allen W.A., Gausman H.W. and Richards A.J.*, "**Mean an effective optical constant of 13 kinds of plant leaves**", Appl. Opt., 9, 2573-2579, (1970).
- *Albihm A.*, "**Infectious Waste Management**", Encyclopedia of Microbiology, 3, 500-512, (2009).
- *Acharya J., Sahu J.N., Sahoo B.K., Mohanty C.R., Meikap B.C.*, "**Removal of lead (II) from waste water by activated carbon developed from Tamarind wood by zinc chloride activation",** Chem. Eng. J., 149 (1–3), 249-262, (2009).
- *Lin L., Zhang Y., Gao Y. and Ju Ming Y.*, "**Adsorption Removal of Dyes from Single and Binary Solutions using a Cellulose-based Bio-adsorbent**", Sustaiable Chem. Engg., 3(3), 432-442, (2015).
- *Abdul Quader A.K.M.*, "**Treatment of Textile Wastewater with Chlorine: An Effective Method**", Chemical Engineering research Bulletin, 14(1), 59-63, (2010).
- *Ahmad R. and Kumar R.*, **"Kinetic and thermodynamic studies of brilliant green adsorption onto carbon/iron oxide nanocomposite",** Journal of the Korean Chemical Society, 54(1), 125–130, (2010).
- *Agarry S.E. and Owabor C.N.* ,"**Evaluation of the adsorption potential of rubber (*Hevea brasiliensis*) seed pericarp – activated carbon in abattoir wastewater treatment and in the removal of iron (11) ions from aqueous solution",** Niger. J. Technol., 31, 346-348, (2012).
- *Adebowale K. O., Olu-Owolabi B. I., and Chigbundu E. C.*, **"Removal of Safranin-O from Aqueous Solution by Adsorption onto Kaolinite Clay",** Journal of Encapsulation and Adsorption Sciences (JEAS), 04, 89–104, (2014).
- *An S., Liu X., Yang L., and Zhang L.*, **"Enhancement removal of crystal violet dye using magnetic calcium ferrite nanoparticle: Study in single- and**

binary-solute systems", Chemical Engineering Research and Design, 94, 726–735, (2015).

- *Atalay S. and Ersoz G.,* "**Advanced Oxidation Processes for Removal of Dyes from Aqueous Mdia**", Green Chemistry, 5, 83-117, (2015).

- *Ameen A., Jalil A., Neelma M. and Sahid R.,* "**Physical and Chemical Analysis of Compost to Check its Maturity and Stability**", European Journal of Pharmaceutical and Medical Research, 3(5), 64-87, (2016).
- *Abkenar S. D.*, **"Application of magnetic-modified Fe3O4 nanoparticles for removal of crystal violet from aqueous solution: kinetic, equilibrium and thermodynamic studies",** *J.* Appl. Chem. Res, 10(1), 65–74, (2016).
- *Ahmet G., Meti A., Kubra G. and Sadi M.*, "**Dyes and Pigments: Their Structure and Properties**", Dyes and Pigments, 23, 13-29, (2016).
- *Ahemed S.***,** *Yesmin M., Jeba F., Hoque S., and James A.R.* **"Risk assessment and evaluation of heavy metals concentrations in blood samples of plastic industry workers in Dhaka, Bangladesh",** Toxicl Resp, 7, 1373-1380, (2016).
- *Ashrafi M., Arab Chamjangali M., Bagherian G., and Goudarzi N.*, **"Application of linear and non-linear methods for modeling removal efficiency of textile dyes from aqueous solutions using magnetic Fe3O4 impregnated onto walnut shell,"** Molecular and Biomolecular Spectroscopy, 171, 268–279, (2017).
- Ajenifuja E., J..A. Ajo and Ajayi E.O.B., " **Equilibrium adsorption isotherm studies of CU(II) and CO(II) in high concentration aqueous solutions on Ag-TiO_2- modified kaolinite ceramic adsorbents**", Appld. Water Sci., 7, 2279-2286, (2017).
- *Alcaraz L., Ana Lopez, Irene G***., "Preparation and characterization of activated carbons from winemaking wastes and their adsorption of methylene blue",** Adsorption Science & Technology**,** https://doi.org/10.1177%2F0263617418770295 (2018).
- *Abdulrshed A.A., Jlil A.A.,Zani M.A. and Gambo Y.*, "**Surface modification of activated carbon for adsorption of SO_2 and NO_X: A review of existing and**

emerging technologies", Renewable and Sustainable Energy Reviews, 94, 1067-1085, (2018).

- *Abbas K., , Znad H., & Awual M. R.*, **"A ligand anchored conjugate adsorbent for effective mercury(II) detection and removal from aqueous media"**, Chem, Eng. J. **334**, 432–443 (2018).
- *Abel Adekanmi A., Sitinurul A., Jamil A. and Abdullah M.*, " **Simultaneous Adsorption of Cationic Dyes from Binary Solutions by Thiourea-Modified Poly (acrylonitrite –co-acrylic acid): Detailed Isotherm and Kinetic Studies**", Dyes and Pigments, 12(18), 2903-2908, (2019).
- *Al Prol, A.E.* "**Study of environmental Concerns of Dyes and Recent Textile Effluents Treatment Technology: A Review**", Asian Journal of fisheries and Aquatic research, 3(2), 1-18, (2019).
- *Awual M.R.,* **"Mesoporous composite material for efficient lead (II) detection and removal from aqueous media"**, J. Environ. Chem. Eng. **7**, 103-124, (2019).
- *Alhujaily A., Yu H., Zhng X. and Ma F.*, "**Adsorption removal of anionic dyes from aqueous solutions using mushroom waste**", Appld. Water Sci., 10(183), 182-194, (2020).
- *Adeniyi A*.G., Chinenye AI. And Ighala J.O., "**ANN modelling of the Adsorption of Herbicides and Pesticides Based on Sorbate-Sorbent Interphase**", Chemistry Africa, 4,443-449, (2021).

B

- *Bohart G.S. and Adams E.Q.*, "**Some aspects of the behavior of charcoal with respect to cholorine**", J.Am.Chem. Soc., 42(3), 523-544, (1920).
- *Bnat F., Al-Basir A. and Sameer MA.*, "**Adsorption of phenols by Bentonite**", Environmental Pollution, 107(3), 391-398, (2000).
- *Bhattacharya, K.G. and Sarma Arunima*, "**Kinetics and thermodynamics of methylene blue adsorption on Neem (Azadirachta indica) leaf powder**," *Dyes and Pigments*, **65**, 51–59 (2005).

- *Bhatnagar A. and Minocha A.K.*, "**Conventional and non-conventional adsorbents for removal of pollutants from water-A review**", Indian Journal of Chemical Technology, 13(3), 203-217, (2006).
- *Batzias F.A., Sidiras D.K.*, "**Simulation of dye adsorption by beech sawdust as affected by pH",** J. Hazard. Mater. 141, 668-679, (2007).
- *Bagher Hayati, Niyaz Mohammad Mahmoodi*, "**Modification of activated carbon by the alkaline treatment to remove the dyes from wastewater: mechanism, isotherm and kinetic**", Desalination and Water Treatment, 47, 322-333, (2012).
- *Baranska M., Rygula A., Mazner K. and Kaczor A.*, "**Raman Spectroscopy of proteins: a review**", Journal of RAMAN SPECTROSCOPY, 44, 1061-1076, (2013).
- *Betiku E. , Okunsolawo S.S. , Ajala S.O. , Odedele O.S. ,* "**Performance evaluation of artificial neural network coupled with generic algorithm and response surface methodology in modeling and optimization of biodiesel production process parameters from shea tree (*Vitellaria paradoxa*) nut butter",** Renew. Energy, 76, 408-417, (2015).
- *Biswas S., Mishra U.,* **"Continuous Fixed-Bed Column Study and Adsorption Modeling: Removal of Lead Ion from Aqueous Solution by Charcoal Originated from Chemical Carbonization of Rubber Wood Sawdust",**Journal of Chemistry,(2015).
- *Barquilha CER, Cossich ES, Tavares CRG, Silva EA.*, "**Biosorption of nickel(II) and copper(II) ions in batch and fixed-bed columns by free and immobilized marine algae Sargassum sp**", J. Clean. Prod., 150, 58–64, (2017).
- *Bhatia D., Singh J, Kanwar RS and Sharma N.*, "**Biological methods for textile dye removal from wastewater: A Review**", Taylor and Francis, 47(3), 1-43, (2017).
- *Batool F. , Akbar J. , Iqbal S., Noreen S., Bukhar S.N.A.*, "**Study of isothermal, kinetic, and thermodynamic parameters for adsorption of cadmium: an overview of linear and nonlinear approach and error analysis'"** Bioinorg. Chem. Appl. 76, 123-128, (2018).
- *Brion-Roby R, Gagnon J, Deschenes J, Chabot B.*, "**Investigation of fixed bed adsorption column operation parameters using a chitosan material for**

treatment of arsenate contaminated water", . J. Environ. Chem. Eng. 6(1), 505–511, (2018).

- *Bidi N. A., Duplay J., and Jada A.*, **"Removal of anionic dye from textile industries effluents by using Tunisian clays as adsorbents: Zeta potential and streaming-induced potential measurements",** Comptes Rendus Chimie, 22, 113–125, (2019).
- Brunolellis C., Polonio Z., Julio AP. And Polinio C., "Effects of textile dyes on health and the environment and bioremediation potential of living organisms", Biotechnology Research and Innovations, 3(2), 275-290, (2019).
- *Benkhaya S***., , Souad R., Ahmed "A review on classifications, recent synthesis and applications of textile dyes**", Inorganic Chemistry Communications,115, 1-36, (2020).

C

- *Crini G.*, "**Non-conventional low-cost adsorbents for dye removal: A review**", Bioresource Technology, 97(9), 1061-1085, (2006).
- *Crini G., and Badot P.M.*, "**Application of Chitosan, a Natural Aminopolysaccharide, for Dye Removal from Aqueous Solutions by Adsorption Processes Using Batch Studies: A Review of Recent Literature**", Progress in Polymer Science, 33, 399-447, (2008).
- Chowdhury A.K., Debsarkar A., Bandyopadhyay A., "**Rice Husk Ash as a Low Cost Adsorbent for the Removal of Methylene Blue and Congo Red in Aqueous Solution**",Clean, 37(7), 581-591, (2009).
- *Cazetta Vargas A.L.., , Nogami E.M., Kunita M.H., Guilherme M.R., Martins A.C., Silva T.L., Moraes J.G. , Almeida V.C.*, "**NaOH-activated carbon of high surface area produced from coconut shell: Kinetics and equilibrium studies from the methylene blue adsorption",** Chem. Eng. J., 174 , 117-125, (2011).
- *Charumathi D. and Nilanjana Das*, "**Packed bed column studies for the removal of synthetic dyes from textile wastewater using immobilised dead C. tropicalis",** Desalination, 285, 22-30, (2012).

- *CPCB, Govt. of India*, "**Report on Inter State River water Monitoring**", 1-20, (2013).
- *Coruh, S Gürkan, E.H. Kılıç, E. Geyikci, F.* "**Prediction of adsorption efficiency for the removal malachite green and acid blue 161 dyes by marble sludge dust using AN**N", Global Nest Journal, 16(4), 676-689, (2014).
- *Canteli AMD, Carpine D, Scheer AP, Mafra MR, Mafra L.*, "**Fixed-bed column adsorption of the coffee aroma compound benzaldehyde from aqueous solution onto granular activated carbon from coconut husk**", WT Food Sci Technol 59(2),1025–1032, (2014).
- *Chi K., L. and Ta Wee S., "***Treatment of landfill leachate using ASBR combined with zeolite adsorption technology**", Biotech, 6, 195-201, (2016).
- *Chen D., Zeng Z., Zeng Y., Zhang F., and Wang M.*, *"***Removal of methylene blue and mechanism on magnetic γ-Fe2O3/SiO2 nanocomposite from aqueous solution***,"* Water Resources and Industry, 15, 1–13, (2016).
- *Chinenye A.M., ShahinA., Abbas R.,Danial K., Rahmin ., Somayeh R.*, "**Modeling of adsorption of Methylene Blue dye onHo-CaWO4nanoparticles using Response SurfaceMethodology (RSM) and Artificial NeuralNetwork (ANN) techniques**", MethodsX, 6, 1779-1797, (2019).

D

- *Dubey S.P., K. Gopal* K., "**Adsorption of chromium (VI) on low cost adsorbents derived from agricultural waste material: a comparative study",** J. Hazard. Mat., 145 , 465-470, (2007).
- *Diwevdi C.P., Sahu J.N. , Mohanty C.R. , Meikap B.C. ,"***Column performance of granular activated carbon packed bed for Pb (II) removal"** ,J. Hazard. Mater, 156 (1–3), 596-603, (2008).
- Demirbas E., Kobya M., Sulak M.T., "**Adsorption kinetics of a basic dye from aqueous solutions onto apricot stone activated carbon",** Bioresour. Technol., 99 , 5368-5373, (2008),

- *Dogan M., Alkan H.*, "**Adsorption of methylene blue onto hazenlnut shell: Kinetics, mechanism and activation parameters**", J. Hazard Mater, 164, 172-181, (2009).
- *Deniz F. and Saygider S.D.*, "**Removl of hazardous Azo dye (Basic red 46) from aqueous solution by princess tree leaf**", Desalination, 268(1-3), 6-11, (2011).
- *Demarchi, CA, Campos, M, Rodrigues, CA*, "**Adsorption of textile dye Reactive Red 120 by the chitosan-Fe (III)-crosslinked: Batch and fixed-bed studies**", Journal of Environmental Chemical Engineering 1(4), 1350–1358, (2013).
- *David Noel S and Rajan MR*, "**Impact of Dyeing Industry Effluent on Groundwater Quality by Water Quality Index and Correlation Analysis**", Journal of Pollution Effects & Control, 2(2), 1-4, (2014).
- *Dang H.T. and Mai P.T.,* "**Optimization of the Photochemical Degradation of Textile Dye Industrial Wastewaters**", Asean Journal on science and Technology for Development, 33(1), 10-17, (2017).
- *Dina A. and Scholz M.*, "**Treatment of synthetic textile wastewater containing dye mixtures with microcosms**", Environmetal Sci. and Pollution Research, 25, 1980-1997, (2018).
- *Dai Y.,* "**Utilizations of agricultural waste as adsorbent for the removal of contaminants: a review**", *Chemosphere,* 211, 235–253 (2018).
- *Department of Chemical and Petrochemicals Report*, **Govt. of India**, **Directory of Chemical Units**, 2019-2020.
- *Das R., Mukherjee A., Sinha I., Roy K. and · Dutta B.K.*, "**Synthesis of potential bio-adsorbent from Indian Neem leaves (Azadirachta indica) and its optimization for malachite green dye removal from industrial wastes using response surface methodology: kinetics, isotherms and thermodynamic studies**", Applied Water Science, 10, 116-134, (2020).

E

- *Ekici B.B. and Aksoy U.T.,* "**Prediction of building energy consumption by using artificial neural networks",** Advances in Engineering Software, 40(5), 356-362, (2009).

- *Ebrahim S.M., Nasifa B., and Abdeltawabd A.,* "**Equilibrium and thermodynamics for uranium onto potassium hydroxide oxidized carbon**", Desalination and water treatment, 72, 335-342, (2017).

F

- *Freundlich H.*, **"Over the adsorption in solution",** The Journal of Physical Chemistry A, 57, 1100–1107, (1906).
- *Futalan, CM, Kan, CC, Dalida, ML,* "**Fixed-bed column studies on the removal of copper using chitosan immobilized on bentonite. Carbohydrate Polymers**", 83(2), 697–704, (2011) .
- *Fayazi M., Afzali D., Taher M. A., Mostafavi A., and Gupta V. K.*, **"Removal of Safranin dye from aqueous solution using magnetic mesoporous clay: Optimization study",** Journal of Molecular Liquids, 212, 675–685, (2015).
- *Fatima S. Nd Wiharto W.*, "**The use of artificial neural network for modelling the decolouriztion of acid orange 7 solution of industrial by ozonation process**", Materials Science and Engineering, 72, 1-8, (2017).
- *Fkih D. Romdhane,Y. Satlaoui, R. Nasraoui, A. Charef, and R. Azouzi*, **"Adsorption, Modeling, Thermodynamic, and Kinetic Studies of Methyl Red Removal from Textile-Polluted Water Using Natural and Purified Organic Matter Rich Clays as Low-Cost Adsorbent",** Journal of Chemistry, 2020, 134-151, (2020).

G

- *Goulden C. H.*, "**Methods of Statistical Analysis**", 2nd ed. New York: Wiley, pp. 50-55, (1956).
- Guibal Larkin E., A., Vincent T. and Tobin J.M., "ChitsanSsorbents for Platinum Sorption from Dilute solutions", Ind. Eng. Chem. Res., 38, 4011-4022, (1999).
- *Gupta V.K., and Suhas*, "**Application of low-cost adsorbents for dye removal – A review**", Journal of Environmental Management, 90(8),2313-2342, (2009).

- *Ghosh A., Das P., Sinha K.*, "**Modeling of biosorption of Cu(II) by alkali-modified spent tea leaves using response surface methodology (RSM) and artificial neural network (ANN)",** Appl. Water Sci., 5 , 191-199, (2015).
- *Gregorio C.*, "**Non Conventional Adsorbents for Dye removal**", Book Chapter, Green Chemistry, 10, 359-407, (2015).
- *Gupta V.K., Khamparia S. and Iyagi I.*, "**Decolorization of mixture of dyes**", Global Journal of Environmental science and Management**,** 1(1), 71-94, (2015).
- *Gupta C., and Majumder D.* , "**Statistical optimization of process parameters for the simultaneous adsorption of Cr(VI) and phenol onto Fe-treated tea waste biomass",** Appl. Water Sci., 7 , 4361-4364, (2017).
- *Gorzin F., Abadi M.M.B.R.,* "**Adsorption of Cr (VI) from aqueous solution by adsorbent prepared from paper mill sludge: kinetics and thermodynamics studies**", Adsorp Sci. Tech., 36, 149–169, (2018).

H

- *Hutchins R.A.*, "**Optimum sizing of activated carbon systems**", Industrial Water Engineering, 10(3), 40–43, (1973).
- *Huang C.P. , and Huang C.*, "**Application of Aspergillus Oryze and Rhizopus Oryzae for Cu(II) Removal**", water research, 30(9), 1985-1990, (1996).
- *Holme I.,* "**Sir William Henry Perkin: a review of his life, work and legacy**", Color Technol., 122, 325-351, (2006).
- *Hubbe MA, Hasan SH, Ducoste JJ*, "**Cellulosic substrates for removal of pollutants from aqueous systems: a review**" Bioresources 6, 2161–2287, (2011).
- *Hasfalina C.M. and Akinbile C.O.*, "**Coconut Husk Adsorbent for the Removal of Methylene Blue Dye from Wastewater**", Biosources, 10(2), 2859-2874, (2015).
- *Heli S., Kimmo S. and Juhani S.*, "**Evaluation of organic and inorganic compounds levels of red wines processed from Pinot Noir Grapes**", Analytical Chem. Research, 3, 26-36, (2015).

- *Hassani, A., Kiransan, M., Soltani, R.D.C., Khataee, A., Karaca, S.*, "**Optimization of the adsorption of a textile dye onto nanoclay using a central composite design**", Turk. J. Chem. **39**, 734–749, (2015).
- *He, W., Li, N., Wang, X., Hu, T., Bu, X.*, "**A cationic metal-organic framework based on Zn_4 cluster for rapid and selective adsorption of dyes**", Chin. Chem. Lett. , 29, 857–860 (2018).
- *Himanshu Patel*, "**A general survey on internet of things based smart cities**", Journal of Advances in Shell Programming, 6(2), 1-7, (2019).

I

- Indra D., Vimal C., Srivastava C. and Nitin K.A., " **Removal of Orange-G and Methyl Violet dyes by adsorption onto bagasse fly ash-kinetic study and equilibrium isotherm analyses**", Dyes and Pigments, 69(3), 210-223, (2006).
- *Istratie R., Stoia M., Păcurariu C., and Locovei C.,* **"Single and simultaneous adsorption of methyl orange and phenol onto magnetic iron oxide/carbon nanocomposites,"** Arabian Journal of Chemistry, 15, 678-682, (2015).
- *India band Equity Foundation report:* ***September 2016***.
- *Indana M.K. , Gangapuram B.R. , Dadigala R., Bandi R., Guttena V., "***A novel green synthesis and characterization of silver nanoparticles using gum tragacanth and evaluation of their potential catalytic reduction activities with methylene blue and Congo red dyes",** J. Analy. Sci. Technol., 7, 19-24, (2016).
- *Isiuku B.O., Ojilbe C.A., Akakuru O.U. and Ibe F.C.,* **"Fixed-bed adsorptive removal of metanil yellow from simulated wastewater in a fixed-bed column by nitric acid-treated-H3PO4-activated carbon (NATPAAC) from oil palm fruit mesocarpfibre"** World News of Natural Science, 17, 157-172, (2018).
- *Islam, M., & Mostafa, M.* ,"Textile Dyeing Effluents and Environment Concerns - A Review", Journal of Environmental Science and Natural Resources, *11*(1-2), 131-144, (2019).

- *Islam M.R. and Mostafa M.G.,* **“Removal of a Reactive Dye from Synthetic Wastewater Using PAC and FeCl3 coagulants**”, Appl Water Sci,10, 119 (2020). https://doi.org/10.1007/s13201-020-01204-4.

J

- *Joylakshmi D., Jekendra S., Salam S. and Kumar S.*, “**Biochemical studies in several dyes yielding plants**”, Nor. Sci. Biol., 5(13), 303-308, (2013).
- *Jayalakshmi R. and Jeyanthi J.*, “**Simultaneous removal of binary die from textile effluent using cobaltaferrite alginate nanocomposite: performane and mechanism**”, Microchemical Journal, 145, 791-800, (2015).

K

- *Khataee, A.R., Fathinia, M., Aber, S., Zarei, M.:*, “**Optimization of photocatalytic treatment of dye solution on supported TiO_2 nanoparticles by central composite design: intermediates identification**”, J. Hazard. Mater., **181**, 886–897 (2010).
- *Kant R.*, “**Textile dyeing industry an environmental hazard**”, Natural Science, 4(1), 22-26, (2012).
- *Kharub M. and Rajor A.*, “**Assesment of total coliform removal and leaching of metal ions from sewage sludge-fly ash mixture at different pH and washing conditions**”, African Journal of Biotechnology, 11(40), 9612-9618, (2012).
- *Kartick H., GonawalaB., and Mehta M.J.*, “**Removal of color from different dye wastewater by using ferric oxide as an adsorbent**”, Int. J. Engg. Res., appl. 4(5), 102-109, (2014).
- *Kassa B.*, “**Removal of Malachite Green from Aqueous Solutions by Adsorption using Low Cost Biosorbent Neem Leaf (Azardirachte Indica)**”, Merit Research Journal of Environmental Science and Toxicology, 2(4), 086-092, (2014).

- *Kayode A., and Olugbenga S.*, "Dye **sequestration using agricultural wastes as adsorbents**", Water Resources and Industry, 12, 8-24, (2015).
- *Kaushal A. and Singh S.K.*, "**Application of statistical tools and hypothesis testing of adsorption data obtained for removal of heavy metals from aqueous solutions**", Int J Adv Res Innov ,4, 82–84, (2016).
- *Kathryn A., Humberto J., Gabriel M., Gerko O. and Paul C., "***What difference does a thiophene make? Evaluation of a 4-4-bis(thiophene) functionalized 2,2-bibyridyl copper (I) complex in a dye-sensitized solar cell**", Dyes and Pigments, 134, 419-426, (2016).
- *Kok B.T., Ahmad A., Bahman H. and Basak S.*, "**Adsorption Mechanism of Microcrystalline cellulose as Green Adsorbent for the removl of Cationic Methylene Blue Dye**", J.Chem.soc. Pak., 38, 512-518, (2016).
- *Kaushal A. and Singh S.K.,* ***"Critical*** **analysis of adsorption data statistically*"*** **A**pplied water Sci., 7, 3191-3196, (2017).
- *Khoshnamvand* N. , *Ahmadi S.* , *Mostafapour F.K.* , "**Kinetic and isotherm studies on ciprofloxacin an adsorption using magnesium oxidenanoparticles",** Int. J. Appl. Pharm. Sci. Res., 7, 79-83,(2017).
- *Katheresan V., Kansedo J. And Sie Y.L., "***Efficiecy of various recent wastewater dye removal methods: A review***",* Journal of Chemical Engineering, 6(4), 4676-4697, (2018).
- *Kamel R. M., Shahat A., Hegazy W., Khodier E.M. , & Awual M. R.*, "**Efficient toxic nitrite monitoring and removal from aqueous media with ligand based conjugate materials**", J. Mol. Liq. 285, 20–26 (2019).
- *Kavithayeni V, Geetha K, Akash Prabhu S.*, "**A Review on Dye Reduction Mechanism using Nano Adsorbents in Waste Water**", International Journal of Recent Technology and Engineering (IJRTE), 7 (6), 632-639, (2019).

L

- *Langmuir I.*, **"The constitution and fundamental properties of solids and liquids. Part-I. Solids**, "The Journal of the American Chemical Society, 38(2), 2221–2295, (1916).

- Lekan T. Popola, "**Nano-magnetic walnut shell-rice husk for Cd(II) sorption: design and optimization using artificial intelligence and design expert**", Heliyon, 5(8), 1-12, (2012).
- *Liu, Y, Kang, Y, Huang, D,* "**Cu^{+2} removal from aqueous solution by modified chitosan hydrogels**", Journal of Chemical Technology and Biotechnology 87(7), 1010–1016, (2012).
- *Lan T, Feng Y, Liao JL, Li XL, Ding CC, Zhang D, Yang JJ, Zeng JH, Yang YY, Tang J, Liu N., "***Biosorption behavior and mechanism of cesium-137 on *Rhodosporidium fluviale* strain UA2 isolated from cesium solution**", J Environ Radioactiv 134, 6–13, (2014).
- *Lin L., Zhang Y., Gao Y. and Ju Ming Y.*, "**Adsorption Removal of Dyes from Single and Binary Solutions using a Cellulose-based Bio-adsorbent**", Sustaiable Chem. Engg., 3(3), 432-442, (2015).
- Lcaraz L. A., Lopez A. and Garcia-Diaz I., "**Preparation and Characterization of activated carbons from winemaking wastes and their adsorption of methylene blue",** Adsorption science & Technology, 36, 1331-1351, (2018).
- *Liang G., Fu W. and Wang K., "Analysis of t-test misuses and SPSS operations in medical research papers, 31(7), 1-5, (2019).*
- *Li X. and Li, Y.* "**Adsorptive Removal of Dyes from Aqueous Solution by $KMnO_4$-Modified Rice Husk and Rice Straw**", Journal of Chemistry, doi. http;org/101155/2019/8359491.

M

- *Mangun C.L., Daley M.A., Braatz B.D. and Economy J.*, "**Effect of Temperature on the Adsorption of Organic Vapours on Activated carbon Fibers**", Carbon, 36, 123-130, (1998).
- *Malik P. K.*, **"Dye removal from wastewater using activated carbon developed from sawdust: adsorption equilibrium and kinetics",** Journal of Hazardous Materials, 113, 81–88, (2004).

- *Mall I.D., Srivastav V.C., Agrawal A.K. and Mishra I.M.,* **"Removal of congo red from aqueous solution by bagasse fly ash and activated carbon: kinetic study and equilibrium isotherm analyses",** Chemosphere, 61, 492-501, (2005)
- *Maji S.K. , Pal A., Pal T.*, "**Arsenic removal from real-life groundwater by adsorption on laterite soil",** J. Hazard. Mater, 151, 811-820, (2008).
- *Muntean S. G., Simu G. M., Kurunczi L., and Szabadai Z.*, **"Investigation of the aggregation of three disazo direct dyes by UV-vis spectroscopy and mathematical analysis",** chemistry magazine, 60(2), 152–155, (2009).
- *Mittal A. , Mittal J., Malviya A. and Gupta V.K.*, " **Adsorptive removal of hazardous anionic dye 'congo red' from wastewater using waste materials and recovery by decomposition**", Journal of Colloid and Interface sci., 340 (1), 16-26, (2009).
- *Mamdouh F. Abdel-Sabour* **"Water hyacinth: Available and renewable resource",** Electronic Journl of Environment, Agriculture, and Chemistry**,** 9(11), 1746-1759, (2010).
- *Mahmoodi N.M, Hayati B., Arami M, Lan C.,* **"Adsorption of textile dyes on pine cone from colored wastewater: kinetic, equilibrium and thermodynamic studies",** Desalination, 268 ,117-125, (2011).
- *Manoj D. and Chaitali M.*, "**Jack fruit leaf as adsorbent of malachite green: recovery of the dye**", Applied Sci., 1(5), 2452-2459, (2012).
- *Muntean S. G., Todea A., Radulescu-Grad M. E., and Popa A.***, "Decontamination of colored wastewater using synthetic sorbents",** Pure and Applied Chemistry, 86(11), 1771–1780, (2014).
- *Mandal N.K.*, "Performance **of Low Cost Bio-Adsorbents for the Removal of Metal Irons_ A Review**", Int. Sci. resh., 3(1), 177-181, (2014).
- *Marisa Punzi , Filip Nilsson , Anbarasan Anbalagan ,Britt-Marie Svensson ,Karin Jönsson ,Bo Mattiasson ,Maria Jonstrup* , "**Combined anaerobic-ozonation process for treatment of textile wastewater: removal of acute toxicity and mutagenicity**", Journl of Hazard. Mater., 292, 52-60, (2015).

- *Mir A.M., Hussain A. and Verma C.*, "**Design considerations and operational performance of anaerobic digester: a review**", Cogent engineering, 3(1), 175-183, (2016).
- *Ma X., Li D., Wu Z., Zhang H. Chen X., Liu Z.*, "**Mercury removal by adsorption on pectin extracted from sugar beet pulp: optimization by response surface methodology**", Chem. Eng Technol. 39:371–377, (2016).
- *Mahmoodi N. M. and Soltani-Gordefaramarzi S.*, **"Dye removal from single and quaternary systems using surface modified nanoparticles: Isotherm and kinetics studies",** Progress in Color, Colorants and Coatings, 9(2), 85–97, (2016).
- *Mohamed A. and Ahmed N.*, "**Health and Environmental Impacts of Dyes: Mini Review**", American Journal of Environmental Science and Engineering, 1(3), 64-67, (2017).
- *Mazhar A., Muhammad A., Syed E.*, **"Vibrio fischeri bioluminescence inhibition assay for eco-toxicity assessment: a review",** Science of the Total Environment, 626, 1295–1309, (2018).
- *Mohamed Gar Alalm and Mahmoud Nasr*, "**Artificial intelligence, regression model, and cost estimation for removal of chlorothalonil pesticide by activated carbon prepared from casuarina charcoal**", Sustainable Environment Research, 28(3), 101-110, (2018).
- *Mohammad K. Uddin and Mukhtar M. Salah*, "**Statistical analysis of Litchi chinensis's adsorption behavior toward Cr(VI)**", Applied Water Science, 8:140-149, (2018).
- *Massoud K., Mojtaba S. And Sahar M.,* "**Removal of Dyes from the Environment by Adsorption Process**", Chemical and Materials Engg., 6(2), 31-35, (2018).
- *Munagapati V.S., Yarramuthi V. and Kim Y.*, "**Removal of anionic dyes 9Reactive Black 5 nd Congo red) from aqueous solutions using Banana Peel Powder as an adsorbent**", Ecotoxicology and Environmental Safety, 148, 601-607, (2018).
- *Manoj D. and Chaitali M.*, "**Jack fruit leaf ash as an adsorbent of malachite green: recovery and reuse of the dye**", Applied Sci., 1(5), 2452-259, (2019).

- *Mohamed B., Hossain S., Gehad G. and Ola A.,* "**Removal of anionic and cationic dyes from wastewater by adsorption using multiwall carbon nanotubes**", Arabian Journal of Chemistry, 13(3), 4797-4810, (2020).

N

- Naimabadi A., Movahedian A. and Shasavani A., "**Decolorization and Biological Degredation of AZO Dye reactiveredz by anaerobic/aerobic sequential process**", Indian J. Environ. Health sci. Engg., 6(2), 67-72, (2009).
- *Nagendrappa G.*, "**Sir William Henry Perkin: The Man and his Mauve**", RESONANCE, 779-793, (2010).
- *Naja G. and Volsky B.*,**"The Mechanism of Metal Cation and Anion Biosorption",** Microbial Biosorption of Metls, 19-58,(2011).
- *Nguyen Thai Anh and Ruey-Shin Juang*, "**Treatment of waters and wastewaters containing sulfur dyes: A review**", Chemical Engineering Journal, 219, 109-117, (2013).

O

- *Ozdemir G. and Baysal S.H.*,"Chromium and aluminum biosorption on Chryseomonas luteola TEM05", Appld. Micro Bio. And Bio Tech., 64(4), 599-603, (2004).
- *Oguz E.*, **"Adsorption characteristics and the kinetics of the Cr (VI) on the Thuja oriantalis",** Colloids and Surfaces A: Physicochemical and Engineering Aspects, 252(2), 121–128, (2005).
- *Ewa Okoniewska E.*,"**Removal of Selected Dyes on Activated Carbons**", Sustainability, 13, 1-13, (2021).

P

- Patel H., "**A study on removal of Toluidine blue dye from aqueous solution by adsorption onto jack fruit leaf and neem leaf powder**", 70, 831-836, (2010).

- *Patil M. R. and Shrivastava V. S.*, **"Adsorption of malachite green by polyaniline–nickel ferrite magnetic nanocomposite: an isotherm and kinetic study",** Applied Nanoscience, 5(7), 809–816, (2015).
- *Panda H., Tiadi N., Mohanty M., Mohanty C. R.*, "**Studies on adsorption behavior of an industrial waste for removal of chromium from aqueous solution**", S Afr J Chem Eng 23:132–138, (2017).
- *Pirkarami A and Ebrahim M.*, "**Removal of dye from industrial wastewater with n emphasis on improving economic efficiency and degradation mechanism**", Journal of Saudi Chemical Society, 21(1), 179-186, (2017).

R

- *Romero-Gonzalez J., Peralta-Videa J., Rodrıguez E., Ramirez S., and Gardea-Torresdey J.*, **"Determination of thermodynamic parameters of Cr (VI) adsorption from aqueous solution onto *Agave lechuguilla* biomass",** The Journal of Chemical Thermodynamics, 37(4), 343–347, (2005).
- *Ryan R., Netta W., Jessey B. and Kirk W.B.*, "**Vitalizing effects of being outdoors and in nature**", Journal of Environmental Psychology, 30, 159-168, (2010).
- *Robati D., Mirza B. and Rajabi M.*, **"Removal of hazardous dyes-BR 12 and methyl orange using graphene oxide as an adsorbent from aqueous phase",** Chemical Engineering Journal, 284, 687–697, (2016).
- *Raval N.P., Shah P.U., Shah N.K.*, "**Adsorptive removal of nickel (II) ions from aqueous environment: a review"**, J Environ Manag 179, 1–20, (2016).
- *Rao R. A. K., and Kashifuddin M.* , "**Adsorption studies of Cd (II) on ball clay: comparison with other natural clays".** Arab J Chem 9:S1233–S1241, (2016).
- *Raheleh Jafri and Sina Razvarz,* **"Solution of fuzzy differential equations using fuzzy Sumudu transforms",** IEEE International Conference, July 3-5, (2017).
- *Recepoglu Y.K., Nalan K., Idil Y., Kazuharu Y., Syouhel N.,* "**Packed bed column dynamic study for boron removal from geothermal brine by a chelating**

fiber and breakthrough curve analysis by using mathematical models", Desalination, 437(1), 1-6, (2018).

- *Rahat Javaid and Umair Yaqub Qazi* , "**Catalytic Oxidation Process for the Degradation of Synthetic Dyes: An Overview**", International Journal of Environmental Research and Public Health, 16, 2066-2093, (2019).

S

- *Sathy C. and Pramada P.N.*, "**Rice husk an adsorbent for methylene blue-effect of ashing temperature**", Adsorption, 12(27), 127-135, (2006).
- *Sousa M.M., Melo M.J., Parola A.J., Rzepa H.S.,* "**A study in mauv: unveiling Perkin's dye in historic samples**", Chem. Eur. J., 14, 8506-8513, (2008).
- *Salleh, M.A.M., Mahmoud, D.K., Karim, W.A.W.A., Idris*, "A Cationic and anionic dye adsorption by agricultural solid wastes: a comprehensive review", Desalination, 280, 1–13, (2011).
- *Sharma, Y.C., Upadhyay, S.N.*, "**An economically viable removal of methylene blue by adsorption on activated carbon prepared from rice husk**", Can. J. Chem. Eng., **89**, 377–383, (2011).
- Saibaba L. N.. King, K.V., P Gopinadh R., "**Application of artificial neural network and statistical methods in coconut oil processing**", International Journal of Advanced Computer and Mathematical Sciences, 3(2), 209-214, (2012).
- *Saeedeh H., Khaterah S., Hamila S. and Zahra A.*, "**Removal of Azo Dyes (Violet B and Violet 5R) from Aqueous Solution using New Activated Carbon Developed from Orange Peel**", Journal of Chemistry, http://dx. Doi. Org/10.1155/2013/283274.(2013).
- *Saikhom J.D., Salam J.S., Kumar S., Manabendra C.,* "**Biochemical Studies in Several Dye Yeilding Plants**", Nor. Sci. Biol., 5(13), 303-308, (2013).
- *Suriga C. L.,* "**Catalytic oxidation of dye waste water by biomass charcoal loaded multiple rare earth composite material**", IOP Conf Ser Mater Sci Eng, 167, 1–7, (2014).

- *Sanmuga Priya E. , Senthamil Selvan P.*, "**Water hyacinth (Eichhornia crassipes) – An efficient and economic adsorbent for textile effluent treatment – A review**", Arabian Journal of Chemistry, http://dx.doi.org/10.1016/j.arabjc.2014.03.002, (2014).
- *Sharma N., Tiwari D.P., Singh S.K.*, "**The efficiency appraisal for removal of malachite green by potato peel and neem bark: isotherm and kinetic studies**", Int J Environ Eng 5, 83–88, (2014).
- *Siddique M., Talha A., Gardazi S.M.H. and Shah J.,* "**Dye Removal from Textile Wastewater using Bioadsorbents**", Scientific J. of COMSATS-SCIENCE VISION, 20, 131-136, (2014).
- *Senthil Kumar P., Ramalingam S. and Sivastava S.*, "**Lead (II) Adsorption onto Sulphuric Acid Treated Cashew Nut Shell", Separation Science and Technology**, 46(15), 2436-2449, (2015).
- *Sumathi S.*, "**Treatment of Textile Dye Containing effluents**", Current Environmental Engineering, 193), 162-184, (2015).
- *Shah P.U., Raval N.P., Shah N.K.*, "**Adsorption of copper from an aqueous solution by chemically modified cassava starch**", J Mater Environ Sci. 6, 2573–2582, (2015).
- *Shrmeen Afroze and H Ming Aug*, "**Adsorption of methylene blue dye from aqueous solution by novel biomass Eucalyptus sheathiana bark: equilibrium, kinetics, thermodynamics and mechanism**", Desalination and water treatment, 43(4), 424-441, (2015)
- *Satapathy M. K., Banerjee P., and Das P.*, **"Plant-mediated synthesis of silver-nanocomposite as novel effective azo dye adsorbent",** Applied Nanoscience, 5(1), 1–9, (2015).
- *Suresh S. and Tygi N.*, "Production **of cellulose from sugarcane molasses using Gluconacetobacter intermedius SNT-1: optimization and characterization**", Journal of cleaner Production, 112, 71-80, (2016).
- *Samchetshabam G., Ajmal H., T. G. Choudhury*,T.G., "**Impact of Textile Dyes Waste on Aquatic Environments and its Treatment**", Environment & Ecology 35 (3), 2349—2353, (2017).

- *Sarala S., Othman N.A., Bakar N.A. and Karim Z.A.,* "**Adsorption studies of packed bed column for the removl of dyes using amine functionalized radiation induced fiber**", S N Applied Sciences, 175, doi. http//doi.org/10.1007/s42452-019-0184-2, (2017).
- *Song Z. J., Ran W., and Wei F. Y.,* **"One-step approach for the synthesis of CoFe2o4@rGO core-shell nanocomposites as efficient adsorbent for removal of organic pollutants",** Water Science and Technology, 75(2), 397–405, (2017).
- *Stephen E.A.,* "**Studies on the mechanism of adsorption of methylene blue onto activated carbon using thermodynamic tools**", 13(2), 17-19, (2018).
- *Sarvanen P., Senthil P. and Yaswanthraj M.* "**Modelling and analysis of a packed-bed column for the effective removal of zinc from aqueous solution using dual surface-modified biomass"** Particulate Sci. and Tech.,36, 934-944, (2018).
- *S. Rahdar, A. Rahdar, C.A. Igwegbe, F. Moghaddam, S. Ahmadi,*"**Synthesis and physical characterization of nickel oxide nanoparticles and its application study in the removal of ciprofloxacin from contaminated water by adsorption: equilibrium and kinetic studies",** Desalin. Water Treat., 141 , pp. 386-393, (2019).
- *S. Sandhya, S. abinaya and P. Lavanya,* "**Engine Oil Condition Monitoring using IOT and Predictive Analysis**", Journal of Critical review, 7(4), 1378-1386, (2020).

T

- *Temkin M. and Pyzhev V.*, "**Kinetics of Ammonia Synthesis on Promoted Iron Catalysts**", Acta Physicochimica USSR, 12, 217-222, (1940).
- *Thomas H.C.,* "**Heterogeneous ion exchange in a flowing system**", *J. Am. Chem. Soc., 66, 1664-1666, (1944).*
- *Tiwari D.P., Singh S.K., Sharma N.*, "**Sorption of methylene blue on treated agricultural adsorbents",** Water Sci, App. doi:10.1007/S13201-014-0171-0, (2014).

- *Thakur S. and Chauhan M.S.*, "**Treatment of Wastewater by Electro Coagulation: A Review**", International Journal of Engineering Science and Innovative Technology, 5(3), 104-110, (2016).

U

- *Uddin T., Rukanuzzaman M., Islam A., "**Adsorption***" **of methylene blue from aqueous solution by jackfruit (Artocarpus hetropyllus) leaf powder: A fixed bed column study",** Journl of Environmentl Management, 90(11), 3443-3450, (2009).
- *Uddin T., Rahaman A. ans Islam R***., "A potential low cost adsorbent for the removal of cationic dyes from aqueous solutions**" Applied Water Science, 7, 2831-2842, (2017).

V

- *Van der Marel H. W.,* "**Quantitative analysis of clay minerals and their admixtures"***,* Contributions to Mineralogy and Petrology, 12, 96–138, (1966).
- *Vital R. K., Saibaba K. V. N., Shaik K. B., and Gopinath R., "Gopinath*, **"Dye removal by adsorption: A review",** Journal of Bioremediation & Biodegradation, 7, 371-384, (2016).
- *Venkatesh S., Venkatesh K. and Quaff A.R.,* "**Dye decomposition by combined ozonation and anaerobic treatment: Cost effective technology**", Journal of Applied Research and Technology, 15(4), 340-345, (2017).

W

- *Wang C., Feng C., Gao Y., Ma X., Wu Q., and Wang Z.*, **"Preparation of a graphene-based magnetic nanocomposite for the removal of an organic dye from aqueous solution",** Chemical Engineering Journal, 173(1), 92–97, (2011).
- World's Worst Pollution Problems, Green Cross, Switzerland and Pure Earth, 1-70, (2015).
- World Bank Report on South Asia Environment and water Resource Unit (2014).

- *Walli F., "***Color Removal and COD Reduction of Dyeing Bath Wastewater by Fenton Reaction**", International Journal of Waste resources, 5(1), 171-178, (2015).
- *Wang T., Zhao P., Lu N., Chen H., Zhang C., and Hou X.*, **"Facile fabrication of Fe3O4/MIL-101(Cr) for effective removal of acid red 1 and orange G from aqueous solution,"** Chemical Engineering Journal, 295, 403–413, (2016).
- *Wang Y., Xu H., Yang S., Wang W. and Wang D.,* "**Adsorption Property and Mechanism of Oxytetracycline onto Willow Residues", Int. J. Environ. Res., 15, 1-11, (2018).**

Y

- Yoon Y.H. and Nelson J.H., "Application of gas adsorption kinetics: theoretical model for respirator cartridge service life", Am. Ind. Hyg., 45, 509-516, (1984).
- *Yao Y., Xu F., Chen M., Xu Z., and Zhu Z.*, **"Adsorption behavior of methylene blue on carbon nanotubes,"** Bioresource Technology, 10199). 9, 3040–3046, (2010).
- *Yang L., Zhang Y., and Liu X.*, "**The investigation of synergistic and competitive interaction between dye Congo red and methyl blue on magnetic MnFe2O4,"** Chemical Engineering Journal, 246, 88–96, (2014).
- Yawei N., Ebelegi A.N. and D. Wankasi, "**Modelling and Interpretation of Adsorption Isotherms**", Journal of Chemistry, 21,1-11, (2017).
- *Yang Z. H., Wang B. , Chai L. Y. , Wang Y. Y. , C.Q. Wang H. Y.* "**Removal of Cr(III) and Cr(VI) from aqueous solution by adsorption on sugarcane pulp residue**", J Cent South Univ Technol., 16, 0101–0107, (2017).
- *Yu J., Zon A., He W. and Liu B.*, "**Adsorption of Mixed Dye system with Cetyltrimrthylammonium Bromide Modified Sepiolite: Characterization, Performance, Kinetics and Thermodynamics**", Wter, 12, 980-994, (2020).

Annexure-I

Variation of different process parameters under Batch Study

Table-1: Spectrophotometer reading using NLA as adsorbent for various initial concentrations (pH, temperature, amount of adsorbent, shaker speed and time were 7, 30^0C, 4gm, 120 r.p.m. and 3 hrs respectively)

Conc. (mg/L)	C_t/C_0	% removal
25	0.0122	98.78
40	0.0276	97.24
50	0.0351	96.49
75	0.0511	94.89
100	0.1047	89.53
150	0.3226	67.74

Table-2: Spectrophotometer reading using NLA as adsorbent for various shaker speeds (pH, temperature, amount of adsorbent, initial conc. and time were 7, 30^0C, 4 gm, 50 mg/L and 3 hrs respectively)

Shaker speed (rpm)	C_t/C_0	% removal
30	0.0687	93.13
50	0.0364	96.36
60	0.0316	96.84
75	0.0295	97.05
90	0.0278	97.22
110	0.0157	98.43
120	0.0143	98.57
130	0.0148	98.52

Table-3: Spectrophotometer reading using NLA as adsorbent for various adsorbent dosages (pH, temperature, initial conc., shaker speed and time were 7, 30^0C, 50mg/L, 120 r.p.m. and 3 hrs respectively)

Dose (gm/L)	C_t/C_0	% removal
0.5	0.4675	53.25
1.25	0.2478	75.22
2.5	0.2078	79.22
5	0.1775	82.25
6	0.1529	84.71
7	0.1105	88.95
10	0.1042	89.58
12	0.1008	89.92
14	0.0981	90.19
16	0.0724	92.76
20	0.0519	94.81
25	0.0219	97.81
30	0.0115	98.85
40	0.0078	99.22
60	0.0079	99.21

Table-4: Spectrophotometer reading using NLA as adsorbent for various contact time (pH, temperature, amount of adsorbent, shaker speed and initial conc. were 7, 30^{0}C, 4 gm, 120 r.p.m. and 50mg/L respectively)

Time (min)	C_t / C_0	% removal
10	0.0349	96.51
30	0.0319	96.81
60	0.0192	98.08
75	0.0095	99.05
90	0.0084	99.16
120	0.0075	99.25
135	0.0042	99.58
165	0.0039	99.61
190	0.004	99.6
210	0.0039	99.61
240	0.0043	99.57
300	0.0039	99.61

Table-5: Spectrophotometer reading using JFLA as adsorbent for various initial concentrations(pH, temperature, amount of adsorbent, shaker speed and time were 7, 30^{0}C, 5gm, 120 r.p.m. and 3 hrs respectively)

Conc. (mg/L)	C_t / C_0	% removal
25	0.1147	88.53
40	0.1524	84.76
50	0.178	82.2
75	0.2171	78.29
100	0.3454	65.46
150	0.4175	58.25

Table-6: Spectrophotometer reading using JFLA as adsorbent for various shaker speeds(pH, temperature, amount of adsorbent, initial conc. and time were 7, 30^{0}C, 5 gm, 50 mg/L and 3 hrs respectively)

Shaker Speed (mg/L)	C_t / C_0	% removal
30	0.0372	96.28
50	0.0214	97.86
60	0.0184	98.16
75	0.0167	98.33
90	0.0161	98.39
110	0.0157	98.43
120	0.0154	98.46
130	0.0157	98.43

Table-7: Spectrophotometer reading using JFLA as adsorbent for various adsorbent dosages (pH, temperature, initial conc., shaker speed and time were 7, 30^{0}C, 50mg/L, 120 r.p.m. and 3 hrs respectively)

Dose (gm)	C_t / C_0	% removal
0.5	0.8417	15.83
1.25	0.6378	36.22
2.5	0.5478	45.22
5	0.4275	57.25
6	0.3814	61.86
7	0.3017	69.83
10	0.2147	78.53
12	0.1785	82.15
14	0.1472	85.28
16	0.1124	88.76
20	0.1051	89.49
25	0.0951	90.49
30	0.0877	91.23
40	0.0798	92.02
60	0.0743	92.57

Table-8: Spectrophotometer reading using JFLA as adsorbent for various contact time (pH, temperature, amount of adsorbent, shaker speed and initial conc. were 7, 30^{0}C, 5 gm, 120 r.p.m. and 50mg/L respectively)

Time (min)	C_t / C_0	% removal
10	0.3147	68.53
30	0.1077	89.23
60	0.1066	89.34
75	0.1001	89.99
90	0.0942	90.58
120	0.081	91.9
135	0.0706	92.94
165	0.0428	95.72
190	0.0428	95.72
210	0.0426	95.74
240	0.0425	95.75
300	0.0426	95.74

Table-9: Spectrophotometer reading using BFA as adsorbent for various initial concentrations (pH, temperature, amount of adsorbent, shaker speed and time were 7, 30^{0}C, 2gm, 120 r.p.m. and 3 hrs respectively)

Conc. (mg/L)	C_t / C_0	% removal
25	0.0346	98.54
40	0.0468	98.32
50	0.0694	98.06
75	0.088	91.2
100	0.1196	88.04
150	0.1551	86.49

Table-10: Spectrophotometer reading using BFA as adsorbent for various shaker speeds (pH, temperature, amount of adsorbent, initial conc. and time were 7, 30^{0}C, 2 gm, 50 mg/L and 3 hrs respectively)

Shaker Speed (rpm)	C_t/C_0	% removal
30	0.0446	95.54
50	0.0418	95.82
60	0.0326	96.74
75	0.0247	97.53
90	0.0219	97.81
110	0.0209	97.91
120	0.0175	98.25
130	0.0176	98.24

Table-11: Spectrophotometer reading using BFA as adsorbent for various adsorbent dosages (pH, temperature, initial conc., shaker speed and time were 7, 30^{0}C, 50mg/L, 120 r.p.m. and 3 hrs respectively)

Dose (gm/L)	C_t/C_0	% removal
0.5	0.0863	91.37
1.25	0.0614	93.86
2.5	0.0382	96.18
5	0.0263	97.37
6	0.0214	97.86
7	0.0209	97.91
10	0.0204	97.96
12	0.0188	98.12
14	0.0181	98.19
16	0.0177	98.23
20	0.0175	98.25
25	0.0174	98.26
30	0.0142	98.58
40	0.0147	98.53
60	0.0143	98.57

Table-12: Spectrophotometer reading using BFA as adsorbent for various contact time (pH, temperature, amount of adsorbent, shaker speed and initial conc. were 7, 30^{0}C, 2 gm, 120 r.p.m. and 50mg/L respectively)

Time (min)	C_t/C_0	% removal
10	0.033	96.7
30	0.0295	97.05
60	0.0292	97.08
75	0.019	98.1
90	0.0176	98.24
120	0.0158	98.42
135	0.0073	99.27
165	0.0071	99.29
190	0.0072	99.28
210	0.0071	99.29
240	0.0072	99.28
300	0.0072	99.28

Table-13: Spectrophotometer reading using RHA as adsorbent for various initial concentrations (pH, temperature, amount of adsorbent, shaker speed and time were 7, 30^{0}C, 4gm, 120 r.p.m. and 3 hrs respectively)

Conc. (mg/L)	C_t/C_0	% removal
25	0.1236	87.64
40	0.2045	79.55
50	0.2727	72.73
75	0.3258	67.42
100	0.3875	61.25
150	0.6258	37.42

Table-14: Spectrophotometer reading using RHA as adsorbent for various shaker speeds (pH, temperature, amount of adsorbent, initial conc. and time were 7, 30^{0}C, 4 gm, 50 mg/L and 3 hrs respectively)

Shaker. Speed (rpm)	C_t/C_0	% removal
30	0.3352	66.48
50	0.2748	72.52
60	0.2103	78.97
75	0.1647	83.53
90	0.1393	86.07
110	0.0905	90.95
120	0.0904	90.96
130	0.0905	90.95

Table-15: Spectrophotometer reading using RHA as adsorbent for various adsorbent dosages (pH, temperature, initial conc., shaker speed and time were 7, 30^{0}C, 50mg/L, 120 r.p.m. and 3 hrs respectively)

Dose (gm)	C_t/C_0	% removal
0.25	0.5498	45.02
0.5	0.4863	51.37
0.75	0.4325	56.75
2.5	0.3709	62.91
5	0.3285	67.15
10	0.201	79.9
12	0.1974	80.26
14	0.1433	85.67
16	0.1031	89.69
20	0.1037	89.63
25	0.079	92.1
30	0.103	89.7
40	0.078	92.2
60	0.07914	92.086

Table-16: Spectrophotometer reading using RHA as adsorbent for various contact time (pH, temperature, amount of adsorbent, shaker speed and initial conc. were 7, 30^{0}C, 4 gm, 120 r.p.m. and 50mg/L respectively)

Time (min)	C_t/C_0	% removal
10	0.4693	53.07
30	0.3685	63.15
60	0.2266	77.34
75	0.2081	79.19
90	0.182	81.8
120	0.1468	85.32
135	0.1247	87.53
165	0.1184	88.16
190	0.1085	89.15
210	0.0952	90.48
240	0.0861	91.39
300	0.0862	91.38

Table-17: Spectrophotometer reading using NLA as adsorbent for various pH (Temperature, amount of adsorbent, shaker speed and initial conc. were 30^{0}C, 4 gm, 120 r.p.m. and 50mg/L respectively)

pH	C_t/C_0	% removal
3	0.0624	93.76
4.1	0.0517	94.83
5.4	0.0218	97.82
7	0.0143	98.57
8.2	0.0102	98.98
9.1	0.0084	99.16

Table-18: Spectrophotometer reading using JFLA as adsorbent for various pH (Temperature, amount of adsorbent, shaker speed and initial conc. were 30^{0}C, 5 gm, 120 r.p.m. and 50mg/L respectively)

pH	C_t/C_0	% removal
3.4	0.0513	94.87
4.2	0.0372	96.28
5.6	0.0242	97.58
7	0.0205	97.95
8.1	0.0154	98.46
9.2	0.0082	99.18

Table-19: Spectrophotometer reading using BFA as adsorbent for various pH (Temperature, amount of adsorbent, shaker speed and initial conc. were 30^0C, 2 gm, 120 r.p.m. and 50mg/L respectively)

pH	C_t/C_0	% removal
3.1	0.0428	95.72
4.7	0.0227	97.73
5.1	0.0214	97.86
7	0.0165	98.35
8.1	0.011	98.9
9.2	0.0092	99.08

Table-20: Spectrophotometer reading using RHA as adsorbent for various pH (Temperature, amount of adsorbent, shaker speed and initial conc. were 30^0C, 4 gm, 120 r.p.m. and 50mg/L respectively)

pH	C_t/C_0	% removal
3.2	0.3456	65.44
4.2	0.2173	78.27
5.1	0.1583	84.17
7	0.0904	90.96
8.2	0.0512	94.88
9.1	0.0127	98.73

Isotherm Study:

Table-21: Langmuir isotherm data for NLA

Conc. (mg/L)	C_t/C_0	% removal	C_e	$1/C_e$	q_e	$1/q_e$
25	0.0122	98.78	0.305	3.27869	12.3475	0.08099
40	0.0276	97.24	1.104	0.9058	19.448	0.05142
50	0.0351	96.49	1.755	0.5698	24.1225	0.04146
75	0.0511	94.89	3.8325	0.26093	35.5838	0.0281
100	0.1047	89.53	10.47	0.09551	44.765	0.02234
150	0.3226	67.74	48.39	0.02067	50.805	0.01968

Table-22: Langmuir isotherm data for JFLA

Conc. (mg/L)	C_t/C_0	% removal	C_e	$1/C_e$	q_e	$1/q_e$
25	0.1147	88.53	2.8675	0.3487358	5.533125	0.1807297
40	0.1524	84.76	6.096	0.164042	8.476	0.1179802
50	0.178	82.2	8.9	0.1123596	10.275	0.0973236
75	0.2171	78.29	16.2825	0.0614156	14.679375	0.0681228
100	0.3454	65.46	34.54	0.0289519	16.365	0.061106
150	0.3541	64.59	53.115	0.018827	24.22125	0.041286

Table-23: Langmuir isotherm data for BFA

Conc. (mg/L)	C_t/C_0	% removal	C_e	$1/C_e$	q_e	$1/q_e$
25	0.0146	98.54	0.365	2.73973	12.3175	
40	0.0168	98.32	0.672	1.4881	19.664	0.05085
50	0.0194	98.06	0.97	1.03093	24.515	0.04079
75	0.088	91.2	6.6	0.15152	34.2	0.02924
100	0.1196	88.04	11.96	0.08361	44.02	0.02272
150	0.1351	86.49	20.265	0.04935	64.8675	0.01542

Table-24: Langmuir isotherm data for RHA

Conc. (mg/L)	C_t/C_0	% removal	C_e	$1/C_e$	q_e	$1/q_e$
25	0.1236	87.64	3.09	0.32362	10.955	0.09128
40	0.2045	79.55	8.18	0.12225	15.91	0.06285
50	0.2727	72.73	13.635	0.07334	18.1825	0.055
75	0.3258	67.42	24.435	0.04092	25.2825	0.03955
100	0.3875	61.25	38.75	0.02581	30.625	0.03265
150	0.6258	37.42	93.87	0.01065	28.065	0.03563

Table-25: Freundlich isotherm data for NLA

Conc. (mg/L)	C_t/C_0	C_e	$\log(C_e)$	q_e	$\log(q_e)$
25	0.0122	0.305	-0.5157	12.3475	1.09158
40	0.0276	1.104	0.04297	19.448	1.28887
50	0.0351	1.755	0.24428	24.1225	1.38242
75	0.0511	3.8325	0.58348	35.5838	1.55125
100	0.1047	10.47	1.01995	44.765	1.65094
150	0.3226	48.39	1.68476	50.805	1.70591

Table-26: Freundlich isotherm data for JFLA

Conc. (mg/L)	C_t/C_0	C_e	$\log(C_e)$	q_e	$\log(q_e)$
25	0.1147	2.8675	1.053441	5.533125	0.74297
40	0.1421	5.684	1.737655	7.2135	0.85815
50	0.178	8.9	2.186051	10.275	1.01178
75	0.2171	16.2825	2.790091	14.67938	1.16671
100	0.3454	34.54	3.542118	16.365	1.21392
150	0.3617	54.255	3.9937	17.2356	1.23643

Table-27: Freundlich isotherm data for BFA

Conc. (mg/L)	C_t/C_0	C_e	$\log(C_e)$	q_e	$\log(q_e)$
25	0.0146	0.365	-0.43771	12.3175	1.090523
40	0.0168	0.672	-0.17263	19.664	1.293672
50	0.0194	0.97	-0.01323	24.515	1.389432
75	0.088	6.6	0.819544	34.2	1.534026
100	0.1196	11.96	1.077731	44.02	1.64365
150	0.1351	20.265	1.306747	64.8675	1.812027

Table-28: Freundlich isotherm data for RHA

Conc. (mg/L)	C_t/C_0	C_e	$\log(C_e)$	q_e	$\log(q_e)$
25	0.136	3.4	0.53148	10.8	1.92315
40	0.2045	8.18	0.91275	15.91	1.20167
50	0.2727	13.635	1.13466	18.1825	1.25965
75	0.3258	24.435	1.38801	25.2825	1.40282
100	0.3875	38.75	1.58827	30.625	1.48608
150	0.491	73.65	1.86717	38.175	1.58178

Table-29: Temkin isotherm data for NLA

Conc. (mg/L)	C_t/C_0	q_e	C_e	$\log(C_e)$
25	0.0122	12.3475	0.305	-1.1874
40	0.0276	19.448	1.104	0.09894
50	0.0351	24.1225	1.755	0.56247
75	0.0511	35.5838	3.8325	1.34352
100	0.1047	44.765	10.47	2.34851
150	0.3226	50.805	48.39	3.87929

Table-30: Temkin isotherm data for JFLA

Conc. (mg/L)	C_t/C_0	q_e	C_e	$\log(C_e)$
25	0.1147	5.533125	2.8675	1.053441
40	0.1524	8.476	6.096	1.807633
50	0.178	10.275	8.9	2.186051
75	0.2171	14.67938	16.2825	2.790091
100	0.3454	16.365	34.54	3.542118
150	0.4175	21.84375	62.625	4.137165

Table-31: Temkin isotherm data for BFA

Conc. (mg/L)	C_t/C_0	q_e	C_e	$\log(C_e)$
25	0.0146	12.3175	0.365	-0.4377
40	0.0168	19.664	0.672	-0.1726
50	0.0194	24.515	0.97	-0.0132
75	0.088	34.2	6.6	0.81954
100	0.1196	44.02	11.96	1.07773
150	0.1351	64.8675	20.265	1.30675

Table-32: Temkin isotherm data for RHA

Conc. (mg/L)	C_t/C_0	q_e	C_e	$\log(C_e)$
25	0.1236	10.955	3.09	1.12817
40	0.2045	15.91	8.18	2.10169
50	0.2727	18.1825	13.635	2.61264
75	0.3258	25.2825	24.435	3.19602
100	0.3875	30.625	38.75	3.65713
150	0.6258	28.065	93.87	4.54191

Table-33: Pseudo-first-order kinetics for NLA

Time (min)	C_t / C_0	% removal	q_t	$q_t - q_e$	$\log(q_t - q_e)$
10	0.0349	96.51	12.06375	0.06375	-1.19552
30	0.0319	96.81	12.10125	0.10125	-0.9946
60	0.0192	98.08	12.26	0.26	-0.58503
75	0.0095	99.05	12.38125	0.38125	-0.41879
90	0.0084	99.16	12.395	0.395	-0.4034
120	0.0075	99.25	12.40625	0.40625	-0.39121
135	0.0042	99.58	12.4475	0.4475	-0.34921
165	0.0039	99.61	12.45125	0.45125	-0.34558
190	0.004	99.6	12.45	0.45	-0.34679
210	0.0039	99.61	12.45125	0.45125	-0.34558
240	0.0043	99.57	12.44625	0.44625	-0.35042
300	0.0039	99.61	12.45125	0.45125	-0.34558

Table-34: Pseudo-second-order kinetics for NLA

Time (min)	C_t / C_0	% removal	q_t	t/q_t
10	0.0349	96.51	12.06375	0.82893
30	0.0319	96.81	12.10125	2.47908
60	0.0192	98.08	12.26	4.89396
75	0.0095	99.05	12.38125	6.05755
90	0.0084	99.16	12.395	7.26099
120	0.0075	99.25	12.40625	9.67254
135	0.0042	99.58	12.4475	10.8456
165	0.0039	99.61	12.45125	13.2517
190	0.004	99.6	12.45	15.261
210	0.0039	99.61	12.45125	16.8658
240	0.0043	99.57	12.44625	19.2829
300	0.0039	99.61	12.45125	24.094

Table-35: Pseudo-first-order kinetics for JFLA

Time (min)	C_t / C_0	% removal	q_t	$q_t - q_e$	$\log(q_t - q_e)$
10	0.3147	68.53	4.28313	1.70125	0.23077
30	0.1077	89.23	5.57688	0.4075	-0.3899
60	0.1066	89.34	5.58375	0.40063	-0.3973
75	0.1001	89.99	5.62438	0.36	-0.4437
90	0.0942	90.58	5.66125	0.32313	-0.4906
120	0.081	91.9	5.74375	0.24063	-0.6187
135	0.0706	92.94	5.80875	0.17563	-0.7554
165	0.0428	95.72	5.9825	0.00188	-2.727
190	0.0428	95.72	5.9825	0.00188	-2.727
210	0.0426	95.74	5.98375	0.00062	-3.2041
240	0.0425	95.75	5.98438	0.00002	-4.699
300	0.0426	95.74	5.98375	0.00062	-3.2041

Table-36: Pseudo-second-order kinetics for JFLA

Time (min)	C_t/C_0	% removal	q_t	t/q_t
10	0.3147	68.53	4.28313	2.33474
30	0.1077	89.23	5.57688	5.37936
60	0.1066	89.34	5.58375	10.7455
75	0.1001	89.99	5.62438	13.3348
90	0.0942	90.58	5.66125	15.8975
120	0.081	91.9	5.74375	20.8923
135	0.0706	92.94	5.80875	23.2408
165	0.0428	95.72	5.9825	27.5804
190	0.0428	95.72	5.9825	31.7593
210	0.0426	95.74	5.98375	35.095
240	0.0425	95.75	5.98438	40.1044
300	0.0426	95.74	5.98375	50.1358

Table-37: Pseudo-first-order kinetics for BFA

Time (min)	C_t/C_0	% removal	q_t	$q_t - q_e$	$\log(q_t-q_e)$
10	0.033	96.7	24.175	0.6475	-0.1888
30	0.0295	97.05	24.2625	0.56	-0.2518
60	0.0292	97.08	24.27	0.5525	-0.2577
75	0.019	98.1	24.525	0.2975	-0.5265
90	0.0176	98.24	24.56	0.2625	-0.5809
120	0.0158	98.42	24.605	0.2175	-0.6625
135	0.0073	99.27	24.8175	0.005	-2.301
165	0.0071	99.29	24.8225	0.0035	-2.4559
190	0.0072	99.28	24.82	0.0025	-2.6021
210	0.0071	99.29	24.8225	0.0025	-2.6021
240	0.0072	99.28	24.82	0.0025	-2.6021
300	0.0072	99.28	24.82	0.0025	-2.6021

Table-38: Pseudo-second-order kinetics for BFA

Time (min)	C_t/C_0	% removal	q_t	t/q_t
10	0.033	96.7	24.175	0.41365
30	0.0295	97.05	24.2625	1.23648
60	0.0292	97.08	24.27	2.47219
75	0.019	98.1	24.525	3.0581
90	0.0176	98.24	24.56	3.6645
120	0.0158	98.42	24.605	4.87706
135	0.0073	99.27	24.8175	5.43971
165	0.0071	99.29	24.8225	6.6472
190	0.0072	99.28	24.82	7.65512
210	0.0071	99.29	24.8225	8.46007
240	0.0072	99.28	24.82	9.66962
300	0.0072	99.28	24.82	12.087

Table-39: Pseudo-first-order kinetics for RHA

Time (min)	C_t/C_0	% removal	q_t	$q_t - q_e$	$\log(q_t - q_e)$
10	0.4693	53.07	6.63375	4.79	0.68034
30	0.3685	63.15	7.89375	3.52875	0.54762
60	0.2266	77.34	9.6675	1.75625	0.24459
75	0.2081	79.19	9.89875	1.52375	0.18291
90	0.182	81.8	10.225	1.19875	0.07873
120	0.1468	85.32	10.665	0.7575	-0.1206
135	0.1247	87.53	10.9413	0.4825	-0.3165
165	0.1184	88.16	11.02	0.4025	-0.3952
190	0.1085	89.15	11.1438	0.28	-0.5528
210	0.0952	90.48	11.31	0.1125	-0.9488
240	0.0861	91.39	11.4238	0.0125	-1.9031
300	0.0862	91.38	11.4225	0.00125	-2.9031

Table-40: Pseudo-second-order kinetics for RHA

Time (min)	C_t/C_0	% removal	q_t	t/q_t
10	0.4693	53.07	6.63375	1.50744
30	0.3685	63.15	7.89375	3.80048
60	0.2266	77.34	9.6675	6.20636
75	0.2081	79.19	9.89875	7.57671
90	0.182	81.8	10.225	8.80196
120	0.1468	85.32	10.665	11.2518
135	0.1247	87.53	10.9413	12.3386
165	0.1184	88.16	11.02	14.9728
190	0.1085	89.15	11.1438	17.0499
210	0.0952	90.48	11.31	18.5676
240	0.0861	91.39	11.4238	21.0089
300	0.0862	91.38	11.4225	26.264

Variation of different process parameters under Column Study

Adsorbent: Neem leaf ash (NLA)

Table-41: Spectrophotometer reading under different bed depths for C_0 = 100 mg/L

Time (min)	$(C_t/C_0)_{H=4}$	$(C_t/C_0)_{H=6}$	$(C_t/C_0)_{H=8}$
0	0.0003	0.0003	0.0053
10	0.0005	0.0004	0.0112
20	0.0019	0.0008	0.0118
30	0.0024	0.005	0.0123
40	0.0029	0.0063	0.0135
50	0.0033	0.008	0.0159
60	0.004	0.0132	0.0162
70	0.006	0.0215	0.0167
80	0.008	0.0227	0.0169
90	0.0197	0.0251	0.0182
100	0.0459	0.0371	0.0184
110	0.1619	0.0845	0.0195
120	0.333	0.2298	0.024
130	0.5285	0.3819	0.0279
140	0.7743	0.6526	0.0387
150	0.9736	0.8155	0.0663
160	0.9736	0.9834	0.1319
170		0.9835	0.1727
180			0.2933
190			0.4487
200			0.5204
210			0.7287
220			0.8943
230			0.9344
240			0.9344

Table-42: Spectrophotometer reading under different bed depths for $C_0 = 75$ mg/L

Time (min)	$(C_t/C_0)_{H=4}$	$(C_t/C_0)_{H=6}$	$(C_t/C_0)_{H=8}$
0	0.0004	0.0003	0.0028
10	0.0007	0.0004	0.0037
20	0.0009	0.0005	0.0065
30	0.0012	0.0009	0.011
40	0.0028	0.0012	0.0134
50	0.0037	0.0052	0.0231
60	0.0035	0.0072	0.0288
70	0.0047	0.0147	0.0324
80	0.0078	0.0215	0.0618
90	0.18	0.0461	0.0857
100	0.2627	0.0976	0.1046
110	0.4191	0.1544	0.1329
120	0.5808	0.2028	0.1346
130	0.6189	0.2445	0.235
140	0.8956	0.3432	0.2893
150	0.9648	0.4225	0.5335
160	0.9741	0.4778	0.6946
170	0.9741	0.6786	0.7355
180		0.7145	0.8123
190		0.8024	0.8904
200		0.9845	0.9135
210		0.9845	0.9273
220			0.9567
230			0.9973
240			0.9973

Table-43: Spectrophotometer reading under different bed depths for $C_0 = 50$ mg/L

Time (min)	$(C_t/C_0)_{H=4}$	$(C_t/C_0)_{H=6}$	$(C_t/C_0)_{H=8}$
0	0.0002	0.0002	0.0008
10	0.0003	0.0004	0.0024
20	0.0005	0.0007	0.0053
30	0.0007	0.0011	0.0077
40	0.0009	0.002	0.0082
50	0.0027	0.0022	0.0093
60	0.0035	0.0027	0.0167
70	0.0049	0.0029	0.0247
80	0.0084	0.0059	0.027
90	0.0361	0.0077	0.0287
100	0.186	0.029	0.0294
110	0.4307	0.0337	0.0309
120	0.5241	0.0376	0.0776
130	0.6042	0.1012	0.1309
140	0.7309	0.3135	0.2224
150	0.8214	0.3915	0.3281
160	0.9051	0.4017	0.3724
170	0.9724	0.5214	0.4816
180	0.9724	0.6247	0.5393
190		0.7056	0.6254
200		0.7873	0.6607
210		0.8125	0.7512
220		0.9531	0.8872
230		0.9741	0.9815
240		0.9741	0.9973
250			0.9973

Table-44: Spectrophotometer reading under different bed depths for $C_0 = 25$ mg/L

Time (min)	$(C_t/C_0)_{H=4}$	$(C_t/C_0)_{H=6}$	$(C_t/C_0)_{H=8}$
0	0.0005	0.0006	0.0008
10	0.0008	0.0009	0.00009
20	0.0009	0.0016	0.0011
30	0.001	0.002	0.0014
40	0.0021	0.0022	0.007
50	0.00235	0.00235	0.0073
60	0.0031	0.0037	0.0078
70	0.0039	0.0045	0.0081
80	0.0042	0.0051	0.0097
90	0.0054	0.0058	0.0135
100	0.0081	0.0061	0.0137
110	0.0124	0.0071	0.0163
120	0.0212	0.0079	0.019
130	0.0483	0.0143	0.0288
140	0.1549	0.0218	0.0327
150	0.273	0.0236	0.0541
160	0.4556	0.0258	0.0724
170	0.6071	0.2472	0.0973
180	0.8122	0.4273	0.1052
190	0.8185	0.6417	0.1862
200	0.9745	0.6943	0.2876
210	0.9745	0.7231	0.5214
220		0.8051	0.6051
230		0.8523	0.7124
240		0.9125	0.8217
250		0.9842	0.8562
260		0.9842	0.9243
270			0.9914
280			0.9914

Table-45: Spectrophotometer reading under different flow rates at H = 4 cm, C_0 = 100 mg/L

Time (min)	$(C_t/C_0)_{q=5\ mLmin-1}$	$(C_t/C_0)_{q=7.5\ mLmin-1}$	$(C_t/C_0)_{q=10\ mLmin-1}$
0	0.0001	0.0003	0.0006
10	0.0002	0.0005	0.0014
20	0.0004	0.0019	0.0047
30	0.0009	0.0024	0.0083
40	0.0014	0.0029	0.019
50	0.0026	0.0033	0.038
60	0.0049	0.004	0.056
70	0.0052	0.006	0.084
80	0.0059	0.008	0.175
90	0.0061	0.0197	0.382
100	0.00741	0.0459	0.621
110	0.00851	0.1619	0.827
120	0.0125	0.333	0.974
130	0.0681	0.5285	
140	0.0853	0.7743	
150	0.159	0.9736	
160	0.438	0.9736	
170	0.826		
180	0.914		
190	0.975		

Table-46: Spectrophotometer reading under different pH at H = 4 cm, C_0 = 100 mg/L

Time (min)	$(C_t/C_0)_{pH=9.2}$	$(C_t/C_0)_{pH=7.0}$	$(C_t/C_0)_{pH=4.1}$
0	0.0002	0.0003	0.0052
10	0.0003	0.0005	0.0086
20	0.0005	0.0019	0.0257
30	0.0008	0.0024	0.0369
40	0.00124	0.0029	0.0589
50	0.00248	0.0033	0.0873
60	0.00486	0.004	0.146
70	0.00501	0.006	0.359
80	0.0062	0.008	0.644
90	0.0073	0.0197	0.812
100	0.0098	0.0459	0.934
110	0.0156	0.1619	0.9736
120	0.0289	0.333	
130	0.0476	0.5285	
140	0.0681	0.7743	
150	0.0953	0.9736	
160	0.156	0.9736	
170	0.571		
180	0.829		
190	0.973		

Adsorbent: Jack fruit leaf ash (JFLA)

Table-47: Spectrophotometer reading under different bed depths for C_0 = 100 mg/L

Time (min)	$(C_t/C_0)_{H=4}$	$(C_t/C_0)_{H=6}$	$(C_t/C_0)_{H=8}$
0	0	0	0
10	0.0001	0	0
20	0.0003	0.0001	0
30	0.0005	0.0002	0.0001
40	0.0007	0.0004	0.0003
50	0.0009	0.0007	0.0006
60	0.0022	0.0015	0.0009
70	0.0028	0.0021	0.0017
80	0.0034	0.0029	0.0021
90	0.0046	0.0037	0.0039
100	0.0073	0.0054	0.0044
110	0.0127	0.0093	0.0084
120	0.0411	0.0321	0.0177
130	0.0725	0.0514	0.0347
140	0.3196	0.1281	0.0918
150	0.4889	0.2711	0.1342
160	0.4905	0.4114	0.3814
170	0.5669	0.5219	0.4179
180	0.6114	0.5624	0.4712
190	0.7217	0.6112	0.5113
200	0.8112	0.6918	0.5431
210	0.8516	0.8233	0.5612
220	0.9217	0.9112	0.6224
230	0.9817	0.9227	0.7341
240	0.9984	0.9658	0.8112
250		0.9856	0.8864
260		0.9986	0.9267
			0.9885
			0.9966

Table-48: Spectrophotometer reading under different bed depths for $C_0 = 75$ mg/L

Time (min)	$(C_t/C_0)_{H=4}$	$(C_t/C_0)_{H=6}$	$(C_t/C_0)_{H=8}$
0	0	0	0
10	0	0	0
20	0.0001	0	0
30	0.0004	0.0001	0
40	0.0007	0.0003	0.0001
50	0.001	0.0005	0.0004
60	0.0019	0.001	0.0009
70	0.0021	0.0015	0.0012
80	0.003	0.0021	0.0019
90	0.0043	0.003	0.0028
100	0.0062	0.0049	0.0041
110	0.012	0.0087	0.0082
120	0.031	0.0215	0.017
130	0.057	0.0411	0.021
140	0.0941	0.0956	0.0704
150	0.2174	0.2105	0.1104
160	0.3721	0.3719	0.02751
170	0.4437	0.4218	0.02912
180	0.5521	0.5014	0.3971
190	0.6214	0.5217	0.4224
200	0.6917	0.6112	0.4983
210	0.7112	0.6914	0.5243
220	0.8416	0.7217	0.6104
230	0.9817	0.8414	0.6948
240		0.9924	0.7152
250			0.8112
260			0.895
270			0.927
280			0.9987

Table-49: Spectrophotometer reading under different bed depths for $C_0 = 50$ mg/L

Time (min)	$(C_t/C_0)_{H=4}$	$(C_t/C_0)_{H=6}$	$(C_t/C_0)_{H=8}$
0	0	0	0
10	0	0	0
20	0	0	0
30	0.0004	0	0
40	0.0007	0.0002	0.0001
50	0.0009	0.0003	0.0002
60	0.0011	0.0009	0.0005
70	0.0017	0.001	0.0007
80	0.0029	0.0017	0.0009
90	0.0041	0.0027	0.0014
100	0.0053	0.042	0.0039
110	0.0092	0.0081	0.0056
120	0.0211	0.0169	0.0041
130	0.0254	0.0178	0.0057
140	0.0263	0.0204	0.0063
150	0.0333	0.0262	0.0069
160	0.0364	0.0305	0.0073
170	0.0372	0.0333	0.0084
180	0.0389	0.0363	0.0097
190	0.0498	0.0411	0.0112
200	0.0529	0.0469	0.053
210	0.0814	0.0614	0.0712
220	0.3511	0.1421	0.2411
230	0.7281	0.3417	0.5012
240	0.9242	0.6124	0.5911
250	0.9862	0.7059	0.6119
260		0.7216	0.6214
270		0.8124	0.7015
280		0.8864	0.7217
290		0.9341	0.8152
300		0.9817	0.8514
			0.8912
			0.9126
			0.9725

Table-50: Spectrophotometer reading under different bed depths for $C_0 = 25$ mg/L

Time (min)	$(C_t/C_0)_{H=4}$	$(C_t/C_0)_{H=6}$	$(C_t/C_0)_{H=8}$
0	0	0	0
10	0	0	0
20	0.0001	0	0
30	0.0003	0	0
40	0.0004	0.0002	0
50	0.0006	0.0003	0.0001
60	0.0007	0.0004	0.0002
70	0.0007	0.0006	0.0003
80	0.0008	0.0006	0.0004
90	0.0009	0.0007	0.0005
100	0.001	0.0008	0.0007
110	0.0013	0.0009	0.0008
120	0.0017	0.001	0.0009
130	0.0029	0.0011	0.0009
140	0.0031	0.0016	0.001
150	0.0057	0.0021	0.0011
160	0.0062	0.0028	0.0012
170	0.0068	0.0037	0.0016
180	0.0074	0.0052	0.0019
190	0.0079	0.0063	0.0034
200	0.0094	0.0084	0.0059
210	0.0125	0.0157	0.0074
220	0.0288	0.0225	0.0088
230	0.0497	0.0342	0.0097
240	0.1128	0.0817	0.0116
250	0.3817	0.1058	0.0724
260	0.7281	0.2167	0.0917
270	0.8476	0.5211	0.1241
280	0.9678	0.7045	0.2253
290	0.9812	0.7261	0.3416
300		0.8415	0.5217
310		0.9127	0.7416
320		0.9621	0.8122
330		0.9835	0.8914
			0.9247
			0.9611
			0.9829
			0.9912

Table-51: Spectrophotometer reading under different flow rates at H = 4 cm, C_0 = 100 mg/L

Time (min)	(C_t/C_0) q= 5 mLmin-1	(C_t/C_0) q= 7.5 mLmin-1	(C_t/C_0) q= 10 mLmin-1
0	0	0	0.0003
10	0	0.0001	0.0005
20	0	0.0003	0.0007
30	0.0001	0.0005	0.0009
40	0.0003	0.0007	0.0012
50	0.0005	0.0009	0.0028
60	0.0008	0.0022	0.0034
70	0.0012	0.0028	0.0046
80	0.0019	0.0034	0.0073
90	0.0028	0.0046	0.0127
100	0.0029	0.0073	0.0411
110	0.0032	0.0127	0.0725
120	0.0039	0.0411	0.3196
130	0.0045	0.0725	0.4889
140	0.0057	0.3196	0.4902
150	0.0099	0.4889	0.5669
160	0.0092	0.4905	0.6114
170	0.0106	0.5669	0.7217
180	0.0217	0.6114	0.8112
190	0.0543	0.7217	0.8516
200	0.0721	0.8112	0.9217
210	0.0843	0.8516	0.9847
220	0.0975	0.9217	0.9924
230	0.1242	0.9817	
240	0.1976	0.9984	
250	0.2148		
260	0.5427		
270	0.5964		
280	0.6412		
290	0.7219		
300	0.8715		
310	0.9214		
320	0.9917		

Table-52: Spectrophotometer reading under different pH at H = 4 cm, C_0 = 100 mg/L

Time (min)	$(C_t/C_0)_{pH=9.2}$	$(C_t/C_0)_{pH=7.0}$	$(C_t/C_0)_{pH=4.1}$
0	0	0	0
10	0	0.0001	0
20	0.0001	0.0003	0
30	0.0004	0.0005	0
40	0.0007	0.0007	0.0001
50	0.001	0.0009	0.00004
60	0.00019	0.0022	0.0009
70	0.0021	0.0028	0.0012
80	0.003	0.0034	0.0019
90	0.0043	0.0046	0.0028
100	0.0062	0.0073	0.0041
110	0.057	0.0725	0.021
120	0.0941	0.3196	0.0704
130	0.2174	0.4889	0.1104
140	0.3721	0.4905	0.2751
150	0.4437	0.5669	0.2912
160	0.5521	0.6114	0.3971
170	0.6214	0.7217	0.4224
180	0.9562	0.8547	0.5623
190	0.9562	0.9012	0.8412
200		0.9635	0.9014
210		0.9653	0.9635
220			0.9651

Adsorbent: Bagasse fly ash (BFA)

Table-53: Spectrophotometer reading under different bed depths for C_0 = 100 mg/L

Time (min)	$(C_t/C_0)_{H=4}$	$(C_t/C_0)_{H=6}$	$(C_t/C_0)_{H=8}$
0	0.0125	0.0014	0.0021
10	0.0672	0.0028	0.003
20	0.1547	0.003	0.0031
30	0.1982	0.0038	0.0042
40	0.2437	0.0128	0.0056
50	0.6392	0.2133	0.0086
60	0.9471	0.4192	0.1339
70	0.9472	0.6512	0.4211
80		0.9322	0.8784
90		0.9322	0.9454
100			0.9454

Table-54: Spectrophotometer reading under different bed depths for C_0 = 75 mg/L

Time (min)	$(C_t/C_0)_{H=4}$	$(C_t/C_0)_{H=6}$	$(C_t/C_0)_{H=8}$
0	0.009	0.0012	0.0007
10	0.0186	0.0048	0.0008
20	0.0232	0.0097	0.00153
30	0.0234	0.0114	0.0026
40	0.0253	0.0216	0.0017
50	0.0319	0.0249	0.0019
60	0.0336	0.0282	0.0024
70	0.034	0.0301	0.0026
80	0.126	0.0655	0.0048
90	0.3401	0.1582	0.0053
100	0.595	0.3412	0.0082
110	0.6216	0.4121	0.0094
120	0.9522	0.6171	0.0281
130	0.9522	0.8965	0.1884
140		0.9633	0.6393
150		0.9633	0.8026
160			0.8965
170			0.9655
180			0.9655

Table-55: Spectrophotometer reading under different bed depths for C_0 = 50 mg/L

Time (min)	$(C_t/C_0)_{H=4}$	$(C_t/C_0)_{H=6}$	$(C_t/C_0)_{H=8}$
0	0.0007	0.0004	0.0003
10	0.0009	0.0006	0.0004
20	0.001	0.0008	0.0006
30	0.0017	0.0009	0.0007
40	0.0024	0.001	0.0009
50	0.0039	0.0023	0.0012
60	0.0042	0.0038	0.0019
70	0.0055	0.0045	0.0024
80	0.0059	0.005	0.0028
90	0.0067	0.0057	0.0033
100	0.0077	0.0062	0.0038
110	0.0092	0.0078	0.0044
120	0.0162	0.0081	0.0047
130	0.0751	0.0096	0.0062
140	0.1042	0.0105	0.0085
150	0.2349	0.019	0.0097
160	0.6531	0.034	0.0112
170	0.9452	0.0478	0.0241
180	0.9651	0.0912	0.0462
190		0.115	0.0815
200		0.6214	0.1252
210		0.8965	0.2344
220		0.9653	0.3576
230		0.9655	0.6211
240			0.8458
250			0.9012
260			0.9703

Table-56: Spectrophotometer reading under different bed depths for C_0 = 25 mg/L

Time (min)	$(C_t/C_0)_{H=4}$	$(C_t/C_0)_{H=6}$	$(C_t/C_0)_{H=8}$
0	0.0004	0.0003	0.0002
10	0.0005	0.0004	0.0003
20	0.0007	0.0005	0.0004
30	0.0008	0.0008	0.0007
40	0.0012	0.0009	0.0008
50	0.0044	0.001	0.0009
60	0.0054	0.0012	0.0011
70	0.0069	0.0014	0.0013
80	0.0083	0.0015	0.0015
90	0.0092	0.0018	0.0017
100	0.0155	0.0019	0.0019
110	0.0156	0.0024	0.0022
120	0.0189	0.0028	0.0025
130	0.0196	0.0044	0.0038
140	0.0239	0.0056	0.0045
150	0.055	0.0063	0.0052
160	0.0768	0.0068	0.0059
170	0.0935	0.0078	0.0064
180	0.122	0.0084	0.0068
190	0.1944	0.0089	0.0069
200	0.2841	0.0094	0.0071
210	0.3602	0.0098	0.0073
220	0.5014	0.01	0.0088
230	0.6124	0.015	0.0101
240	0.9012	0.021	0.0189
250	0.9633	0.033	0.0263
260	0.9633	0.042	0.0355
270		0.067	0.0421
280		0.078	0.0747
290		0.115	0.1063
300		0.326	0.1354
310		0.487	0.1379
320		0.651	0.1925
330		0.651	0.2642
340		0.8012	0.3433
350		0.9533	0.4879
360		0.9533	0.5542
370			0.6412
380			0.6421
			0.8012
			0.9562
			0.9566

Table-57: Spectrophotometer reading under different flow rates at H = 4 cm, C_0 = 100 mg/L

Time (min)	$(C_t/C_0)_{q=5\ mLmin-1}$	$(C_t/C_0)_{q=7.5\ mLmin-1}$	$(C_t/C_0)_{q=10\ mLmin-1}$
0	0.0084	0.0125	0.0125
10	0.0045	0.0672	0.0672
20	0.0128	0.1547	0.1547
30	0.0161	0.1982	0.1982
40	0.0644	0.2437	0.2437
50	0.152	0.6392	0.6392
60	0.932	0.8523	0.8562
70		0.9633	0.9633
80			0.9644

Table-58: Spectrophotometer reading under different pH at H = 4 cm, C_0 = 100 mg/L

Time (min)	$(C_t/C_0)_{pH=9.2}$	$(C_t/C_0)_{pH=7.0}$	$(C_t/C_0)_{pH=4.1}$
0	0.0087	0.0125	0.1124
10	0.02412	0.0672	0.2148
20	0.08641	0.1547	0.3812
30	0.11247	0.1982	0.6325
40	0.2149	0.2437	
50	0.3664	0.6392	
60	0.4287		
70	0.5214		
80	0.5214		
90	0.6349		

Adsorbent: Rice husk ash (RHA)

Table-59: Spectrophotometer reading under different bed depths for C_0 = 100 mg/L

Time (min)	$(C_t/C_0)_{H=4}$	$(C_t/C_0)_{H=6}$	$(C_t/C_0)_{H=8}$
0	0.0712	0.0705	0.0692
10	0.0901	0.0852	0.0715
20	0.0933	0.091	0.0812
30	0.1533	0.1047	0.0951
40	0.3412	0.2142	0.1156
50	0.5474	0.3156	0.1951
60	0.7251	0.4271	0.2147
70		0.5679	0.4173
80		0.725	0.5159
90		0.7558	0.6168
100			0.7252
110			0.7553

Table-60: Spectrophotometer reading under different bed depths for C_0 = 75 mg/L

Time (min)	$(C_t/C_0)_{H=4}$	$(C_t/C_0)_{H=6}$	$(C_t/C_0)_{H=8}$
0	0.0612	0.0602	0.0604
10	0.0756	0.0751	0.0667
20	0.0875	0.0815	0.0714
30	0.0939	0.0905	0.0816
40	0.1153	0.1721	0.0952
50	0.2147	0.3346	0.1056
60	0.5214	0.4217	0.1562
70	0.6917	0.5191	0.5147
80	0.7552	0.6192	0.6017
90	0.9563	0.755	0.7106
100		0.9655	0.7551
110			0.9544
120			0.9562

Table-61: Spectrophotometer reading under different bed depths for C_0 = 50 mg/L

Time (min)	$(C_t/C_0)_{H=4}$	$(C_t/C_0)_{H=6}$	$(C_t/C_0)_{H=8}$
0	0.0579	0.0564	0.0438
10	0.0612	0.0579	0.0518
20	0.0695	0.0614	0.0597
30	0.0708	0.0697	0.061
40	0.0914	0.0756	0.0698
50	0.2158	0.0917	0.0784
60	0.3478	0.2246	0.0819
70	0.4812	0.3147	0.0951
80	0.5967	0.4978	0.1158
90	0.6812	0.5279	0.2143
100	0.755	0.6114	0.3416
110	0.9544	0.7215	0.4228
120	0.9612	0.7552	0.5716
130		0.9551	0.7105
140		0.9556	0.8521
150			0.9744
160			0.9745

Table-62: Spectrophotometer reading under different bed depths for C_0 = 25 mg/L

Time (min)	$(C_t/C_0)_{H=4}$	$(C_t/C_0)_{H=6}$	$(C_t/C_0)_{H=8}$
0	0.0092	0.00358	0.0041
10	0.0131	0.0467	0.0091
20	0.0475	0.0498	0.0105
30	0.0516	0.0502	0.0216
40	0.0682	0.0534	0.0412
50	0.0716	0.0597	0.0498
60	0.0915	0.0712	0.0512
70	0.1074	0.0853	0.0614
80	0.1191	0.0917	0.0779
90	0.165	0.1072	0.0814
100	0.2164	0.2151	0.0905
110	0.3792	0.2782	0.1142
120	0.4065	0.3156	0.2147
130	0.4981	0.3857	0.3152
140	0.5346	0.4716	0.3981
150	0.715	0.5127	0.4217
160	0.7554	0.6114	0.5141
170	0.9552	0.715	0.6214
180	0.9563	0.7559	0.7341
190		0.9566	0.7553
200		0.9578	0.9688
210			0.9701

Table-63: Spectrophotometer reading under different flow rates at H = 4 cm, C_0 = 100 mg/L

Time (min)	(C_t/C_0) q= 5 mLmin-1	(C_t/C_0) q= 7.5 mLmin-1	(C_t/C_0) q= 10 mLmin-1
0	0.0614	0.0712	0.1245
10	0.0725	0.0901	0.4179
20	0.0814	0.0933	0.6959
30	0.0952	0.1533	0.7552
40	0.1157	0.3412	0.9632
50	0.1963	0.5474	0.9633
60	0.2155	0.7251	
70	0.5229	0.7552	
80	0.6172	0.9566	
90	0.7211	0.9566	
100	0.7557		
110	0.9533		
120	0.9542		

Table-64: Spectrophotometer reading under different pH at H = 4 cm, C_0 = 100 mg/L

Time (min)	$(C_t/C_0)_{pH=9.2}$	$(C_t/C_0)_{pH=7.0}$	$(C_t/C_0)_{pH=4.1}$
0	0.0814	0.0579	0.0414
10	0.0914	0.0612	0.0514
20	0.1152	0.0695	0.0609
30	0.2142	0.0708	0.0714
40	0.3146	0.0914	0.0923
50	0.5134	0.1976	0.1145
60	0.6147	0.2158	0.1861
70	0.7552	0.4812	0.2153
80	0.9412	0.5967	0.4451
90	0.9414	0.6812	0.5217
100		0.755	0.6111
110		0.9633	0.7142
120		0.9654	0.7294
130			0.9622
140			0.9641

Data Modeling under Column Study

Adsorbent: Neem Leaf Ash

Thomas Model

Table-65 (a): Thomas model constants under different bed depths and concentrations

C_0 (mg/L)	H (cm)	R^2	K_{Th}	q_e
25	4	0.931	1.0	18.36
50	4	0.977	0.64	30.55
75	4	0.955	0.43	43.23
100	4	0.924	0.30	61.68

C_0 (mg/L)	H (cm)	R^2	K_{Th}	q_e
25	6	0.916	0.72	12.28
50	6	0.986	0.44	20.60
75	6	0.979	0.32	27.33
100	6	0.939	0.28	31.45

C_0 (mg/L)	H (cm)	R^2	K_{Th}	q_e
25	8	0.932	0.68	7.73
50	8	0.931	0.38	12.14
75	8	0.963	0.25	16.56
100	8	0.838	0.13	30.51

Table-65 (b): Thomas model constants under different flow rates

C_0 (mg/L)	H (cm)	Q (mL/min)	R^2	K_{Th}	q_e
100	4	5.0	0.975	0.57	34.35
100	4	7.5	0.924	0.70	38.02
100	4	10.0	0.914	0.81	39.51

Table-65 (c): Thomas model constants under different pH

C_0 (mg/L)	H (cm)	pH	R^2	K_{Th}	q_e
100	4	4.1	0.927	0.68	43.56
100	4	7.0	0.917	0.68	40.37
100	4	9.2	0.967	0.71	29.34

Yoon Nelson Model

Table-66 (a): Yoon-Nelson model constants under different bed depths and concentrations

C_0 (mg/L)	H (cm)	R^2	K_{YN}	T
25	4	0.931	0.053	167.02
50	4	0.977	0.073	128.35
75	4	0.995	0.075	119.24
100	4	0.924	0.077	115.61

C_0 (mg/L)	H (cm)	R^2	K_{YN}	T
25	6	0.958	0.043	197.33
50	6	0.996	0.051	170.42
75	6	0.997	0.056	149.86
100	6	0.989	0.066	127.98

C_0 (mg/L)	H (cm)	R^2	K_{YN}	T
25	8	0.932	0.039	206.0
50	8	0.931	0.043	164.14
75	8	0.963	0.044	145.30
100	8	0.978	0.056	108.04

Table-66 (b): Yoon-Nelson model constants under different flow rates

C_0 (mg/L)	H (cm)	q (mL/min)	R^2	K_{YN}	*T*
100	4	5.0	0.914	0.057	165.84
100	4	7.5	0.924	0.070	127.17
100	4	10.0	0.914	0.081	91.79

Table 66 (c): Yoon-Nelson model constants under different pH

C_0 (mg/L)	H (cm)	pH	R^2	K_{YN}	*T*
100	4	4.1	0.975	0.079	71.97
100	4	7.0	0.924	0.070	127.17
100	4	9.2	0.918	0.052	172.85

Adams-Bohart Model

Table-67 (a): Adams-Bohart model constants under different bed depths and concentrations

C_0 (mg/L)	H (cm)	R^2	K_{AB}	N_0
25	4	0.961	1.6	0.0005
50	4	0.938	1.1	0.0007
75	4	0.922	0.72	0.0011
100	4	0.962	0.53	0.0015

C_0 (mg/L)	H (cm)	R^2	K_{AB}	N_0
25	6	0.937	1.24	0.0004
50	6	0.950	0.76	0.0007
75	6	0.937	0.56	0.0009
100	6	0.967	0.48	0.001

C_0 (mg/L)	H (cm)	R^2	K_{AB}	N_0
25	8	0.940	1.12	0.0003
50	8	0.952	0.54	0.0005
75	8	0.943	0.33	0.0007
100	8	0.900	0.22	0.001

Table-67(b): Adams-Bohart model constants under different flow rates

C_0 (mg/L)	H (cm)	q (mL/min)	R^2	K_{AB}	N_0
100	4	5.0	0.962	0.46	1.83
100	4	7.5	0.962	0.53	1.46
100	4	10.0	0.978	0.61	1.06

Table-63 (c): Adams-Bohart model constants under different pH

C_0 (mg/L)	H (cm)	pH	R^2	K_{AB}	N_0
100	4	4.1	0.969	0.53	0.94
100	4	7.0	0.962	0.50	1.47
100	4	9.2	0.984	0.43	1.88

Adsorbent: Jack Fruit Leaf Ash

Thomas Model

Table-68 (a): Thomas model constants under different bed depths and concentrations

C_0 (mg/L)	H (cm)	R^2	K_{Th}	q_e
25	4	0.845	1.56	14.09
50	4	0.866	0.82	24.89
75	4	0.982	0.73	29.55
100	4	0.980	0.57	37.125

C_0 (mg/L)	H (cm)	R^2	K_{Th}	q_e
25	6	0.916	0.72	12.28
50	6	0.986	0.44	20.60
75	6	0.979	0.32	27.33
100	6	0.939	0.28	31.45

C_0 (mg/L)	H (cm)	R^2	K_{Th}	q_e
25	8	0.919	1.64	12.72
50	8	0.958	0.82	22.05
75	8	0.973	0.76	25.38
100	8	0.985	0.59	30.00

Table-68 (b): Thomas model constants under different flow rates

C_0 (mg/L)	H (cm)	q (mL/min)	R^2	K_{Th}	q_e
100	4	5.0	0.958	1.66	3.73
100	4	7.5	0.924	2.59	3.83
100	4	10.0	0.914	2.55	4.60

Table-68 (c): Thomas model constants under different pH

C_0 (mg/L)	H (cm)	pH	R^2	K_{Th}	q_e
100	4	4.1	0.971	0.25	41.65
100	4	7.0	0.917	0.25	37.52
100	4	9.2	0.967	0.23	40.89

Yoon-Nelson Model

Table-69 (a): Yoon-Nelson model constants under different bed depths and concentrations

C_0 (mg/L)	H (cm)	R^2	K_{YN}	*T*
25	4	0.845	0.039	270.25
50	4	0.866	0.041	229.90
75	4	0.982	0.055	181.09
100	4	0.980	0.057	171.42

C_0 (mg/L)	H (cm)	R^2	K_{YN}	*T*
25	6	0.919	0.041	280.00
50	6	0.958	0.041	242.078
75	6	0.973	0.057	186.32
100	6	0.985	0.059	176.95

C_0 (mg/L)	H (cm)	R^2	K_{YN}	*T*
25	8	0.931	0.041	300.0
50	8	0.963	0.041	258.29
75	8	0.956	0.051	202.55
100	8	0.974	0.052	195.00

Table-69 (b): Yoon-Nelson model constants under different flow rates

C_0 (mg/L)	H (cm)	q (mL/min)	R^2	K_{YN}	*T*
100	4	5.0	0.958	0.038	270.20
100	4	7.5	0.924	0.057	171.42
100	4	10.0	0.914	0.058	166.40

Table-69 (c): Yoon-Nelson model constants under different pH

C_0 (mg/L)	H (cm)	pH	R^2	K_{YN}	*T*
100	4	4.1	0.971	0.0594	167.63
100	4	7.0	0.972	0.0590	169.08
100	4	9.2	0.947	0.0530	202.45

Adams-Bohart Model

Table-70 (a): Adams-Bohart model constants under different bed depths and concentrations

C_0 (mg/L)	H (cm)	R^2	K_{AB}	N_0
25	4	0.931	1.24	0.75
50	4	0.957	0.66	1.04
75	4	0.961	0.58	1.51
100	4	0.946	0.45	1.90

C_0 (mg/L)	H (cm)	R^2	K_{AB}	N_0
25	6	0.960	1.28	0.52
50	6	0.962	0.64	0.88
75	6	0.944	0.60	1.01
100	6	0.923	0.41	1.39

C_0 (mg/L)	H (cm)	R^2	K_{AB}	N_0
25	8	0.959	1.24	0.42
50	8	0.944	0.64	0.73
75	8	0.901	0.49	0.87
100	8	0.901	0.37	1.13

Table-70(b): Adams-Bohart model constants under different flow rates

C_0 (mg/L)	H (cm)	q (mL/min)	R^2	K_{AB}	N_0
100	4	5.0	0.981	1.33	0.295
100	4	7.5	0.937	1.84	0.204
100	4	10.0	0.929	1.87	0.187

Table-70(c): Adams-Bohart model constants under different flow rates

C_0 (mg/L)	H (cm)	pH	R^2	K_{AB}	N_0
100	4	4.1	0.954	0.211	1.99
100	4	7.0	0.937	0.180	2.03
100	4	9.2	0.877	0.170	2.28

Adsorbent: Bagasse Fly Ash

Thomas Model

Table-71 (a): Thomas model constants under different bed depths and concentrations

C_0 (mg/L)	H (cm)	R^2	K_{Th}	q_e
25	4	0.980	1.36	11.56
50	4	0.867	0.80	19.90
75	4	0.829	0.59	17.53
100	4	0.918	0.54	9.38

C_0 (mg/L)	H (cm)	R^2	K_{Th}	q_e
25	6	0.909	0.88	13.63
50	6	0.90	0.62	18.42
75	6	0.950	0.56	16.03
100	6	0.909	0.42	16.66

C_0 (mg/L)	H (cm)	R^2	K_{Th}	q_e
25	8	0.936	0.84	13.78
50	8	0.982	0.60	17.57
75	8	0.951	0.54	17.65
100	8	0.936	0.35	16.42

Table-71 (b): Thomas model constants under different flow rates

C_0 (mg/L)	H (cm)	q (mL/min)	R^2	K_{Th}	q_e
100	4	5.0	0.812	1.0	11.65
100	4	7.5	0.995	0.86	13.63
100	4	10.0	0.984	0.62	13.78

Table-71 (c): Thomas model constants under different pH

C_0 (mg/L)	H (cm)	pH	R^2	K_{Th}	q_e
100	4	4.1	0.995	0.86	5.011
100	4	7.0	0.918	0.84	9.388
100	4	9.2	0.924	0.56	14.31

Yoon-Nelson Model

Table-72 (a): Yoon-Nelson model constants under different bed depths and concentrations

C_0 (mg/L)	H (cm)	R^2	K_{YN}	*T*
25	4	0.98	0.034	229.42
50	4	0.867	0.040	196.0
75	4	0.829	0.044	115.75
100	4	0.918	0.084	46.23

C_0 (mg/L)	H (cm)	R^2	K_{YN}	*T*
25	6	0.909	0.022	379
50	6	0.899	0.030	264.67
75	6	0.950	0.042	148.62
100	6	0.909	0.072	107.34

C_0 (mg/L)	H (cm)	R^2	K_{YN}	*T*
25	8	0.936	0.021	402
50	8	0.982	0.029	292.86
75	8	0.751	0.041	194.27
100	8	0.936	0.065	116.31

Table-72 (b): Yoon-Nelson model constants under different flow rates

C_0 (mg/L)	H (cm)	q (mL/min)	R^2	K_{YN}	*T*
100	4	5.0	0.958	0.038	270.20
100	4	7.5	0.924	0.057	171.42
100	4	10.0	0.914	0.058	166.40

Table-72 (c): Yoon-Nelson model constants under different pH

C_0 (mg/L)	H (cm)	pH	R^2	K_{YN}	*T*
100	4	4.1	0.971	0.0594	167.63
100	4	7.0	0.972	0.0590	169.08
100	4	9.2	0.947	0.0530	202.45

Adams-Bohart Model

Table-73 (a): Adams-Bohart model constants under different bed depths and concentrations

C_0 (mg/L)	H (cm)	R^2	K_{AB}	N_0
25	4	0.982	0.52	0.609
50	4	0.902	0.32	1.0
75	4	0.859	0.21	0.96
100	4	0.892	0.29	0.53

C_0 (mg/L)	H (cm)	R^2	K_{AB}	N_0
25	6	0.938	0.036	0.502
50	6	0.934	0.24	0.90
75	6	0.956	0.26	0.645
100	6	0.900	0.42	0.48

C_0 (mg/L)	H (cm)	R^2	K_{AB}	N_0
25	8	0.964	0.32	0.42
50	8	0.950	0.26	0.28
75	8	0.794	0.21	0.68
100	8	0.844	0.34	0.44

Table-73 (b): Adams-Bohart model constants under different flow rates

C_0 (mg/L)	H (cm)	q (mL/min)	R^2	K_{AB}	N_0
100	4	5.0	0.880	0.34	0.702
100	4	7.5	0.892	0.39	0.539
100	4	10.0	0.971	0.41	0.448

Table-73 (c): Adams-Bohart model constants under different pH

C_0 (mg/L)	H (cm)	pH	R^2	K_{AB}	N_0
100	4	4.1	0.997	0.25	0.356
100	4	7.0	0.892	0.21	0.539
100	4	9.2	0.865	0.19	0.836

Adsorbent: Rice Husk Ash

Thomas Model

Table-74 (a): Thomas model constants under different bed depths and concentrations

C_0 (mg/L)	H (cm)	R^2	K_{Th}	q_e
25	4	0.974	0.52	10.98
50	4	0.949	0.30	15.0
75	4	0.932	0.25	17.49
100	4	0.926	0.23	18.77

C_0 (mg/L)	H (cm)	R^2	K_{Th}	q_e
25	6	0.926	0.44	8.48
50	6	0.954	0.26	11.86
75	6	0.974	0.22	12.66
100	6	0.964	0.19	14.23

C_0 (mg/L)	H (cm)	R^2	K_{Th}	q_e
25	8	0.980	0.48	6.89
50	8	0.909	0.22	11.20
75	8	0.941	0.20	11.60
100	8	0.956	0.16	13.22

Table-74 (b): Thomas model constants under different flow rates

C_0 (mg/L)	H (cm)	q (mL/min)	R^2	K_{Th}	q_e
100	4	5.0	0.978	0.15	27.79
100	4	7.5	0.926	0.26	15.77
100	4	10.0	0.845	0.31	6.04

Table-74 (c): Thomas model constants under different pH

C_0 (mg/L)	H (cm)	pH	R^2	K_{Th}	q_e
100	4	4.1	0.984	0.34	7.18
100	4	7.0	0.949	0.30	10.11
100	4	9.2	0.967	0.26	12.32

Yoon-Nelson Model

Table-75 (a): Yoon-Nelson model constants under different bed depths and concentrations

C_0 (mg/L)	H (cm)	R^2	K_{YN}	T
25	4	0.974	0.031	136.51
50	4	0.949	0.035	96.34
75	4	0.932	0.045	72.10
100	4	0.926	0.061	49.85

C_0 (mg/L)	H (cm)	R^2	K_{YN}	T
25	6	0.926	0.029	143.17
50	6	0.954	0.031	110.61
75	6	0.974	0.039	79.43
100	6	0.964	0.045	66.78

C_0 (mg/L)	H (cm)	R^2	K_{YN}	T
25	8	0.980	0.027	181.60
50	8	0.909	0.028	135.37
75	8	0.941	0.036	91.81
100	8	0.956	0.038	82.55

Table-75 (b): Yoon-Nelson model constants under different flow rates

C_0 (mg/L)	H (cm)	q (mL/min)	R^2	K_{YN}	*T*
50	4	5.0	0.978	0.039	88.31
50	4	7.5	0.949	0.035	96.34
50	4	10.0	0.931	0.013	237.30

Table-75 (c): Yoon-Nelson model constants under different pH

C_0 (mg/L)	H (cm)	pH	R^2	K_{YN}	*T*
50	4	4.1	0.984	0.040	67.86
50	4	7.0	0.972	0.035	96.34
50	4	9.2	0.967	0.032	111.34

Adams-Bohart Model

Table-76 (a): Adams-Bohart model constants under different bed depths and concentrations

C_0 (mg/L)	H (cm)	R^2	K_{AB}	N_0
25	4	0.943	0.40	0.35
50	4	0.965	0.20	0.65
75	4	0.955	0.17	0.74
100	4	0.946	0.14	0.76

C_0 (mg/L)	H (cm)	R^2	K_{AB}	N_0
25	6	0.872	0.36	0.30
50	6	0.966	0.18	0.49
75	6	0.976	0.16	0.51
100	6	0.963	0.13	0.59

C_0 (mg/L)	H (cm)	R^2	K_{AB}	N_0
25	8	0.951	0.32	0.29
50	8	0.939	0.16	0.44
75	8	0.943	0.16	0.49
100	8	0.963	0.11	0.55

Table-76 (b): Adams-Bohart model constants under different flow rates

C_0 (mg/L)	H (cm)	q (mL/min)	R^2	K_{AB}	N_0
100	4	5.0	0.976	0.10	1.20
100	4	7.5	0.946	0.14	0.76
100	4	10.0	0.945	0.17	0.39

Table-76 (c): Adams-Bohart model constants under different pH

C_0 (mg/L)	H (cm)	pH	R^2	K_{AB}	N_0
100	4	4.1	0.989	0.11	0.57
100	4	7.0	0.946	0.14	0.76
100	4	9.2	0.977	0.10	0.1.38

Annexure-II

Kinetic Model

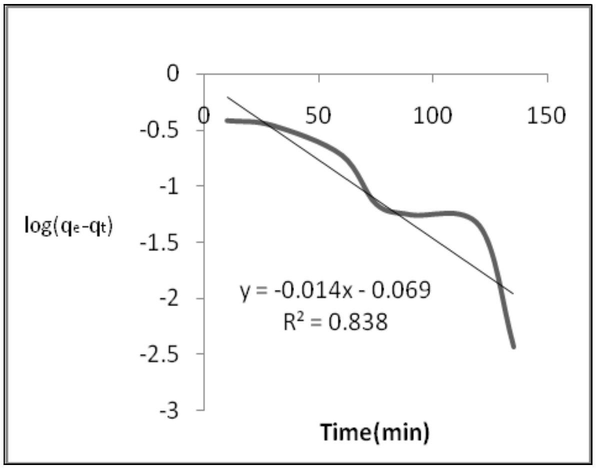

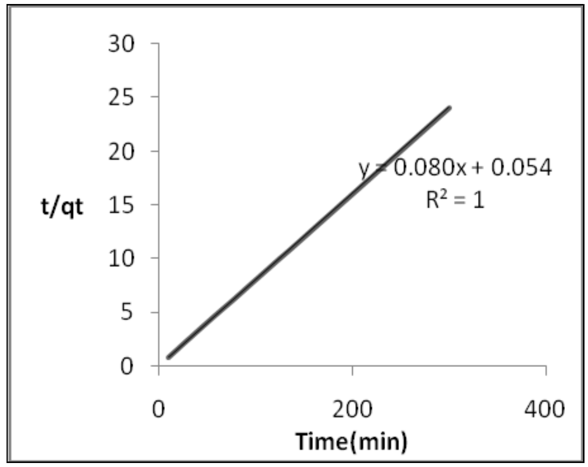

Fig.1: Pseudo-first order reaction for NLA

Fig.2:Pseudo-second order reaction for NLA

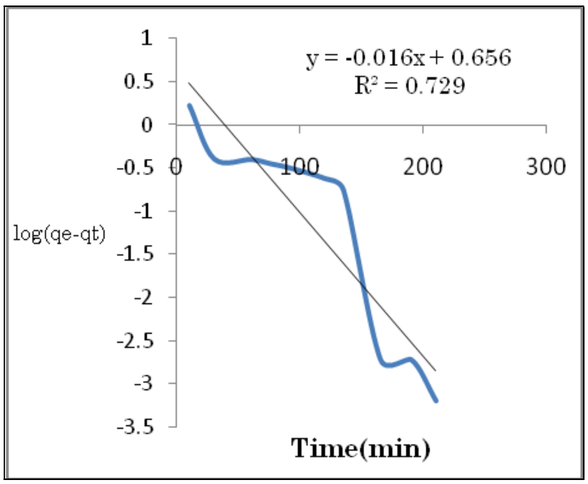

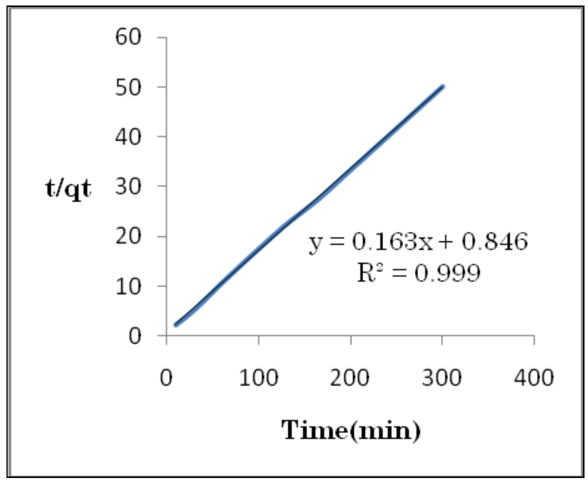

Fig.3: Pseudo-first order reaction for JFLA

Fig.4:Pseudo-second order reaction for JFLA

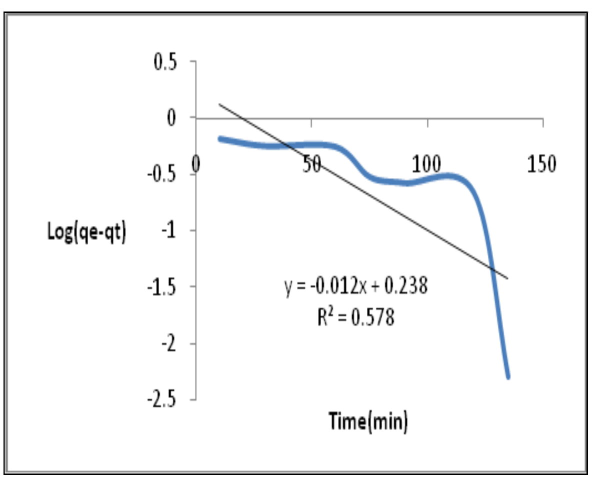

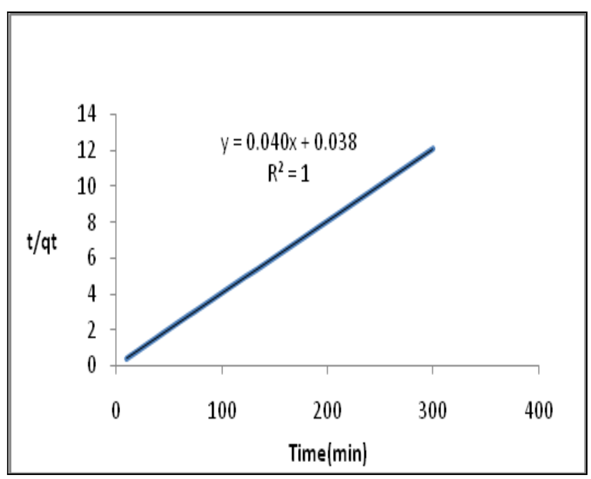

Fig.5: Pseudo-first order reaction for BFA

Fig.6:Pseudo-second order reaction for BFA

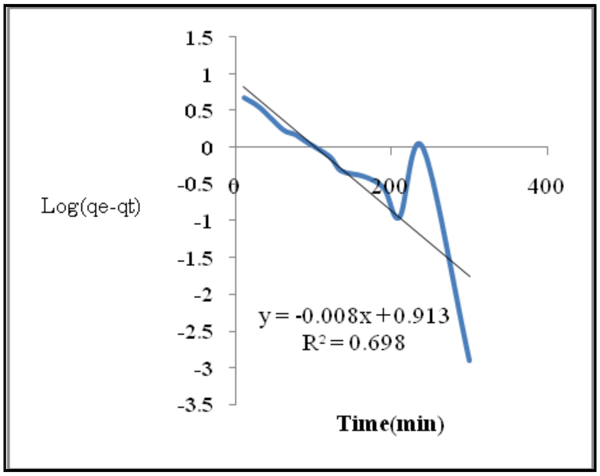

Fig.7: Pseudo-first order reaction for RHA

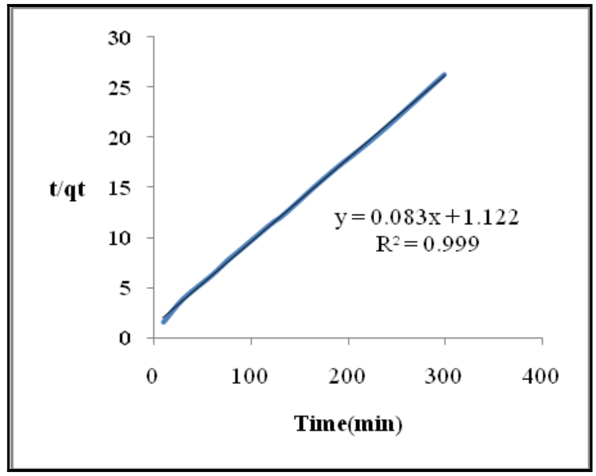

Fig.8:Pseudo-second order reaction for RHA

Column study: Variation of process parameters

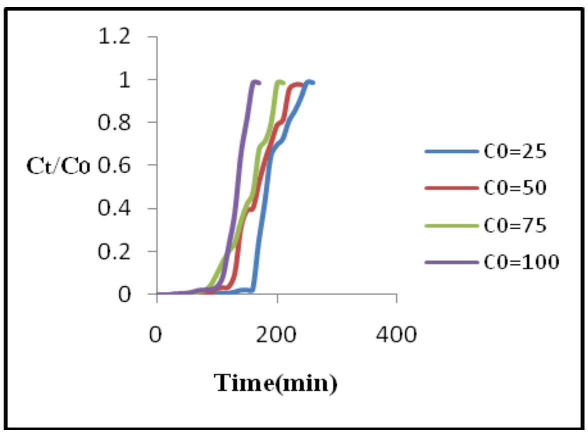

Fig. 9(a): Effect of initial concentration for NLA at H=6cm, q= 7.5mL/min

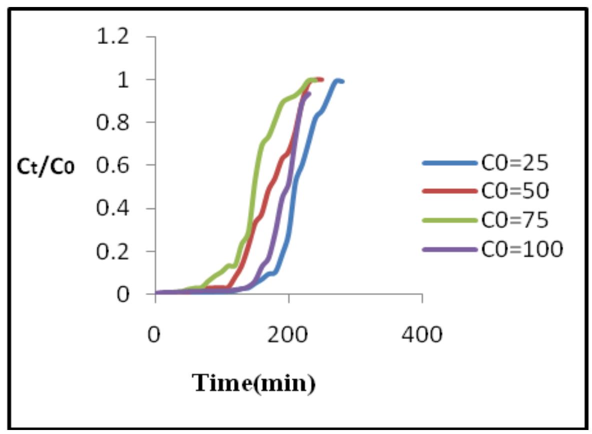

Fig. 9(b): Effect of initial concentration for JFLA at H=6cm, q= 7.5mL/min

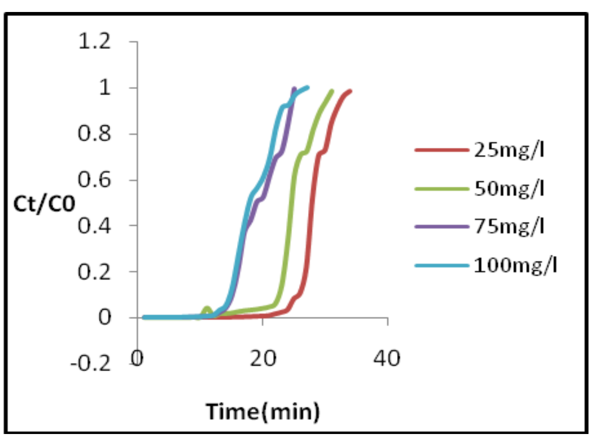

Fig. 9(c): Effect of initial concentration for BFA at H=6cm, q= 7.5mL/min

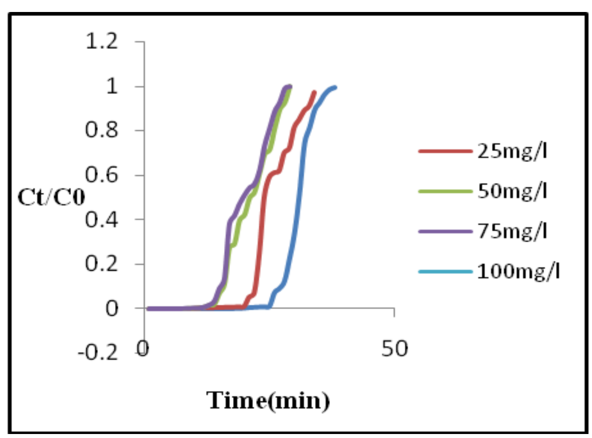

Fig. 9(d): Effect of initial concentration for RHA at H=6cm, q= 7.5mL/min

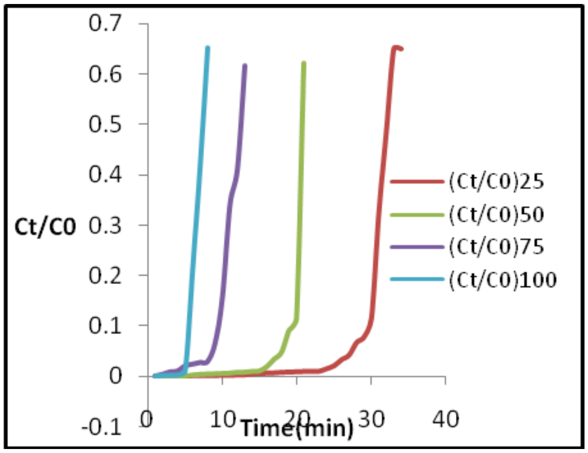

Fig. 10(a): Effect of initial concentration for NLA at H=8cm, q= 7.5mL/min

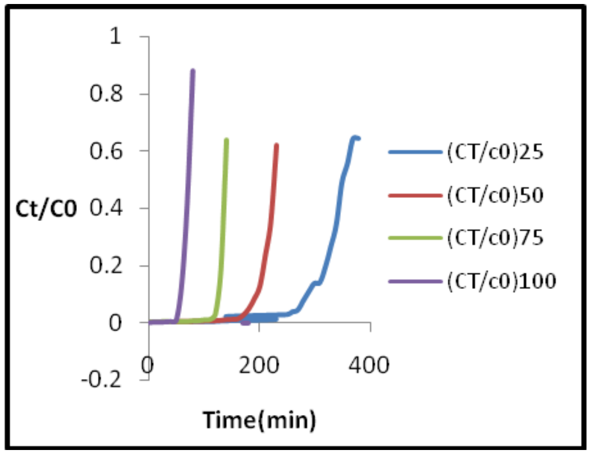

Fig. 10(b): Effect of initial concentration for JFLA at H=8cm, q= 7.5mL/min

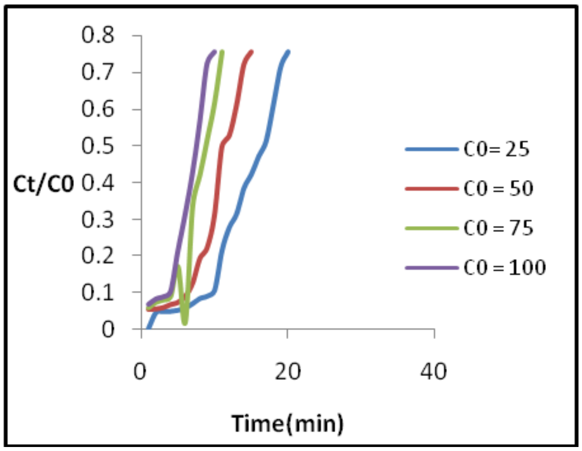

Fig. 10(c): Effect of initial concentration for BFA at H=8cm, q= 7.5mL/min

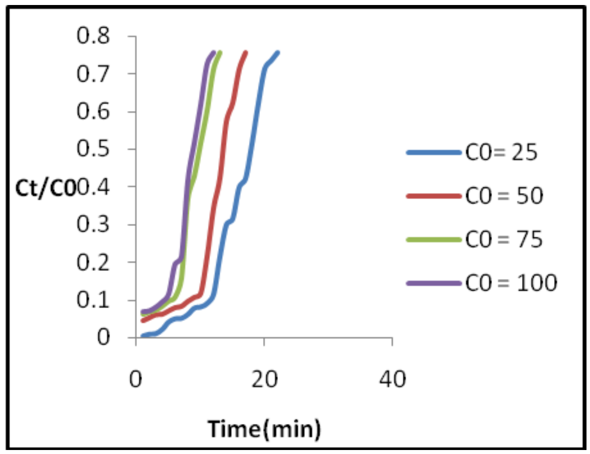

Fig. 10(d): Effect of initial concentration for RHA at H=8cm, q= 7.5mL/min

Model Analysis under Column Study

Neem leaf ash

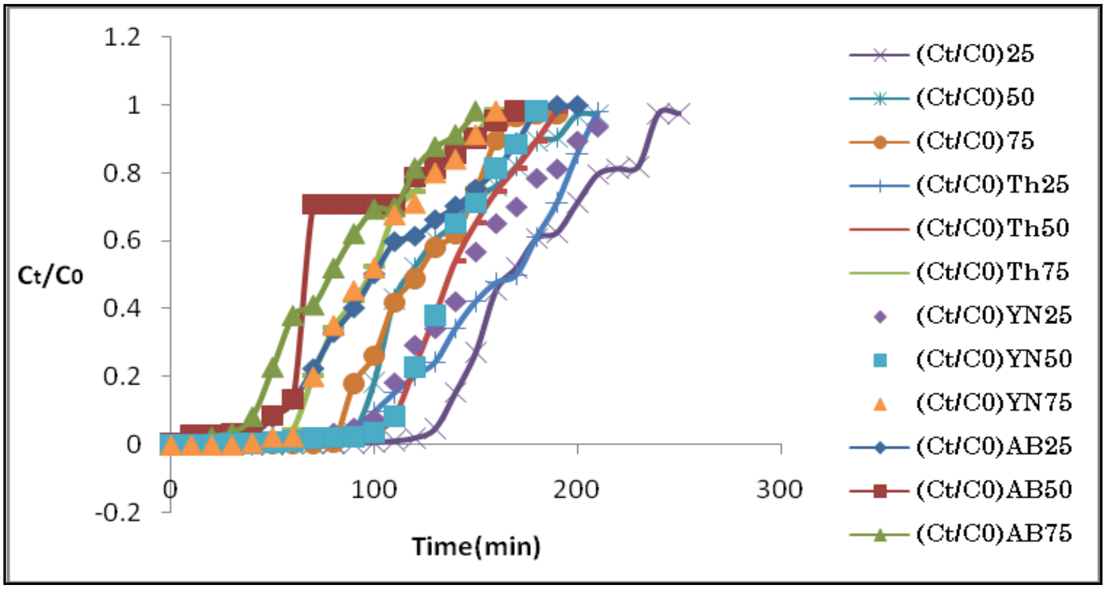

Fig. 11: Model analysis of NLA for variation of concentrations at H=8 cm, q=7.5mLmin^{-1}

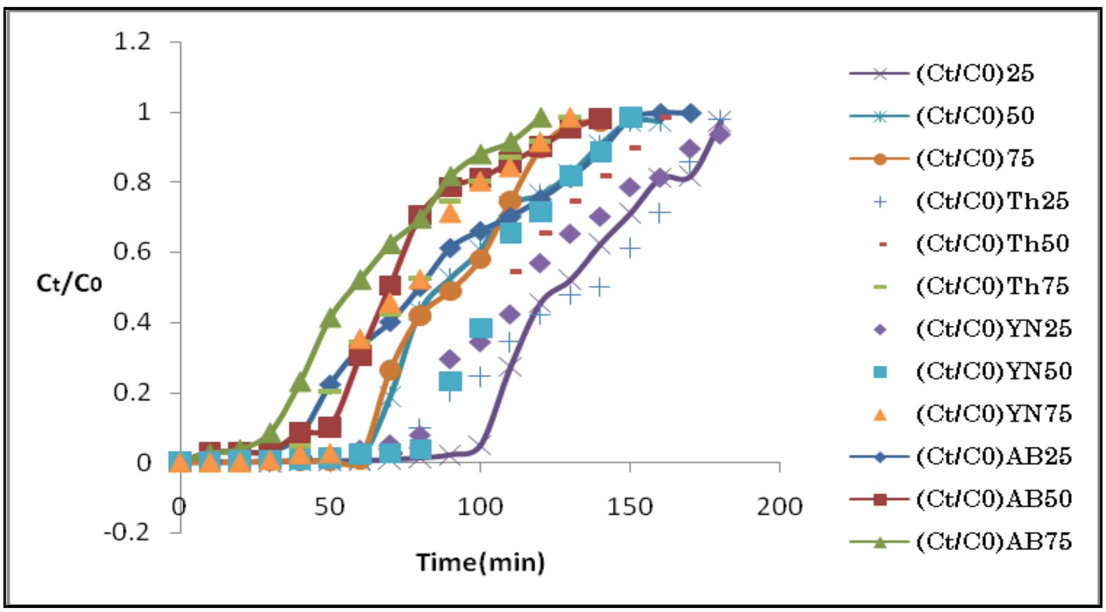

Fig. 12: Model analysis of NLA for variation of concentrations at H=6 cm, q=7.5mLmin^{-1}

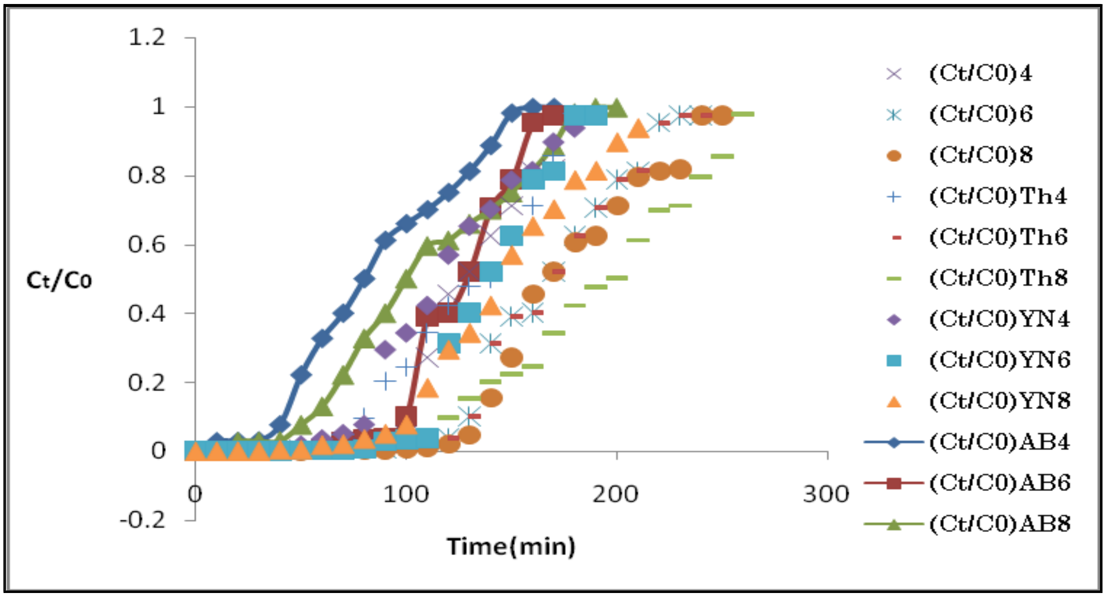

Fig. 13: Model analysis of NLA for variation of bed depth at C_0= 25mgL^{-1}, q=7.5mLmin^{-1}

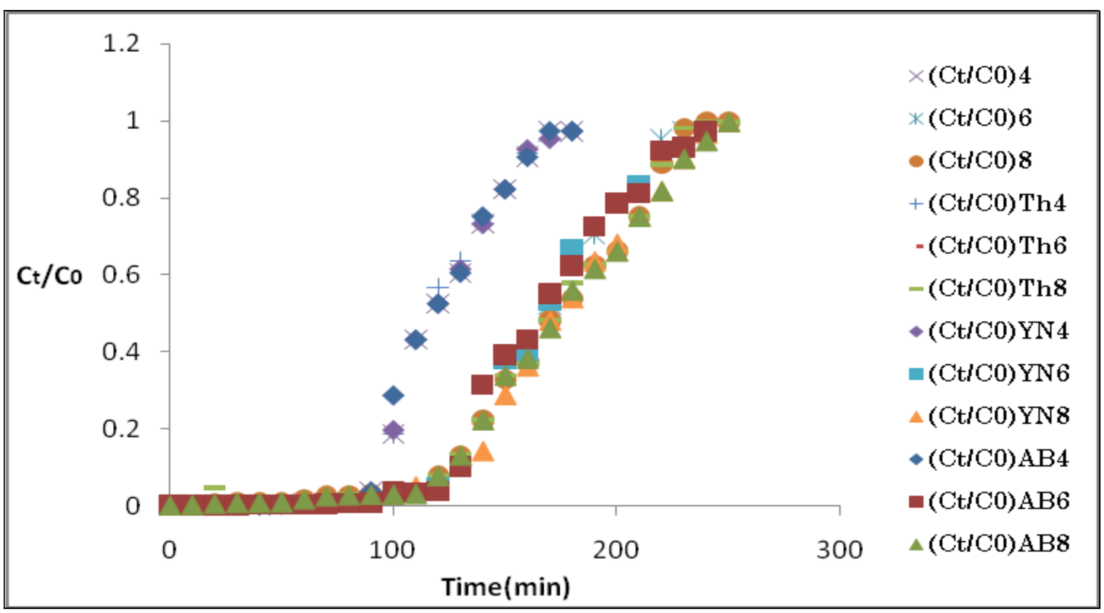

Fig. 14: Model analysis of NLA for variation of bed depth at C_0= 50 mgL^{-1},

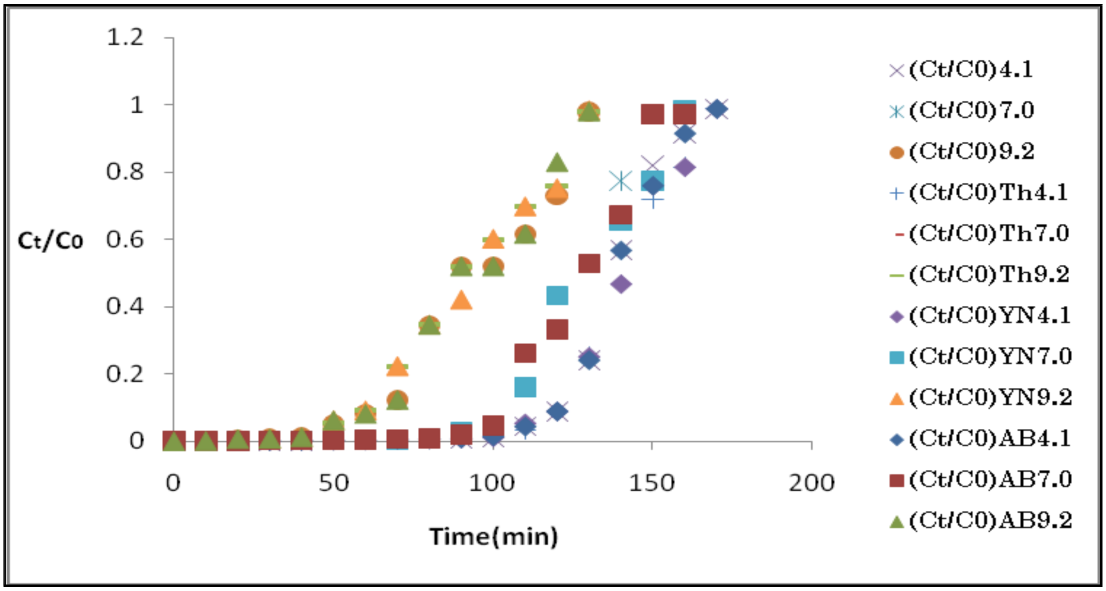

Fig. 15: Model analysis of NLA for variation of pH at C_0= 100 mgL^{-1}, H=4 cm, q=7.5mLmin^{-1}

Jack fruit leaf ash

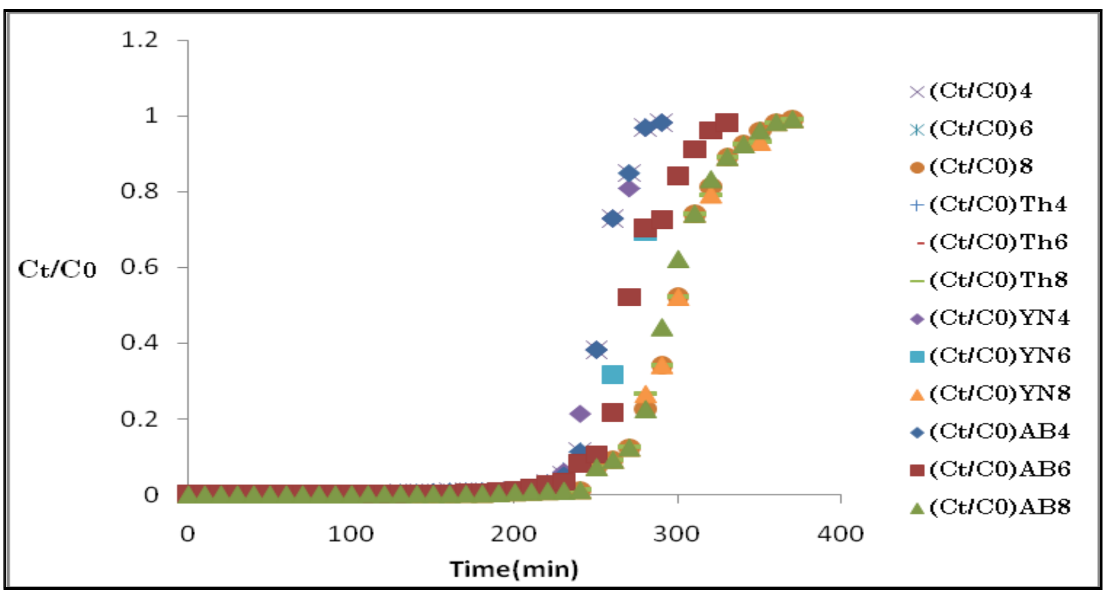

Fig. 16: Model analysis of JFLA for variation of bed depth at C_0= 25 mgL^{-1}, q=7.5mLmin^{-1}

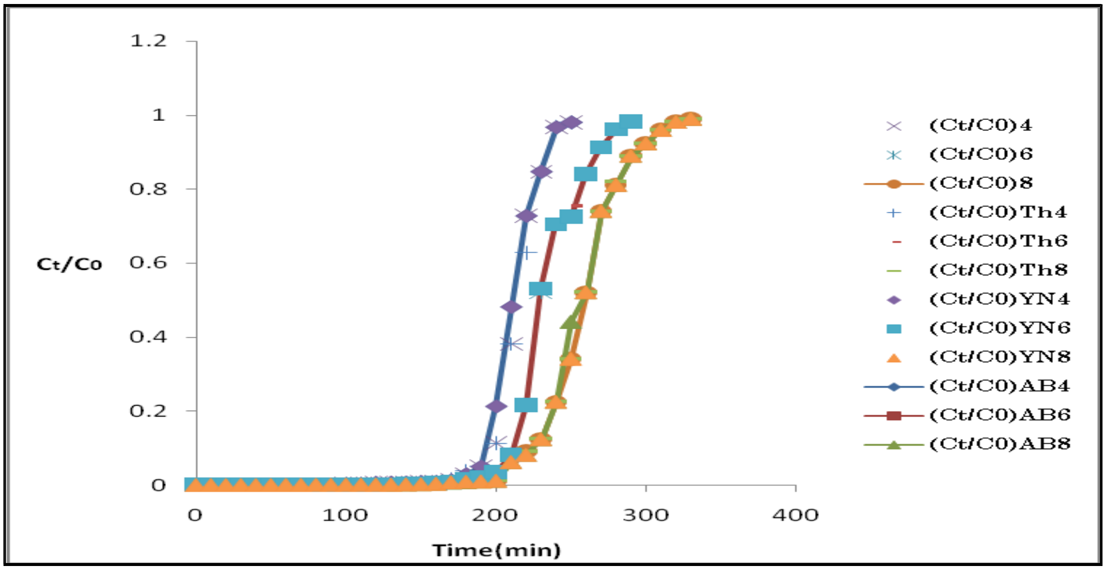

Fig. 17: Model analysis of JFLA for variation of bed depth at C_0= 50 mgL^{-1}, q=7.5mLmin^{-1}

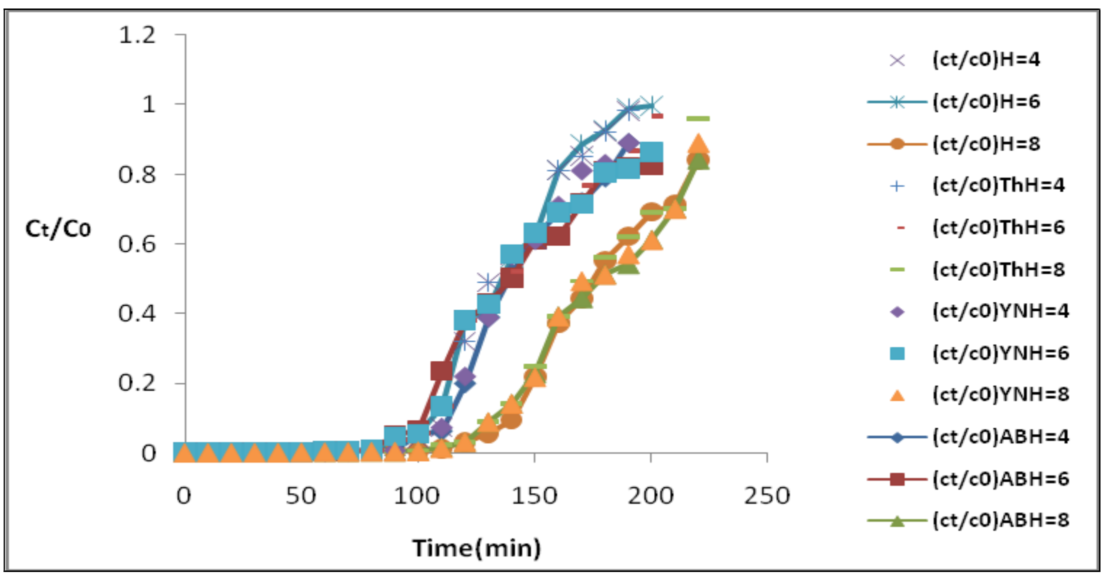

Fig.18: Model analysis of JFLA for variation of bed depth at C_0= 75 mgL^{-1}, q=7.5mLmin^{-1}

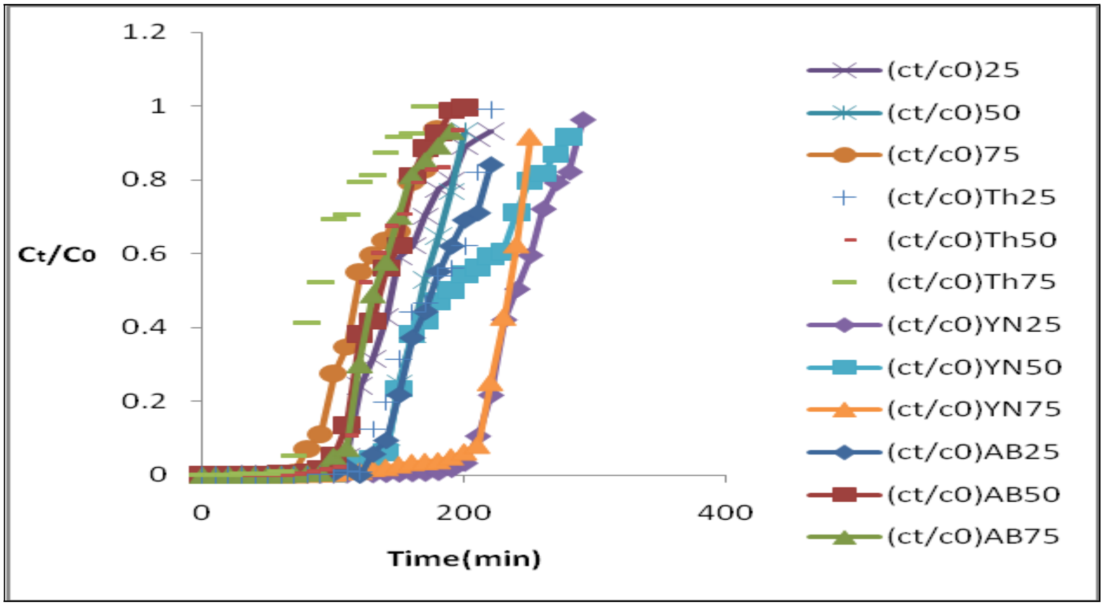

Fig.19: Model analysis of JFLA for variation of concentrations at H=4 cm, q=7.5mLmin^{-1}

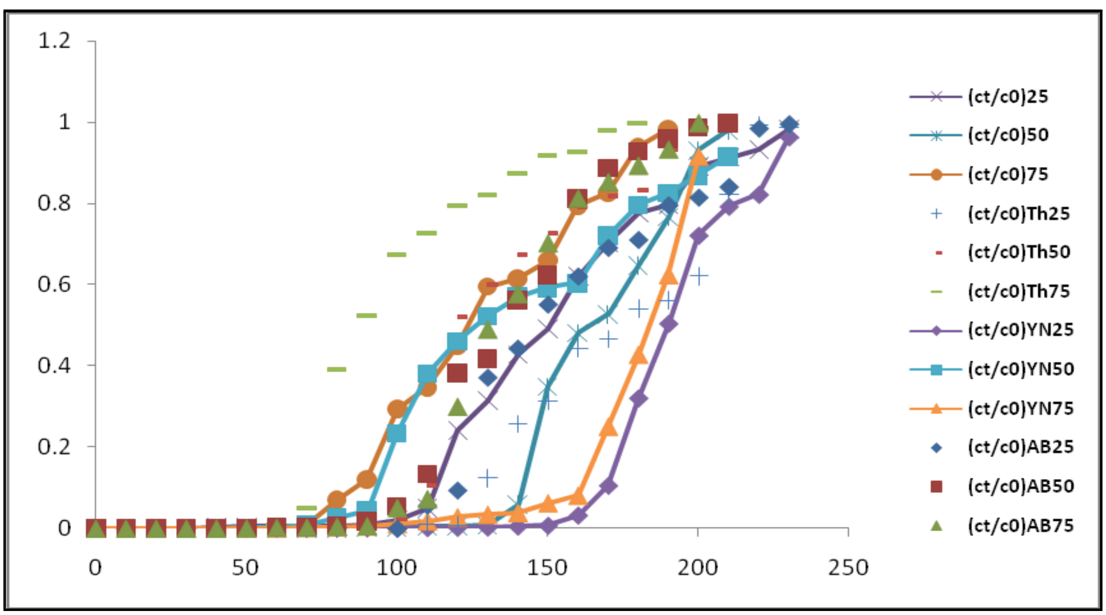

Fig.20: Model analysis of JFLA for variation of concentrations at H=8 cm, q=7.5mLmin^{-1}

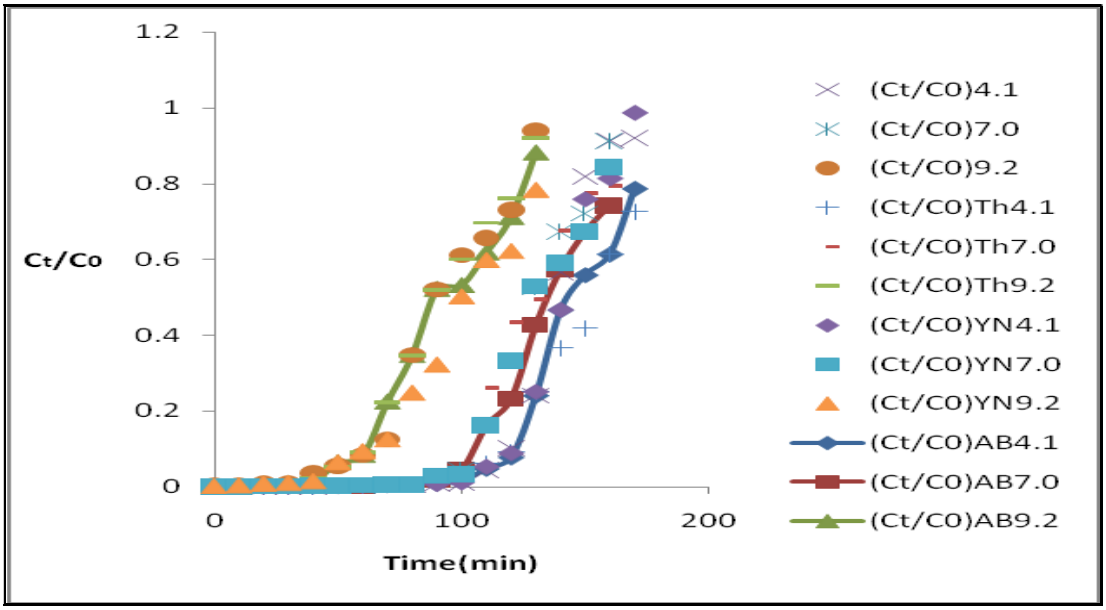

Fig.21: Model analysis of JFLA for variation of pH at C_0= 100 mgL^{-1}, q=7.5mLmin^{-1}

Bagasse fly ash

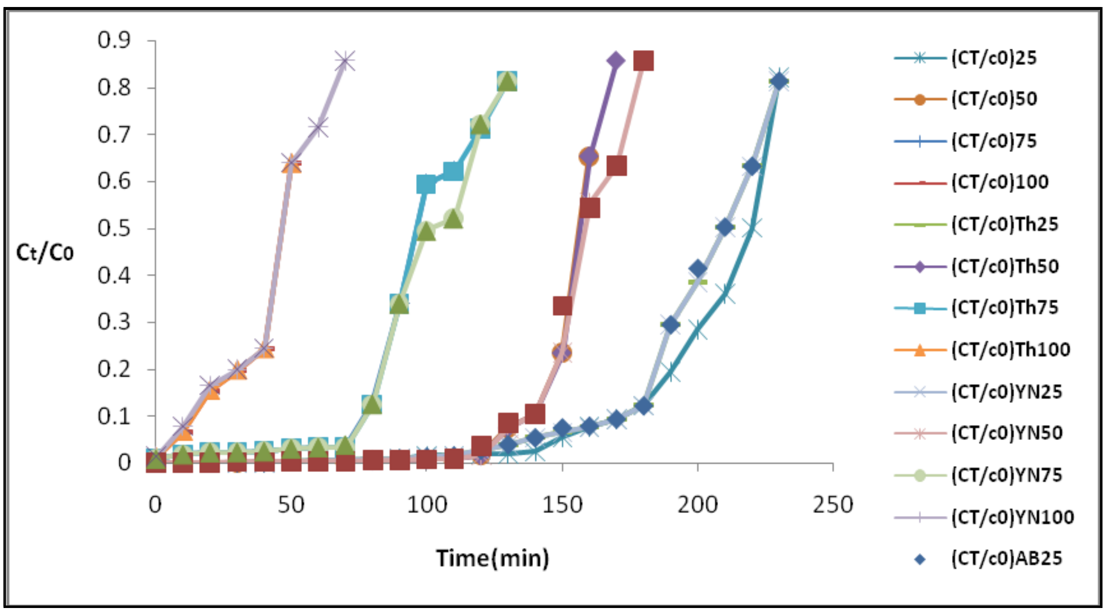

Fig.22: Model analysis of BFA for variation of concentration at H=4cm q=7.5 mLmin^{-1}

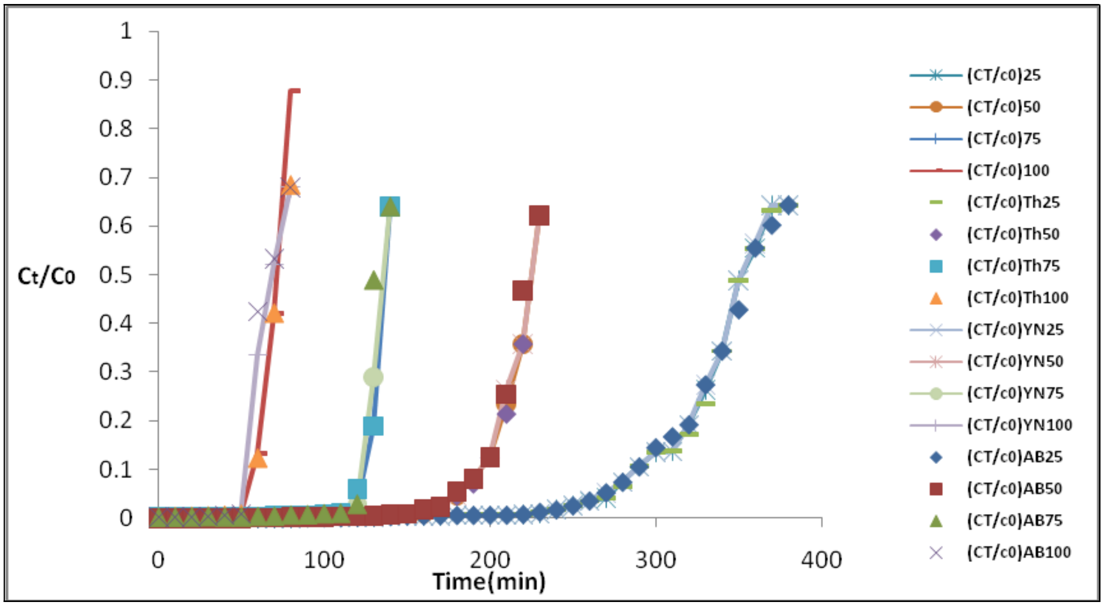

Fig. 23: Model analysis of BFA for variation of concentration at H=6 cm q=7.5 mLmin^{-1}

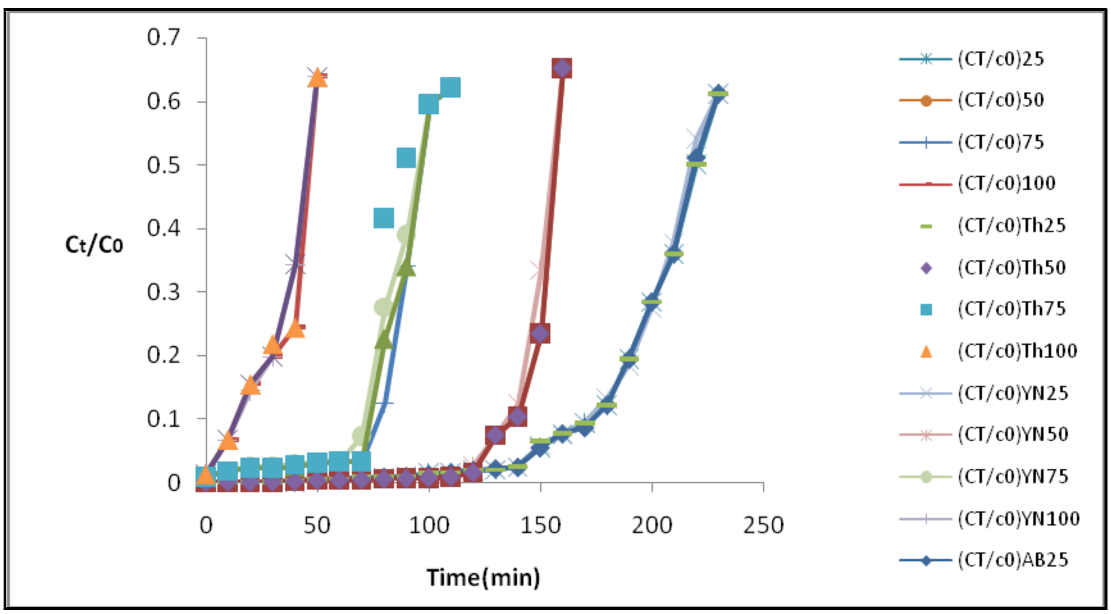

Fig.24: Model analysis of BFA for variation of concentration at H=8 cm q=7.5 mLmin^{-1}

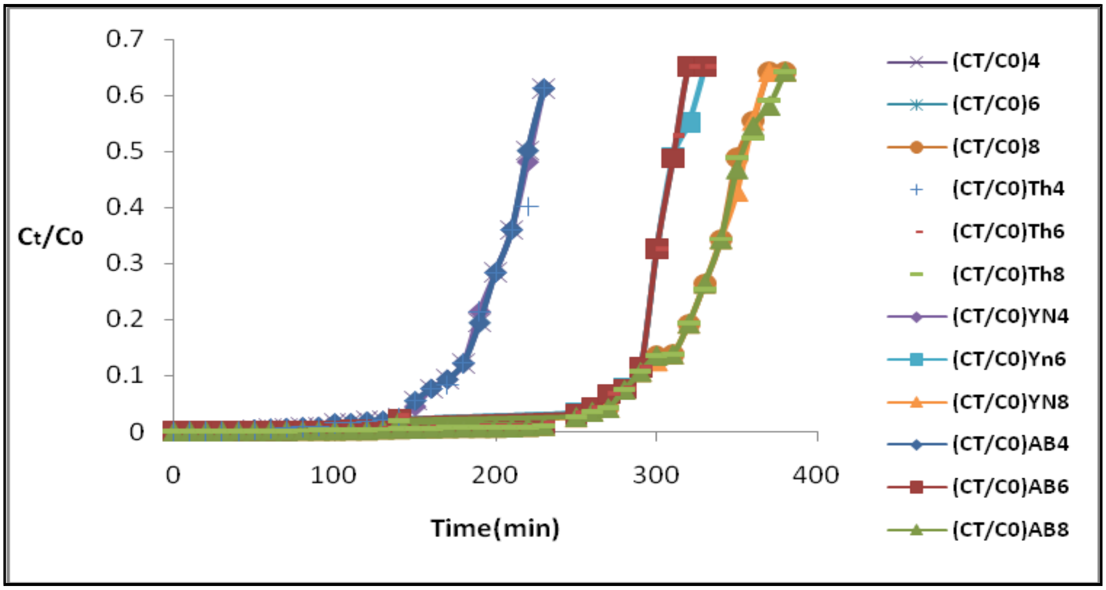

Fig.25: Model analysis of BFA for variation of bed depth at C_0= 25 mgL^{-1}, q=7.5mLmin^{-1}

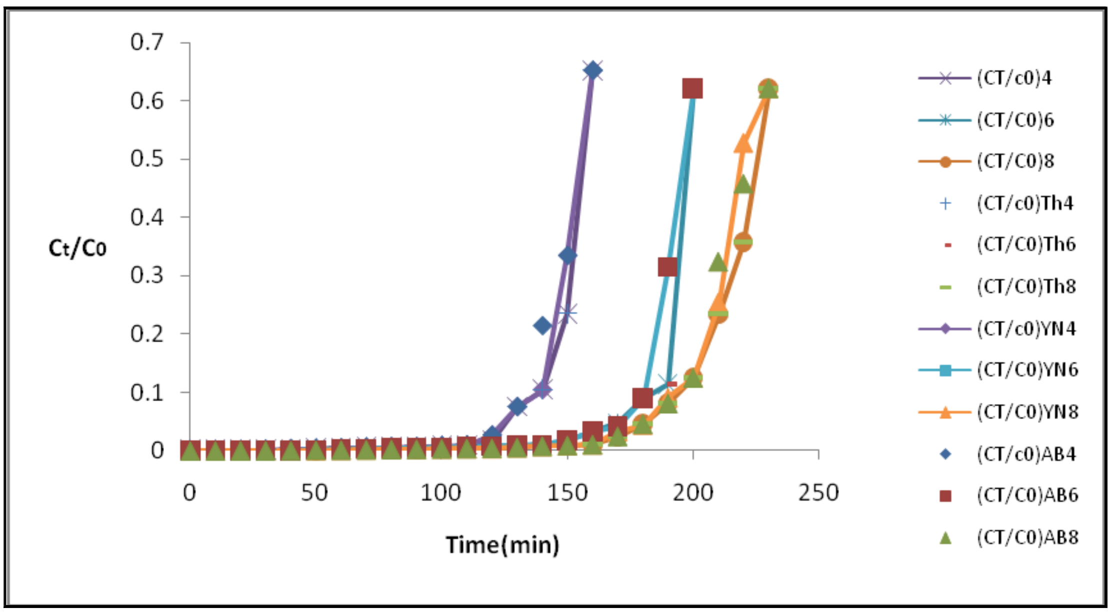

Fig.26: Model analysis of BFA for variation of bed depth at C_0= 50 mgL^{-1}, q=7.5mLmin^{-1}

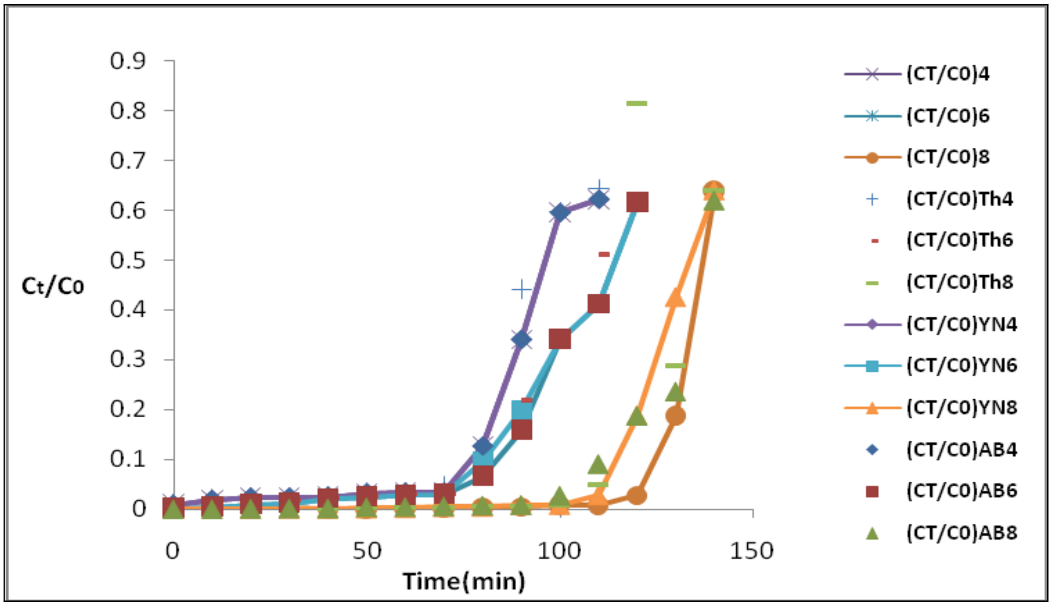

Fig.27: Model analysis of BFA for variation of bed depth at C_0= 75 mgL^{-1}, q=7.5mLmin^{-1}

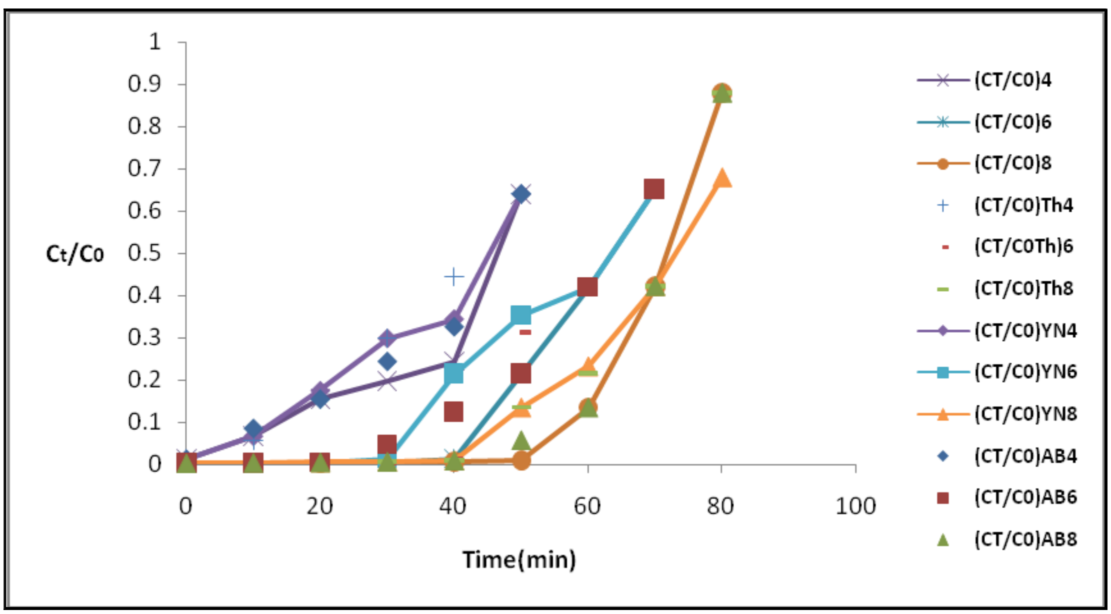

Fig.28: Model analysis of BFA for variation of bed depth at C_0= 100 mgL^{-1}, q=7.5mLmin^{-1}

Rice husk ash

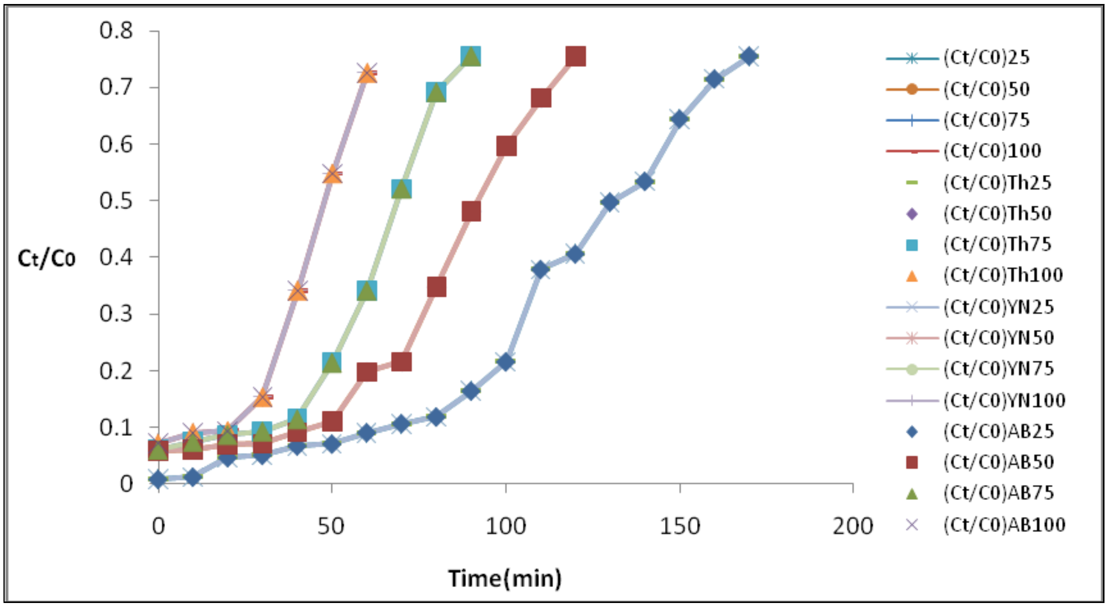

Fig.29: Model analysis of RHA for variation of concentrations at H=4 cm, q=7.5mLmin^{-1}

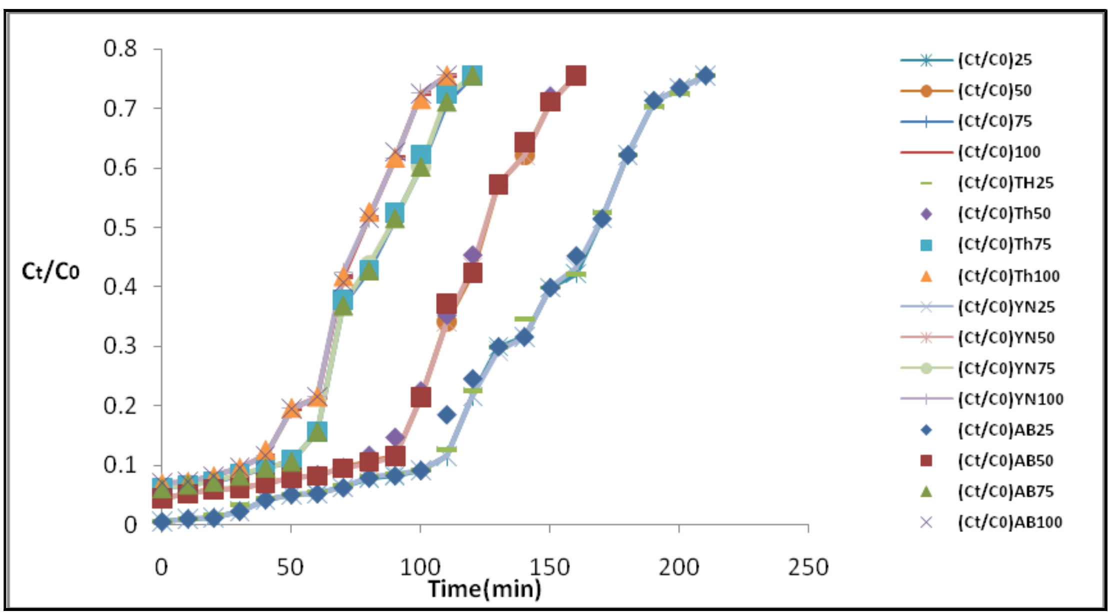

Fig.30: Model analysis of RHA for variation of concentrations at H=8 cm, q=7.5mLmin^{-1}

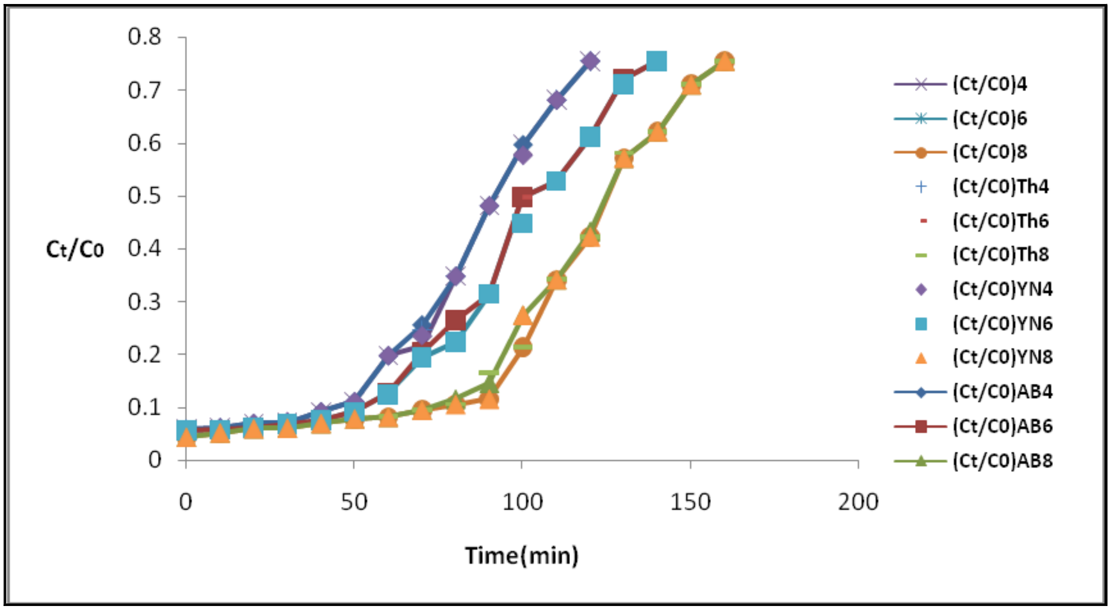

Fig.31: Model analysis of RHA for variation of bed depth at C_0= 50 mgL^{-1}, q=7.5$mLmin^{-1}$

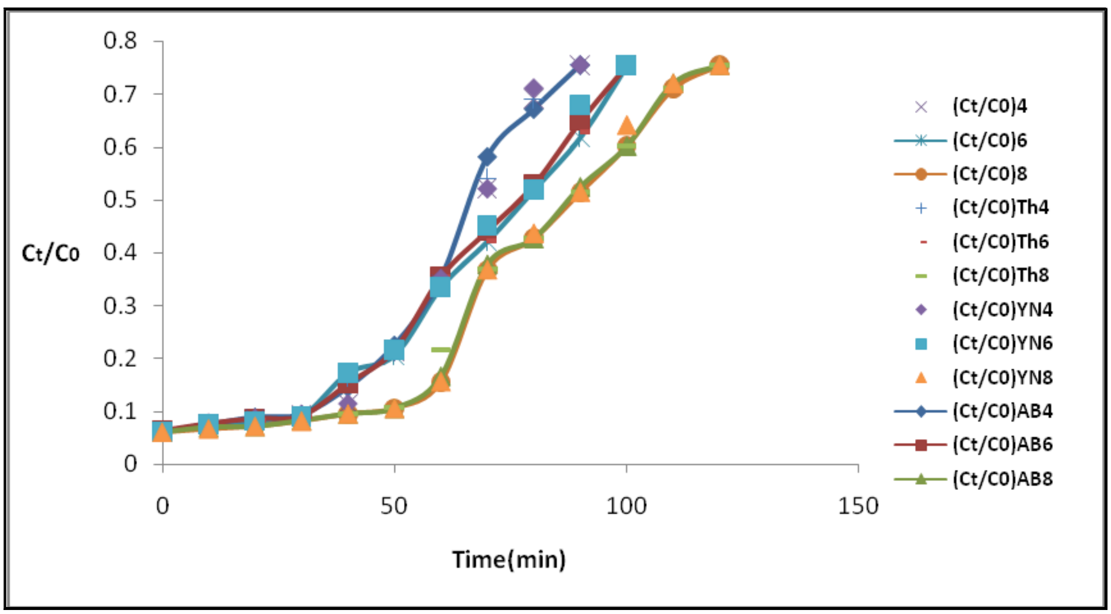

Fig.32: Model analysis of RHA for variation of bed depth at C_0= 75 mgL^{-1}, q=7.5$mLmin^{-1}$

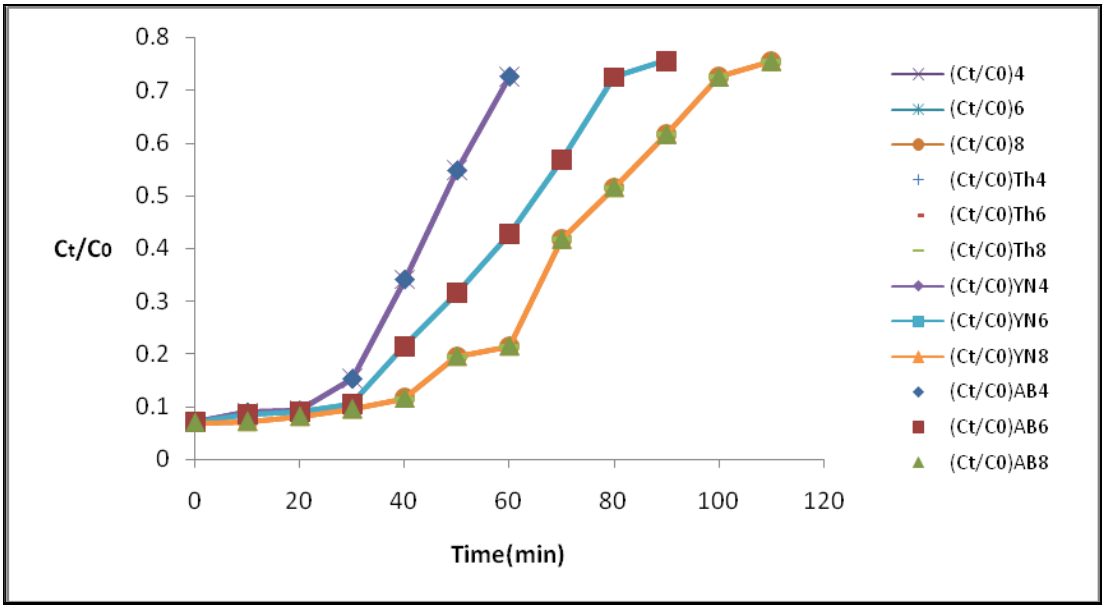

Fig.33: Model analysis of RHA for variation of bed depth at C_0= 100 mgL^{-1}, q=7.5$mLmin^{-1}$

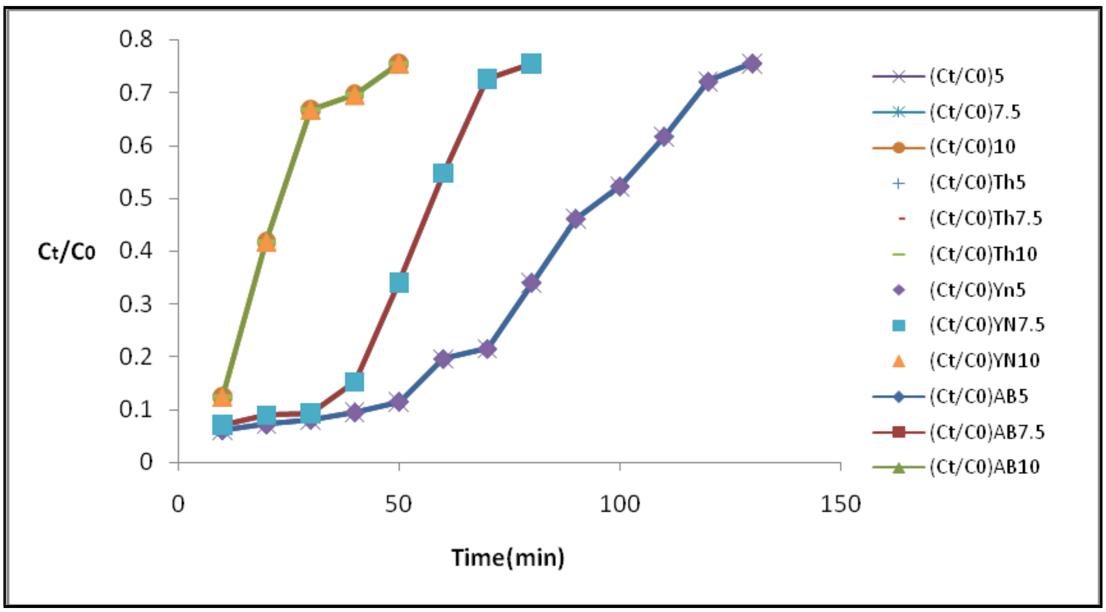

Fig.34: Model analysis of RHA for variation of flow rate at C_0= 100 mgL^{-1}, H=4 cm

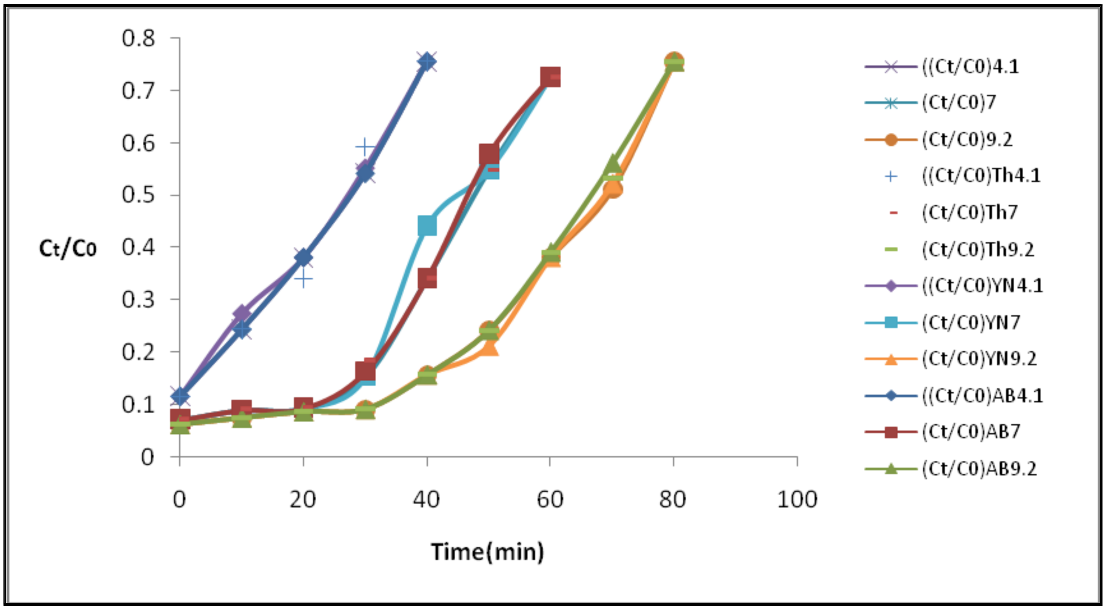

Fig.35: Model analysis of RHA for variation of pH at C_0= 100 mgL^{-1}, H=4, q=7.5$mLmin^{-1}$

Annexure-III

Statistical t-test output using STATA-10

Column Study

Adsorbent: Neem leaf ash (NLA)

Variable Parameter: Adsorbent bed height from 4 to 8 cm at low concentration 25 mg/L

Variable	Obs	Mean	Std. Err.	Std. Dev.	[95% Conf.	Interval]
var1	46	.2097565	.048169	.3266984	.1127391	.306774
var2	46	.210266	.0485027	.3289611	.1125766	.3079554
combined	92	.2100113	.0339905	.3260255	.1424933	.2775292
diff		-.0005095	.0683576		-.1363138	.1352949

```
    diff = mean(var1) - mean(var2)                              t =  -0.0075
Ho: diff = 0                                  degrees of freedom =       90

    Ha: diff < 0                 Ha: diff != 0                 Ha: diff > 0
 Pr(T < t) = 0.4970         Pr(|T| > |t|) = 0.9941          Pr(T > t) = 0.5030
```

Variable Parameter: Adsorbent bed height from 4 to 8 cm at high concentration 100 mg/L

Variable	Obs	Mean	Std. Err.	Std. Dev.	[95% Conf.	Interval]
var1	14	.1697786	.0837061	.3131997	-.0110575	.3506147
var2	14	.1685643	.0819638	.3066806	-.0085078	.3456364
combined	28	.1691714	.0574816	.3041638	.051229	.2871139
diff		.0012143	.1171528		-.2395969	.2420254

```
    diff = mean(var1) - mean(var2)                              t =   0.0104
Ho: diff = 0                                  degrees of freedom =       26

    Ha: diff < 0                 Ha: diff != 0                 Ha: diff > 0
 Pr(T < t) = 0.5041         Pr(|T| > |t|) = 0.9918          Pr(T > t) = 0.4959
```

Variable Parameter: Initial concentrations of dye solution from 25 to 100 mg/L

Variable	Obs	Mean	Std. Err.	Std. Dev.	[95% Conf.	Interval]
var1	46	.2714587	.0485576	.3293334	.1736588	.3692586
var2	46	.2737026	.0482327	.3271298	.176557	.3708481
combined	92	.2725806	.0340324	.3264269	.2049795	.3401817
diff		-.0022439	.0684414		-.1382147	.1337269

```
    diff = mean(var1) - mean(var2)                              t =  -0.0328
Ho: diff = 0                                  degrees of freedom =       90

    Ha: diff < 0                 Ha: diff != 0                 Ha: diff > 0
 Pr(T < t) = 0.4870         Pr(|T| > |t|) = 0.9739          Pr(T > t) = 0.5130
```

Variable Parameter: Inflow rate of mixed-dye solution at C_0 =100 mg/l, H = 4 cm

Variable	Obs	Mean	Std. Err.	Std. Dev.	[95% Conf.	Interval]
var1	15	.2235267	.0818259	.3169103	.0480276	.3990258
var2	15	.2218962	.0813037	.3148877	.0475172	.3962752
combined	30	.2227114	.0566724	.3104074	.1068034	.3386195
diff		.0016304	.1153506		-.2346545	.2379154

diff = mean(var1) - mean(var2)   t = 0.0141
Ho: diff = 0   degrees of freedom = 28

Ha: diff < 0   Ha: diff != 0   Ha: diff > 0
Pr(T < t) = 0.5056   Pr(|T| > |t|) = 0.9888   Pr(T > t) = 0.4944

Variable Parameter: pH of mixed-dye solution at C_0 = 100 mg/l, H = 4 cm

Variable	Obs	Mean	Std. Err.	Std. Dev.	[95% Conf.	Interval]
var1	16	.2209075	.0885533	.3542132	.0321606	.4096544
var2	16	.2170019	.0874717	.3498866	.0305604	.4034433
combined	32	.2189547	.0612244	.3463374	.0940867	.3438226
diff		.0039056	.1244708		-.2502976	.2581089

diff = mean(var1) - mean(var2)   t = 0.0314
Ho: diff = 0   degrees of freedom = 30

Ha: diff < 0   Ha: diff != 0   Ha: diff > 0
Pr(T < t) = 0.5124   Pr(|T| > |t|) = 0.9752   Pr(T > t) = 0.4876

Adsorbent: Jack fruit leaf ash (JFLA)

Variable Parameter: Adsorbent bed height from 4 to 8 cm at concentration 50 mg/L

Variable	Obs	Mean	Std. Err.	Std. Dev.	[95% Conf.	Interval]
var1	24	.1999417	.0726223	.3557752	.049711	.3501724
var2	24	.2058863	.074152	.3632692	.0524911	.3592814
combined	48	.202914	.0513422	.355709	.0996269	.3062011
diff		-.0059446	.1037908		-.2148646	.2029754

diff = mean(var1) - mean(var2)   t = -0.0573
Ho: diff = 0   degrees of freedom = 46

Ha: diff < 0   Ha: diff != 0   Ha: diff > 0
Pr(T < t) = 0.4773   Pr(|T| > |t|) = 0.9546   Pr(T > t) = 0.5227

Variable Parameter: Initial concentration of mixed dyes at H = 4 cm

Variable	Obs	Mean	Std. Err.	Std. Dev.	[95% Conf.	Interval]
var1	33	.2389925	.0608729	.3496885	.1149984	.3629866
var2	33	.2470122	.0615708	.3536972	.1215966	.3724278
combined	66	.2430023	.0429597	.349006	.157206	.3287987
diff		-.0080197	.0865822		-.1809875	.1649481

diff = mean(var1) - mean(var2) t = -0.0926
Ho: diff = 0 degrees of freedom = 64

Ha: diff < 0 Ha: diff != 0 Ha: diff > 0
Pr(T < t) = 0.4632 Pr(|T| > |t|) = 0.9265 Pr(T > t) = 0.5368

Variable Parameter: Initial concentration of mixed dyes at H = 8 cm

Variable	Obs	Mean	Std. Err.	Std. Dev.	[95% Conf.	Interval]
var1	22	.2865577	.0815963	.3827204	.1168689	.4562464
var2	22	.2884629	.0816142	.3828044	.1187369	.4581889
combined	44	.2875103	.0570289	.3782868	.1725006	.40252
diff		-.0019053	.1154072		-.2348065	.2309959

diff = mean(var1) - mean(var2) t = -0.0165
Ho: diff = 0 degrees of freedom = 42

Ha: diff < 0 Ha: diff != 0 Ha: diff > 0
Pr(T < t) = 0.4935 Pr(|T| > |t|) = 0.9869 Pr(T > t) = 0.5065

Variable Parameter: Influent flow rate of mixed-dye solution at C_0 = 100 mg/L, H = 4 cm

Variable	Obs	Mean	Std. Err.	Std. Dev.	[95% Conf.	Interval]
var1	19	.3094737	.0856311	.3732572	.1295695	.4893779
var2	19	.3079295	.0853343	.3719635	.1286489	.4872102
combined	38	.3087016	.0596232	.367542	.1878936	.4295097
diff		.0015441	.1208909		-.243634	.2467223

diff = mean(var1) - mean(var2) t = 0.0128
Ho: diff = 0 degrees of freedom = 36

Ha: diff < 0 Ha: diff != 0 Ha: diff > 0
Pr(T < t) = 0.5051 Pr(|T| > |t|) = 0.9899 Pr(T > t) = 0.4949

Variable Parameter: pH of mixed-dye solution at C_0 = 100 mg/L, H = 4 cm

Variable	Obs	Mean	Std. Err.	Std. Dev.	[95% Conf.	Interval]
var1	25	.2406296	.0656293	.3281466	.1051773	.3760819
var2	25	.2422344	.0657574	.3287868	.1065179	.3779509
combined	50	.241432	.0459759	.3250989	.1490399	.3338241
diff		-.0016048	.0929045		-.1884017	.1851921

```
    diff = mean(var1) - mean(var2)                                t =  -0.0173
Ho: diff = 0                                     degrees of freedom =       48

    Ha: diff < 0                 Ha: diff != 0                 Ha: diff > 0
 Pr(T < t) = 0.4931         Pr(|T| > |t|) = 0.9863          Pr(T > t) = 0.5069
```

Adsorbent: Bagasse fly ash (BFA)

Variable Parameter: Adsorbent bed height from 4 to 8 cm at concentration 25 mg/L

Variable	Obs	Mean	Std. Err.	Std. Dev.	[95% Conf.	Interval]
var1	19	.0866737	.0386873	.1686342	.0053946	.1679528
var2	19	.0865803	.0375877	.1638409	.0076115	.1655491
combined	38	.086627	.0266031	.1639928	.0327239	.1405301
diff		.0000934	.0539402		-.1093024	.1094892

```
    diff = mean(var1) - mean(var2)                                t =   0.0017
Ho: diff = 0                                     degrees of freedom =       36

    Ha: diff < 0                 Ha: diff != 0                 Ha: diff > 0
 Pr(T < t) = 0.5007         Pr(|T| > |t|) = 0.9986          Pr(T > t) = 0.4993
```

Variable Parameter: Adsorbent bed height from 4 to 8 cm at concentration 75 mg/L

Variable	Obs	Mean	Std. Err.	Std. Dev.	[95% Conf.	Interval]
var1	10	.12454	.0648927	.2052088	-.0222575	.2713375
var2	10	.1216614	.0620105	.1960943	-.018616	.2619388
combined	20	.1231007	.0436829	.1953558	.0316714	.21453
diff		.0028786	.0897572		-.1856944	.1914515

```
    diff = mean(var1) - mean(var2)                                t =   0.0321
Ho: diff = 0                                     degrees of freedom =       18

    Ha: diff < 0                 Ha: diff != 0                 Ha: diff > 0
 Pr(T < t) = 0.5126         Pr(|T| > |t|) = 0.9748          Pr(T > t) = 0.4874
```

Variable Parameter: Adsorbent bed height from 4 to 8 cm at concentration 100 mg/L

Variable	Obs	Mean	Std. Err.	Std. Dev.	[95% Conf.	Interval]
var1	9	.1280556	.0740436	.2221307	-.0426892	.2988003
var2	9	.1178122	.0651098	.1953293	-.0323312	.2679556
combined	18	.1229339	.0478436	.2029831	.0219927	.223875
diff		.0102433	.0985988		-.1987768	.2192635

```
    diff = mean(var1) - mean(var2)                              t =   0.1039
Ho: diff = 0                                   degrees of freedom =       16

    Ha: diff < 0                 Ha: diff != 0                 Ha: diff > 0
 Pr(T < t) = 0.5407         Pr(|T| > |t|) = 0.9185          Pr(T > t) = 0.4593
```

Variable Parameter: Initial concentration of mixed dyes at H = 4 cm

Variable	Obs	Mean	Std. Err.	Std. Dev.	[95% Conf.	Interval]
var1	15	.1309067	.0533623	.2066713	.0164559	.2453574
var2	15	.1337425	.052272	.2024486	.0216302	.2458549
combined	30	.1323246	.0367007	.201018	.0572632	.207386
diff		-.0028359	.0746987		-.1558493	.1501775

```
    diff = mean(var1) - mean(var2)                              t =  -0.0380
Ho: diff = 0                                   degrees of freedom =       28

    Ha: diff < 0                 Ha: diff != 0                 Ha: diff > 0
 Pr(T < t) = 0.4850         Pr(|T| > |t|) = 0.9700          Pr(T > t) = 0.5150
```

Variable Parameter: Initial concentration of mixed dyes at H = 6 cm

Variable	Obs	Mean	Std. Err.	Std. Dev.	[95% Conf.	Interval]
var1	20	.04429	.0196222	.087753	.0032203	.0853597
var2	20	.0459764	.020348	.090999	.0033876	.0885652
combined	40	.0451332	.0139522	.0882414	.0169122	.0733542
diff		-.0016864	.0282678		-.0589117	.0555388

```
    diff = mean(var1) - mean(var2)                              t =  -0.0597
Ho: diff = 0                                   degrees of freedom =       38

    Ha: diff < 0                 Ha: diff != 0                 Ha: diff > 0
 Pr(T < t) = 0.4764         Pr(|T| > |t|) = 0.9527          Pr(T > t) = 0.5236
```

Variable Parameter: Influent flow rate of mixed-dye solution at $C_0 = 100$ mg/L, H = 4 cm

Variable	Obs	Mean	Std. Err.	Std. Dev.	[95% Conf.	Interval]
var1	10	.223216	.0735267	.2325119	.056887	.389545
var2	10	.2219318	.0732429	.2316144	.0562448	.3876187
combined	20	.2225739	.0505072	.2258751	.1168611	.3282867
diff		.0012842	.103782		-.2167536	.2193221

diff = mean(var1) - mean(var2)   t = 0.0124
Ho: diff = 0   degrees of freedom = 18

Ha: diff < 0   Ha: diff != 0   Ha: diff > 0
Pr(T < t) = 0.5049   Pr(|T| > |t|) = 0.9903   Pr(T > t) = 0.4951

Variable Parameter: pH of mixed-dye solution at $C_0 = 100$ mg/L, H = 4 cm.

Variable	Obs	Mean	Std. Err.	Std. Dev.	[95% Conf.	Interval]
var1	13	.2389146	.0634143	.2286437	.1007466	.3770826
var2	13	.2401364	.0596552	.2150899	.1101589	.370114
combined	26	.2395255	.0426526	.2174865	.1516808	.3273702
diff		-.0012218	.0870639		-.1809129	.1784693

diff = mean(var1) - mean(var2)   t = -0.0140
Ho: diff = 0   degrees of freedom = 24

Ha: diff < 0   Ha: diff != 0   Ha: diff > 0
Pr(T < t) = 0.4945   Pr(|T| > |t|) = 0.9889   Pr(T > t) = 0.5055

Adsorbent: Rice husk ash (RHA)

Variable Parameter: Adsorbent bed height from 4 to 8 cm at low concentration 25 mg/L

Variable	Obs	Mean	Std. Err.	Std. Dev.	[95% Conf.	Interval]
var1	18	.1382556	.0478235	.2028979	.0373568	.2391543
var2	18	.1392631	.047679	.2022849	.0386692	.239857
combined	36	.1387593	.0332795	.1996772	.0711983	.2063204
diff		-.0010075	.0675306		-.1382461	.1362311

diff = mean(var1) - mean(var2)   t = -0.0149
Ho: diff = 0   degrees of freedom = 34

Ha: diff < 0   Ha: diff != 0   Ha: diff > 0
Pr(T < t) = 0.4941   Pr(|T| > |t|) = 0.9882   Pr(T > t) = 0.5059

Variable Parameter: Adsorbent Bed Height from 4 to 8 cm at high concentration 100 mg/L

Variable	Obs	Mean	Std. Err.	Std. Dev.	[95% Conf.	Interval]
var1	10	.31264	.0855378	.2704942	.1191401	.5061399
var2	10	.325241	.0864844	.2734875	.1295998	.5208822
combined	20	.3189405	.0592154	.2648194	.1950012	.4428798
diff		-.012601	.1216399		-.2681569	.2429549

```
    diff = mean(var1) - mean(var2)                          t =  -0.1036
Ho: diff = 0                                  degrees of freedom =       18

    Ha: diff < 0                 Ha: diff != 0                 Ha: diff > 0
 Pr(T < t) = 0.4593         Pr(|T| > |t|) = 0.9186          Pr(T > t) = 0.5407
```

Variable Parameter: Initial concentration of mixed dyes at H = 4 cm

Variable	Obs	Mean	Std. Err.	Std. Dev.	[95% Conf.	Interval]
var1	17	.2142176	.0538312	.2219516	.1001007	.3283346
var2	17	.2226582	.0515505	.2125481	.113376	.3319403
combined	34	.2184379	.0367051	.2140258	.1437608	.293115
diff		-.0084405	.0745335		-.1602603	.1433793

```
    diff = mean(var1) - mean(var2)                          t =  -0.1132
Ho: diff = 0                                  degrees of freedom =       32

    Ha: diff < 0                 Ha: diff != 0                 Ha: diff > 0
 Pr(T < t) = 0.4553         Pr(|T| > |t|) = 0.9105          Pr(T > t) = 0.5447
```

Variable Parameter: Initial concentration of mixed dyes at H = 6 cm

Variable	Obs	Mean	Std. Err.	Std. Dev.	[95% Conf.	Interval]
var1	18	.1022133	.0460169	.195233	.0051263	.1993004
var2	18	.0959059	.0433733	.1840173	.0043963	.1874156
combined	36	.0990596	.0311676	.1870056	.035786	.1623332
diff		.0063074	.063236		-.1222036	.1348184

```
    diff = mean(var1) - mean(var2)                          t =   0.0997
Ho: diff = 0                                  degrees of freedom =       34

    Ha: diff < 0                 Ha: diff != 0                 Ha: diff > 0
 Pr(T < t) = 0.5394         Pr(|T| > |t|) = 0.9211          Pr(T > t) = 0.4606
```

Variable Parameter: Influent flow rate of mixed-dye solution at C_0 = 100 mg/L, H = 4 cm

Variable	Obs	Mean	Std. Err.	Std. Dev.	[95% Conf.	Interval]
var1	10	.353962	.0945788	.2990844	.1400099	.5679141
var2	10	.3508205	.0927844	.2934099	.1409276	.5607133
combined	20	.3523912	.06448	.2883635	.2174329	.4873495
diff		.0031415	.1324918		-.2752135	.2814966

diff = mean(var1) - mean(var2) t = 0.0237
Ho: diff = 0 degrees of freedom = 18

Ha: diff < 0 Pr(T < t) = 0.5093
Ha: diff != 0 Pr(|T| > |t|) = 0.9813
Ha: diff > 0 Pr(T > t) = 0.4907

Variable Parameter: pH of mixed-dye solution at C_0 = 100 mg/l, H = 4 cm

Variable	Obs	Mean	Std. Err.	Std. Dev.	[95% Conf.	Interval]
var1	8	.3423	.0790766	.2236623	.1553136	.5292864
var2	8	.3427882	.0681833	.1928515	.1815603	.5040162
combined	16	.3425441	.0504363	.2017452	.2350417	.4500465
diff		-.0004882	.104413		-.2244318	.2234553

diff = mean(var1) - mean(var2) t = -0.0047
Ho: diff = 0 degrees of freedom = 14

Ha: diff < 0 Pr(T < t) = 0.4982
Ha: diff != 0 Pr(|T| > |t|) = 0.9963
Ha: diff > 0 Pr(T > t) = 0.5018

Statistical t-test output using STATA-10

Batch Study

Adsorbent: Neem leaf ash

Variable Parameter: Adsorbent Dose

Variable	Obs	Mean	Std. Err.	Std. Dev.	[95% Conf.	Interval]
var1	16	.1164	.0298081	.1192324	.0528655	.1799345
var2	16	.1214295	.0297996	.1191984	.0579132	.1849459
combined	32	.1189148	.0207367	.1173046	.0766219	.1612076
diff		-.0050295	.042149		-.0911093	.0810502

diff = mean(var1) - mean(var2) t = -0.1193
Ho: diff = 0 degrees of freedom = 30

Ha: diff < 0 Ha: diff != 0 Ha: diff > 0
Pr(T < t) = 0.4529 Pr(|T| > |t|) = 0.9058 Pr(T > t) = 0.5471

Variable Parameter: Contact Time

Variable	Obs	Mean	Std. Err.	Std. Dev.	[95% Conf.	Interval]
var1	12	.0113	.0032413	.0112282	.0041659	.0184341
var2	12	.0111608	.0032955	.0114158	.0039075	.018414
combined	24	.0112304	.0022604	.0110738	.0065543	.0159064
diff		.0001392	.0046224		-.0094469	.0097254

diff = mean(var1) - mean(var2) t =0.0301
Ho: diff = 0 degrees of freedom = 22

Ha: diff < 0 Ha: diff != 0 Ha: diff > 0
Pr(T < t) =0.5119 Pr(|T| > |t|) =0.9762 Pr(T > t) 0.4881

Variable Parameter: Initial Concentration

Variable	Obs	Mean	Std. Err.	Std. Dev.	[95% Conf.	Interval]
EXP	6	.0922167	.0478759	.1172716	-.0308524	.2152857
ANN	6	.1161938	.0566225	.1386962	-.029359	.2617465
combined	12	.1042052	.0355339	.1230931	.0259956	.1824149
diff		-.0239771	.0741499		-.1891935	.1412392

diff = mean(var1) - mean(var2) t = -0.3234
Ho: diff = 0 degrees of freedom = 10

Ha: diff < 0 Ha: diff != 0 Ha: diff > 0
Pr(T < t) = 0.3765 Pr(|T| > |t|) = 0.7531 Pr(T > t) = 0.6235

Variable Parameter: Shaker Speed

Variable	Obs	Mean	Std. Err.	Std. Dev.	[95% Conf.	Interval]
var1	8	.02985	.0063078	.0178411	.0149344	.0447656
var2	8	.0381274	.0069672	.0197061	.0216527	.0546021
combined	16	.0339887	.0046639	.0186557	.0240478	.0439296
diff		-.0082774	.0093984		-.0284349	.0118801

diff = mean(var1) - mean(var2) t = -0.8807
Ho: diff = 0 degrees of freedom = 14

Ha: diff < 0 Ha: diff != 0 Ha: diff > 0
Pr(T < t) = 0.1967 Pr(|T| > |t|) = 0.3933 Pr(T > t) = 0.8033

Variable Parameter: pH of dye mixture

Variable	Obs	Mean	Std. Err.	Std. Dev.	[95% Conf.	Interval]
var1	8	.02985	.0063078	.0178411	.0149344	.0447656
var2	8	.0381274	.0069672	.0197061	.0216527	.0546021
combined	16	.0339887	.0046639	.0186557	.0240478	.0439296
diff		-.0082774	.0093984		-.0284349	.0118801

diff = mean(var1) - mean(var2) t = -0.8807
Ho: diff = 0 degrees of freedom = 14

Ha: diff < 0 Ha: diff != 0 Ha: diff > 0
Pr(T < t) = 0.1967 Pr(|T| > |t|) = 0.3933 Pr(T > t) = 0.8033

Adsorbent: Jack fruit leaf ash

Variable Parameter: Adsorbent Dose

Variable	Obs	Mean	Std. Err.	Std. Dev.	[95% Conf.	Interval]
var1	14	.2970286	.0640151	.2395225	.1587324	.4353247
var2	14	.2981562	.0643787	.2408831	.1590745	.437238
combined	28	.2975924	.0445458	.2357143	.2061919	.3889929
diff		-.0011277	.0907885		-.1877461	.1854908

```
    diff = mean(var1) - mean(var2)                                t =  -0.0124
Ho: diff = 0                                     degrees of freedom =       26

    Ha: diff < 0                 Ha: diff != 0                 Ha: diff > 0
 Pr(T < t) = 0.4951         Pr(|T| > |t|) = 0.9902          Pr(T > t) = 0.5049
```

Variable Parameter: Contact Time

Variable	Obs	Mean	Std. Err.	Std. Dev.	[95% Conf.	Interval]
var1	11	.0950636	.0234227	.0776844	.0428745	.1472528
var2	11	.0988339	.0251844	.0835273	.0427194	.1549483
combined	22	.0969487	.0167871	.0787386	.062038	.1318595
diff		-.0037702	.034393		-.0755128	.0679724

```
    diff = mean(var1) - mean(var2)                                t =  -0.1096
Ho: diff = 0                                     degrees of freedom =       20

    Ha: diff < 0                 Ha: diff != 0                 Ha: diff > 0
 Pr(T < t) = 0.4569         Pr(|T| > |t|) = 0.9138          Pr(T > t) = 0.5431
```

Variable Parameter: Initial Concentration

Variable	Obs	Mean	Std. Err.	Std. Dev.	[95% Conf.	Interval]
var1	6	.2375167	.0484151	.1185923	.1130617	.3619716
var2	6	.2292732	.0465355	.1139881	.10965	.3488964
combined	12	.2333949	.0320382	.1109836	.1628793	.3039106
diff		.0082435	.0671533		-.1413835	.1578704

```
    diff = mean(var1) - mean(var2)                                t =   0.1228
Ho: diff = 0                                     degrees of freedom =       10

    Ha: diff < 0                 Ha: diff != 0                 Ha: diff > 0
 Pr(T < t) = 0.5476         Pr(|T| > |t|) = 0.9047          Pr(T > t) = 0.4524
```

Variable Parameter: **Shaker Speed**

Variable	Obs	Mean	Std. Err.	Std. Dev.	[95% Conf.	Interval]
var1	8	.019575	.0026157	.0073984	.0133898	.0257602
var2	8	.0197444	.0029693	.0083984	.0127231	.0267656
combined	16	.0196597	.0019116	.0076464	.0155852	.0237342
diff		-.0001694	.0039571		-.0086565	.0083178

```
    diff = mean(var1) - mean(var2)                          t =  -0.0428
Ho: diff = 0                                  degrees of freedom =       14

    Ha: diff < 0                 Ha: diff != 0                 Ha: diff > 0
 Pr(T < t) = 0.4832         Pr(|T| > |t|) = 0.9665          Pr(T > t) = 0.5168
```

Variable Parameter: **pH of the mixed dyes solution**

Variable	Obs	Mean	Std. Err.	Std. Dev.	[95% Conf.	Interval]
var1	6	.2375167	.0484151	.1185923	.1130617	.3619716
var2	6	.2292732	.0465355	.1139881	.10965	.3488964
combined	12	.2333949	.0320382	.1109836	.1628793	.3039106
diff		.0082435	.0671533		-.1413835	.1578704

```
    diff = mean(var1) - mean(var2)                          t =   0.1228
Ho: diff = 0                                  degrees of freedom =       10

    Ha: diff < 0                 Ha: diff != 0                 Ha: diff > 0
 Pr(T < t) = 0.5476         Pr(|T| > |t|) = 0.9047          Pr(T > t) = 0.4524
```

Adsorbent: Bagasse fly ash

Variable Parameter: Adsorbent Dose

Variable	Obs	Mean	Std. Err.	Std. Dev.	[95% Conf.	Interval]
var1	15	.0271733	.0052686	.0204052	.0158733	.0384734
var2	15	.0266693	.005418	.0209838	.0150488	.0382897
combined	30	.0269213	.0037132	.0203382	.0193269	.0345157
diff		.0005041	.0075573		-.0149764	.0159845

```
    diff = mean(var1) - mean(var2)                          t =   0.0667
Ho: diff = 0                                  degrees of freedom =       28

    Ha: diff < 0                 Ha: diff != 0                 Ha: diff > 0
 Pr(T < t) = 0.5264         Pr(|T| > |t|) = 0.9473          Pr(T > t) = 0.4736
```

Variable Parameter: Contact Time

Variable	Obs	Mean	Std. Err.	Std. Dev.	[95% Conf.	Interval]
var1	12	.0156083	.0029128	.0100901	.0091974	.0220193
var2	12	.0150182	.0026523	.009188	.0091804	.0208559
combined	24	.0153132	.0019274	.0094423	.0113261	.0193004
diff		.0005902	.0039394		-.0075797	.00876

diff = mean(var1) - mean(var2) t = 0.1498
Ho: diff = 0 degrees of freedom = 22

Ha: diff < 0	Ha: diff != 0	Ha: diff > 0
Pr(T < t) = 0.5589	Pr(|T| > |t|) = 0.8823	Pr(T > t) = 0.4411

Variable Parameter: Initial Concentration

Variable	Obs	Mean	Std. Err.	Std. Dev.	[95% Conf.	Interval]
var1	12	.0156083	.0029128	.0100901	.0091974	.0220193
var2	12	.0150182	.0026523	.009188	.0091804	.0208559
combined	24	.0153132	.0019274	.0094423	.0113261	.0193004
diff		.0005902	.0039394		-.0075797	.00876

diff = mean(var1) - mean(var2) t = 0.1498
Ho: diff = 0 degrees of freedom = 22

Ha: diff < 0	Ha: diff != 0	Ha: diff > 0
Pr(T < t) = 0.5589	Pr(|T| > |t|) = 0.8823	Pr(T > t) = 0.4411

Variable Parameter: Shaker Speed

Variable	Obs	Mean	Std. Err.	Std. Dev.	[95% Conf.	Interval]
var1	8	.0277	.0037876	.0107129	.0187438	.0366562
var2	8	.0296081	.0037124	.0105003	.0208296	.0383865
combined	16	.028654	.0025737	.0102947	.0231684	.0341397
diff		-.0019081	.0053036		-.0132831	.0094669

diff = mean(var1) - mean(var2) t = -0.3598
Ho: diff = 0 degrees of freedom = 14

Ha: diff < 0	Ha: diff != 0	Ha: diff > 0
Pr(T < t) = 0.3622	Pr(|T| > |t|) = 0.7244	Pr(T > t) = 0.6378

Variable Parameter: pH of the Dye mixture

Variable	Obs	Mean	Std. Err.	Std. Dev.	[95% Conf.	Interval]
var1	6	.0227667	.0054646	.0133855	.0087195	.0368139
var2	6	.0229883	.0052595	.012883	.0094684	.0365082
combined	12	.0228775	.0036159	.0125258	.014919	.030836
diff		-.0002216	.0075844		-.0171208	.0166775

```
    diff = mean(var1) - mean(var2)                                t =  -0.0292
Ho: diff = 0                                     degrees of freedom =       10

    Ha: diff < 0                 Ha: diff != 0                 Ha: diff > 0
 Pr(T < t) = 0.4886         Pr(|T| > |t|) = 0.9773          Pr(T > t) = 0.5114
```

Adsorbent: Rice husk ash

Variable Parameter: **Adsorbent Dose**

Variable	Obs	Mean	Std. Err.	Std. Dev.	[95% Conf.	Interval]
var1	14	.2325457	.0447644	.1674931	.1358381	.3292533
var2	14	.233183	.04275	.1599558	.1408273	.3255388
combined	28	.2328644	.0303707	.1607068	.1705488	.2951799
diff		-.0006373	.0618984		-.1278713	.1265967

```
    diff = mean(var1) - mean(var2)                                t =  -0.0103
Ho: diff = 0                                     degrees of freedom =       26

    Ha: diff < 0                 Ha: diff != 0                 Ha: diff > 0
 Pr(T < t) = 0.4959         Pr(|T| > |t|) = 0.9919          Pr(T > t) = 0.5041
```

Variable Parameter: Contact Time

Variable	Obs	Mean	Std. Err.	Std. Dev.	[95% Conf.	Interval]
var1	12	.1850333	.0347896	.1205147	.1084619	.2616047
var2	12	.1864395	.0350734	.1214979	.1092434	.2636355
combined	24	.1857364	.024158	.1183496	.1357617	.2357111
diff		-.0014061	.049401		-.1038576	.1010453

```
    diff = mean(var1) - mean(var2)                                t =  -0.0285
Ho: diff = 0                                     degrees of freedom =       22

    Ha: diff < 0                 Ha: diff != 0                 Ha: diff > 0
 Pr(T < t) = 0.4888         Pr(|T| > |t|) = 0.9775          Pr(T > t) = 0.5112
```

Variable Parameter: Initial Concentrations

Variable	Obs	Mean	Std. Err.	Std. Dev.	[95% Conf.	Interval]
var1	6	.2375167	.0484151	.1185923	.1130617	.3619716
var2	6	.2405739	.047652	.1167232	.1180805	.3630674
combined	12	.2390453	.0323885	.1121971	.1677586	.310332
diff		-.0030573	.0679319		-.1544189	.1483044

```
    diff = mean(var1) - mean(var2)                          t =  -0.0450
Ho: diff = 0                               degrees of freedom =       10

    Ha: diff < 0             Ha: diff != 0             Ha: diff > 0
 Pr(T < t) = 0.4825      Pr(|T| > |t|) = 0.9650      Pr(T > t) = 0.5175
```

Variable Parameter: Shaker Speed

Variable	Obs	Mean	Std. Err.	Std. Dev.	[95% Conf.	Interval]
var1	8	.1744625	.0326469	.0923395	.0972647	.2516603
var2	8	.1753397	.0330006	.0933398	.0973056	.2533738
combined	16	.1749011	.0224235	.0896941	.1271065	.2226957
diff		-.0008772	.0464205		-.1004393	.0986849

```
    diff = mean(var1) - mean(var2)                          t =  -0.0189
Ho: diff = 0                               degrees of freedom =       14

    Ha: diff < 0             Ha: diff != 0             Ha: diff > 0
 Pr(T < t) = 0.4926      Pr(|T| > |t|) = 0.9852      Pr(T > t) = 0.5074
```

Variable Parameter: pH of the dye mixture

Variable	Obs	Mean	Std. Err.	Std. Dev.	[95% Conf.	Interval]
var1	6	.1459167	.0499741	.1224111	.0174541	.2743792
var2	6	.1496797	.0478421	.1171887	.0266977	.2726617
combined	12	.1477982	.0329866	.1142688	.0751953	.2204011
diff		-.003763	.0691829		-.1579122	.1503862

```
    diff = mean(var1) - mean(var2)                          t =  -0.0544
Ho: diff = 0                               degrees of freedom =       10

    Ha: diff < 0             Ha: diff != 0             Ha: diff > 0
 Pr(T < t) = 0.4788      Pr(|T| > |t|) = 0.9577      Pr(T > t) = 0.5212
```

Annexure-IV

Evaluation of adsorption potential by using ANN tool: Column study

Adsorbent: Neem leaf ash

Variation of bed depth at C_0 = 50 mg/L

Test	Input	Sl. No	2	3	8	9	13	14	18	22	23	26	29	34	41	42	50	53	54	63	66
		H	4	4	4	4	4	4	4	6	6	6	6	6	6	6	8	8	8	8	8
		Time	10	20	70	80	120	130	170	30	40	70	100	150	220	230	70	100	110	200	230
		q	7.5	7.5	7.5	7.5	7.5	7.5	7.5	7.5	7.5	7.5	7.5	7.5	7.5	7.5	7.5	7.5	7.5	7.5	7.5
		pH	7	7	7	7	7	7	7	7	7	7	7	7	7	7	7	7	7	7	7
		C0	50	50	50	50	50	50	50	50	50	50	50	50	50	50	50	50	50	50	50
	Target	Ct/C0	0.0003	0.0005	0.0049	0.0084	0.5241	0.6042	0.9724	0.0011	0.002	0.0029	0.029	0.3915	0.9531	0.9741	0.0247	0.0309	0.0776	0.7512	0.9973
		Model	0.0473367	0.0504418	0.0030499	0.1446068	0.5029658	0.6293304	1.0754408	-0.0076085	-0.0105137	0.0021221	0.0153986	0.3222811	0.8099172	0.7769649	0.0389213	0.1320172	0.1704213	0.7916826	0.911088

Variation of bed depth at C_0 = 100 mg/L

Test	Input	Sl. No	3	4	5	10	15	21	22	28	36	38	41	42	53	55
		H	4	4	4	4	4	6	6	6	8	8	8	8	8	8
		Time	20	30	40	90	140	40	50	110	20	40	70	80	190	210
		q	7.5	7.5	7.5	7.5	7.5	7.5	7.5	7.5	7.5	7.5	7.5	7.5	7.5	7.5
		pH	7	7	7	7	7	7	7	7	7	7	7	7	7	7
		C0	100	100	100	100	100	100	100	100	100	100	100	100	100	100
	Target	Ct/C0	0.0019	0.0024	0.0029	0.0197	0.7743	0.0063	0.008	0.0845	0.0118	0.0153	0.0169	0.0182	0.5204	0.8943
		Model	0.0018806	0.0042501	0.0039647	-0.0120491	0.7431227	0.005979	0.0470781	0.1191347	-0.0218865	0.0125185	-0.0799198	-0.0975576	0.6440474	0.8134473

Variation of bed depth at C_0 = 25 mg/L

		Sl. No	3	4	9	16	25	27	42	43	47	51	54	56	57	61	62	66	67	71	72
Test	Input	H	4	4	4	4	6	6	6	6	6	8	8	8	8	8	8	8	8	8	8
		Time	20	30	80	150	30	50	200	210	250	30	60	80	90	130	140	180	190	230	240
		q	7.5	7.5	7.5	7.5	7.5	7.5	7.5	7.5	7.5	7.5	7.5	7.5	7.5	7.5	7.5	7.5	7.5	7.5	7.5
		pH	7	7	7	7	7	7	7	7	7	7	7	7	7	7	7	7	7	7	7
		C0	25	25	25	25	25	25	25	25	25	25	25	25	25	25	25	25	25	25	25
	Target	Ct/C0	0.0009	0.001	0.0042	0.273	0.002	0.0023	0.6943	0.7231	0.9842	0.0014	0.0097	0.0135	0.0288	0.0327	0.1052	0.1862	0.7124	0.8217	0.8417
		Model	0.0104717	0.001046645	0.01163259	0.311781536	0.00211982	-0.001563739	0.7374758	0.8077549	0.8890897	0.0010423	0.0059301	0.005453	0.006878	0.035382	0.04908007	0.1258686	0.245677	0.68689	0.76526761

Variation of initial concentration at H = 4 cm.

		Sl. No	5	6	7	13	14	21	22	27	33	34	45	46	53	61	62	69	70
Test	Input	C0	25	25	25	25	25	25	50	50	50	50	75	75	75	100	100	100	100
		Time	40	50	60	120	130	200	0	50	110	120	50	60	130	40	50	120	130
		q	7.5	7.5	7.5	7.5	7.5	7.5	7.5	7.5	7.5	7.5	7.5	7.5	7.5	7.5	7.5	7.5	7.5
		pH	7	7	7	7	7	7	7	7	7	7	7	7	7	7	7	7	7
		H	4	4	4	4	4	4	4	4	4	4	4	4	4	4	4	4	4
	Target	Ct/C0	0.0021	0.0023	0.0031	0.0212	0.0483	0.9745	0.0002	0.0027	0.4307	0.5241	0.0037	0.0035	0.6189	0.0029	0.0033	0.333	0.5285
		Model	0.010258082	0.002232314	0.014279181	-0.026472005	0.00585537	0.90077697	0.027473019	0.00296364	0.250476663	0.382410779	0.003876515	-0.038347469	0.752539702	0.002008837	0.002915687	0.356178802	0.569864105

Variation of initial concentration at H = 8 cm.

Test	Input	Sl. No	2	3	9	16	21	22	32	33	34	37	42	43	53	54	60	61	62	76	77	85
		H	25	25	25	25	25	25	50	50	50	50	50	50	50	75	75	75	75	75	75	100
		Time	10	20	80	150	200	210	30	40	50	80	130	140	240	0	60	70	80	220	230	70
		q	7.5	7.5	7.5	7.5	7.5	7.5	7.5	7.5	7.5	7.5	7.5	7.5	7.5	7.5	7.5	7.5	7.5	7.5	7.5	7.5
		pH	7	7	7	7	7	7	7	7	7	7	7	7	7	7	7	7	7	7	7	7
		C0	8	8	8	8	8	8	8	8	8	8	8	8	8	8	8	8	8	8	8	8
	Target	Ct/C0	0.0009	0.0011	0.0097	0.0541	0.2876	0.5214	0.0077	0.0082	0.0093	0.027	0.1309	0.2224	0.9973	0.0028	0.0288	0.0324	0.0618	0.9567	0.9973	0.0167
		Model	0.002471	0.006323	0.00705	0.0548707	0.3046835	0.4399853	0.0299883	0.0388668	0.0379489	0.048655	0.1372302	0.210008	1.1241	0.02966	0.023991	0.0297066	0.058204	0.948088	0.994567	0.016826

Variation of flow rate at C_0 = 100 mg/L and H = 4 cm.

Test	**Input**	**Sl. No**	2	3	6	11	12	19	20	26	27	35	36	37	43	44	47
		C0	100	100	100	100	100	100	100	100	100	100	100	100	100	100	100
		Time	10	20	50	100	110	50	60	120	130	50	60	70	130	140	170
		q	5	5	5	5	5	7.5	7.5	7.5	7.5	10	10	10	10	10	10
		pH	7	7	7	7	7	7	7	7	7	7	7	7	7	7	7
		H	4	4	4	4	4	4	4	4	4	4	4	4	4	4	4
	Target	**Ct/C0**	0.0014	0.0047	0.038	0.621	0.827	0.0033	0.004	0.333	0.5285	0.0026	0.0049	0.0051	0.0681	0.0853	0.826
		Model	0.0012641	0.0051313	0.0349004	0.3565719	0.6011311	0.0048627	0.0058207	0.2243055	0.4444398	0.0046771	0.0071721	0.0086763	0.0279867	0.0637786	0.6181742

Variation of pH at C_0 = 100 mg/L and H = 4 cm.

Test	Input	**Sl. No**	2	3	4	11	12	18	19	24	25	33	34	39	42	43	44	47
		C0	100	100	100	100	100	100	100	100	100	100	100	100	100	100	100	100
		Time	10	20	30	100	110	50	60	110	120	40	50	100	130	140	150	180
		q	7.5	7.5	7.5	7.5	7.5	7.5	7.5	7.5	7.5	7.5	7.5	7.5	7.5	7.5	7.5	7.5
		pH	4.1	4.1	4.1	4.1	4.1	7	7	7	7	9.2	9.2	9.2	9.2	9.2	9.2	9.2
		H	4	4	4	4	4	4	4	4	4	4	4	4	4	4	4	4
	Target	**Ct/C0**	0.0086	0.0257	0.0369	0.934	0.9736	0.0033	0.004	0.1619	0.333	0.00124	0.00248	0.0098	0.0476	0.0681	0.0953	0.829
		Model	-0.00082	-0.0046	-0.00051	0.904971	0.920818	-0.01747	-0.02353	0.144852	0.308912	-0.01764	-0.01399	0.018215	0.060684	0.094904	0.161921	0.747439

Adsorbent: Jack fruit leaf ash

Variation of bed depth at C_0 = 25 mg/L

Test	input	Sl. No	4	5	11	17	18	23	24	25	31	32	41	42	50	51	59	60	69	70	79	80	89	99	101
		H	4	4	4	4	4	4	4	4	6	6	6	6	6	6	6	6	8	8	8	8	8	8	8
		Time	30	40	100	160	170	220	230	240	0	10	100	110	190	200	280	290	40	50	140	150	240	340	360
		q	7.5	7.5	7.5	7.5	7.5	7.5	7.5	7.5	7.5	7.5	7.5	7.5	7.5	7.5	7.5	7.5	7.5	7.5	7.5	7.5	7.5	7.5	7.5
		pH	7	7	7	7	7	7	7	7	7	7	7	7	7	7	7	7	7	7	7	7	7	7	7
		C0	25	25	25	25	25	25	25	25	25	25	25	25	25	25	25	25	25	25	25	25	25	25	25
		(Ct/C0)exp	0.0003	0.0004	0.001	0.0062	0.0068	0.0288	0.0497	0.1128	0	0	0.0008	0.0009	0.0063	0.0084	0.7045	0.7261	0	0.0001	0.001	0.0011	0.0116	0.9247	0.9829
		(Ct/C0)ANN	4.89E-05	0.00017	0.002714	0.01835	0.01989172	0.03309	0.116657	0.260191	-0.166067	-0.1195	0.00269	0.0111683	-0.005631	-0.00594	0.6018671	0.74764	-0.00459	-0.0054	0.0018647	0.0174752	0.04255	0.946966	1.0063

Variation of bed depth at C_0 = 100 mg/L

		Sl. No	2	3	4	12	13	19	20	26	33	34	38	42	43	51	52	61	62	65	69	70	71	78	79	80
		H	4	4	4	4	4	4	4	6	6	6	6	6	6	6	6	8	8	8	8	8	8	8	8	8
Test	input	Time	10	20	30	110	120	180	190	0	70	80	120	160	170	250	260	80	90	120	160	170	180	250	260	270
		q	7.5	7.5	7.5	7.5	7.5	7.5	7.5	7.5	7.5	7.5	7.5	7.5	7.5	7.5	7.5	7.5	7.5	7.5	7.5	7.5	7.5	7.5	7.5	7.5
		pH	7	7	7	7	7	7	7	7	7	7	7	7	7	7	7	7	7	7	7	7	7	7	7	7
		C0	100	100	100	100	100	100	100	100	100	100	100	100	100	100	100	100	100	100	100	100	100	100	100	100
		(Ct/C0)exp	0.0001	0.0003	0.0005	0.0127	0.0411	0.6114	0.7217	0	0.0021	0.0029	0.0321	0.4114	0.5219	0.9856	0.999	0.0021	0.004	0.0117	0.3814	0.4179	0.4712	0.886	0.9267	0.9885
		(Ct/C0)ANN	0.0073	-0.00095	-0.01022	-0.0099	0.03882	0.6542	0.70014	-0.1123	0.0063	0.0084	0.02714	0.3437	0.43136	1.00657	1.063	-0.0045	-0.003	0.01836	0.21291	0.31	0.4102	0.983	1.1105	1.2163

Variation of concentration at H = 6 cm

		Sl. No	2	3	4	5	6	7	16	17	18	19	24	25	26	33	34	35	44	45	49	55	56	61	62	71	72
		C0	25	25	25	25	25	25	25	25	25	25	25	25	25	25	50	50	50	50	50	50	50	50	50	75	75
Test	input	Time	10	20	30	40	50	60	150	160	170	180	230	240	250	320	0	10	100	110	150	210	220	270	280	60	70
		q	7.5	7.5	7.5	7.5	7.5	7.5	7.5	7.5	7.5	7.5	7.5	7.5	7.5	7.5	7.5	7.5	7.5	7.5	7.5	7.5	7.5	7.5	7.5	7.5	7.5
		pH	7	7	7	7	7	7	7	7	7	7	7	7	7	7	7	7	7	7	7	7	7	7	7	7	7
		H	6	6	6	6	6	6	6	6	6	6	6	6	6	6	6	6	6	6	6	6	6	6	6	6	6
		(Ct/C0)exp	0	0	0	0.0002	0.0003	0.0004	0.0028	0.0037	0.0052	0.0063	0.0817	0.106	0.2167	0.9835	0	0	0.042	0.0081	0.0262	0.0614	0.1421	0.8124	0.8864	0.001	0.0015
		(Ct/C0)ANN	-0.1914729	-0.1666	-0.120958	-0.0732	-0.03651	-0.01393	0.0021	-0.00176	-6E-04	0.002	0.09997	0.167	0.266	1.01657	0.024	0.01824	0.04971	0.05393	0.01279	0.18191	0.286808	0.8454	0.902298	-0.009	-0.009225

Variation of concentration at H = 8 cm

		Sl. No	2	3	4	10	11	17	18	26	27	38	39	49
		C0	25	25	25	25	25	25	25	25	25	25	50	50
Test	input	Time	10	20	30	90	100	160	170	250	260	370	0	100
		q	7.5	7.5	7.5	7.5	7.5	7.5	7.5	7.5	7.5	7.5	7.5	7.5
		pH	7	7	7	7	7	7	7	7	7	7	7	7
		H	8	8	8	8	8	8	8	8	8	8	8	8
		(Ct/C0)exp	0	0	0	0.0005	0.0007	0.0012	0.0016	0.0724	0.0917	0.9912	0	0.0039
		(Ct/C0)ANN	-0.01961	-0.01875	-0.00994	-0.00168	-0.00169	0.004057	0.00514	0.11358	0.245045	0.981186	0.0085	0.003136

		Sl. No	50	51	61	62	86	87	88	101	102	109	110	124	125	12
		C0	50	50	50	50	75	75	75	75	100	100	100	100	100	10
Test	input	Time	110	120	220	230	130	140	150	280	0	70	80	220	230	24
		q	7.5	7.5	7.5	7.5	7.5	7.5	7.5	7.5	7.5	7.5	7.5	7.5	7.5	7.
		pH	7	7	7	7	7	7	7	7	7	7	7	7	7	7
		H	8	8	8	8	8	8	8	8	8	8	8	8	8	8
		(Ct/C0)exp	0.0056	0.0041	0.2411	0.5012	0.021	0.0704	0.1104	0.9987	0	0.002	0.0021	0.6224	0.7341	0.8
		(Ct/C0)ANN	-4E-04	-9E-04	0.31885	0.502	0.0106	0.01475	0.0225	0.8667	0.02017	0.004	0.0091	0.69273	0.79422	0.864

Variation of flow rate at C_0 = 100 mg/L and H = 4 cm.

		Sl. No	6	7	13	14	15	22	23	30	31
		C0	100	100	100	100	100	100	100	100	100
Test	input	Time	50	60	120	130	140	210	220	290	300
		q	5	5	5	5	5	5	5	5	5
		pH	7	7	7	7	7	7	7	7	7
		H	4	4	4	4	4	4	4	4	4
		(Ct/C0)exp	0.0005	0.0008	0.0039	0.0045	0.0057	0.0843	0.0975	0.7219	0.8715
		(Ct/C0)ANN	0.0155457	0.0124794	0.0396742	0.024109	0.009849	0.081253	0.100923	0.688908	0.8228157

		Sl. No	41	42	51	52	59	60	71	77	78	79
		C0	100	100	100	100	100	100	100	100	100	100
Test	input	Time	70	80	170	180	0	10	120	180	190	200
		q	7.5	7.5	7.5	7.5	10	10	10	10	10	10
		pH	7	7	7	7	7	7	7	7	7	7
		H	4	4	4	4	4	4	4	4	4	4
		(Ct/C0)exp	0.0028	0.0034	0.5669	0.6114	0.0003	0.0005	0.3196	0.8112	0.8516	0.9217
		(Ct/C0)ANN	-0.003891	-0.0142145	0.5957006	0.6475956	0.0150063	0.0073626	0.3379305	0.8596468	1.0210431	1.1277182

Variation of pH at C_0 = 100 mg/L and H = 4 cm

		Sl. No	2	3	4	10	11	18	19	24	25	27	34	35	41	42	43	51	52	53	54	62	63	70	71	75	76
		pH	4	4	4	4	4	4	4	7	7	7	7	7	7	7	7	10	10	10	10	10	10	10	10	10	10
Test	input	Time	10	20	30	90	100	170	180	0	10	30	100	110	170	180	190	20	30	40	50	130	140	210	220	260	270
		q	7.5	7.5	7.5	7.5	7.5	7.5	7.5	7.5	7.5	7.5	7.5	7.5	7.5	7.5	7.5	7.5	7.5	7.5	7.5	7.5	7.5	7.5	7.5	7.5	7.5
		C0	100	100	100	100	100	100	100	100	100	100	100	100	100	100	100	100	100	100	100	100	100	100	100	100	100
		H	4	4	4	4	4	4	4	4	4	4	4	4	4	4	4	4	4	4	4	4	4	4	4	4	4
		(Ct/C0)exp	0	0.0001	0.0004	0.0043	0.0062	0.4437	0.5521	0	0.0001	0.0005	0.0073	0.0127	0.5669	0.6114	0.7217	0	0	0.0001	0.0004	0.021	0.0704	0.5243	0.6104	0.895	0.927
		(Ct/C0)ANN	0.0025	0.002	0.0003	-0.009518	-0.03599	0.4889	0.5952	-0.022882	-0.0064	0.00035	-0.02755	-0.019	0.66075	0.75168	0.82354	0.01181	0.00241	-0.009	-0.014	0.04798	0.099489	0.5643	0.6214	0.86667	0.9347

Adsorbent: Bagasse fly ash

Variation of bed depths at C_0 = 25 mg/L

		Sl. No	3	4	12	13	20	21	33	36	43	44	51	52	62	63	69	76	77	92	95
		H	4	4	4	4	4	4	6	6	6	6	6	6	8	8	8	8	8	8	8
Test	input	Time	20	30	110	120	190	200	80	110	180	190	260	270	40	50	110	180	190	340	370
		q	7.5	7.5	7.5	7.5	7.5	7.5	7.5	7.5	7.5	7.5	7.5	7.5	7.5	7.5	7.5	7.5	7.5	7.5	7.5
		pH	7	7	7	7	7	7	7	7	7	7	7	7	7	7	7	7	7	7	7
		C0	25	25	25	25	25	25	25	25	25	25	25	25	25	25	25	25	25	25	25
		(Ct/C0)exp	0.0007	0.0008	0.0156	0.0189	0.1944	0.2841	0.0015	0.0024	0.0084	0.0089	0.042	0.067	0.0008	0.0009	0.0022	0.0068	0.0069	0.3433	0.6412
		(Ct/C0)ANN	0.002222	0.00402	0.00807	0.01124	0.15504	0.22754	-0.00228	0.0028	0.01	0.0105	0.06199	0.09043	0.05193	0.07312	0.0022	0.00541	0.00548	0.385	0.596

Variation of bed depths at C_0 = 75 mg/L

		Sl. No	2	5	10	16	20	25	32	33	37	39
		H	4	4	4	6	6	6	8	8	8	8
		Time	10	40	90	30	70	120	60	70	110	130
Test	input	q	7.5	7.5	7.5	7.5	7.5	7.5	7.5	7.5	7.5	7.5
		pH	7	7	7	7	7	7	7	7	7	7
		C0	75	75	75	75	75	75	75	75	75	75
		(Ct/C0)exp	0.0186	0.0253	0.3401	0.0114	0.0301	0.6171	0.0024	0.0026	0.0094	0.1884
		(Ct/C0)ANN	0.006708	0.028031	0.331151	0.011048	0.033548	0.486884	0.000764	0.002819	-0.19465	0.393825

Variation of bed depths at C_0 = 100 mg/L

		Sl. No	2	5	8	11	15	16	20	21	23
		H	4	4	6	6	8	8	8	8	8
Test	input	Time	10	40	10	40	0	10	50	60	80
		q	7.5	7.5	7.5	7.5	7.5	7.5	7.5	7.5	7.5
		pH	7	7	7	7	7	7	7	7	7
		C0	100	100	100	100	100	100	100	100	100
		(Ct/C0)exp	0.0672	0.2437	0.0028	0.0128	0.0021	0.003	0.0086	0.1339	0.6784
		(Ct/C0)ANN	0.140146	0.339727	-0.09543	0.053879	-0.20552	-0.16069	0.05811	0.23061	0.529221

Variation of initial concentrations at H = 4 cm

		Sl. No	3	6	7	13	19	24	25	32	33	39	44	45	52	53	58
		C0	25	25	25	25	25	25	50	50	50	50	75	75	75	100	100
Test	input	Time	20	50	60	120	180	230	0	70	80	140	20	30	100	110	40
		q	7.5	7.5	7.5	7.5	7.5	7.5	7.5	7.5	7.5	7.5	7.5	7.5	7.5	7.5	7.5
		pH	7	7	7	7	7	7	7	7	7	7	7	7	7	7	7
		H	4	4	4	4	4	4	4	4	4	4	4	4	4	4	4
		(Ct/C0)exp	0.0007	0.0044	0.0054	0.0189	0.122	0.6124	0.0007	0.0055	0.0059	0.1042	0.0232	0.0234	0.595	0.1982	0.2437
		(Ct/C0)ANN	0.000717	0.002292	0.00378	0.017884	0.162774	0.389629	0.000753	0.007225	0.007439	0.132194	0.021046	0.023803	0.7192	0.198204	0.343398

Variation of initial concentrations at H= 6 cm.

		Sl. No	2	3	10	11	19	25	26	37	38	39	45	46	53	54	60	61	66	69	72	73
		C0	25	25	25	25	25	25	25	50	50	50	50	50	50	50	75	75	75	100	100	100
Test	input	Time	10	20	90	100	180	240	250	20	30	40	100	110	180	190	40	50	100	0	30	40
		q	7.5	7.5	7.5	7.5	7.5	7.5	7.5	7.5	7.5	7.5	7.5	7.5	7.5	7.5	7.5	7.5	7.5	7.5	7.5	7.5
		pH	7	7	7	7	7	7	7	7	7	7	7	7	7	7	7	7	7	7	7	7
		H	6	6	6	6	6	6	6	6	6	6	6	6	6	6	6	6	6	6	6	6
		(Ct/C0)exp	0.0002	0.0004	0.0015	0.0018	0.0078	0.015	0.021	0.0008	0.0009	0.001	0.0062	0.0078	0.0912	0.115	0.0216	0.0249	0.3412	0.0014	0.0128	0.2133
		(Ct/C0)ANN	0.000801	0.00085	0.00132	0.00171	0.00786	0.01473	0.02294	0.001622	0.00232	0.002355	0.006037	0.007285	0.05273	0.06527	0.0113	0.02129	0.3412	-0.01105	0.0215	0.1241

Variation of flow rate at H = 4 cm and C_0 = 100 mg/L

		Sl. No	3	4	7	8	12	13	18	19
		q	5	5	5	7.5	7.5	7.5	10	10
		Time	20	30	60	0	40	50	40	50
Test	input	C0	25	25	25	25	25	25	25	25
		pH	7	7	7	7	7	7	7	7
		H	8	8	8	8	8	8	8	8
		(Ct/C0)exp	0.0128	0.0161	0.832	0.0125	0.2437	0.6392	0.4533	0.49316
		(Ct/C0)ANN	-0.0087	-0.01488	0.430054	0.022455	0.210594	0.042283	0.196786	-0.05225

Variation of pH at H = 4cm and C_0 = 100 mg/L

		Sl. No	2	3	5	8	10	13	14	17	18	19
		pH	4.2	4.2	7	7	7	9.2	9.2	9.2	9.2	9.2
		Time	10	20	0	30	50	20	30	60	70	80
		q	7.5	7.5	7.5	7.5	7.5	7.5	7.5	7.5	7.5	7.5
Test	input	H	4	4	4	4	4	4	4	4	4	4
		C0	100	100	100	100	100	100	100	100	100	100
	Target	(Ct/C0)exp	0.2148	0.3812	0.0125	0.1982	0.6392	0.08641	0.11247	0.4287	0.5214	0.5307
		(Ct/C0)ANN	0.630769	0.363854	0.0125	0.151559	0.026481	0.181406	0.186316	0.478977	0.5214	0.536266

Adsorbent: Rice husk ash

Variation of bed depths at C_0 = 25 mg/L

		Sl. No	3	4	9	10	17	18	28	29	40	41	51	52	60	61	69	70	79	80
		H	4	4	4	4	4	4	6	6	6	6	8	8	8	8	8	8	8	8
		Time	20	30	80	90	160	170	60	70	180	190	20	30	110	120	200	210	300	310
Test	input	q	7.5	7.5	7.5	7.5	7.5	7.5	7.5	7.5	7.5	7.5	7.5	7.5	7.5	7.5	7.5	7.5	7.5	7.5
		pH	7	7	7	7	7	7	7	7	7	7	7	7	7	7	7	7	7	7
		C0	25	25	25	25	25	25	25	25	25	25	25	25	25	25	25	25	25	25
		(Ct/C0)exp	0.0256	0.05	0.1599	0.17	0.6018	0.6712	0.0051	0.0057	0.0729	0.0814	0.007	0.0072	0.0098	0.0145	0.0237	0.028	0.2228	0.332
		(Ct/C0)ANN	0.04465	0.06303	0.16411	0.18706	0.6071	0.66792	-0.00874	-0.00124	0.08883	0.13048	0.00684	0.00667	0.00369	0.001723	0.02695	0.02335	0.22425	0.31228

Variation of bed depths at C_0 = 100 mg/L

		Sl. No	3	4	5	8	10	11	16	17	19	20	22	23
		H	4	4	4	6	6	6	8	8	8	8	8	8
		Time	20	30	40	10	30	40	10	20	40	50	70	80
Test	input	q	7.5	7.5	7.5	7.5	7.5	7.5	7.5	7.5	7.5	7.5	7.5	7.5
		pH	7	7	7	7	7	7	7	7	7	7	7	7
		C0	100	100	100	100	100	100	100	100	100	100	100	100
		(Ct/C0)exp	0.0933	0.1533	0.3447	0.0825	0.1124	0.4641	0.0652	0.0852	0.1525	0.5988	0.6923	0.7093
		(Ct/C0)ANN	0.113395	0.17455	0.3447	0.0825	0.08143	0.399973	0.017948	0.108457	0.107714	0.766312	0.732063	0.726629

Variation of initial concentrations at H = 4 cm

		Sl. No	2	3	9	13	14	19	20	24	25	31	32	40	41	49	50	56	57
		C0	25	25	25	25	25	25	25	50	50	50	50	75	75	75	75	100	100
		Time	10	20	80	120	130	180	190	20	30	90	100	10	20	100	110	20	30
<u>Test</u>	input	q	7.5	7.5	7.5	7.5	7.5	7.5	7.5	7.5	7.5	7.5	7.5	7.5	7.5	7.5	7.5	7.5	7.5
		pH	7	7	7	7	7	7	7	7	7	7	7	7	7	7	7	7	7
		H	4	4	4	4	4	4	4	4	4	4	4	4	4	4	4	4	4
		(Ct/C0)exp	0.0237	0.0256	0.1599	0.2687	0.3182	0.6947	0.7248	0.0214	0.0374	0.1367	0.1876	0.0264	0.0378	0.3344	0.3978	0.0933	0.1533
		(Ct/C0)ANN	0.01762	0.04541	0.13618	0.2921	0.46331	0.69034	0.71007	-0.0101	0.01295	0.1385	0.15647	0.044722	0.05136	0.3306	0.35687	0.29148	0.12135

Variation of initial concentrations at H = 4 cm

		Sl. No	2	3	8	14	15	23	24	33	34	41	42	54	55	61	62	73	74	79
		C0	25	25	25	25	25	25	25	50	50	50	50	75	75	75	75	100	100	100
<u>Test</u>	input	Time	10	20	70	130	140	220	230	50	60	130	140	20	30	90	100	0	10	60
		q	7.5	7.5	7.5	7.5	7.5	7.5	7.5	7.5	7.5	7.5	7.5	7.5	7.5	7.5	7.5	7.5	7.5	7.5
		pH	7	7	7	7	7	7	7	7	7	7	7	7	7	7	7	7	7	7
		H	6	6	6	6	6	6	6	6	6	6	6	6	6	6	6	6	6	6
		(Ct/C0)exp	0.0021	0.0029	0.0057	0.0163	0.0249	0.3417	0.4448	0.00314	0.0047	0.0246	0.0297	0.0089	0.0097	0.0314	0.0342	0.0612	0.0825	0.7114
		(Ct/C0)ANN	0.005217	0.0053	0.005186	0.013376	0.021764	0.31202	0.363244	0.00545	0.005529	0.020567	0.030866	0.004243	0.005239	0.038694	0.038558	-2.043728	-1.231779	0.704158

Variation of flow rate at H = 4cm and C_0 = 100 mg/L

	Sl. No	2	3	8	9	13	14	21	22	25	26
	C0	100	100	100	100	100	100	100	100	100	100
input	Time	10	20	70	80	120	130	200	210	240	250
	q	5	5	5	5	5	7.5	7.5	10	10	10
	pH	7	7	7	7	7	7	7	7	7	7
	H	4	4	4	4	4	4	4	4	4	4
	(Ct/C0)exp	0.01152	0.0426	0.3417	0.5217	0.7512	0.0061	0.7252	0.0912	0.4269	0.6215
	(Ct/C0)ANN	-0.08871	-0.07819	0.191232	0.291431	0.716228	0.121407	0.423968	0.436642	0.619563	0.64243

Variation of pH at H = 4 cm and C_0 = 100mg/L

	Sl. No	2	3	8	9	13	14	21	22	25	26
	C0	100	100	100	100	100	100	100	100	100	100
input	Time	10	20	70	80	120	130	200	210	240	250
	q	5	5	5	5	5	7.5	7.5	10	10	10
	pH	7	7	7	7	7	7	7	7	7	7
	H	4	4	4	4	4	4	4	4	4	4
	(Ct/C0)exp	0.01152	0.0426	0.3417	0.5217	0.7512	0.0061	0.7252	0.0912	0.4269	0.6215
	(Ct/C0)ANN	-0.08871	-0.07819	0.191232	0.291431	0.716228	0.121407	0.423968	0.436642	0.619563	0.64243

Evaluation of adsorption potential by using ANN tool: Batch study

Adsorbent: Neem leaf ash

Variation of adsorbent dosages

		Sl. No	1	3	5	6	8	9	11	12	14	15
		C0	25	25	25	25	25	25	25	25	25	25
	Input	Time	135	135	135	135	135	135	135	135	135	135
		Dose	0.1	0.5	1.2	1.4	2.4	2.8	4	5	8	12
Training		pH	7	7	7	7	7	7	7	7	7	7
		S	165	165	165	165	165	165	165	165	165	165
		Ct/C0	0.47	0.2	0.2	0.1	0.1	0.1	0.1	0.02	0.008	0.008
Target												
		Model	0.28	0.3	0.2	0.2	0.06	0.1	0.1	0.01	0.017	0.044

Variation of initial pH of the solution dyes

		Sl. No	1	2	5
		C0	25	25	25
	Input	Time	135	135	135
		Dose	4	4	4
Training		pH	3	4.1	8.2
		S	165	165	165
		Ct/C0	0.06	0.1	0.12
Target					
		Model	0.06	0.1	0.13

Variation of contact time

		Sl. No	1	3	4	7	8	10
		C0	25	25	25	25	25	25
	Input	Time	10	60	75	135	165	210
		Dose	4	4	4	4	4	4
Training		pH	7	7	7	7	7	7
		S	165	165	165	165	165	165
		Ct/C0	0.03	0.02	0.01	0.004	0	0.004
Target								
		Model	0.04	0.02	0.01	0.004	0.02	0.004

Variation in shaker speed

		Sl. No	1	4	5	8
		C0	25	25	25	25
	Input	Time	135	135	135	135
		Dose	4	4	4	4
Training		pH	7	7	7	7
		S	30	75	90	130
		Ct/C0	0.07	0.03	0.028	0.01
Target						
		Model	0.03	0.04	0.028	0.08

Variation of initial concentrations

		Sl. No	1	4	6
		C0	25	75	150
	Input	Time	135	135	135
		Dose	4	4	4
Training		pH	7	7	7
		S	165	165	165
		Ct/C0	0.0122	0.0511	0.3226
Target					
		Model	0.0122001	0.0511	0.3226001

Adsorbent: Jack fruit leaf ash

Variation of adsorbent dosages

		Sl. No	1	2	5	6	7	8	9	11	12	15
		C_0	25	25	25	25	25	25	25	25	25	25
	Input	Time	135	135	135	135	135	135	135	135	135	135
		Dose	0.1	0.25	1.2	1.4	2	2.4	2.8	4	5	12
Training		pH	7	7	7	7	7	7	7	7	7	7
		S	165	165	165	165	165	165	165	165	165	165
		Ct/C0	0.842	0.638	0.381	0.302	0.215	0.179	0.147	0.105	0.1	0.0743
	Target											
		Model	0.838	0.811	0.425	0.311	0.195	0.18	0.156	0.096	0.1	0.0744

Variation of initial pH of the solution dyes

		Sl. No	1	4	6
		C_0	25	25	25
	Input	Time	135	135	135
		Dose	4	4	4
Training		pH	3	7	9.1
		S	165	165	165
		Ct/C0	0.051	0.021	0.008
Target					
		Model	0.051	0.02	0.008

Variation of contact time

		Sl. No	1	4	5	6	9	10	12
		C0	25	25	25	25	25	25	25
	Input	Time	10	75	90	120	190	210	300
		Dose	4	4	4	4	4	4	4
Training		pH	7	7	7	7	7	7	7
		S	165	165	165	165	165	165	165
		Ct/C0	0.315	0.1	0.094	0.08	0.0427	0.0426	0.0426
Target									
		Model	0.332	0.315	0.36	0.29	0.2661	0.3863	0.1517

Variation of shaker speed

		Sl. No	1	2	5	7	8
		C0	25	25	25	25	25
	Input	Time	135	135	135	135	135
		Dose	4	4	4	4	4
Training		pH	7	7	7	7	7
		S	30	50	90	120	130
		Ct/C0	0.037	0.021	0.02	0.015	0.016
	Target						
		Model	0.019	0.019	0.02	0.019	0.014

Variation of initial concentration

		Sl. No	1	4	5	6
		C0	25	75	100	150
	Input	Time	135	135	135	135
		Dose	4	4	4	4
Training		pH	7	7	7	7
		S	165	165	165	165
		Ct/C0	0.1147	0.2171	0.3454	0.4175
	Target					
		Model	0.1147	0.2171	0.308219	0.4175

Adsorbent: Bagasse fly ash

Variation of adsorbent dosages

Training	Input	Sl. No	1	2	5	6	7	10	11	14	15
		C_0	25	25	25	25	25	25	25	25	25
		Time	135	135	135	135	135	135	135	135	135
		Dose	0.1	0.25	1.2	1.4	2	3.2	4	8	12
		pH	7	7	7	7	7	7	7	7	7
		S	165	165	165	165	165	165	165	165	165
Target		Ct/C0	0.086	0.061	0.021	0.02	0.02	0.0177	0.0175	0.0147	0.01
		Model	0.077	0.061	0.021	0.02	0.02	0.0177	0.0175	0.0147	0.01

Variation of initial pH of the solution dyes

Training	Input	Sl. No	1	4	5	6
		C0	25	25	25	25
		Time	135	135	135	135
		Dose	4	4	4	4
		pH	3	7	8.2	9.1
		S	165	165	165	165
	Target	Ct/C0	0.0428	0.0175	0.011	0.0092
		Model	0.0428	0.0175	0.0111	0.0092

Variation of contact time

Training	Input	Sl. No	1	4	5	6
		C0	25	25	25	25
		Time	135	135	135	135
		Dose	4	4	4	4
		pH	3	7	8.2	9.1
		S	165	165	165	165
	Target	Ct/C0	0.0428	0.0175	0.011	0.0092
		Model	0.0428	0.0175	0.0111	0.0092

Variation of shaker speed

Training	Input	Sl. No	1	4	6	8
		C0	25	25	25	25
		Time	135	135	135	135
		Dose	4	4	4	4
		pH	7	7	7	7
		S	30	75	110	130
	Target	Ct/C0	0.045	0.0247	0.021	0.018
		Model	0.045	0.0559	0.021	0.021

Variation of initial concentrations

Training	Input	Sl. No	1	4	6
		C_0	25	75	150
		Time	135	135	135
		Dose	4	4	4
		pH	7	7	7
		S	165	165	165
	Target	C_t/C_0	0.0146	0.0888	0.1351
		Model	0.0146	0.0888	0.1351

Adsorbent: Rice husk ash

Variation of adsorbent dosages

Training	Input	Sl. No	1	2	3	7	8	10	11	12
		C0	25	25	25	25	25	25	25	25
		Time	10	30	60	135	165	210	240	300
		DOSE	4	4	4	4	4	4	4	4
		pH	7	7	7	7	7	7	7	7
		S	165	165	165	165	165	165	165	165
	Target	Ct/C0	0.4693	0.3685	0.2266	0.1247	0.1184	0.0952	0.0861	0.0862
		Model	0.46898	0.38068	0.22649	0.12465	0.08173	0.095468	0.085372	0.086364

Variation of initial pH of the solution dyes

		Sl. No	2	3	5
		C0	25	25	25
	Input	Time	135	135	135
		Dose	4	4	4
Test		pH	4.1	5.4	8.2
		H	165	165	165
		Ct/C0	0.2173	0.1583	0.0512
Target					
		Model	0.226439	0.17001	0.06625

Variation of Contact time of the solution dyes

		Sl. No	1	2	3	7	8	10	11	12
		C0	25	25	25	25	25	25	25	25
	Input	Time	10	30	60	135	165	210	240	300
		DOSE	4	4	4	4	4	4	4	4
Training		pH	7	7	7	7	7	7	7	7
		S	165	165	165	165	165	165	165	165
		Ct/C0	0.4693	0.3685	0.2266	0.1247	0.1184	0.0952	0.0861	0.0862
	Target									
		Model	0.46898	0.38068	0.22649	0.12465	0.08173	0.095468	0.085372	0.086364

Variation of shaker speed

		Sl. No	1	5	6	7	8
		C0	25	25	25	25	25
	Input	Time	135	135	135	135	135
		Dose	4	4	4	4	4
Training		pH	7	7	7	7	7
		S	30	90	110	120	130
		Ct/C0	0.3352	0.1393	0.0905	0.0904	0.0905
	Target						
		Model	0.3352	0.20203	0.0905	0.063475	0.0904999

Variation of initial concentrations

		Sl. No	1	5	6
		C0	25	100	150
	Input	Time	135	135	135
		Dose	4	4	4
Training		pH	7	7	7
		S	165	165	165
		Ct/C0	0.1147	0.3454	0.4175
Target					
		Model	0.1147	0.3454	0.4175